How sediment damages corals

Dissertation zur Erlangung des Doktorgrades der Naturwissenschaften

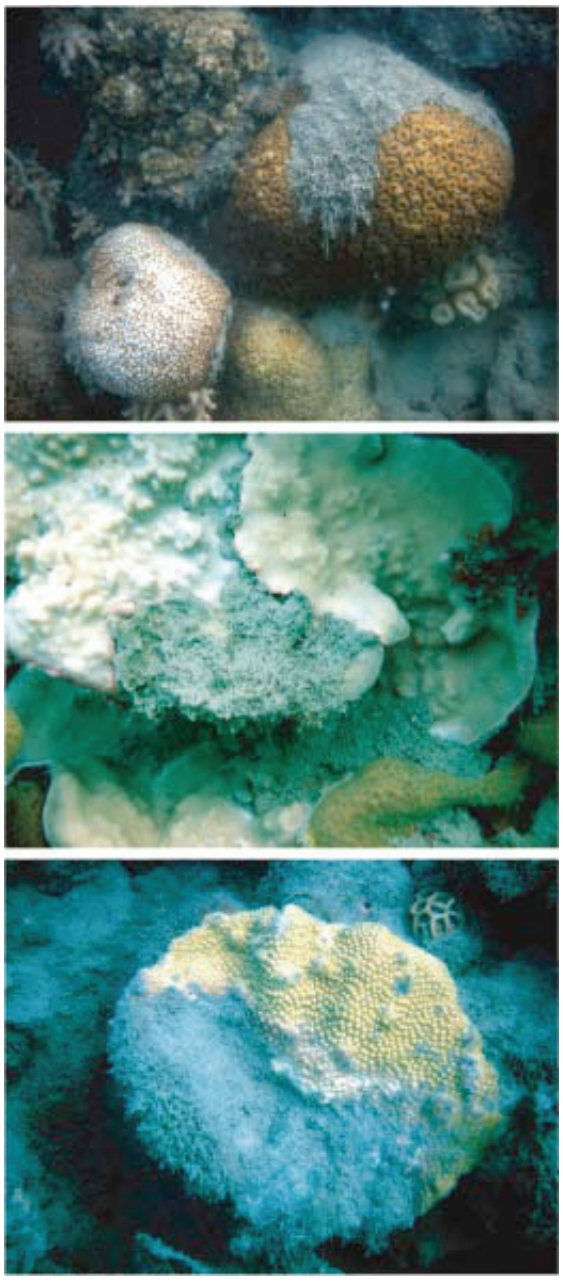

dem Fachbereich Biologie/Chemie
der Universität Bremen vorgelegt

von **Miriam Weber**

Bremen
Februar 2009

Die vorliegende Arbeit wurde von Januar 2004 bis Februar 2009* in Form eines Kooperationsprojektes an den folgenden Instituten angefertigt:

1. Max-Planck-Institut für Marine Mikrobiologie in Bremen, Deutschland
2. HYDRA Institut für Meereswissenschaften, Feldstation Elba, Italien
3. Australian Institute of Marine Science, Townsville, Australien

*Auf Grund anderweitiger Berufstätigkeit wurden folgende Pausen eingelegt: 08-09.2004, 09-10.2005, 08-09.2006, 03-11.2007 und 05-09.2008 (total 20 Monate)

Gutachter

Prof. Dr. Bo Barker Jørgensen

Prof. Dr. Kai Bischof

Prüfer

Dr. Dirk de Beer

Prof. Dr. Wilhelm Hagen

Weitere Mitglieder des Prüfungsausschusses

MSc LS Katharina Kohls

BSc Stefan Häusler

Datum des Promotionskolloquiums: 24. April 2009

Table of contents

Summary	i
Zusammenfassung	I
Chapter 1: Introduction	1
1. Warm-water coral reefs	2
2. Sediment on the continental shelf	6
3. How sediment damages corals: a hypothesis	12
4. Methods and technological developments	16
5. Objectives of the thesis	19
6. Overview of chapters 2-8	20
7. References	22
Chapter 2: Effects of different types of sediment, dissolved inorganic nutrients and salinity on fertilisation and embryo development in the coral *Acropora millepora* (Ehrenberg, 1834)	27
Chapter 3: Sedimentation stress in a scleractinian coral exposed to terrestrial and marine sediments with contrasting physical, organic and geochemical properties	43
Chapter 4: A cascade of microbial processes kills sediment-covered corals	61
Chapter 5: *In situ* applications of a new diver-operated motorized microsensor profiler	101
Chapter 6: *In situ* measurement of gross photosynthesis using a microsensor-based light-shade shift method	123
Chapter 7: Heterogeneous oxygenation resulting from active and passive flow in two Mediterranean sponges	135
Chapter 8: The H_2S microsensor and the dissociation constant pK_1: problems and solutions	157
Chapter 9: Conclusions and outlook	171
Acknowledgements	175
Erklärung / Statement	176

Summary

Recent reports state that worldwide about 50-80% of the warm-water coral reefs have been harmed, and about 25% irreversibly damaged from direct human pressures. Poor coastal management results in overfishing and elevated river discharge of sediment, nutrients and pollutants. The effects of sedimentation on reef-building corals are well documented, as previous studies focused mostly on the coral response. The processes of how sediment actually damages corals, and the role of contrasting sediment properties have remained poorly understood. In this study we therefore focused on the sediments and investigated the harming processes. Our central hypothesis was that bacteria play a crucial role in the damage that sediment causes to corals.

In summary, this work revealed that harmful effects of sediment exposure on reef-building warm-water corals are tightly linked to sediment properties, primarily the percentage of silt grains, the organic matter content and the microbial activity. A chain reaction of microbial degradation processes starting with oxygen depletion and pH decrease, followed by increased sulfide concentrations, resulted in the rapid death of the entire sediment-covered coral. An increase of 3-5% of total organic carbon in the sediment was enough to trigger the deadly cascade, killing the coral within one day. Hence, the exposure to fine sediment enriched in organic matter is particularly dangerous for coral reefs. The new submersible microsensor system DOMS proved itself as a valuable instrument to gain environmentally relevant information about *in situ* microprocesses in shallow water ecosystems, an area of research that was previously not amenable to flexible and easily replicated field measurements.

We tested the effect of different types of natural sediments on the photosynthetic activity of the coral *Montipora peltiformis* (Chapter 3), and on the fertilisation rates of the coral *Acropora millepora* (Chapter 2). Adult corals covered with medium sand, fine sand or organic-poor silt were not affected, but corals covered with organic-rich silt died within one day. The coral health status correlated most with the organic matter content and the grain size fraction of the ten sediment types tested. It was to a lesser extent related to the measured sedimentation rate, sedimentation volume, or light transmission, and unrelated to the concentrations of trace elements and metals found in the sediments (Chapter 3). Fertilisation rates of *A. millepora* were lowest in gametes simultaneously exposed to suspended sediment with the smallest average grain size and highest dissolved inorganic nutrient levels. Coral fertilisation was not reduced by exposure to elevated dissolved nutrients only, or by exposure

to low concentrations of suspended sediments. A significant interaction between the effects of salinity, suspended sediment and nutrients was shown, when salinity was <30 ppt (Chapter 2). As organic-rich sediments are also rich in microbes, we investigated if microbial processes play an important role in the mechanisms harming sediment-covered corals. For the coral *M. peltiformis* a microbially mediated cascade in the sediment layer was documented that led to coral death. We exposed coral fragments to natural reef sediment (containing 12.5 μg TOC g^{-1} DW) enriched with organic matter derived from natural concentrated seawater plankton, at environmentally relevant concentrations (up to + 0.6 μg TOC g^{-1} DW). After being covered by the sediment, first necrotic areas of square millimetre size were detected within one or two days, depending on the content of organic matter in the sediment. Contrary to our expectation, sulfide from sulfate reduction rates was not the inducer of the tissue necrosis. Immediately after accumulation of the sediment on the coral, the degradation of sedimentary organic matter depleted oxygen to zero and decreased the pH to 7. Although sulfide was also increased by sulfate reduction, it was not high enough to kill the coral. A simulation experiment revealed that anoxia combined with pH 7 was enough to kill the coral within one day. The corals survived anoxia at pH 8.2 for the entire exposure time of four days. This experiment also showed that concentrations of sulfide two orders of magnitude higher than measured are needed to kill the coral within one day. However after the initial killing microbially mediated sulfide release from the necrotic tissue accelerated the damage of the neighbouring coral polyps, and set off further necrosis and sulfide release. We showed that this cascade could kill the entire sediment-covered coral in less than one day (Chapter 4).

During this thesis technical development and major extensions of methods were needed. Working with the hydrogen sulfide microsensor resulted in an improvement of the existing calibration protocol (Chapter 8). The “2-way-calibration-method” was developed to determine the precise dissociation constant pK_1 for total sulfide. For a commonly used calibration buffer we observed that the previously used pK_1 compared to the newly determined pK_1, results in an error of ± 30% deviance in the H_2S concentration. We confirmed that the sensor is sensitive to ionic strength and temperature, and recommend to calibrate the sensor not in a buffer, but in the same media in which the profiling will be done, but to acidify it to pH <4 (no pK_1 needed).

The development of the new diver-operated microsensor system (DOMS) resulted in an easy-to-use instrument for shallow water applications (Chapter 5). The stand with a ball-head and the interactive capacities of the logger allow for a totally flexible positioning of the motorized

microsensor and an adjustable use of the measuring protocol. On land and in the water the system is transported in a small compact suitcase, giving the diver autonomy and flexibility to find the best study site. The high-speed measuring amplifiers allow to measure rapid dynamics (<0.5 s) as needed e.g. for photosynthesis studies. For that purpose we modified the light-dark-shift gross photosynthesis measurement method, for which complete darkening of the sample is necessary. The light-shade shift method allows the quantification of the gross photosynthesis with microsensors at the ambient light intensity from 4-5 light transition measurements by shading the sample. The total exclusion of light is not needed for this method, and thus it is more readily applicable *in situ*, where, during day light, complete sample darkening is practically very difficult to achieve (Chapter 6). It is often debated whether findings from tank experiments are artefacts due to unnatural conditions. We used the DOMS to compare laboratory tank measurements with field measurements from sediment-covered corals (Chapter 4), and, in a cooperation project, from the sponge *Dysidea avara* that had unexpectedly shown anoxic conditions in the tissue (Chapter 7). The results obtained by the *in situ* measurements confirmed concepts based on laboratory studies.

Zusammenfassung

Durch direkte anthropogene Einflüsse sind weltweit 50-80% der Warmwasser-Korallenriffe beschädigt, und ungefähr 25% irreversibel zerstört. Ungenügendes Küstenzonenmanagement führt zu Überfischung und erhöhten Einträgen von Sediment, Nährstoffen und Schadstoffen durch Flüsse. Der Einfluss von Sediment auf riffbildende Korallen ist gut dokumentiert, da sich vorangegangene Studien meist auf die Reaktion der Koralle konzentrierten. Die Prozesse wie Sediment die Korallen schädigt, und die Rolle unterschiedlicher Sedimentparameter sind nur wenig untersucht. In dieser Studie legten wir den Schwerpunkt auf die Sedimente und untersuchten die schädigenden Prozesse. Unsere Haupthypothese war, dass Bakterien einen entscheidenden Anteil an diesen auf die Koralle schädlich wirkenden Prozessen haben.
Diese Arbeit zeigte, dass die schädigenden Effekte durch Sedimentation auf Korallen eng mit den Sedimentparametern wie dem Anteil an Siltpartikeln, dem organischen Gehalt und der mikrobiellen Aktivität verknüpft sind. Eine Kettenreaktion mikrobieller Degradationsprozesse, beginnend mit rascher Sauerstoffzehrung und einem sofortigen pH-Abfall, gefolgt von ansteigender Sulfidkonzentration, brachte die gesamte sedimentbedeckte Koralle in einem Tag zum Absterben. Eine Erhöhung des organischen Gesamtkohlenstoffgehalts von 3-5% genügte, um diese tödliche Kaskade in Gang zu bringen. Das während dieser Arbeit neu entwickelte Mikrosensorinstrument DOMS erwies sich für die Untersuchung von umweltrelevanten Mikroprozessen in Flachwasserökosystemen als sehr geeignet. Ein solch flexibles und hoch auflösendes Instrument stand bisher für solche Feldmessungen nicht zur Verfügung.

Im Rahmen dieser Arbeit untersuchten wir die Wirkung von verschiedenen natürlichen Sedimenten auf die Photosyntheseaktivität der Koralle *Montipora peltiformis* (Kapitel 3), und auf die Fertilisationsrate der Koralle *Acropora millepora* (Kapitel 2). Adulte Korallen waren nicht beeinträchtigt, wenn sie mit Mittelsand, Feinsand oder organikarmem Silt bedeckt waren. Waren die Korallen mit organikreichem Silt bedeckt starben sie innerhalb eines Tages. Die Photosyntheseaktivität korrelierte am stärksten mit dem organischen Gehalt und mit der Korngrößenklasse der 10 getesteten Sedimente. Sie korrelierte weniger mit der Sedimentationsrate, dem Sedimentationsvolumen, oder der Lichtdurchlässigkeit. Und sie korrelierte nicht mit dem Gehalt an Spurenelementen und Metallen, die in den Sedimenten gemessen wurden (Kapitel 3). Die Fertilisationsraten in den Gameten waren am niedrigsten, wenn diese gleichzeitig suspendiertem Sediment der kleinsten Korngröße und der höchsten

Konzentration von gelösten anorganischen Nährstoffen ausgesetzt waren. Die Befruchtung war nicht beeinflusst wenn die Gameten nur mit erhöhten Nährstoffen, oder mit niedrigen Konzentrationen von suspendiertem Sediment inkubiert wurden. Wenn die Salinität unter 30 ppt blieb, wurden signifikante Interaktionen zwischen der Wirkung suspendierten Sediments, der gelösten Nährstoffe und der Salinität gemessen (Kapitel 2).

Da organikreiches Sediment auch reich an Mikroben ist, haben wir untersucht, ob mikrobielle Prozesse in der Sedimentschicht auf der adulten Koralle eine Rolle bei deren Schädigung spielen. Wir haben Korallenstücke natürlichem Riffsediment (mit 12,5 μg TOC g^{-1} DW) ausgesetzt, welches in umweltrelevanten Konzentrationen (+ 0,6 μg TOC g^{-1} DW) mit organischem Material angereichert war. Der Zusatz an organischem Material wurde aus natürlichem konzentriertem Plankton hergestellt. Erste Millimeter große Stellen abgestorbenen Gewebes wurden, abhängig von der Konzentration des organischen Materials, nach ein bis zwei Tagen detektiert. Entgegen unserer Erwartung war nicht Sulfid aus dem Prozess der Sulfatreduktion der Auslöser für das Absterben. Auf Grund des Abbaus des sedimentären organischen Materials war der Gehalt an Sauerstoff direkt nach dem Absetzen des Sediments auf der Koralle gleich Null und der pH auf 7 abgesunken. Obwohl der Gehalt an Sulfid durch Sulfatreduktion anstieg, war die Konzentration nicht hoch genug, um die Koralle zu töten. In einem Simulationsexperiment konnte gezeigt werden, dass Anoxie kombiniert mit pH 7 ausreichend war, um die Koralle binnen eines Tages irreversibel zu schädigen. Anoxie bei pH 8,2 hingegen schädigte die Koralle während vier Tagen nicht. Dieses Experiment zeigte außerdem, dass Sulfid in um zwei Größenordnungen höherer Konzentration notwendig gewesen wäre, um die Koralle binnen eines Tages zu töten. Nach dem initialen Absterben von kleinen Stellen, wurde totes Korallengewebe sofort abgebaut und dadurch Sulfid in höheren Konzentrationen frei. Dies tötete dann die Nachbarpolypen und beschleunigte so das Absterben. Wir konnten zeigen, dass diese Kaskade die gesamte sedimentbedeckte Fläche binnen weniger als einem Tag irreversibel schädigen kann (Kapitel 4).

Während dieser Arbeit waren technische Entwicklungen und Erweiterungen von bestehenden Methoden nötig. Die Arbeit mit dem Schwefelwasserstoff-Mikrosensor ergab eine weit reichende Verbesserung des bestehenden Protokolls bezüglich der Sensorkalibrierung (Kapitel 8). Für die präzise Bestimmung der Dissoziationskonstante pK_1 haben wir die so genannte „2-Weg-Kalibrier-Methode“ entwickelt. Bei der Sensorkalibrierung mit dem herkömmlichen Puffer und dem bislang verwendeten pK_1 gegenüber dem von uns neu

bestimmten pK_1 stellten wir eine Abweichung von ± 30% fest. Wir konnten bestätigen, dass der Sensor empfindlich auf die Ionenstärke und die Temperatur reagiert und empfehlen, den Sensor nicht in dem herkömmlichen Puffer, sondern in dem Medium, worin später die Messungen gemacht werden, zu kalibrieren. Das Medium sollte außerdem auf pH <4 angesäuert werden (kein pK_1 mehr nötig).

Die Entwicklung des neuen Taucher-betriebenen Mikrosensorsystems (DOMS) ergab ein einfach zu handhabendes Instrument für Flachwassereinsätze (Kapitel 5). Eine totale Flexibilität für die Positionierung des Mikrosensors wird durch das Stativ mit einem Kugelkopf erreicht. Der interaktive Datenlogger erlaubt jederzeit den Zugriff auf das Messprotokoll. An Land wie auch im Wasser wird das System in einem kleinen handlichen Koffer transportiert, so dass der Taucher autonom und flexibel ist, um den besten Platz zum Messen zu finden. Die hochempfindlichen Messverstärker ermöglichen Messungen von sich schnell ändernden Konzentrationen (<0.5 s). Dies wird z.B. für Bruttophotosynthese-messungen mit Sauerstoffmikrosensoren nach der Licht-Dunkel-Methode benötigt. Die Probe muss dabei komplett abdunkelt werden, was im Feld bei Tageslicht nur schwer möglich ist. Für diese Anwendung haben wir die Licht-Schatten-Methode entwickelt. Diese ermöglicht die Quantifizierung der Bruttophotosynthese bei Tageslicht mittels 4-5 Übergangsmessungen, bei welchen die Probe verschieden stark beschattet wird, aber nicht abdunkelt werden muss (Kapitel 6). Es wird immer wieder diskutiert, ob Aquarienversuche im Labor zu Artefakten in den Messergebnissen führen, da die natürlichen Bedingungen nur bedingt simuliert werden können. Mit dem DOMS haben wir Labormessungen direkt mit Feldmessungen vergleichen können. Dies haben wir an sedimentbedeckten Korallen (Kapitel 4), und in einem Kooperationsprojekt an dem Schwamm *Dysidea avara*, in dessen Gewebe unerwartet anoxische Bedienungen gemessen wurden, durchgeführt (Kapitel 7). Die im Feld erhobenen Messdaten konnten die im Labor gewonnenen Ergebnisse bestätigen.

Chapter 1

Introduction

Introduction

In this study we investigated how sediment damages reef-building warm water corals. Central in this thesis was the hypothesis that bacteria are important for the death of sediment-covered corals. We determined the geophysical properties of different sediments, their chemical composition, their microbial communities and the biogeochemical processes within the sediment, and related those to the health status of the corals. A multi-method approach was chosen which is outlined at the end of this chapter. For the experimental work in the coral reef a new submersible microsensor system was developed that was further applied in studies in related fields.

Because this is an interdisciplinary study, the introduction is broad, ranging from coral physiology, reef ecology and geography, to sedimentology, biogeochemistry, and microbiology, and to human impacts and coastal management. This chapter therefore also contains a literature overview of side topics. To underline in which context the chapters 2-8 stand to each other, the chapter number is given in brackets each time at the corresponding part of the introduction.

1. Warm-water coral reefs

Coral reefs are made from organisms that build calcium carbonate skeletons. The main warm water reef-builders are Scleractinia, also called stony corals, and calcareous algae. The majority of Scleractinia are colonial cnidarians that are marine animals living in symbiosis with phototrophic dinoflagellates, called zooxanthellae. During the day the zooxanthellae supply the symbiontic consortium with photosynthates as oxygen and organics (carbohydrates, amino acids, and mainly lipids), and the particle-feeding polyps supply the algae with inorganic nutrients. Light respiration in corals is about 80% of their net photosynthesis (Kühl et al. 1995, Al-Horani et al. 2003), which supplies energy for e.g. calcification and growth. Calcification of the coral is highest during the day because of the coupling to photosynthesis. Particularly at night corals catch planktonic organisms for food with their tentacles (Chapter 3-6).

Most corals reproduce sexually once a year by external fertilization (Harrison et al. 1984). The period from fertilisation to larval settlement lasts from a few days to maximally six weeks (Schuhmacher 1991) (Chapter 2).

Warm-water coral reefs are regarded as the most diverse and very productive shallow water marine ecosystems (Smith 1978, Roberts et al. 2002). With an area of 284300 km^2 they cover about 1.2% of the world's continental shelf (Spalding et al. 2001), and are found along coastlines in tropical and subtropical regions. Corals with zooxanthellae are restricted by the light availability and grow between 0 and 100 m depth. However, high coral cover and diversity are documented from nearshore turbid waters to offshore clear waters such as along the Great Barrier Reef in Australia (DeVantier 2006). Coral reefs tolerate salinities between 30 and 44 ppt and are usually not found in the direct influence of large rivers discharging episodically or constantly freshwater, such as e.g. the Amazon River (Schuhmacher 1991, Veron 2000). Corals can tolerate seawater temperatures from about 16 to 35°C. For optimal growth 25 to 30°C are needed. Cold- and warm-water currents shape the biogeography of coral reefs. In upwelling regions like at the west coasts of Africa and South America temperatures are too low, whereas warm currents let reefs grow in subtropical regions like Bermuda or South Australia (Fig. 1).

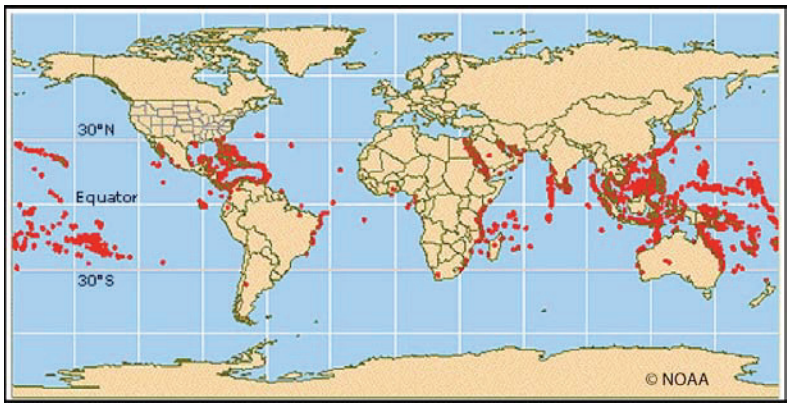

Figure 1. The red dots on this map show the global distribution of warm-water coral reefs. The majority of reefs are located between the 30° northern and 30° southern latitude. Some coral reefs grow further north or south because of warm-water currents (modified from NOAA).

The Great Barrier Reef (GBR), our study site, is the world's largest warm-water coral reef complex, and listed as marine World Heritage Area. It is about 2300 km long, ranging from 10° northern to 24° southern latitude, and consists of nearly 3000 reefs. Since 1975 the GBR is a Marine Park, which is divided in four sections called "Far Northern", "Northern", "Central" and "Southern" Section (Fig. 2).

A healthy, productive and biodiverse GBR is an essential part of Australia's international "brand". Reef-associated tourism, commercial fishing, cultural and recreational activity is worth about US$3.7 x 10^9 per year (Access Economics 2007). Worldwide coral reefs have an immense overall ecological and economical importance. It is estimated that warm-water coral reefs as an ecosystem provide US$375 x 10^9 each year (Costanza et al. 1997). 15% of all

humans live within 100 km of coral reefs and depend partly or completely on their well-being (Pomerance 1999). Reefs provide natural coastal protection, are attractive for tourism, are valuable for commercial fisheries, harbour potentially important natural products for mankind, and are ecosystems with the highest marine biodiversity (Burke et al. 1998, Carte 1996, Roberts et al. 2002). It is estimated that about 10% of the reef biodiversity, including viruses, bacteria and fungi, is known (Reaka-Kudla et al. 1997), and that only a small fraction of the biochemistry is tested for useful active compounds, of interest e.g. for medicine, science or cosmetics (Adey 2000).

Figure 2. The GRB is located along the northeast coast of Australia, stretching out for 2300 km in length. It is a Marine Park, a World Heritage Area, and home of nearly 3000 warm-water coral reefs (modified from Google maps).

Recent reports state that about 50-80% of the reefs have been harmed, and about 25% irreversibly damaged (Wilkinson 2002, 2004, 2008). The estimations for the future are that 60% of all coral reefs could be lost by the year 2030 (EC 2008), and 32% of stony coral species might be extinct (Carpenter et al. 2008). Coral reefs survived natural impacts like cyclones, sea level changes, bleaching (release of zooxanthellae) events and Crown-of-Thorns starfish mass appearances since the Triassic (200 x 10^6 years ago) (Veron 2000). Today coral reefs face additional anthropogenically caused impacts.

Global threats are ocean acidification and global warming. They possibly decrease calcification below sustainable rates by 2050 (Hoegh-Guldberg 2007, De'ath et al. 2009), and increase the intensity and frequency of mass coral bleaching (Hoegh-Guldberg 1999). Local threats include dynamite fishing, damage by anchors, ship groundings and diving tourism. Regional problems arise from overfishing, metals from mining, oil spills, and pollution with agrochemicals, sewage, warming by power plants, nutrients, and sediment (overview in Dubinsky & Stambler 1996, Wilkinson 2004). Reefs are more threatened by direct human pressures from poor coastal management resulting in river discharge of more sediment, nutrients and pollutants or overfishing, than by global climate change (Wilkinson 2004,

Kleypas & Eakin 2007). In fact, nowadays the effects of coastal development by urbanisation and agriculture on coral reefs are regarded as the most damaging impacts (Burke et al. 1998, Fabricius 2005).

Figure 3. On the left picture is an intact reef located in coastal waters of the far northern Great Barrier Reef. In the catchment on land the natural vegetation is predominant. On the right picture is an impacted reef close to an urbanised coastal area in North Queensland, Australia.

Typical examples for coral reefs threatened by human pressure are found at the northeast coast of Australia (Fig. 3). Since European settlement 200 year ago coastal development caused drastic change in the natural vegetation also along the GBR. In the "Northern" and "Central Section" of the GBR about 85% of the natural vegetation is removed due to intensive agriculture. The "Far Northern Section" is hardly inhabited and the natural vegetation mostly remained (Fig. 4) (Furnas 2003). Depending on the distance to shore the GBR is zoned in "nearshore", mid-shelf", and "offshore" reefs. Nearshore reefs include 900 reefs within 20 km off the coast. Four consecutive "Status of Coral Reefs of the World" reports conclude that nearshore reefs in the "Northern" and "Central Section" are under acute threat due to changes in the catchments (Wilkinson 1998, 2000, 2002, 2004) (Fig. 5) (Chapter 2-4).

Following intensive changes in land-use, increased sediment input (Maede 1972, McCulloch 2003) and an accumulation of terrestrial sediment in coral reefs has been observed at various places (Nemeth & Nowlis 1999, Brooks et al. 2007, Ryan et al. 2008). The imported sediment was finer, and had a higher content of organic matter than the autochthonous reef sediment, originating from skeletons of calcifying organisms (Ryan et al. 2008). In Micronesia and in Australia direct observations could be made when after road constructions fine soil was

imported to the reef by runoff, quickly smothering and killing reef organisms (Hopley et al. 1983, Fabricius et al. 2007) (Chapter 3-4).

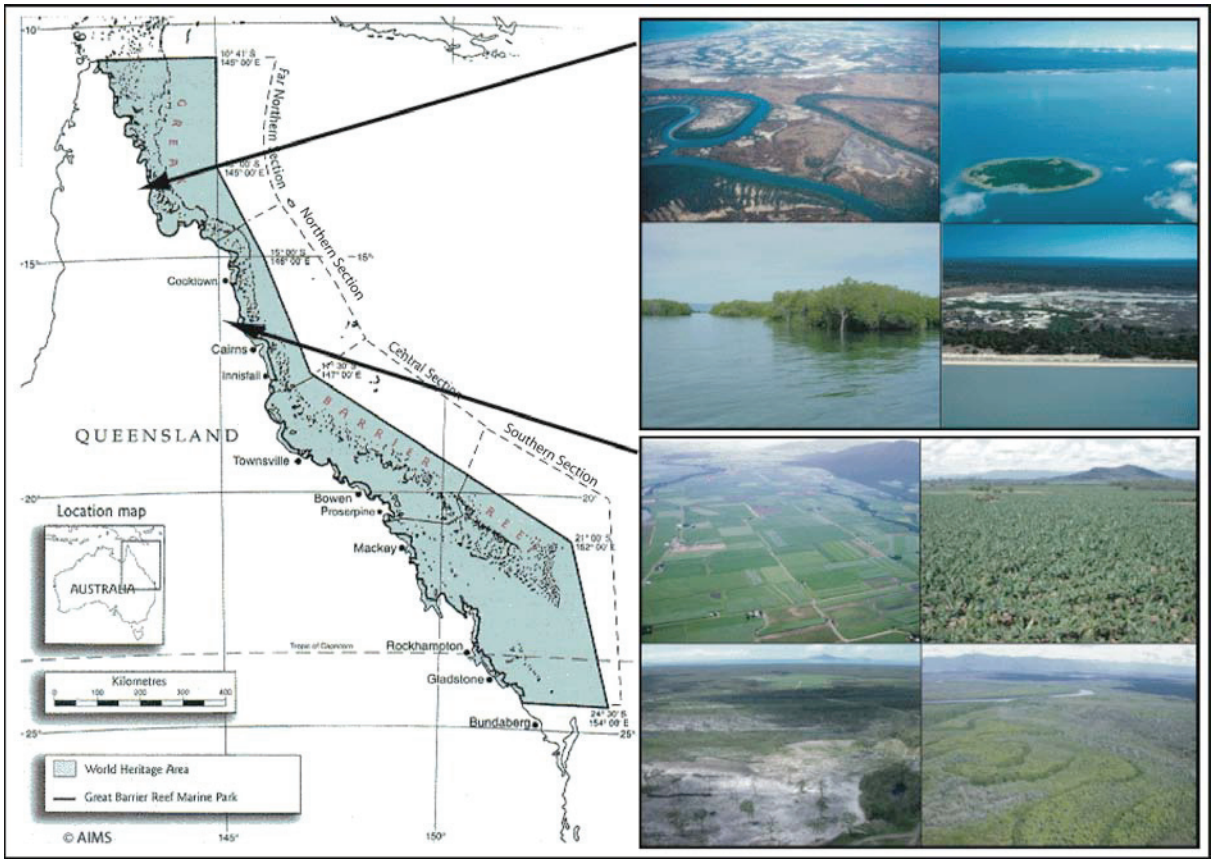

Figure 4. The Great Barrier Reef Marine Park is divided in four sections: "Far Northern", "Northern", "Central" and "Southern" GBR Section. The upper pictures show the catchment of the "Far Northern Section", where mainly natural vegetation remained. The lower pictures show the catchment of the developed "Northern Section", where about 15% of the natural vegetation remained (modified from Furnas 2003 and AIMS. Photos K. Fabricius).

2. Sediment on the continental shelf

The definition of sediment commonly follows a pure geoscientific approach. It describes unconsolidated rock fragments or minerals that were deposited by the action of wind, ice, and water, or by chemical and biological processes. In this thesis, the broadest possible definition is used and sediment is defined as "matter that settles to the bottom of a liquid" (Oxford English Dictionary). In nature sediment is far more than the suspended mineral particles that are eventually deposited. Besides mineral particles, sediment also contains pollutants and organic matter such as detritus, exopolymeric substances and living organisms. Chemicals adsorb to the minerals, altering their properties. Different salinities change solubility leading to the precipitation, adsorption or leaching of substances. Natural particles coagulate depending on their organic coating and ambient salinity (Gibbs 1983). Microorganisms settle on particles, coating them with biofilms. Some bacteria may use substances from the mineral

phase, e.g. iron, or significantly modify the chemical microenvironment by the release of exudates such as mucus. These "living particles" become trapped in mucous substances released by planktonic microalgae. Biological and physico-chemical processes cause the flocculation of particular matter to larger aggregates (Edzwald et al. 1974), known as marine snow (Alldredge & Silver 1988), a microcosm of its own (Chapter 2-4).

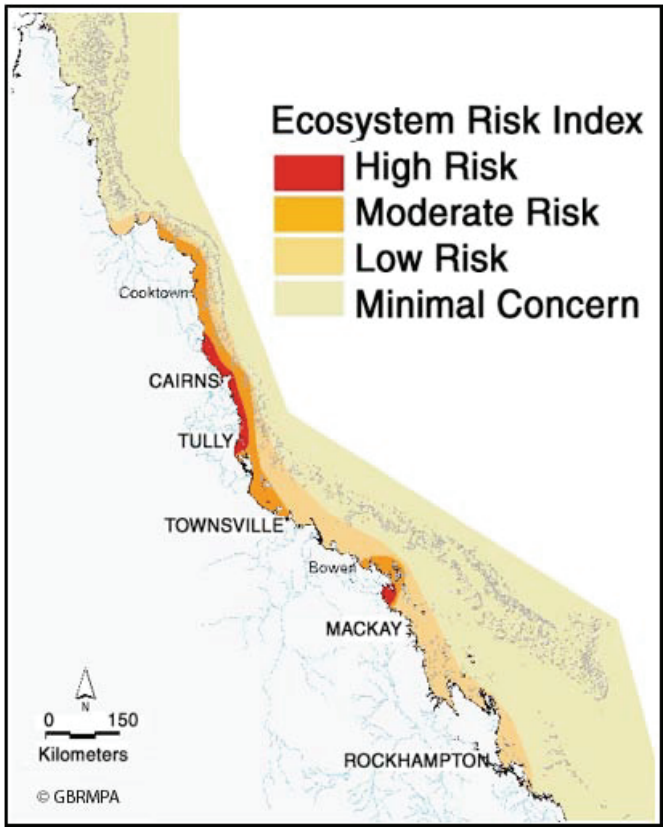

Figure 5. The coastal waters of northern Queensland in Australia are impacted by coastal development. A risk evaluation of the marine ecosystems by the "Ecosystem Risk Index" is shown in this map. Nearshore areas close to bigger towns and catchments of large rivers are ranked as at high risk. Under minimal concern are areas far away from the coast and along catchments with remaining natural vegetation (modified from Devlin et al. 2003 and GBRMPA).

This scenario results in a variety of sediment types, characterized by different properties such as e.g. mineral origin, organic matter content, total organic carbon, nitrogen, and phosphorous, the microbial community, sedimentation rate and volume, and grain size distribution. Sediment can be characterised by sorting the particles into different grain size fractions, e.g. with a series of sieves. The most commonly known sediment categories are gravel, sand, silt and clay. Sand includes grains between 63-2000 μm and silt includes all grains between 3.9-63 μm. Further divisions are made within the sand fraction: very coarse, coarse, medium and fine sand; and within the silt fraction: coarse, medium, fine and very fine silt (Wentworth 1922). Depending on their grain size, sediment particles carry adsorbed and particulate nutrients and contaminants. Silty sediment particles have higher adsorption capacities than sandy particles, transporting higher amounts of biocides, metals and nutrients

(Alkhatib & Castor 2000, Cantwell et al. 2002). Also a higher diversity of the microbial community is associated with smaller grain size (Sessitisch et al. 2001) (Chapter 2-4).

On land silt gets easily washed out during rainfalls, or in the water, resuspended during moderate turbulences, and then it can be transported over large distances (McCave 1972, Crocket & Nittouer 2004). New terrestrial fine sediments are imported into coastal ecosystems by river discharge, also called runoff. In many rivers 90% of the sediment discharge occurs in 10% of the time (Maede 1972). Thus runoff is an irregular phenomenon, occurring in events. Since European settlement in Australia sediment input increased up to 4-10 times, phosphorous input up to 3-15 and nitrogen input up to 2-4 times (overview in Neil et al. 2002, Furnas 2003). High nutrient and sediment concentrations in the rivers are reached after rainfall and thereafter in flood plumes reaching the reefs (Nemeth & Nowlis 1999, Mitchell et al. 2005) (Fig. 6). In cores drilled from corals it was shown that since 200 years increased amounts of sediment have reached the reefs (McCullow 2003), and that mostly nearshore reefs were affected (Lough 2002). However, sediment source studies and recent satellite pictures revealed that flood plumes sporadically reach offshore reefs and that this impact has been underestimated so far (Deslarzes & Lugo-Fernández 2007, Devlin & Brodie 2005). The residence time of dissolved nutrients in the water column exceeds the flooding event by up to ten months. Because of this, primary production followed by marine snow development is promoted for prolonged periods (Luick et al. 2007, Wolanski et al. 2007).

Figure 6. The pictures on the left show the mouth of the Herbert River nearby Ingham in North-Queensland, Australia. The river carries A) clear water before and B) murky water after heavy rainfalls. C) The picture on the right shows a major runoff event, bringing nutrients and sediments into the coastal area. Such flood plumes occur mainly during the wet season (November to April) (modified from Johnson & Murray 1997 and GBRMPA).

Where the turbulence intensities decrease the marine snow particles can more easily settle, thus this will especially happen in areas sheltered from currents and waves. During runoff events most aggregates settle in the estuary and the nearby nearshore reefs (Wolanski et al. 2003, Victor et al. 2006). Within a coral reef sedimentation is highest in areas sheltered from waves or in deeper reef parts and lowest in shallow wave-exposed areas (Wolanski et al. 2005). In coastal areas particulate matter is subject to wind-driven resuspension and deposition several times before it is deposited in deeper waters. South-easterly winds generate regular wave-induced shear stress and resuspension in the GBR lagoon (Larcombe et al. 1995, Orpin et al. 1999). Coastal ecosystems experience sedimentation stress far more often from wave-driven resuspension than from flood plumes (Furnas 2003). Short-term sedimentation at nearshore reefs in the GBR can then reach 120-210 mg cm^{-2} d^{-1} concentrated within a few hours (Hopley et al. 1983, Larcombe et al. 2001) (Fig. 7). Sedimentation rates measured in different coral reefs of the world were between 10 to 500 mg cm^{-2} d^{-1} (Bastidas et al. 1999, Cortes & Risk 1985, Victor et al. 2006). In stagnant water most marine suspended matter sinks with a velocity of 0.1-0.3 cm s^{-1} (Gibbs 1985, Wolanski et al. 1998), reaching 10 m water depth within 1-3 hours. Settling of marine snow is accelerated by a factor of 10 when silt grains become incorporated (Wolanski et al. 2003) (Chapter 2-5).

In marine snow aggregates active phytoplankton (Kovac et al. 2005) and aerobic heterotrophic bacterial communities are present (Ploug et al. 1997, Rath et al. 1998, Kiørboe 2003). In shelf areas the microbial community of marine snow does not degrade all organic carbon during the sedimentation event, and about 80% of the totally produced organic matter reaches the shelf seafloor (Jørgensen 1996). At the seafloor the degradation of organic matter in the settled sediment continues rapidly by aerobic and anaerobic processes releasing inorganic nutrients. Degradation of dead cells is a very complex process involving hydrolysis and fermentation of many different compounds by a large diversity of specialized bacteria. Under oxic conditions aerobic respiration is the main degradation process (Gibson 1984). Under anoxic conditions denitrification, manganese, iron, and sulfate reduction, and methanogenesis occur (Fröhlich et al. 1979, Fenchel & Finlay 1995) (Fig. 8). Different respiration reactions can co-occur, e.g. iron with sulfate reduction and methanogenesis. In tropical seas nitrate concentrations are so low that denitrification is possibly insignificant for mineralization (Capone et al. 1992, Miyajima et al. 2001). Manganese and iron reduction are depending on physical disturbance of sediments (e.g. by bioturbation) and control the oxidation processes in the suboxic zone (Canfield et al. 2005). In marine shelf sediments

>50% of the carbon mineralisation occurs by sulfate reduction (Jørgensen 1982). This leads to a high hydrogen sulfide production, H_2S being a highly toxic agent (National Research Council 1979). Its production is enhanced by anthropogenic pollution via river discharge (Sorokin 1978). However, sulfide rarely escapes the sediments in measurable quantities, because microbial and geochemical processes scavenge it efficiently in the suboxic zone (Jørgensen & Nelson 2004). Nevertheless the microbial degradation of organic matter in sediments and the development of toxic metabolites, as we suggest, might play a crucial role for reef organisms getting smothered with such kinds of sediment (Chapter 2-4).

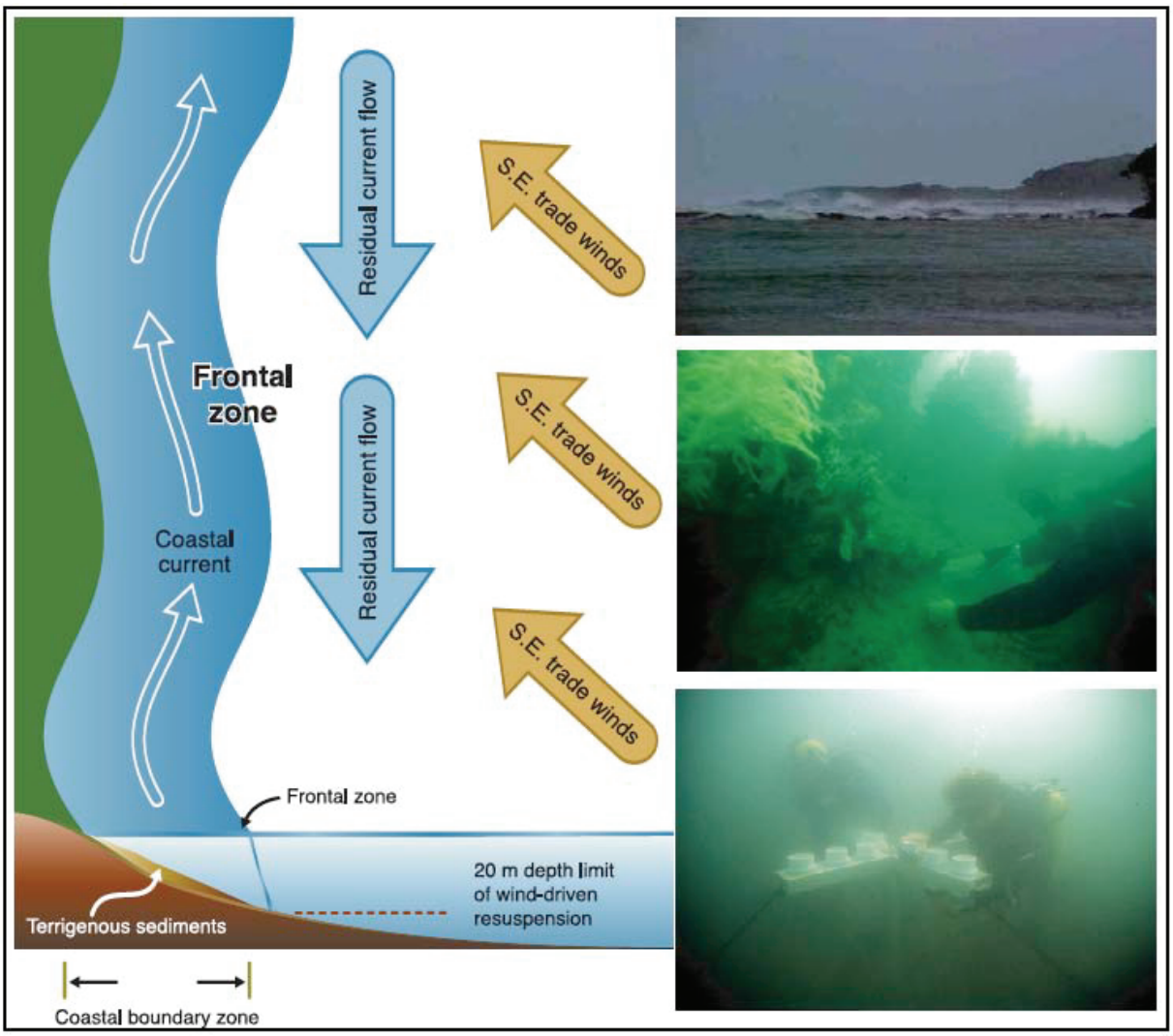

Figure 7. This illustration shows the relationships of the coastal water flow regime in the Great Barrier Reef, Australia. It includes the wind-wave stress, the wind-driven currents, and the 20 m depth zone of frequent resuspension. The pictures on the right side illustrate the turbid coastal waters at nearshore reefs after wave-induced resuspension (modified from Furnas 2003).

Increased nutrient and sediment loads are tightly linked and therefore have a high potential of harming the coastal ecosystems of the GBR World Heritage Area (Wilkinson 2004).

However, whether the harming potential is linked to the composition or simply to the amount of runoff or resuspended material is still under scientific and political debate. Frequent criticism on the scientific work was that laboratory studies would not mirror the "real world" and field data would to a large extend be missing (Williams 2001, Neil et al. 2002). Such debates lead to uncertainty for coastal management action and to the postponement of protective measures, while sediment, nutrient and contaminant discharge into the GBR lagoon is increasing (Brodie et al. 2001) (Chapter 2-7).

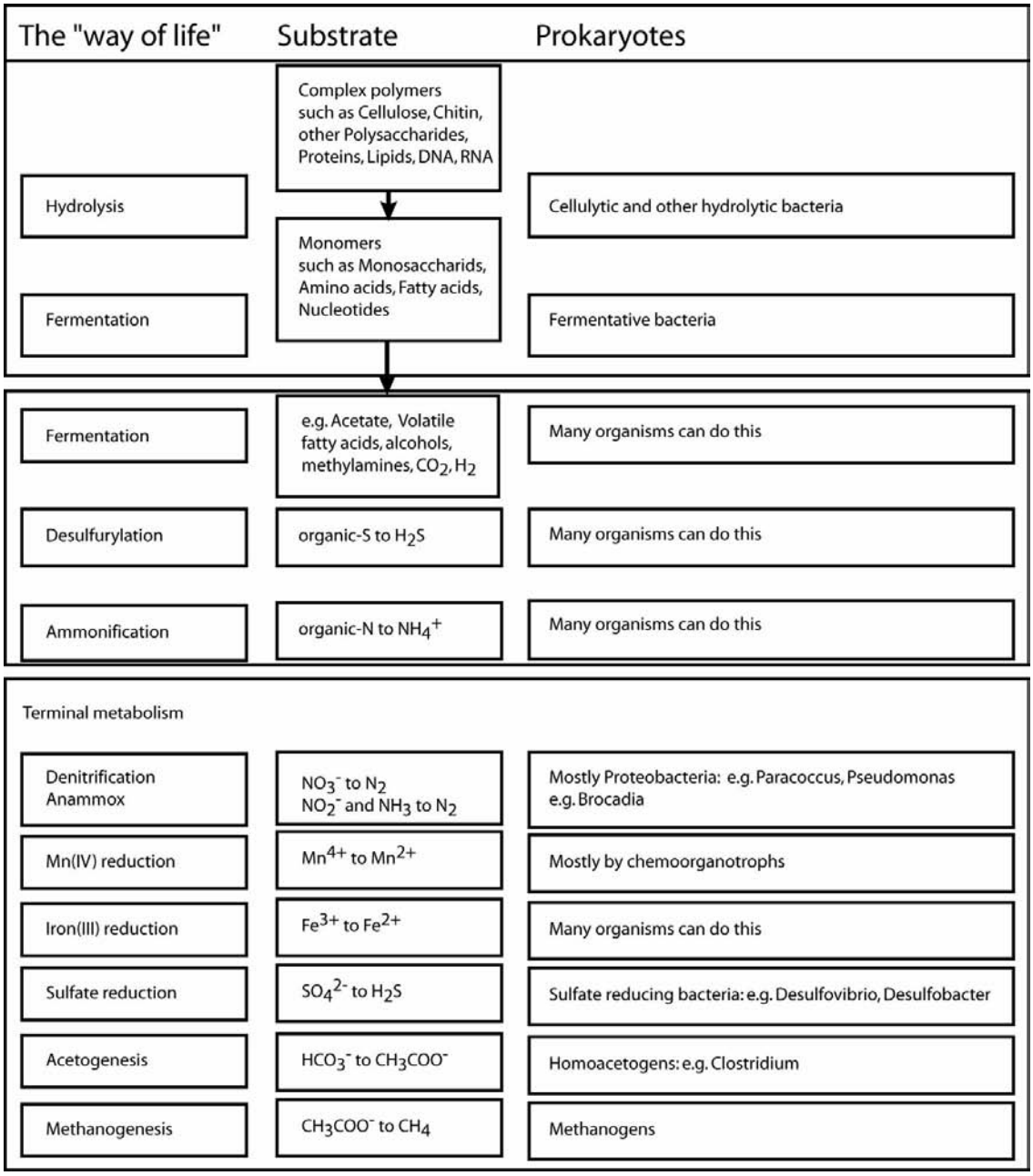

Figure 8. Metabolic pathways of organic matter degradation and their mostly used C-sources are listed. Examples of known prokaryotes performing the corresponding pathway are named. Note that rare, more specific and interconnections between pathways were omitted for clarity and can be found in e.g. Madigan & Martinko 2006 (modified from Capone & Kiene 1988, Jørgensen 2006, Madigan & Martinko 2006)

3. How sediment damages corals: a hypothesis

Numerous sessile organisms, such as macroalgae, sponges, and corals, cannot escape sediment exposure. They are impaired by sediment input in their habitat because of increased concentrations of suspended solids and nutrients altering the turbidity of the water column, and by settling sediment eventually smothering the organisms with a blanket of sediment (Rogers 1990, Fabricius 2005) (Fig. 9). Corals are affected in their metabolism, eventually resulting in the death of the colony, and in their reproduction and recruitment success. Reduced fertilisation rates were reported after exposure to increased suspended sediments of 50-100 mg l^{-1} (Gilmour 1999) and to increased nitrogen and phosphorous concentrations (Harrison & Ward 2001) (Chapter 2-4).

Figure 9. Reef-building corals smothered by terrigenous sediment in coastal waters of the Great Barrier Reef, Australia.

Sublethal stress responses are recognized by e.g. changes in gene expression and biomarker profiles. Suspended soil triggered a change in heat-shock proteins in *Pocillopora damicornis* (Hashimoto 2004), or reduced the lysosome membrane stability in corals (Rees et al. 1999). Significant relationships were documented between sedimentation rates and physiological parameters, such as respiration and growth (Cortes & Risk 1985, Nugues & Roberts 2003, Dutra et al. 2006). Increased turbidity reduced the photosynthesis rates of the zooxanthellae, leading to insufficient energy supply to the coral polyps (Yentsch et al. 2002). Some coral species acclimatised to reduce light conditions phototropically and/or heterotrophically within days (Anthony & Fabricius 2000, Titlyanov et al. 2001). Complete sediment coverage however, possibly suppresses photosynthesis by shading, and disables polyps to catch plankton (Fabricius et al. 2003). If the sediment remains for hours to few days the coral starts to bleach, and then eventually dies. Algal overgrowth or coral diseases can also cause tissue mortality (Smith et al. 2006, Peters 1997). However, a 15-month monitoring revealed that most important for tissue mortality was sediment smothering (Nugues & Roberts 2003) (Chapter 3-5).

Necrosis starts with the death of single polyps and smaller areas under the accumulated sediment layer, and ends in dying of the complete smothered tissue (Peters & Pilson 1985, Philip & Fabricius 2003). If single polyps were not covered with sediment they remained unaffected, even though the neighbouring polyps have died (Philipp & Fabricius 2003). Sediment coverage is therefore a local impact phenomenon, not necessarily affecting the whole colony (Fig. 10) (Chapter 3-5).

Corals have different mechanisms to free themselves from sediment. Enhanced mucus production, tissue swelling, and an increased movement of cilia and tentacles are used to reject sediment (Fig. 11). Certain species are able to free themselves efficiently and do not suffer subsequent damage. However the rejection efficiencies depend among others on the particle size of the sediment and the morphology of the coral (Stafford-Smith 1993, Wesseling et al. 1999). The chances for recovery after sediment removal depend on the amount of sediment deposited and the duration of coverage (Philipp & Fabricius 2003). (Chapter 3)

Figure 10. Local death of sediment-covered areas of the reef-building flat-foliose coral *Montipora sp*. The dead coral skeleton and bleached areas became visible after sediment removal (Photo: K. Fabricius).

The damage of reef-building corals by sediment exposure is well studied (Rogers 1990, Fabricius 2005). Previous studies focused mostly on the coral response, and so sediment characteristics were hardly described. We aimed to determine the causal link between the damaging process and sediment type; and to investigate the combined effects of certain sediment properties, such as e.g. grain size, organic matter or metals. This work put therefore the focus on the properties of the sediments, their compounds and on the biogeochemical processes within the sediment layer after accumulation on the coral. (Chapter 2-4)

We realised that previous experimental designs partly were not environmentally relevant, as either too much sediment was used, and/or sandy sediments, and/or sediments, which were free of organic matter (Peters & Pilson 1985, Vargas-Ángel et al. 2006, Sofonia & Anthony 2008). It was proposed that fine sand is less harmful to corals than coarse sand, as corals could reject it better (Pastorok & Bilyard 1985 and references therein). Our data from the reefs along the Great Barrier Reef in Australia contradicts this notion (unpublished). We found that mainly fine sand to coarse silt accumulates on corals, but so far mainly the effects of coarser sediments have been tested. Further we know that the sediment collected in sediment traps and those covering corals have higher organic matter contents then seafloor sediment. It is essential to characterize the used sediment in detail and measure besides the grain size fraction also other physical properties and the chemical composition.

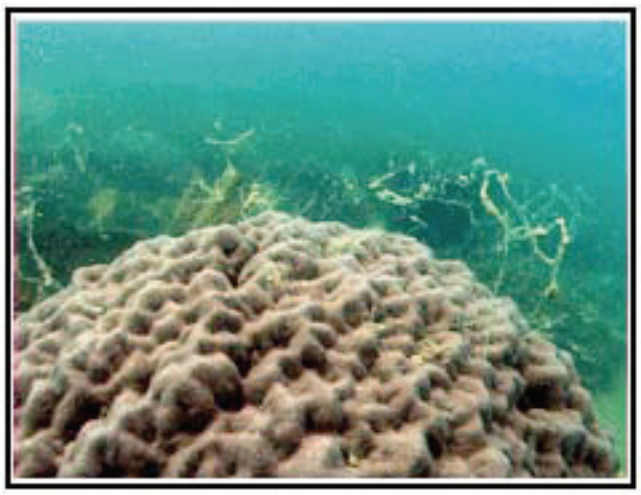

Figure 11. Mucus secretion is a method of sediment rejection of corals, as shown by this *Porites sp*. The mucus-sediment mixture is then resuspended by wave action.

Previous studies showed that corals quickly respond to copper, iron and lead by increased respiration, bleaching (Howard et al 1986, Harland & Brown 1989), and reduced fertilisation success (Reichlett-Brushett & Harrison 2000). Thus metals and trace elements in the sediments were measured in this study, because they could harm the corals during sediment coverage. Only a few studies were done on combination effects of exposure of sediment with increased organic matter content on coral reefs. In a pilot study Fabricius and Wolanski (2000) exposed an *Acropora sp.* coral that harboured barnacles (Cirripedia / Fam. Pyrgomatidae) to estuarine silt enriched with marine snow, and sheer silt particles. Both organisms were able to free themselves from settling silt without enrichment, but died within one hour from settling enriched silt. A further study showed that marine snow, in combination with silty sediment, significantly reduced the survival of four-week old coral juveniles (Fabricius et al. 2003) (Chapter 2-3).

We aimed to study, which processes during sediment coverage on corals contribute to their death within hours to few days. Sediment coverage could lead to energy deficits by restricting the movement of the polyps and so blocking heterotrophy, and/or due to reduced or suppressed photosynthesis, and/or due to the diffusional barrier of the sediment hindering oxygen supply from the overlaying water and so hampering corals respiration, so that finally the coral suffocates (Bak & Elgerhuizen 1976, Stafford-Smith & Ormond 1992, Philipp & Fabricius 2003). Oxygen depletion in sediments also occurs by metazoan and microbial aerobic respiration (Canfield 2005), so that the coral would suffocate due to respiration of the microbial community within the covering sediment layer using up any oxygen diffusing through the sediment. Various invertebrates related to corals have high tolerance to anoxic conditions (von Brand 1946, Hochachka & Mustafa 1972), and also corals could survive 0.5 to >6 days of anoxia (Yonge et al. 1932, Sassaman & Mangum 1973). Sea anemones, close relatives of scleractinian corals, survive anoxia even up to weeks (Sassaman & Mangum 1973, Mangum 1980). Thus corals and sea anemones can adapt to anoxia and survive on anaerobic metabolism (fermentation). Indeed under anoxia sea anemones produced typical end-products for anaerobic metabolic activity, such as succinate, fumarate, and lactate (Ellington 1977, 1980). Thus we found the hypothesis of coral death by suffocation not very plausible. However, we think that microbial activity is connected to the death of sediment covered coral tissue, but in possibly two different ways. The degradation of organic matter in the sediment increases toxic metabolites or the sediment acts as a vector for pathogens, potentially killing the coral when covered with sediment. Indeed, it is has been reported that pathogens can be transported with mineral particles or marine snow (Rosenberg & Loya 2004, Lyons et al 2005). For coral diseases five bacteria and one fungus are known as infectious agents, but many more invertebrate disease and pathogens are known. The cultivation of microbes is often not practicable and the fulfilment of Koch's postulates almost impossible (Richardson 1998). Therefore mostly modern diagnostics based on molecular tools are used to identify new pathogens (Webster 2007, Sussman et al. 2008 and references therein). A quorum is needed to successfully infect the host, implying that a high abundance of the pathogens should be present. We aim to follow the microbial community changes during the sediment exposure experiment with molecular tools such as cloning and fingerprinting techniques (Chapter 4).

We hypothesized that the exposure to a toxic substance, produced by microbes in organic-rich sediments, kills the corals. We aimed to test the hypothesis that corals die from coverage under sediments by the exposure to H_2S, generated by sulfate reducing bacteria in the

sediments. This hypothesis is similar to the one proposed for the spreading of the black band diseases over coral colonies (Carlton & Richier 1995) (Chapter 4, 5 and 8).

H_2S freely crosses membranes at a penetration rate directly proportional to its concentration in the surrounding water (Jacques 1936). H_2S inhibits the oxygenic photosynthesis, the cytochrome c oxidase, the key enzyme of the mitochondrial respiratory chain, and 20 other enzymes, among others ATPase, catalase, and monoamine oxidase. This results in complex effects on multiple metabolic parameters such as photosynthesis, respiration, cell division, assimilation and fermentative ability (Bagarinao 1992 and references therein). Organisms typical for silty bottoms are more tolerant to H_2S than those of hard or sand bottoms, and species more tolerant to hypoxia are also more tolerant to H_2S (Bagarinao, 1992). Because corals are found in oxygenated waters growing on hard substratum, it is likely that corals are rather sensitive to H_2S. The inhibition of both photosystem II and the cytochrome c oxidase, would lead to a general disruption of the energy metabolism of corals, and other essential enzyme activities would be blocked, which together could lead to coral death within hours (Chapter 4 and 8).

4. Methods and technological developments

A multi-method approach was chosen for this thesis to reveal the causal link of declined coral health to sediment properties, and the mechanism killing sediment-covered corals. The chemical microenvironment at a sediment-covered coral surface depends on biogeochemistry and transport characteristics of the sediment. Hence its physical properties and chemical composition were determined. Our main hypothesis was that bacteria are important for the damage that sediment causes to reef-building warm-water corals possibly by their activity or through pathogenesis. Hence the investigation of the microbial activity and composition was central in this thesis. In sediments covering corals we followed the microbial community composition change with molecular fingerprinting technique and sequencing, which was also used for screening of pathogens. We monitored oxygen consumption, hydrogen sulfide development and changes in pH using microsensors. Sulfate reduction rates were measured with the radiotracer technique (Chapter 2-4).

The consequences of covering the coral surface with a 2 to 5 mm layer of sediment needed to be studied on the microenvironment level. Microsensors were the ideal tool for this (Fig. 12). They have a sensing tip diameter of 1-20 µm and are therefore minimally invasive, not disturbing the chemical environment or the structures in which they are measuring. Microsensors have been used successfully in coral polyps and on coral surfaces to measure

photosynthesis and respiration (Kühl et al. 1995, de Beer et al. 2000) as well as to measure penetrating light within sediment layers (Kühl et al. 1994). Microsensor measurements allow the characterization of microenvironments in and under the sediments with high spatial resolution, and the determination of fluxes (e.g. O_2 and H_2S) from concentration profiles above the coral surface, using Fick's law of diffusion. This information allows to assess underlying mechanisms of processes by following the dynamics of microenvironmental parameters after a perturbation with high temporal resolution (Chapter 4-8).

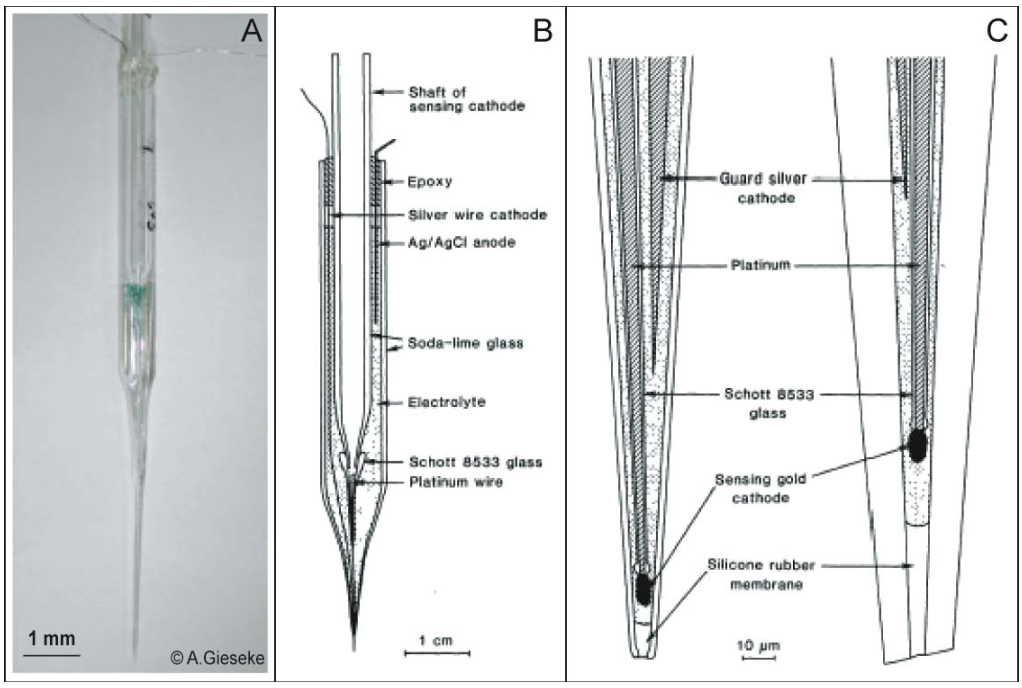

Figure 12. A) Shows an amperometric Clark-type oxygen microsensor, B) shows the scheme of the microsensor, C) shows the sensing tip of the microsensor (modified from Revsbech 1989).

To compare the data from our laboratory experiment with actual conditions in the field, microsensor measurements have been done with an instrumentation that had to be specially developed for the use *in situ* within this study. Microsensor measurements by divers have been done previously in the field (Ziebis et al. 1996, Vopel et al. 2005). We have developed and used an improved diver-operated microsensor system, that allows interactive control of the profiling with amperometric and potentiometric microsensors (Revsbech & Jørgensen 1986), and measurements of the light penetration depth with a spherical light microsensor (Lassen et al. 1992). The high-speed measuring amplifiers allow to measure rapid dynamics (<0.5 s) as needed e.g. for photosynthesis studies. For that we extended the light-dark-shift method (Revsbech & Jørgensen 1983) to a measuring procedure called light-shade shift method. It allows the quantification of gross photosynthesis at the ambient light intensity

from 4-5 light transition measurements by shading the sample, without the necessity of achieving complete darkness (Chapter 4-7).

The potential photochemical efficiency of the reaction centre photosystem II (PSII) of the zooxanthellae has been successfully used as a measure of the overall health status of the coral (Beer at al. 1998, Ralph et al. 1999). The quantum yield of the photosynthetic energy conversion can be derived with the saturation pulse method using the pulse-amplitude modulated (PAM) fluorometry, a non-intrusive optical method (Schreiber et al. 1986). Other parameters for the determination of the coral fitness have been used and some have been also considered for this work. These are RNA/DNA ratio (Buckley & Szmant 2004), protein content, tissue thickness (Cooper & Fabricius 2007), and gross photosynthesis performance measured with microsensors (Kühl et al. 1995). However they turned out to be not so efficient and diagnostically conclusive so that we focused on the PAM instrument and so-called colour chart measurements. Standardised colour charts and image analysis have been used to quantify bleaching and necrosis (Siebeck et al. 2006) (Chapter 3, 4 and 6).

High priority of this study was to conduct experiments as environmentally relevant as possible and to confirm mesocosm data in the field. For the mesocosm studies we chose to work with natural sediments. Different sediment types have been collected from different catchment areas and reefs. For the enrichment experiments plankton mixture has been used as natural organic matter. We designed the mesocosm experiments based on the settings in the reef. Water flow and light conditions were adjusted. And a large sampling campaign where sediments have been collected from sediment traps, from on top of corals and from the seafloor along the GBR gave us insight in the sediments' grain size and the amount of organic matter, which effectively settles on corals (unpublished and not shown in this thesis). In our experiments these parameters were adjusted according to our findings from the field (Chapter 2-7).

5. Objectives of the thesis

This work is divided in two parts. Part one included experiments in controlled mesocosms, and field measurements to confirm mesocosm data. The second part was the development of technical equipment and the extension of existing methods, including their application under different circumstances. Both parts are integrally linked: the mesocosm work was important to reveal the complexity of how sediment damages corals, the field work was necessary for confirming laboratory observations, and the technical development was essential for the *in situ* work.

In summary the main objectives of this thesis are:
The investigation of

- effects of sediment types, differing in geochemical-, physical-, and organic-nutrient-related parameters, on the fertilisation and the early development of scleractinian corals,
- effects of coverage by sediment types, differing in geochemical-, physical-, and organic-nutrient-related characteristics on adult scleractinian corals,
- the lethal process on adult corals during coverage of sediment, which is possibly microbially mediated, via the generation of toxic hydrogen sulfide from sulfate reduction, and
- the development of a new diver-operable microsensor system (DOMS) for the investigation of the microenvironment in sediments accumulated on corals in the coral reef.

6. Overview of chapters 2-8

Chapter 2: Effects of different types of sediment, dissolved inorganic nutrients and salinity on fertilisation and embryo development in the coral *Acropora millepora* (Ehrenberg, 1834)

C. Humphrey, M. Weber, C. Lott, T. Cooper, and K.E. Fabricius

K. Fabricius initiated the study of sediment, inorganic nutrient and salinity. M. Weber initiated the study of different sediment types. C. Humphrey, M. Weber, C. Lott, T. Cooper, and K.E. Fabricius carried out the experiment. C. Humphrey did the fertilization and development success analysis, and M. Weber did the sediment sample analysis. K. Fabricius did the statistics. C. Humphrey wrote the manuscript with help of all authors. This article is published in Coral Reefs (2008) 27:837-850.

Chapter 3: Sedimentation stress in a scleractinian coral exposed to terrestrial and marine sediments with contrasting physical, organic and geochemical properties

M. Weber, C. Lott, and K.E. Fabricius

K. Fabricius initiated this study. All authors designed the experiments. M. Weber and C. Lott carried out the experiments. M. Weber did the data analysis and K. Fabricius the multivariate statistics. M. Weber wrote the manuscript with help of all authors. This article is published in JEMBE (2006) 336:18-32.

Chapter 4: A cascade of microbial processes kills sediment-covered corals

M. Weber, C. Lott, K. Kohls, L. Polerecky, R.M.M. Abed, T. Ferdelman, K.E. Fabricius, and

D. de Beer

M. Weber, D. de Beer and K. Fabricius initiated this study. M. Weber, C. Lott, K. Fabricius and D. de Beer designed the experiments. M. Weber and C. Lott did the field measurements. M. Weber carried out the laboratory experiments and did the data analysis. R. Abed and K. Kohls helped with the molecular work. T. Ferdelman helped with the radiotracer work. L. Polerecky did the modelling analysis. M. Weber wrote the manuscript with help of all authors. This article will be submitted to a peer-reviewed international journal. These data were presented at ASLO 2009 during an invited talk, which got then selected for an outstanding student presentation award.

Chapter 5: *In situ* applications of a new diver-operated motorized microsensor profiler

M. Weber, P. Färber, V. Meyer, C. Lott, G. Eickert, K.E. Fabricius, and D. de Beer

M. Weber and D. de Beer initiated this study. M. Weber and C. Lott designed the concept of the system. P. Färber developed the logger instrument. V. Meyer developed the measuring devices. G. Eickert extended the pH microsensor. M. Weber and C. Lott did the scuba diving work in Italy, and in Australia with additional help of K. Fabricius. M. Weber wrote the manuscript with help of all authors. This article is published in ES&T 41 (2007) 41:6210-6215.

Chapter 6: *In situ* measurement of gross photosynthesis using a microsensor-based light-shade shift method

L. Polerecky, C. Lott, and M. Weber

M. Weber and L. Polerecky initiated the study. All authors did the land-based measurements. M. Weber and C. Lott did the diving operated measurements. L. Polerecky did the calculations and wrote the manuscript with help of all authors. This article is published in Limnol. Oceanogr. Methods (2008) 6:373-383.

Chapter 7: Ventilation behaviour and oxygen dynamics in *Dysidea avara* and *Chondrosia reniformis* (Porifera: Demospongiae) *in situ* and *ex situ*

M-L. Schläppy, M. Weber, D. Mendola, F. Hoffmann, and D. de Beer.

F. Hoffmann, M-L. Schläppy and D. de Beer initiated the study. M-L. Schläppy and D. Mendola did the laboratory measurements. M. Weber did the field measurements. M-L. Schläppy did the data analysis and wrote the manuscript with help of all authors. This article is a chapter in the electronically published PhD thesis of M-L. Schläppy (2008) p75-101, and has been submitted to Limnol. Oceanogr. in January 2009.

Chapter 8: The H_2S microsensor and the dissociation constant pK_1: problems and solutions

M. Weber*, A. Lichtschlag*, S. Jansen, and D. de Beer
M. Weber and D. de Beer initiated this study. A. Lichtschlag, M. Weber and S. Jansen did the laboratory work. M. Weber and A. Lichtschlag wrote the manuscript with help of all authors. This extended protocol will be electronically published within this PhD thesis and maybe submitted as a note to an international journal. *These authors contributed equally to this work.

7. References

Access Economics (2007) Measuring economics and financial value of the GBR. Access Economics PYT Ltd. For GBRMPA 2005-2006. Online at http://www.gbrmpa.gov.au/corp_site/info_services/publications/research_publications/rp088/access_economics_report_0607 (accessed 23.02.2009)

Adey WH (2000) Coral Reef Ecosystems and Human Health: Biodiversity Counts! Ecosystem Health 6:227-236

Al-Horani FA, Al-Moghrabi SM, de Beer D (2003) The mechanism of calcification and its relation to photosynthesis and respiration in the scleractinian coral *Galaxea fascicularis*. Mar. Biol. 142:419-426

Alkhatib E, Castor K (2000) Parameters influencing sediments resuspension and the link to sorption of inorganic compounds. Environ. Monit. Assess. 65:531-546

Alldredge A, Silver MW (1988) Characterstics, dynamics and significance of marine snow. Prog. Oceanogr. 20:41-82

Anthony KRN, Fabricius KE (2000) Shifting roles of heterotrophy and autotrophy in coral energetics under varying turbidity. JEMBE 252:221-253

Bagarinao T (1992) Sulfide as an environmental factor and toxicant: tolerance and adaptations in aquatic organisms. Aquat. Toxicol. 24:21-62

Bak RM, Elgershuizen JHBW (1976) Patterns of Oil-Sediment Rejection in Corals. Mar. Biol. 37:105-113

Bastidas C, Bone D, Garcia EM (1999) Sedimentation rates and metal content of sediments in a Venezuelan coral reef. Mar. Poll. Bull. 38:16-24

Beer S, Ilan M, Eshel A, Weil A, Brickner I (1998) Use of pulse amplitude modulated (PAM) fluorometry for *in situ* measurements of photosynthesis in two Red Sea *faviid* corals. Mar. Biol. 131:607-612

Brodie JE, Christie C, Devlin M, Haynes D, Morris S, Ramsay M, Waterhouse J, Yorkston H (2001) Catchment management and the Great Barrier Reef. Water Sci. Technol. 43:203-211

Brooks G, Devine B, Larson RA, Rood BP (2007) Sedimentary development of Coral Bay, St. John, USVI: A shift from natural to anthropogenic influences. Carib. J. Sci. 43:226-243

Buckley B, Szmant A (2004) RNA/DNA ratios as indicators of metabolic activity in four species of Caribbean reef-building corals. MEPS 282:143-149

Burke L, Bryant D, McManus J, Spalding M (1998) Reefs at Risk: A map-based indicator of potential threats to the world's coral reefs, pp 56

Canfield DE, Kristensen E, Thamdrup B (2005) Aquatic Geomicrobiology. Elsevier Academic Press, San Diego, pp 640

Cantwell MG, Burgess RM, Kester DR (2002) Release and phase partitioning of metals from anoxic estuarine sediments during periods of simulated resuspension. ES&T 36:5328-5334

Capone DG, Kiene RP (1988) Comparison of microbial dynamics in marine and freshwater sediments: Contrast in anaerobic carbon catabolism. Limnol.Oceanogr. 33:725-749

Capone GC, Dunham SE, Horrigan SG, Duguay LE (1992) Microbial nitrogen transformations in unconsolidated coral reef sediments. MEPS 80:75-88

Carlton RG, Richardson LL (1995) Oxygen and sulfide dynamics in a horizontally migrating cyanobacterial mat: Black band disease of corals. FEMS Microbiol. Ecol. 18:155-162

Carpenter KE, Abrar M, Aeby G, Aronson RB, Banks S, Bruckner A, Chiriboga A, Cortes J, Delbeek JC, DeVantier L, Edgar GJ, Edwards AJ, Fenner D, Guzman HM, Hoeksema BW, Hodgson G, Johan O, Licuanan WY, Livingstone SR, Lovell ER, Moore JA, Obura DO, Ochavillo D, Polidoro BA, Precht WF, Quibilan MC, Reboton C, Richards ZT, Rogers AD, Sanciangco J, Sheppard A, Sheppard C, Smith J, Stuart S, Turak E, Veron JEN, Wallace C, Weil E, Wood E (2008) One-Third of Reef-Building Corals Face Elevated Extinction Risk from Climate Change and Local Impacts. Science 321:560-563

Carte BK (1996) Biomedical potential of marine natural products: Marine organisms are yielding novel molecules for use in basic research and medical applications. Bioscience 46:271-286

Cooper T, Fabricius KE (2007) Coral-based indicators of changes in water quality on nearshore coral reefs of the Great Barrier Reef. Report to Marine and Tropical Science Research Facility, Reef and Rainforest Research Centre Limited, Cairns. http://www.rrrc.org.au/mtsrf/theme_3/project_3_7_1.html (accessed 23.02.2009)

Cortes JN, Risk MJ (1985) A reef under siltation stress: Cahuita, Costa Rica. Bull. Mar. Sci. 36:339-356

Costanza R, d'Arge R, de Groot R, Farber S, Grasso M, Hannon B, Limburg K, Naeem S, O'Neill RV, Paruelo J, Raskin RG, Sutton P, van den Belt M (1997) The value of the world's ecosystem services and natural capital. Nature 387:253-260

Crockett JS, Nittrouer CA (2004) The sandy inner shelf as a repository for muddy sediment: an example from Northern California. Cont. Shelf Res. 24:55-73

de Beer D, Kühl M, Stambler N, Vaki L (2000) A microsensor study of light enhanced Ca^{2+} uptake and photosynthesis in the reef-building hermatypic coral *Favia* sp. MEPS 194:75-85

De'ath G, Lough JM, Fabricius KE (2009) Declining Coral Calcification on the Great Barrier Reef. Science 323:116-119

Deslarzes K, Lugo-Fernández A (2007) Influence of terrigenous runoff on offshore coral reefs: An example from the flower garden banks, Gulf of Mexico. In: Aronson RB (ed) Geological Approaches to Coral Reef Ecology, pp 126-160

DeVantier L, De'ath G, Turak E, Done T, Fabricius KE (2006) Species richness and community structure of reef-building corals on the nearshore Great Barrier Reef. Coral Reefs 25:329-340

Devlin M, Brodie J, Waterhouse A, Mitchell D, Audas A, Hanes D (2003) Exposure of Great Barrier Reef inner-shelf reefs to riverbourne contaminants. In Proceedings of the 2nd National Conference on Aquatic Environments: sustaining our aquatic environments, implementing solutions. Queensland Department of Natural Resources and Mines, Brisbane, Australia

Devlin MJ, Brodie J (2005) Terrestrial discharge into the Great Barrier Reef Lagoon: nutrient behavior in coastal waters. Mar. Poll. Bull. 51:9-22

Dubinsky Z, Stambler N (1996) Marine pollution and coral reefs. Global Change Biology 2:511-526

Dutra LXC, Kikuchi RKP, Leao, ZMAN (2006) Effects of sediment accumulation on reef corals from Abrolhos, Bahia, Brazil. J. Coast. Res. 2:633-638

EC (2008) The economics of ecosystems & biodiversity. European Communities. Online at http://ec.europa.eu/environment/nature/biodiversity/economics/index_en.htm (accessed 23.02.2009)

Edzwald JK, Upchurch JB, O'Melia CR (1974) Coagulation in estuaries. ES&T 8:58-63

Ellington WR (1977) Aerobic and anaerobic degradation of glucose by the estuarine sea anemone, *Diadumene leucolena*. Comp. Biochem. Physiol. 58B:173-175

Ellington WR (1980) Some aspects of the metabolism of the sea anemone *Haliplanella luciae* (Verrill) during air exposure and hypoxia. Mar. Biol. Lett. 1:255-262

Fabricius KE (2005) Effects of terrestrial runoff on the ecology of corals and coral reefs: review and synthesis. Mar. Poll. Bull. 50:125-146

Fabricius KE, Golbuu Y, Victor S (2007) Selective mortality in coastal reef organisms from an acute sedimentation event. Coral Reefs 26:69-69

Fabricius KE, Wild C, Wolanski E, Abele D (2003) Effects of transparent exopolymer particles and muddy terrigenous sediments on the survival of hard coral recruits. Estuar. Coast. Shelf Sci. 57:613-621

Fabricius KE, Wolanski E (2000) Rapid smothering of coral reef organisms by muddy marine snow. Estuar. Coast. Shelf Sci. 50:115-120

Fenchel T, Finley BJF (1995) Ecology and Evolution in Anoxic worlds. Oxford University Press, Oxford

Froelich PN, Klinkhammer GP, Bender ML, Luedtke NA, Heath GR, Cullen D, Dauphin P, Hammond D, Hartman B, Maynard V (1979) Early oxidation of organic matter in pelagic sediments of the eastern equatorial Atlantic: suboxic diagenesis. Geochim. Cosmochim. Acta 43:1075-1090

Furnas M (2003) Catchments and corals: terrestrial runoff to the Great Barrier Reef. Australian Institute of Marine Science & CRC Reef Research Centre and Rainforest CRC

Gibbs RJ (1983) Effect of natural organic coatings on the coagulation of particles. ES&T 17:237-240

Gibson DT (1984) Microbial degradation of organic compounds. Marcel Dekker Ltd

Gilmour J (1999) Experimental investigation into the effects of suspended sediment on fertilisation, larval survival and settlement in a scleractinian coral. Mar. Biol. 135:451-462

Harland AD, Brown BE (1989) Metal tolerance in the scleractinian coral *Porites lutea*. Mar. Poll. Bull. 20:353-357

Harrison P, S W (2001) Elevated levels of nitrogen and phosphorus reduce fertilisation success of gametes from scleractinian reef corals. Mar. Biol. 139:1057–1068

Harrison PL, Babcock RC, Bull GD, Oliver JK, Wallace CC, Willis BL (1984) Mass Spawning in Tropical Reef Corals. Science 223:1186-1189

Hashimoto K, Shibuno T, Murayama-Kayano E, Tanaka H, Kayano T (2004) Isolation and characterization of stress-responsive genes from the scleractinian coral *Pocillopora damicornis*. Coral Reefs 23:485-491

Hochachka PW, Mustafa T (1972) Invertebrate Facultative Anaerobiosis: A reinterpretation of invertebrate enzyme pathways suggests new approaches to helminth chemotherapy. Science 178:1056-1060

Hoegh-Guldberg O (1999) Climate change, coral bleaching and the future of the world´s coral reefs. Mar. Freshw. Res. 50:839-866

Hoegh-Guldberg O, Mumby PJ, Hooten AJ, Steneck RS, Greenfield P, Gomez E, Harvell CD, Sale PF, Edwards AJ, Caldeira K, Knowlton N, Eakin CM, Iglesias-Prieto R, Muthiga N, Bradbury RH, Dubi A, Hatziolos ME (2007) Coral reefs under rapid climate change and ocean acidification. Science 318:1737-1742

Hopley D, van Woesik R, Hoyal DCJD, Rasmussen CE, Steven ADL (1983) Sedimentation resulting from road development, Cape Tribulation area. GBRMPA TM-24

Howard L, Crosby D, Alino P (1986) Evaluation of some methods for quantitatively assessing the toxicity of heavy metals to corals. In: Jokiel P, Richmond R, Rogers R (eds) Coral reef population biology. Sea grant coop. rep. Hawaii Univ., pp 452-464

Jacques AG (1936) The kinetics of penetration: XII. Hydrogen sulfide. J. Gen. Physiol. 19:397-418

Johnson AKL, Murray AE (1997) Herbert River Catchment Atlas. CSIRO Tropical Agriculture, Townsville, pp 48

Jørgensen BB (1982) Mineralization of organic matter in the seabed - the role of sulphate reduction. Nature 296:643-645

Jørgensen BB (1996) Case Study - Aarhus Bay. In: Jørgensen BB, Richardson K (eds) Eutrophication in Coastal Marine Ecosystems, vol 52. Amer. Geophys. Union, pp 137-154

Jørgensen BB (2006) Bacteria and marine biogeochemistry. In: Schulz HD, Zabel M (eds) Marine Geochemistry. Springer Verlag, Berlin, pp 173-208

Jørgensen BB, Nelson DC (2004) Sulfide oxidation in marine sediments: geochemistry meets microbiology. In: Amend JP, Edwards KJ, Lyons TW (eds) Sulfur Biogeochemistry - Past and Present, vol 379. Geological Society of America, Boulder, pp 63-81

Kiørboe T (2003) Marine snow microbial communities: scaling of abundances with aggregate size. Aqu. Microb. Ecol. 33:67-75

Kleypas J, Eakin CM (2007) Scientists' perception of threats to coral reefs: Results of a survey of coral reef researchers. Bull. Mar. Sci. 80:419-436

Kovac N, Mozetic P, Trichet J, Defarge C (2005) Phytoplankton composition and organic matter organization of mucous aggregates by means of light and cryo-scanning electron microscopy. Mar. Biol. 147:261-271

Kühl M, Cohen Y, Dalsgaard T, Jørgensen BB, Revsbech NP (1995) Microenvironment and photosynthesis of zooxanthellae in scleractinian corals studied with microsensors for O_2, pH and light. MEPS 117:159-172

Kühl M, Lassen C, Jorgensen BB (1994) Light penetration and light-intensity in sandy marine-sediments measured with irradiance and scalar irradiance fiberoptic microprobes. MEPS 105:139-148

Larcombe P, Costen A, Woolfe KJ (2001) The hydrodynamic and sedimentary setting of nearshore coral reefs, central Great Barrier Reef shelf, Australia: Paluma Shoals, a case study. Sedimentol. 48:811-835

Larcombe P, Ridd PV, Prytz A, Wilson B (1995) Factors controlling suspended sediment on inner-shelf coral reefs, Townsville, Australia. Coral Reefs 14:163-171

Lassen C, Ploug H, Jørgensen BB (1992) A fiberoptic scalar irradiance microsensor - application for spectral light measurements in sediments. FEMS Microbiol. Ecol. 86:247-254

Lough J, Barnes D, McAllister F (2002) Luminescent lines in corals from the Great Barrier Reef provide spatial and temporal records of reefs affected by land runoff. Coral Reefs 21:333-343

Luick J, Mason L, Hardey T, Furnas MJ (2007) Circulation in the Great Barrier Reef Lagoon using numerical tracers and in situ data. Cont. Shelf Res. 27:757–778

Lyons MM, Ward JE, Smolowitz R, Uhlinger KR, Gast RJ (2005) Lethal marine snow: Pathogen of bivalve mollusc concealed in marine aggregates. Limnol. Oceanogr. 50:1983-1988

Madigan MT, Martinko JM (2006) Biology of microorganisms. Brock 11th edn. Prentice-Hall, Upper Saddle River NJ, USA

Maede R (1972) Sources, sinks, and storage of river sediment in the Atlantic drainage of the United States. J. Geol. 90:235-252

Magnum DC (1980) Sea anemone neuromuscular responses in anaerobic conditions. Science 208:1177-1178

McCave IN (1972) Transport and escape of fine-grained sediment from shelf areas. Hutchinson & Ross, Dowden

McCulloch M, Fallon S, Wyndham T, Hendy E, Lough J, Barnes D (2003) Coral record of increased sediment flux to the inner Great Barrier Reef since European settlement. Nature 421:727-730

Mitchell C, Brodie J, White I (2005) Sediments, nutrients and pesticide residues in event flow conditions in streams of the Mackay Whitsunday Region, Australia. Mar. Poll. Bull. 51:23-36

Miyajima T, Suzumura M, Umezawa Y, Kioke, I (2001) Microbiological nitrogen transformation in carbonate sediments of coral-reef lagoon and associated seagrass beds. MEPS 217:273-286

National Research Council (1979) Division of Medical Science, Subcommittee on Hydrogen Sulfide University Park Press, Baltimore

Neil DT, Orpin AR, Ridd EV, Yu BF (2002) Sediment yield and impacts from river catchments to the Great Barrier Reef lagoon. Mar. Freshw. Res. 53:733-752

Nemeth RS, Nowlis JS (2001) Monitoring the effects of land development on the near-shore reef environment of St. Thomas, USVI. Bull. Mar. Sci. 69:759-775

Nugues MM, Roberts CM (2003) Coral mortality and interaction with algae in relation to sedimentation. Coral Reefs 22:507-516

Orpin AR, Ridd PV, Stewart LK (1999) Assessment of the relative importance of major sediment transport mechanisms in the central Great Barrier Reef lagoon. Australian J. Earth Sci. 46:883-896

Pastorok RA, Bilyard GR (1985) Effects of sewage pollution on coral-reef communities. MEPS 21:175-189

Peters E (1997) Diseases of Coral-Reef Organisms Life and Death of Coral Reefs. Chapman & Hall, London, pp 114-139

Peters EC, Pilson MEQ (1985) A comparative study of the effects of sedimentation on symbiotic and asymbiotic colonies of the coral *Astrangia danae*. JEMBE 92:215-230

Philipp E, Fabricius K (2003) Photophysiological stress in scleractinian corals in response to short-term sedimentation. JEMBE 287:57-78

Ploug H, Kühl M, Buchholz-Cleven B, Jørgensen BB (1997) Anoxic aggregates - an ephemeral phenomenon in the pelagic environment? Aqu. Microb. Ecol. 13:285-294

Pomerance R (1999) Coral bleaching, coral mortality, and global climate change. Report presented by Deputy Assistant Secretary of State for the Environment and Development to the US Coral Reef Task Force M, Maui, Hawaii.

Ralph PJ, Gademann R, Larkum AWD, Schreiber U (1999) *In situ* underwater measurements of photosynthetic activity of coral zooxanthaellae and other-dwelling dinoflagellate endosymbionts. MEPS 180:139-147

Rath J, Ke Ying W, Gerhard JH, Edward FD (1998) High phylogenetic diversity in a marine-snow-associated bacterial assemblage. Aqu. Microb. Ecol. 14:261-269

Reaka-Kudla M (1997) The global biodiversity of coral reefs: a comparison with rain forests. In: Reaka-Kudla ML, Wilson DE, Wilson EO (eds) Biodiversity II: Understanding and Protecting Our Biological Resources. Joseph Henry Press, Washington, D.C., pp 83-108

Rees JG, Setiapermana D, Sharp VA, Weeks JM, Williams TM (1999) Evaluation of the impacts of land-based contaminants on the benthic faunas of Jakarta Bay, Indonesia. Oceanol. Acta 22:627-640

Reichelt-Brushett AJ, Harrison PL (2000) The effect of copper on the settlement success of larvae from the scleractinian coral *Acropora tenuis*. Mar. Poll. Bull. 41:385-391

Revsbech NP, Jørgensen BB (1983) Photosynthesis of benthic microflora measured with high spatial-resolution by the oxygen microprofile method - capabilities and limitations of the method. Limnol. Oceanogr. 28:749-756

Revsbech NP, Jørgensen BB (1986) Microelectrodes: Their use in microbial ecology. Adv. Microb. Ecol. 9:293-352

Revsbech NP (1989) An oxygen microsensor with a guard cathode. Limnol. Oceanogr. 34:474-478

Richardson LL (1998) Coral diseases: what is really known? Trends Ecol. Evol. 13:438-443

Roberts CM, McClean CJ, Veron JEN, Hawkins JP, Allen GR, McAllister DE, Mittermeier CG, Schueler FW, Spalding M, Wells F, Vynne C, Werner TB (2002) Marine biodiversity hotspots and conservation priorities for tropical teefs. Science 295:1280-1284

Rogers CS (1990) Responses of coral reefs and reef organisms to sedimentation. MEPS 62:185-202

Rosenberg E, Loya Y (2004) Coral health and disease. Springer Verlag, Berlin

Ryan K, Walsh JP, Corbett DR, Winter A (2008) A record of recent change in terrestrial sedimentation in a coral-reef environment, La Parguera, Puerto Rico: A response to coastal development? Mar. Poll. Bull. 56:1177–1183

Sassaman C, Mangum CP (1973) Relationship between aerobic and anaerobic metabolism in estuarine anemones. Comp. Biochem. Physiol. 44A:1313-1319

Schläppy M-L (2008) Chemical micro-environments, ventilation behavior, and microbial processes in sponges. PhD thesis. University of Bremen

Schreiber U, Schliwa U, Bilger W (1986) Continuous recording of photochemical and non-photochemical chlorophyll fluorescence quenching with a new type of modulation fluorometer. Photosynth. Res. 10:51-62

Schuhmacher H (1991) Korallenriffe. BLV Verlagsgesellschaft, München

Sessitsch A, Weilharter A, Gerzabek MH, Kirchmann MH, Kandeler E (2001) Microbial population structures in soil particle size fractions of a long-term fertilizer field experiment. Appl. Environ. Microbiol. 67:4215-4224

Siebeck U, Marshall N, Klüter A, Hoegh-Guldberg O (2006) Monitoring coral bleaching using a colour reference card. Coral Reefs 25:453-460

Smith JE, Shaw M, Edwards RA, Obura D, Pantos O, Sala E, Sandin SA, Smriga S, Hatay M, Rohwer FL (2006) Indirect effects of algae on coral: algae-mediated, microbe-induced coral mortality. Ecol. Lett. 9:835-845

Smith SV (1978) Coral-reef area and the contributions of reefs to processes and resources of the world's oceans. Nature 273:225-226

Sofonia J, Anthony KRN (2008) High-sediment tolerance in the reef coral *Turbinaria mesenterina* from the inner Great Barrier Reef lagoon (Australia). Estuar. Cost. Shelf Sci. 78:748-752

Sorokin YI (1978) Microbial production in the coral-reef community. Arch. Hydrobiol. 83:281-323

Spalding M, Ravilious C, Green EP (2001) World Atlas of Coral Reefs. University of California Press, Berkeley, USA

Stafford-Smith MG (1993) Sediment-rejection efficiency of 22 species of Australian scleractinian corals. Mar. Biol. 115:229-243

Stafford-Smith MG, Ormond RFG (1992) Sediment-rejection mechanisms of 42 species of Australian scleractinian corals. Aust. J. Mar. Freshw. Res. 43:683-705

Sussman M, Willis BL, Victor S, Bourne DG (2008) Coral pathogens identified for white syndrome (WS) epizootics in the Indo-Pacific. PLoS One 3:e2393

Titlyanov EA, Titlyanov TV, Ymazato K, van Woesik R (2001) Photo-acclimation dynamics of the coral *Stylophora pistillata* to low and extremely low light. JEMBE 263:211-225

Vargas-Ángel B, Riegl B, Gilliam D, Dodge RE (2006) An experimental histopathological rating scale of sediment stress in the Caribbean coral *Montastrea cavernosa*. Proceedings of the 10th International Coral Reef Symposium, Okinawa, pp 1168-1173

Veron J (2000) Corals of the World. Australian Institute of Marine Science, Townsville

Victor S, Neth L, Golbuu Y, Wolanski E, Richmond RH (2006) Sedimentation in mangroves and coral reefs in a wet tropical island, Pohnpei, Micronesia. Estuar.Coast. Shelf Sci. 66:409-416

von Brand T (1976) Anaerobiosis in Invertebrates. Biodynamica, University of Michigan

Vopel K, Thistle D, Ott J, Bright M, Røy H (2005) Wave-induced H_2S flux sustains a chemoautotrophic symbiosis. Limnol. Oceanogr. 50:128-133

Webster NS (2007) Sponge disease: a global threat? Environ. Microbiol. 9:1363-1375

Wentworth CK (1922) A scale of grade and class terms for clastic sediments. J. Geol. 30:377-392

Wesseling I, Uychiaoco AJ, Alino PM, Aurin T, Vermaat JE (1999) Damage and recovery of four Philippine corals from short-term sediment burial. MEPS 176:11-15

Wilkinson C (1998) Status of coral reefs of the world: 1998. Australian Institute of Marine Science, Townsville

Wilkinson C (2002) Status of coral reefs of the world: 2002. Australian Institute of Marine Science, Townsville

Wilkinson C (2004) Status of coral reefs of the world: 2004. Australian Institute of Marine Science, Townsville

Wilkinson C (2008) Status of coral reefs of the world: 2008. Australian Institute of Marine Science, Townsville

Williams DM (2001) Impacts of terrestrial run-off on the Great Barrier Reef World Heritage Area. Report to CRC Reef Research Centre, Australian Institute of Marine Science, Townsville, pp 52

Wolanski E, Fabricius K, Spagnol S, Brinkman R (2005) Fine sediment budget on an inner-shelf coral-fringed island, Great Barrier Reef of Australia. Estuar. Coast. Shelf Sci. 65:153-158

Wolanski E, Fabricius KE, Cooper TF, Humphrey C (2008) Wet season fine sediment dynamics on the inner shelf of the Great Barrier Reef. Estuar. Coast. Shelf Sci. 77:755-762

Wolanski E, Richmond RH, Davis G, Bonito V (2003) Water and fine sediment dynamics in transient river plumes in a small, reef-fringed bay, Guam. Estuar. Coast. Shelf Sci. 56:1029-1040

Wolanski E, Spagnol S, Ayukai T (1998) Field and model studies of the fate of particulate carbon in mangrove-fringed Hinchinbrook Channel, Australia. Mangr. Salt Mar. 2:205-221

Yentsch CS, Yentsch CM, Cullen JJ, Lapointe B, Phinney DA, Yentsch SW (2002) Sunlight and water transparency: cornerstones in coral research. JEMBE 268:171-183

Yonge C, Yonge MJ, Nicholls AG (1932) Studies on the physiology of corals - VI. The relationship between respiration in corals and the production of oxygen by their zooxanthellae. Great Barrier Reef Expedition 1928-29 Science Reports 1:213-251

Ziebis W, Forster S, Hüttel M, Jørgensen BB (1996) Complex burrows of the mud shrimp *Callianassa truncata* and their geochemical impact in the seabed. Nature 382:619-622

Chapter 2

Effects of suspended sediments, dissolved inorganic nutrients and salinity on fertilisation and embryo development in the coral *Acropora millepora* (Ehrenberg, 1834)

Coral Reefs
DOI 10.1007/s00338-008-0408-1

REPORT

Effects of suspended sediments, dissolved inorganic nutrients and salinity on fertilisation and embryo development in the coral *Acropora millepora* (Ehrenberg, 1834)

C. Humphrey · M. Weber · C. Lott · T. Cooper · K. Fabricius

Received: 1 January 2008 / Accepted: 22 July 2008

Abstract Exposure of coral reefs to river plumes carrying increasing loads of nutrients and sediments is a pressing issue for coral reefs around the world including the Great Barrier Reef (GBR). Laboratory experiments were conducted to investigate the effects of changes in inorganic nutrients (nitrate, ammonium and phosphate), salinity and various types of suspended sediments in isolation and in combination on rates of fertilisation and early embryonic development of the scleractinian coral *Acropora millepora*. Dose–response experiments showed that fertilisation declined significantly with increasing sediments and decreasing salinity, while inorganic nutrients at up to 20 μM nitrate or ammonium and 4 μM phosphate had no significant effect on fertilisation. Suspended sediments of ≥100 mg l^{-1} and salinity of 30 ppt reduced fertilisation by >50%. Developmental abnormality occurred in 100% of embryos at 30 ppt salinity, and no fertilisation occurred at ≤28 ppt. Another experiment tested interactions between sediment, salinity and nutrients and showed that fertilisation was significantly reduced when nutrients and low concentrations of sediments co-occurred, although both on their own had no effect on fertilisation rates. Similarly, while slightly reduced salinity on its own had no effect, fertilisation was reduced when it coincided with elevated levels of sediments or nutrients. Both these interactions were synergistic. A third experiment showed that sediments with different geophysical and nutrient properties had differential effects on fertilisation, possibly related to sediment and nutrient properties. The findings highlight the complex nature of the effects of changing water quality on coral health, particularly stressing the significance of water quality during coral spawning time.

Keywords Great Barrier Reef · Coral fertilisation · Salinity · Sediment · Nutrients · Terrestrial runoff

Communicated by Environment Editor Professor Rob van Woesik

C. Humphrey (✉) · T. Cooper · K. Fabricius
Australian Institute of Marine Science, PMB 3, Townsville, QLD 4810, Australia
e-mail: c.humphrey@aims.gov.au

M. Weber · C. Lott
Max Planck Institute for Marine Microbiology, Celsiusstrasse 1, 28359 Bremen, Germany

M. Weber · C. Lott
HYDRA Institute for Marine Sciences, Elba Field Station, Via del Forno 80, 57034 Campo nell'Elba, Livorno, Italy

Introduction

One of the most pressing concerns for the management of the Great Barrier Reef (GBR) is to understand the consequences of increasing terrestrial runoff of nutrients and sediments (Hutchings and Haynes 2005; Hutchings et al. 2005). Nearshore reefs of the GBR have developed in an environment driven by the influence of river runoff, yet in the past 150 years, expanding agriculture, urban development and industry have led to greater runoff of freshwater (McCulloch et al. 2003), nutrients (Devlin et al. 2001; Furnas 2003), sediments (Neil et al. 2002; Furnas 2003; McCulloch et al. 2003), and agrochemicals (Haynes and Johnson 2000; Haynes and Michalek-Wagner 2000). River plume waters are characterised by elevated levels of dissolved organic and inorganic nitrogen and phosphorus, suspended particulate matter, turbidity, and chlorophyll *a*, as well as by reduced salinity, when compared with ambient marine coastal waters (Table 1). Generally, flood plumes in this region remain within 20 km of the coast due to prevailing south-easterly winds and Coriolis forcing (Chao 1988), impinging upon the approximately 900 nearshore reefs

Table 1 Water quality parameters of flood plumes of the Great Barrier Reef compared to ambient values

	Salinity (ppt)	NH_4 (μM)	NO_3	DON	PN	DIP	DOP	PP	Si	Chl *a* (μg l^{-1})	SS (mg l^{-1})
Flood plume[a]	0	12.8	14.3	40.4	20.3	2.5	2.8	1.3	221	4.6	500[c]
Ambient (non-flood)[b]	35	0.03	0.02	5.43	1.43	0.10	<0.10	0.10	4.77	0.4	1.7

Salinities are minimum values recorded while all other values are maximum values

[a] Devlin et al. (2001), values recorded in flood plumes on the GBR between 1991 and 1999

[b] Furnas (2003), median values from inshore waters of the Central GBR

[c] Wolanski et al. (2008)

(~27% of all reefs) within the GBR Marine Park. In the absence of strong south-easterly winds, flood plumes may extend to some of the mid- and outer-shelf reefs of the GBR (Devlin and Brodie 2005).

Some reefs in the northern wet tropical section of the GBR (Herbert to Daintree Rivers) are exposed to floods nearly annually. Reefs in the southern, central and far northern sections are characterised by dryer subtropical to tropical climates with fewer floods (on average every 2–3 years; Devlin and Brodie 2005). The majority of river floods occur in the monsoonal wet season (October to April), often associated with tropical cyclones or rain depressions (Devlin et al. 2001). Although average rainfall is highest in January to March, early floods can coincide with the coral mass spawning event in the GBR that occurs annually in October to December (Babcock et al. 1986).

The residency time of dissolved materials in the GBR has been estimated to be up to 300 days (disregarding biological uptake; Luick et al. 2007), while particulate materials remain for an unknown period whilst undergoing cycles of wind-driven re-suspension and deposition until they are finally deposited in deeper water or in north-facing bays. Terrestrial runoff therefore not only affects biological processes during acute flood events but can also chronically alter water quality near inshore reefs year-round.

The reproductive processes and early life history stages of corals, including fertilisation, embryonic development, metamorphosis and settlement, are sensitive to changes in water quality (Fabricius 2005). Successful coral reproduction is critical for the resilience of coral reefs, determining the speed of recovery after disturbance. Several investigators have studied the effects of individual water quality parameters on coral reproduction. In particular, exposure to increased levels of nitrogen and phosphorus resulted in reduced fertilisation rates and increased levels of developmental abnormalities in *Acropora longicyathus* (Harrison and Ward 2001), as well as the production of smaller and fewer eggs per polyp in *A. longicyathus* and *Acropora aspera* (Ward and Harrison 2000). Enhanced ammonium has also been shown to reduce larval survival and settlement in *Diploria strigosa* with more pronounced reductions at higher temperatures (Bassim and Sammarco 2003). Reduction in salinity from 35 to 28 ppt reduced fertilisation success in *Acropora digitifera* from 86% to 25%, with a further 50% reduction in development to actively swimming planulae larvae (Richmond 1993). Suspended sediments of 50–100 mg l^{-1} have also been shown to reduce fertilisation rates, larval survival and larval settlement in *Acropora digitifera* (Gilmour 1999).

Understanding the effects of changes in water quality on coral reproduction is complicated by the fact that high nutrients often co-occur with reduced salinity and increased levels of suspended sediments. Few studies have examined these interactive effects between water quality parameters on coral reproduction. One of the few studies to investigate interactions in water quality parameters on corals is that of Bassim and Sammarco (2003) who showed that the effects of temperature and ammonium were additive in reducing survivorship, ciliary activity and settlement rates of larvae of the coral *Diploria strigosa*. Another study showed that the effects of sedimentation on adult corals depended upon the physical and chemical properties of the sediments, as nutrient-rich sediments exerted greater photo-physiological stress on corals than nutrient-poor sediments (Weber et al. 2006). The effects of sedimentation on the photo-physiology of reef-inhabiting crustose coralline algae were also substantially exacerbated by the presence of trace concentrations of the herbicide diuron (Harrington et al. 2005).

This study investigates the synergistic effects of varying but environmentally relevant levels of suspended sediments, salinity and dissolved inorganic nitrogen (as nitrate and ammonium) and phosphorus on fertilisation and embryonic development in the coral *Acropora millepora*. The effects of five contrasting sediment types on coral fertilisation and development were also compared, to better understand how sediment properties determine reproductive impairment. The results help to better understand the effects of increased terrestrial runoff and changes in water quality on coral reproduction and resilience on coral reef systems that are within the reach of river flood plumes and seafloor resuspension on the GBR.

Materials and methods

Spawning and gamete collection

The broadcast-spawning coral *Acropora millepora* (Ehrenberg, 1834), abundant in nearshore waters of the GBR, was selected as the study species. Eleven gravid colonies (each ~30 × 30 cm) were collected from Davies Reef, GBR (18°50′ S, 147°38′ E), from a depth of 5–8 m on 28 Nov. 2004. They were transported to aquarium facilities at the Australian Institute of Marine Science and maintained outdoors in 27–29°C temperature-controlled, flow-through seawater tanks until spawning commenced.

Prior to sunset, colonies were isolated in 50 l plastic containers and shielded from artificial light. Synchronous spawning occurred in 8 of the 11 colonies between 2100 and 2200 h on 1 Dec. 4 days after the full moon. The released gametes were collected following the methods of Negri and Heyward (2000). Briefly, the floating egg–sperm bundles from individual colonies were collected from the water surface by gentle suction through a plastic tube into 250 ml plastic containers. Gametes from each colony were kept separate to prevent fertilisation until the experiments were ready to proceed. Gametes in the plastic jars were gently agitated to separate the eggs and sperm, and passed through a 150 µm plankton mesh to retain all eggs and collect the concentrated sperm in a glass beaker. The eggs thus retained on the mesh were washed five times with sperm-free seawater to remove residual sperm. Eggs from all colonies that had spawned were pooled, as was the concentrated sperm.

The sperm concentration in the stock solution was determined with a haemocytometer viewed with a compound microscope at 400× magnification. Sperm concentration was diluted with sperm-free seawater to achieve a working stock of $\sim 1.4 \times 10^7$ cells ml^{-1}. The concentrations of the egg and sperm slurries were adjusted to obtain ~100–500 eggs and a sperm concentration of $\sim 2 \times 10^6$ sperm ml^{-1} per treatment chamber. This concentration has been found to be slightly suboptimal for fertilisation, thereby increasing the sensitivity of the assay (Harrison and Ward 2001). Gamete-free seawater treatments with varying concentrations of dissolved inorganic nutrients, various types of sediments and/or freshwater (see below) were made up a few hours prior to spawning in 70 ml plastic jars. To each of five replicate jars holding 20 ml of modified seawater per treatment, 5 ml of egg solution was added, and 5 ml of sperm was added to another set of five plastic jars per treatment. Gametes remained in separate jars for 30 min before the eggs and sperm from the appropriate treatments were combined, resulting in a final gamete and seawater volume of 50 ml per chamber. The 30 min pre-fertilisation exposure period simulated the time required for sperm to find and appropriate eggs in the field, and reflecting the time required for polar body extrusion in acroporid gametes (Babcock and Heyward 1986). Chambers were sealed and then placed in a flow-through seawater bath to maintain a constant ambient temperature during fertilisation and development. At 10 min intervals all chambers were gently agitated to keep the sediment in suspension.

Development was terminated after 3 h by adding to each jar 2 ml of Bouin's preservative (75 ml saturated aqueous picric acid, 25 ml concentrated formalin, 5 ml glacial acetic acid), which preserved embryo integrity. Three aliquots of fertilised eggs were then collected with a wide bore pipette, placed on glass well-slides, and photographed for later analysis of rates of fertilisation, abnormal and normal development (both expressed as a percentage of fertilised eggs). Coral embryos undergo radial holoblastic cleavage with regular cleavage up to the eight cell stage which generally occurs within 3–8 h (Hayashibara et al. 1997; Ball et al. 2002; Okubu and Motokawa 2007). Aberrant development was characterised as deviation from this pattern of division, generally resulting in irregularly shaped blastomeres.

Treatment types

Three experiments were conducted. Experiment 1 investigated the main effects of gamete exposure to increasing concentrations of suspended sediments, salinity, and dissolved inorganic nitrogen and phosphate. Experiment 2 investigated the combined effects of suspended sediment, salinity and nutrients, to assess potential interactions. Experiment 3 investigated main effects of increasing concentrations of five different types of sediments. Concentrations for all the treatments were within the range of those measured on nearshore reefs of the GBR during flood events (Devlin et al. 2001).

Experiment 1: response curves

Suspended sediment

Coastal sediment was collect from a jetty off the Australian Institute of Marine Science (19°17′ S; 147°03′ E) from 3 m water depth. The sediment was placed into a 100 l tank and suspended by agitation, and the coarser grain fraction was allowed to settle for 1 h. The fine particles, still in suspension after 1 h, were then collected by siphoning directly from the top of the tank, and allowed to settle for a further 3 h. This sediment was then passed through a 63 µm mesh, keeping only the <63 µm fraction.

The suspended sediment treatments consisted of filtered seawater, to which 0, 25, 50, 100, 200 and 400 mg dry

weight (DW) l^{-1} of suspended sediment solution was added. Final amounts of suspended sediment were calculated by determining the DW of a known volume of the stock solution. Twenty-nine water chemical and geological parameters were analysed for each of the sediment types used; these and the methods used for determination are listed in Table 2.

Salinity

Salinity was manipulated by adding Super-Q water to filtered seawater, resulting in 36, 34, 32, 30 and 28 ppt salinity.

Dissolved inorganic nutrients

Two sources of dissolved inorganic nutrients were compared: a nitrate (potassium nitrate) and phosphate (dipotassium hydrogen phosphorus) treatment, and an ammonium (ammonium chloride) and phosphate (as above) treatment. Nutrients were added to filtered seawater at a nitrogen to phosphorus molar ratio of 5:1. The nutrient treatments consisted of a filtered seawater control and nominal concentrations of nitrate/phosphate and ammonium/phosphate of 1.25:0.25, 2.5:0.5, 5:1, 10:2 or 20:4 μM. Final concentrations of nutrients were confirmed as outlined in Table 2.

Experiment 2: interactions between suspended sediment, salinity and nutrients

The second experiment investigated interactions between the main effect treatments of Experiment 1. There were three nutrient treatments with nominal concentrations of 0:0, 5:1 and 10:2 μM nitrate and phosphate, three sediment treatments with nominal concentrations of 0, 50 and 100 mg DW l^{-1}, and two salinity treatments (36 and 32 ppt). An extra replicate of each treatment was added to the experiment and filtered seawater added in place of eggs or sperm for later analysis of the various water quality parameters to confirm the nominal concentrations. A filtered seawater control and all possible interactions of the above treatments were investigated in five replicates of each. The experiment proceeded as described above.

Experiment 3: comparison of suspended sediment types

Five different types of sediments were collected 4 weeks prior to the spawning event. The upper 5 cm of sediment was collected from just below the water level at the estuarine shore of the Chester River (13°04′ S; 143°33′ E), a catchment in the far northern section of the GBR with minimal agriculture (Fabricius et al. 2005). The upper 5 cm of marine sediments was collected by SCUBA from 5 to 10 m depth from the leeward sides of the near-shore fringing reefs of High Island (17°10′ S, 146°00′ E), Wilkie Island (13°46′ S, 143°38′ E), and the lagoon of the offshore reef 14-077 (14°19′ S, 145°13′ E). The fifth sediment type was aragonite silt, a by-product of slicing coral skeletons of massive *Porites* sp. for growth band analyses (for details see Weber et al. 2006). All sediments were prepared as described above.

Treatments (each with five replicates) consisted of filtered seawater, with 0, 4, 16, 32, 64, 128, 256 and 512 mg DW l^{-1} suspended sediment solution from either

Table 2 The 29 chemical and geochemical parameters measured, and the analytical methods employed to characterise the suspended sediments

Parameter	Method	Description
Grain size distribution (GSD)[a]	Laser diffraction	Master series X Malvern Particle Sampler (32 detector ranges); Detector lens = 1000 μm
Ash free dry weight (AFDW)[b]	Combustion	Sediments dried at 100°C for 24 h, weighed, heated at 500°C for 1 h, and re-weighed.
Total organic carbon (TOC)[c] and dissolved organic carbon (DOC)[c]	Combustion	Shimadzu TOC-5000 Carbon Analyser (Shimadzu Corporation, Kyoto, Japan)
Total nitrogen (TN)[d]	Combustion	ANTEK Solid Auto Sampler (Antek Instruments, Inc., Houston, Texas, USA)
Chlorophyll *a* (Chl *a*) and phaeophytin (Phaeo)[e]	Fluorometry	Turner Designs (Model 10-AU or TD700) Digital Fluorometer after 24 h extraction in acetone in dark.
Al, Ba, Ca, Cd, Co, Cu, Fe, Mg, Mn, Mo, Ni, Pb, Sn, Zn, V and Total phosphorous (TP)[f]	Spectrophotometry	Varian Liberty 220 ICP Atomic Emission Spectrometer (ICP-AES)
Total inorganic nutrients (PO_4, Si, NO_2, NO_3, $NO_2 + NO_3$)[g]	Colorimetry	Segmented Flow Analysis—Bran+Luebbe AA3
Total suspended solids (TSS)[c]	Gravimetry	Re-weighed filters after drying at 60°C until constant weight.

[a] Woolfe and Michibayashi (1995); [b] Parker (1983); [c] Furnas and Mitchell (1999); [d] Furnas et al. (1995); [e] Strickland and Parsons (1972); [f] Loring and Rantala (1992); [g] Ryle et al. (1981) and Ryle and Wellington (1982)

one of the five stock solutions. A treatment with 1,024 mg DW l^{-1} was additionally tested, but samples were lost in two of the sediments; results of the successful treatments are included in the graphics but not in the statistical analyses. Sediment and water quality properties (29 parameters) were analysed as detailed in Table 2. To characterise the sediments, the sediment parameters were *z*-transformed, parameters were grouped into four categories, and *z*-transformed parameter values summed for each sediment type to form the following four indices: grain size (GSI), organic and nutrient related parameters (ONP), geochemical parameters (GCP), and dissolved nutrients (DNI). GSI was calculated as the sum of *z*-scores of the four parameters: mean grain size, and the 25, 50 and 75 percentiles of sediment volume. ONP was calculated as the sum of *z*-scores of the six parameters: chlorophyll *a* (Chl *a*) and phaeophytin (Phaeo) (an indicator of nutrient status; Brodie et al. 2007), ash-free dry weight (AFDW) (an indicator of organic matter), total organic carbon (TOC), total nitrogen (TN) and total phosphorous (TP). GCP was calculated as the sum of *z*-scores of fifteen metal and trace elements. DNI was calculated based on the six parameters: dissolved organic carbon (DOC), ammonium (NH_4), nitrate (NO_3), nitrite (NO_2), silicate (Si) and phosphate (PO_4).

Statistical analysis

Experiment 1

The data from the fertilisation and embryo development experiments were analysed using analysis of variance (ANOVA). One-factor ANOVAs were conducted to test the main effects of differing concentrations of suspended sediment and salinity, while a two-factor ANOVA was conducted to test for the effects of dissolved nutrients on fertilisation success and development of *A. millepora* embryos in isolation. Data were tested for deviation from homogeneity of variances and arcsine transformed where required. Post hoc comparisons of means for significant factors in the ANOVAs were done using Student-Newman Keuls (SNK) tests.

Experiment 2

To test for synergistic effects among the water quality parameters on the fertilisation success and development on *A. millepora* embryos, a three-factor ANOVA was used with suspended sediment (three levels), nutrients (three levels, fixed and orthogonal) and salinity (three levels, fixed and orthogonal) as the factors. Data were tested for deviation from homogeneity of variances and arcsine transformed where required.

Experiment 3

Analysis of variance (ANOVA) was used to test for differences in fertilisation and early development abnormalities between sediment type and concentration. Data were tested for deviation from homogeneity of variances and arcsine transformed where required. A Spearman non-parametric rank correlation test was used to test the correlation of ranked rates of fertilisation with the four sediment indices for the five sediments. The AIMS jetty sediment was not included in this analysis as gametes were exposed to different treatment concentrations.

All results were given as the mean ± standard error, and as not all the data required transformation all plots are of untransformed data to maintain consistency. Data analyses were conducted with Statistica 6.0 (StatSoft) and the statistical software package R (R Development Core Team 2008).

Results

Experiment 1: response curves

The responses of gametes exposed to increasing sediments and nutrients, and decreasing salinity are shown in Fig. 1 and Table 3. The controls were characterised by high levels of fertilisation (87.1 ± 2.2% SE) and moderate rates of developmental abnormalities (20.1 ± 1.6%). Sediment significantly affected rates of fertilisation yet had no effect on successful embryo development (Table 3; Fig. 1a, b). Fertilisation declined to 75.6 ± 5.4% at 100 mg l^{-1} suspended sediments, and 35.5 ± 4.8% at 200 mg l^{-1} (Fig. 1a). Fertilisation was not affected by 36–32 ppt salinity, while it dropped to 33.6 ± 4.6% at 30 ppt, and no fertilisation was observed at 28 ppt (Table 3; Fig. 1c). Salinity of 32 ppt led to an increase in developmental abnormality of ~10%, while salinity of 30 ppt resulted in 100% developmental abnormality (Fig. 1d). Neither the nitrate/phosphate nor the ammonium/phosphate treatments significantly affected fertilisation or development, even at the highest nutrient concentrations (Table 3; Fig. 1e, f).

Experiment 2: interactions between suspended sediment, salinity and nutrients

Fertilisation rates of gametes exposed simultaneously to combinations of sediments, salinity and nutrients are shown in Fig. 2. There was a significant interactive effect between sediments, salinity and nutrients on fertilisation (Table 4). While in Experiment 1, fertilisation was not affected by sediments at ≤50 mg l^{-1}, salinity at ≥32 ppt or any of the nutrient treatments (Fig. 1 a, c, e), fertilisation was significantly

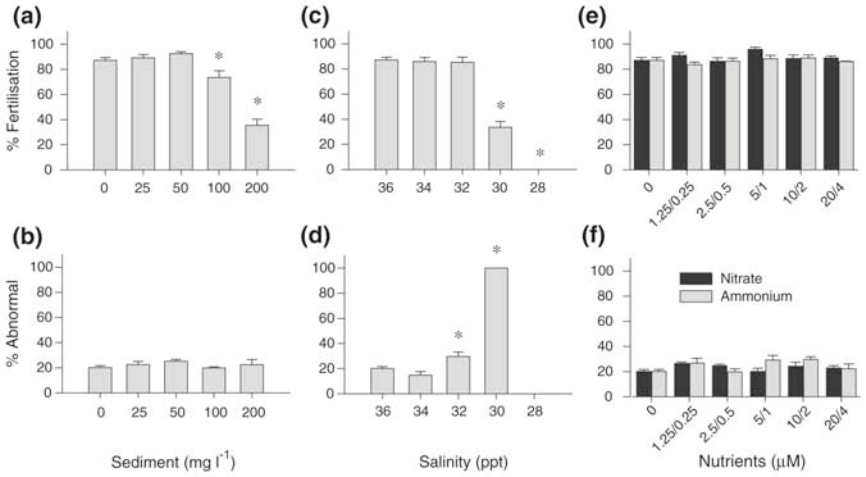

Fig. 1 Percentage of fertilisation and abnormal development in gametes of the coral *Acropora millepora* in response to exposure to various concentrations of suspended sediment (AIMS jetty), salinity and dissolved inorganic nutrients (Experiment 1). * Represents significant difference ($P < 0.05$; Table 3)

Table 3 Effects of exposure to changes in salinity, suspended sediment, and dissolved inorganic nutrients on gamete fertilisation and early development of *A. millepora* (Experiment 1)

	df	MS	*F*	*P*	Pairwise multiple comparison, SNK
Sediment					
Fertilisation (%)	5	3,018	41.27	<0.0001	0 = 25 = 50 > 100 > 200
Abnormal development (%)	5	19.87	19.87	0.5688	
Salinity					
Fertilisation (%)	4	7,915	150.01	<0.0001	28 < 30 < 32 = 34 = 36
Abnormal development (%)	3	7,883	262.00	<0.0001	36 = 34 < 32 < 30
Nitrate and phosphate/Ammonium and phosphate (Fertilisation (%))					
Concentration	5	6.9	0.36	0.8759	
Nutrient type	1	51.7	2.68	0.1080	
Concentration × nutrient type	5	17.4	0.90	0.4867	
Nitrate and phosphate/Ammonium and phosphate (Abnormal (%))					
Concentration	5	31.63	1.95	0.1032	
Nutrient type	1	12.08	0.75	0.39	
Concentration × nutrient type	5	28.85	1.78	0.1351	

reduced at these levels and higher when in combination (Fig. 2). At the highest nutrient concentration of 10:2 µM NO_3:PO_4 and salinity of 32 ppt, fertilisation was reduced at 100 mg l^{-1} sediments compared with treatments with 0 and 50 mg l^{-1}. At 36 ppt salinity, there was no sediment effect at 0 and 50 mg l^{-1} at the lowest two nutrient concentrations, though when nutrients were increased to 10:2 µM NO_3:PO_4 there was a significant effect at all sediment concentrations (Fig. 2c).

There were no interactive effects of salinity, sediment or nutrients on proportion of embryonic abnormalities.

Experiment 3: comparison of suspended sediment types

In the control treatments, the level of fertilisation averaged 71.0 ± 2.4%, and 24.5 ± 2.3% of embryos showed developmental abnormalities. Fertilisation was significantly reduced at the highest sediment levels for two of the five sediment types (Wilkie and High Islands; Fig. 3). Consequently, the analyses showed strong interactions between the effects of sediment type and sediment concentration on fertilisation success (Tables 5, 6).

Levels of abnormal development averaged 34% over all treatments, and showed weak and complex interactions between sediment types and amount (Tables 5, 6). The highest level of abnormal development (45.1 ± 3.3%) was observed in embryos exposed to Chester River sediment at 16 mg DW l^{-1}. The lowest levels of abnormalities were found for the lowest concentrations of Wilkie Island sediments (22.2% and 20.8%, respectively).

The concentrations and derived indices of each of the five sediments, and of the AIMS jetty sediment from Experiment

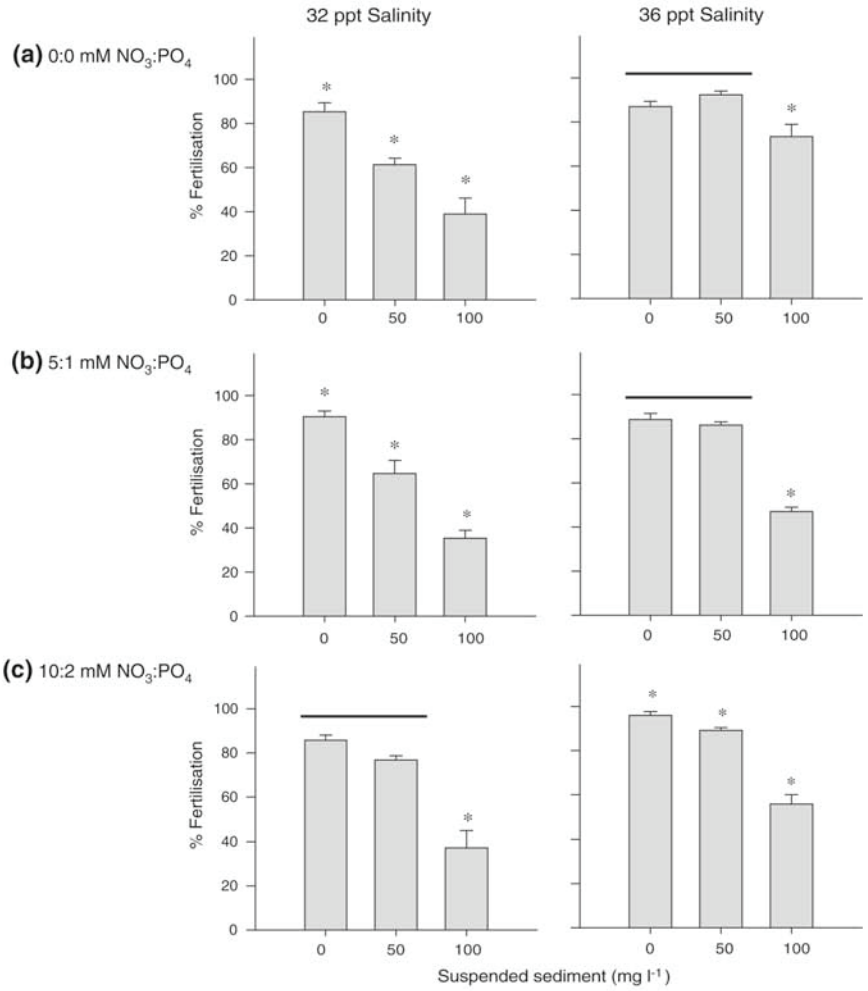

Fig. 2 Percentage of fertilisation and abnormal development in gametes of the coral *Acropora millepora* in response to combined exposure to suspended sediment (AIMS jetty), salinity, and dissolved inorganic nutrients (Experiment 2). Line above bars represent that there is no significant difference between treatments, while * represents significant difference ($P < 0.05$; Table 4)

1, are listed in Table 7. Median grain sizes of the silt-sized sediments ranged from 11 to 23 μm, with smallest grain size in the AIMS jetty sediment (Experiment 1) or High Island (Experiment 3) and highest for aragonite silt. The organic and nutrient-related parameters (ONP) were highest for Chester River sediment, and lowest for aragonite silt. The geochemical parameters were highest in the AIMS jetty and High Island sediment, and lowest in aragonite silt. The index characterising dissolved inorganic nutrients was highest in the two inshore sediments Wilkie and High Island, and lowest in the AIMS jetty and Chester River sediments.

In order to investigate the role various sediment properties may play in determining their effects on coral reproduction, fertilisation rates exposed to 512 mg l^{-1} of the five sediment types were rank ordered (in increasing order) as follows: Wilkie Island sediments (49.9 ± 3.6%), followed by High Island sediment (58.2 ± 8.7%), offshore sediments (64.8 ± 1.0%), Chester River sediment (76.1 ± 3.5%) and aragonite silt (76.8 ± 4.3%). Chester River and aragonite silt were given the same rank order. The ranking of fertilisation rates was strongly related to the index characterising the dissolved nutrients in the sediment treatment (DNI, $P = 0.005$), with higher nutrient concentrations resulting in lower fertilisation rates (Table 8, Fig. 4). The apparent positive relationship of fertilisation rate to grain size was non-significant (GSD, $P = 0.054$). Fertilisation rates were also clearly unrelated to the geochemical and the organic and nutrient-related sediment parameters ($P > 0.1$).

Discussion

This study investigated the interactive effects of suspended sediments, salinity and dissolved inorganic nutrients on fertilisation success and embryonic development in a scleractinian coral. The results from this experiment confirm

Table 4 Effects of combined exposure to 3 levels of suspended sediment, 2 levels of salinity, and 3 levels of dissolved inorganic nutrients on gamete fertilisation and early development of *A. millepora* (Experiment 2)

	df	MS	*F*	*P*
Fertilisation (%)				
Sediment	2	6057.8	164.5	<0.0001
Salinity	1	2602.5	70.7	<0.0001
Nutrients	2	90.64	2.46	0.0925
Sediment × nutrients	4	127.34	3.46	0.0122
Sediment × salinity	2	308.29	8.37	0.0005
Salinity × nutrients	2	138.71	3.77	0.0278
Sediment × salinity × nutrients	4	114.49	3.11	0.0203
Residual	72			
Abnormal development (%)				
Sediment	2	94.51	4.64	0.0128
Salinity	1	1121.77	55.0	<0.000
Nutrients	2	2.49	0.122	0.8852
Sediment × nutrients	4	26.73	1.31	0.2740
Sediment × salinity	2	22.59	1.11	0.3357
Salinity × nutrients	2	50.04	2.45	0.0930
Sediment × salinity × nutrients	4	41.21	2.02	0.1004
Residual	72	20.38		

previous studies that have shown that suspended sediments, salinity and nutrients at environmentally relevant levels (see Table 1) affect the reproductive successes in corals; it furthermore demonstrates that these effects are interactive. Suspended sediments with different organic, nutritive and geophysical properties also differed in their effects on fertilisation and embryonic development.

Increased suspended sediments in the water column negatively affect the physiology of corals, including their rates of photosynthesis, growth, survival and energy expenditure (see reviews by Rogers (1990) and Fabricius (2005)). While mean suspended sediment concentrations are typically <5 mg l^{-1} (Rogers 1990), they exceed ~80 mg l^{-1} for 20–30 days per year due to wind resuspension around some GBR inshore reefs (Wolanski 1994; Wolanski et al. 2005). Wolanski et al. (2008) measured suspended sediment levels of 280 mg l^{-1} as a result of a flood plume during calm weather, and 500 mg l^{-1} due to a combination of flood plume and resuspension during a storm event. Here, levels of suspended sediment ≥50 mg l^{-1} inhibited fertilisation yet had no effect on early development, a finding that closely matches that of Gilmour (1999) who found that suspended sediment ≥50 mg l^{-1} inhibited fertilisation yet had no effect on larval development. Interestingly, Gilmour (1999) found no difference in fertilisation between the 50 and 100 mg l^{-1} treatments, whereas in the present study there was a continued decline in the fertilisation with increasing concentrations of suspended sediments: fertilisation dropped from 92% at 50 mg l^{-1} to 75% at 100 mg l^{-1} and 35% at 200 mg l^{-1}. Such differences are likely to be attributable to the different coral species or sediment types used. Gilmour (1999) used *Acropora digitifera* and sourced sediment from spoil dredged from a large port that comprised grain sizes of ~50–200 μm, while the present study used fresh (presumably biologically active) coastal marine sediments with <63 μm grain size.

The effect of differences in sediment properties on coral fertilisation and early development was further investigated by exposing the gametes to various types of sediments with contrasting properties including grain size, organic and nutrient related parameters, geochemical properties and dissolved nutrients. A reduction in fertilisation was only found in sediments containing high dissolved nutrients and small sediment grain sizes. The AIMS Jetty sediment used in Experiment 1 appeared to reduce fertilisation more than any of the sediments used in Experiment 3; however, results were not strictly comparable as different concentrations were used in the two studies. Nevertheless it is noteworthy that the AIMS Jetty sediment had the lowest GSI of all sediments, strengthening the evidence for a potential correlation between GSI and fertilisation.

The mechanisms by which coral fertilisation could be impaired by suspended sediments are presently unknown. It is possible that suspended sediments may act as physical barrier between sperm and egg: suspended sediment may hinder, damage or adhere to sperm affecting its viability and movement hence reducing the number of egg–sperm contacts, or sediment particles may cover the micropyle blocking access to the sperm (Galbraith et al. 2006). Gilmour (1999) observed greater aggregation of eggs in treatments exposed to suspended sediment and suggested that this may result in fewer contacts between sperm and egg. These suggestions may help to explain the role of sediment presence in reducing fertilisation success, yet they fail to account for the interactive effects of dissolved nutrients. A number of studies have shown that sediment microorganisms rapidly recycle coral spawning products (Wild et al. 2004), and that sediment properties, including particle size, are responsible for binding nutrients (Pailles and Moody 1992) and harbouring microorganisms (Crump and Baross 1996). We speculate that microbial communities attached to suspended sediment particles might be one of the mechanisms responsible for low fertilisation in sediment-exposed coral gametes; however, this hypothesis requires further study.

The correlation between sediment nutrients and fertilisation rate shown in Experiment 3 have to be interpreted with caution, as the number of sediment variables is high compared with the number of sediments investigated, and some of the sediment parameters are highly correlated with each

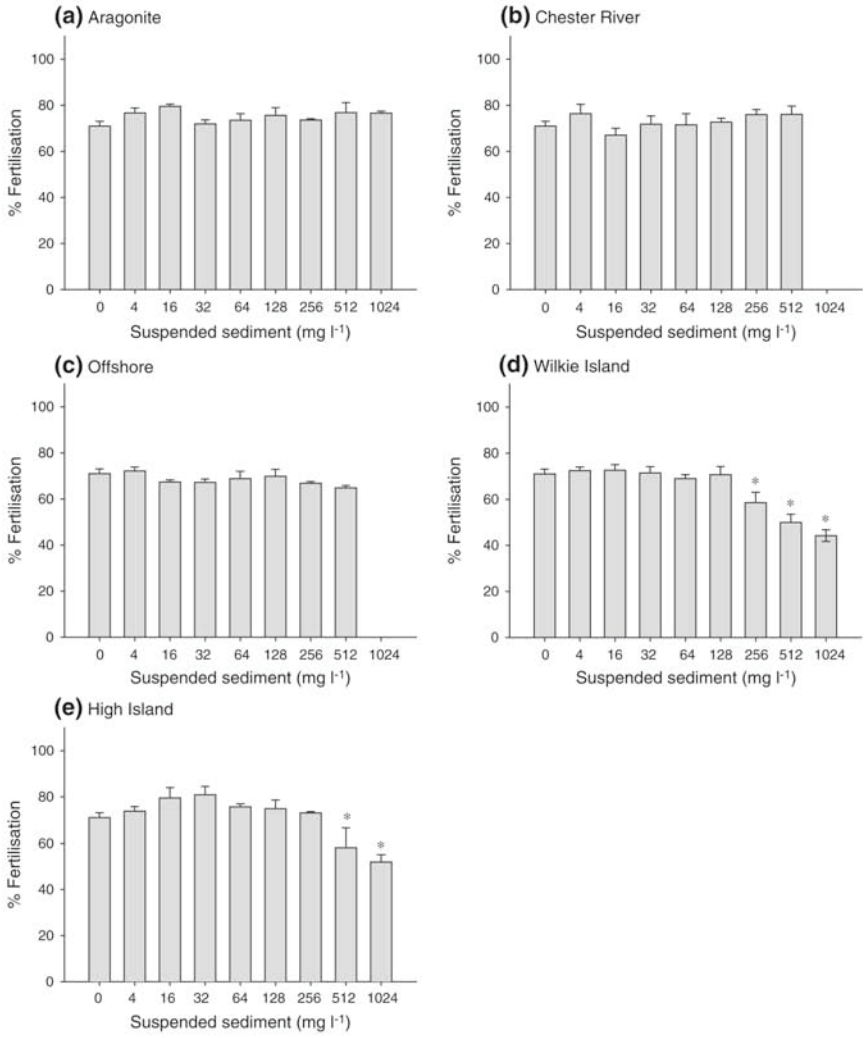

Fig. 3 Percentage of fertilisation in gametes of the coral *Acropora millepora* in response to exposure to five types of suspended sediments (Experiment 3). * Represents significant difference ($P < 0.05$; Table 5)

Table 5 Effects of exposure to five types of suspended sediments on gamete fertilisation and early development of *A. millepora* (Experiment 3)

	df	MS	*F*	*P*
Fertilisation (%)				
Sediment type	5	335.02	1.76	0.2560
Concentration	6	190.83	4.97	0.0002
Sediment type × concentration	24	108.08	2.82	0.0001
Residual	112	38.38		
Abnormal development (%)				
Sediment type	5	331.02	7.68	0.0138
Concentration	6	43.12	1.02	0.4151
Sediment type × concentration	24	78.30	1.86	0.0167
Residual	112	42.21		

other. Nevertheless, the results agree with the findings of Experiment 2, showing that interactions between high nutrient concentrations and sedimentation negatively affect coral fertilisation rates.

Salinity is an important environmental factor for corals, as corals lack mechanisms for osmoregulation (Muthiga and Szmant 1987). Some inshore coral reefs of the GBR are exposed to reduced salinity from flood plumes almost annually (Devlin et al. 2001), yet only a relatively small proportion of these floods coincide with spawning. Heavy localised monsoonal rainfall can also occur during the coral mass spawning period, resulting in the formation of low salinity surface water layers. Anecdotal evidence by Harrison et al. (1984) suggested that the entire reproductive output of a coral reef flat in the GBR was destroyed when the mass

Table 6 Summary of post-hoc comparisons of mean rates of fertilisation and abnormal development in Experiment 3

	Sediment	Concentration (mg DW l^{-1})
Fertilisation	CR	Ns
	HI	512 < (0 = 4 = 16 = 32 = 64 = 128 = 256)
	Ar	Ns
	OS	Ns
	WI	256 = 512 < (0 = 4 = 16 = 32 = 64 = 128)
Abnormal	CR	0 = 4 < (16 = 32 = 64 = 128 = 256 = 512)
	HI	0 < (4 = 16 = 32 = 64 = 128 = 256 = 512)
	Ar	Ns
	OS	Ns
	WI	512 = 0 < (4 = 16 = 32 = 64 = 128 = 256)

Sediment concentrations are presented in ascending order of percentage fertilisation or abnormality (Ns = no significant difference). Sediment types: CR, Chester River; HI, High Island; Ar, Aragonite; OS, Offshore; WI, Wilkie Island

spawning event coincided with heavy rainfall destroying all coral propagules on the surface, most probably due to reduced salinity.

Effects of reduced salinity on adult corals are well documented in the literature (e.g. Moberg et al. 1997; Alutoin et al. 2001; Kerswell and Jones 2003). However; there are fewer studies on the effects of reduced salinity on reproductive processes including fertilisation and larval development. This study demonstrated a significant reduction in fertilisation in response to a reduction in salinity to 30 ppt, while at 28 ppt no fertilisation of coral eggs occurred. These results are similar to those of Richmond (1993) who found that the rate of fertilisation dropped from 88% to 25% with a drop in salinity from 34 to 28 ppt, and from 58% to 34% with a drop in salinity from 35 to 31.5 ppt in corals from Guam and Okinawa, respectively. The present study also showed increased levels of developmental abnormalities at 30 ppt salinity treatment compared to 32 or 35 ppt, again confirming previous studies which also recorded a reduction in embryo viability and planulae survival in response to reductions in salinity (Richmond 1993; Vermeij et al. 2006). Increasing rates of abnormal development, in addition to reduction in fertilisation levels, can bring about a marked reduction in viable larvae and may have a profound impact on recruitment (Bassim et al. 2002).

Nutrient concentrations vary widely around inshore coral reefs of the GBR, with lowest concentrations during the dry season and orders of magnitude greater values in flood plumes (Table 1). This study showed that dissolved inorganic nutrients on their own did not affect rates of fertilisation or early larval development in *A. millepora*. This result contrasts with Harrison and Ward (2001) who found that fertilisation rates and development in the sympatric species *Acropora longicyathus* were significantly affected by ammonium, phosphate and ammonium/phosphate at levels similar to those investigated in the present study. In *Goniastrea aspera* exposed to the same levels of nutrients, fertilisation rates were affected at the highest treatment (50 μM) of ammonium plus phosphate, and most treatments adversely affected larval development (Harrison and Ward 2001). The sensitivity of coral fertilisation experiments is known to strongly depend on sperm density and gamete viability (Oliver and Babcock 1992; Marshall 2006), and it is possible that differences in the viability of different crosses may explain the different outcomes between the two sets of experiments. Additionally, the differences may also have been due to species-specific differences in sensitivities to elevated nutrients, as reviewed by Koop et al. (2001). Cox and Ward (2002) also showed different effects of increased ammonia on the reproduction in a broadcasting coral, *Montipora capitata,* and a brooding coral, *Pocillopora damicornis*. Planulation in *P. damicornis* ceased after 4 months of exposure to ammonium, while in *M. capitata* there was no change in fecundity or fertilisation success.

This study showed that there was a significant synergistic interaction between salinity, sediment and nutrients on fertilisation rates of *A. millepora*. This finding highlights the complex nature of the effects of changing water quality on coral ecology. Nutrients and low concentrations of sediments on their own had no effect on fertilisation rates yet when occurring in combination there was a significant reduction in fertilisation. Similarly, while slightly reduced salinity on its own had no effect, fertilisation was reduced when water with slightly reduced salinity carried elevated levels of sediments or nutrients. This interaction is particularly relevant when considering the changed nature of flood plumes: nutrient and sediment loads carried in flood plume waters into the Great Barrier Reef have increased around fivefold since onset of western agriculture, due to soil erosion from overgrazing, and increasing fertiliser application (Devlin et al. 2001; Furnas 2003; McCulloch et al. 2003). Thus, while exposure to low amounts of sediment-poor freshwater seems to reduce fertilisation success only in a minor way, it constitutes a major problem for coral fertilisation if that freshwater carries enhanced levels of dissolved inorganic nutrients and sediments, as often found in flood plumes from agriculturally modified catchments. The GBR lagoon, which covers an area of 30,000 km^2, currently receives on average 66 km^3 of freshwater, 14 to 28 million tonnes of sediment, and 43,000 and 1,300 to 22,000 tonnes of nitrogen and phosphorus, respectively, from the land per year (Furnas 2003). A significant proportion of these nutrients are associated with particulate matter (Verstraeten and Poesen 2000; Vaze and Chiew 2004), increasing the potential of synergistic detrimental effects on coral reproduction and on the resilience of nearshore reefs.

The early life history stages of coral have been shown to be extremely sensitive to changes in water quality (Ward and Harrison 1997; Negri et al. 2005; Markey et al. 2007), partic-

Table 7 Results of the sediment and water quality properties measured to characterise each of the six sediments (means ± s.e.) used in Experiments 1–3, including Grain Size Index (GSI), Geochemical Parameters (GCP), Organic and Nutrient related Parameters (ONP) and Dissolved Nutrient Index (DNI)

	AIMS Jetty	Chester river	High island	Wilkie island	Offshore	Aragonite
Grain size parameters (PP)						
Mean grain size (μm)	11	20	13	15	17	23
50% of sample volume = median of grain size distribution (GSD) (μm)	7	14	7	9	12	19
25% of sample volume (GSD) (μm)	3	7	3	4	6	6
75% of sample volume (GSD) (μm)	14	26	14	19	23	35
Organic and nutrient related parameters (ONP)						
AFDW [%]	13.0 ± 0.8	16.3 ± 0.4	11.9 ± 0.8	12.0 ± 0.3	10.2 ± 0.7	6.5 ± 0.6
C/N ratio	11.35	11.03	6.57	6.20	4.30	3.28
Chlorophyll *a* (μg g DW^{-1})	3.54 ± 0.32	11.12 ± 0.68	2.82 ± 0.42	3.89 ± 0.66	9.36 ± 0.58	0.55 ± 0.18
Phaeophytin (μg g DW^{-1})	19.84 ± 0.68	37.54 ± 2.36	15.88 ± 0.64	19.87 ± 3.63	21.31 ± 1.50	1.98 ± 0.70
TOC (mg g DW^{-1})	20.07 ± 1.19	50.15 ± 2.84	12.53 ± 0.25	13.16 ± 0.42	17.37 ± 1.12	2.78 ± 0.35
TN (mg g DW^{-1})	1.77 ± 0.18	4.55 ± 0.54	1.91 ± 0.12	2.12 ± 0.22	4.04 ± 0.49	0.85 ± 0.26
TP (μg kg DW^{-1})	4.83 ± 0.27	11.42 ± 0.41	5.58 ± 0.36	5.76 ± 0.28	14.39 ± 0.62	0.64 ± 0.18
Geochemical parameters (GCP)						
Ca (mmol g^{-1})	0.197 ± 0.003	0.267 ± 0.006	1.41 ± 0.034	1.86 ± 0.009	7.30 ± 0.207	10.1 ± 0.008
Mg (mmol g^{-1})	0.759 ± 0.006	0.677 ± 0.011	0.615 ± 0.010	0.887 ± 0.011	0.757 ± 0.000	0.084 ± 0.000
Al (mmol g^{-1})	2.39 ± 0.034	2.35 ± 0.039	2.28 ± 0.007	1.86 ± 0.058	0.287 ± 0.001	0.010 ± 0.000
Fe (mmol g^{-1})	0.721 ± 0.006	0.489 ± 0.013	0.572 ± 0.022	0.464 ± 0.011	0.067 ± 0.002	0.004 ± 0.000
Mn (μmol g^{-1})	8.90 ± 0.070	4.37 ± 0.012	8.94 ± 0.181	5.61 ± 0.068	0.760 ± 0.001	0.091 ± 0.001
Ba (μmol g^{-1})	0.662 ± 0.011	0.660 ± 0.006	0.489 ± 0.008	0.508 ± 0.017	0.103 ± 0.002	0.111 ± 0.000
Zn (μmol g^{-1})	1.133 ± 0.006	0.863 ± 0.005	0.989 ± 0.009	0.707 ± 0.006	0.130 ± 0.004	0.221 ± 0.004
V (μmol g^{-1})	1.60 ± 0.055	0.97 ± 0.029	1.34 ± 0.015	1.08 ± 0.138	<0.196	<0.196
Cu (μmol g^{-1})	0.346 ± 0.001	0.141 ± 0.001	0.235 ± 0.002	0.136 ± 0.005	0.038 ± 0.002	0.069 ± 0.001
Co (μmol g^{-1})	0.196 ± 0.008	0.133 ± 0.001	0.171 ± 0.001	0.107 ± 0.007	<0.017	<0.017
Pb (μmol g^{-1})	0.091 ± 0.001	0.115 ± 0.002	0.109 ± 0.010	0.083 ± 0.000	0.016 ± 0.000	0.010 ± 0.000
Ni (μmol g^{-1})	0.343 ± 0.017	0.179 ± 0.004	0.469 ± 0.009	0.223 ± 0.013	0.131 ± 0.006	0.036 ± 0.006
Cd (μmol g^{-1})	0.154 ± 0.011	0.117 ± 0.030	0.185 ± 0.066	0.082 ± 0.025	0.285 ± 0.027	0.190 ± 0.001
Dissolved nutrients (DNI)						
DOC	1.16 ± 0.14	1.41 ± 0.05	1.21 ± 0.11	1.77 ± 0.22	1.47 ± 0.06	1.38 ± 0.06
PO_4	1.27 ± 0.95	0.17 ± 0.03	0.41 ± 0.19	2.93 ± 2.71	0.23 ± 0.04	0.22 ± 0.04
Si	5.60 ± 1.77	5.79 ± 2.74	8.43 ± 4.36	6.67 ± 2.87	7.06 ± 3.99	4.04 ± 3.99
NH_4	0.66 ± 0.50	0.22 ± 0.01	0.24 ± 0.02	0.19 ± 0.00	1.85 ± 1.08	0.75 ± 0.37
NO_2	0.30 ± 0.03	0.35 ± 0.07	0.46 ± 0.06	0.40 ± 0.02	0.40 ± 0.03	0.48 ± 0.03
NO_3	1.01 ± 0.15	1.48 ± 0.14	2.23 ± 0.78	1.53 ± 0.25	1.16 ± 0.15	1.41 ± 0.15
Indices						
GSI	−4.17	3.08	−3.83	−1.63	1.11	5.43
ONP	0.35	9.80	−2.14	−1.39	2.29	−8.90
GCP	9.38	2.20	8.07	0.59	−5.78	−14.47
DNI	−3.75	−2.28	2.24	3.27	1.44	−0.92

ularly fertilisation (Harrison and Ward 2001; Reichelt-Brushett and Harrison 2005). The finding that environmentally realistic changes in suspended sediment, salinity and dissolved inorganic nutrients can have a negative impact on fertilisation, and to a lesser extent on development, is clearly a reason for concern. Coral reefs around the world are under increasing threat from overfishing (Jackson et al. 2001), urban development (Hughes and Connell 1999), and climate change (Hoegh-Guldberg 1999; Hughes et al. 2003). An important aspect of the ability of coral reefs to withstand these ongoing disturbances is successful reproduction and recruitment. If recruitment is a limiting event in the life history

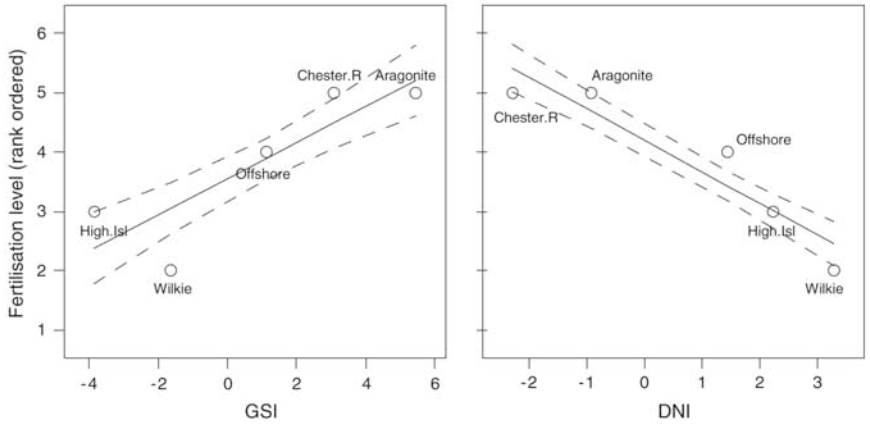

Fig. 4 Level of fertilisation in *Acropora millepora* (rank ordered) after exposure to five different sediment types characterised by indices for sediment grain size (GSI) and dissolved nutrients (DNI). The solid and dashed lines indicate the linear regression fit and 95% confidence intervals of the regression line, respectively

Table 8 Spearman rank correlation analysis testing the relationship between the ranks of % fertilisation and the properties of sediments used in Experiment 3. Sediment properties are: the indices for sediment grain size (GSI), geochemical parameters (GCP), organic and nutrient related parameters (ONP) and dissolved nutrients (DNI)

	S	rho	*P*
GSI	2.558	0.872	0.054
GCP	27.182	−0.359	0.553
ONP	17.948	0.103	0.870
DNI	39.494	−0.975	0.005

of corals, then any reduction in fertilisation levels and additional increases in embryonic abnormalities will have profound consequences for the ability of coral reefs to recover from disturbances. This study therefore again confirms that the prevention of terrestrial runoff of nutrients and sediments through sustainable land management is an important management tool for reef conservation.

Acknowledgements This study was supported by the Australian Institute of Marine Science, the Catchment-to-Reef Program of the Cooperative Research Centre of the Great Barrier Reef World Heritage Area, and the Marine and Tropical Sciences Research Facility (MTSRF), part of the Australian Government's Commonwealth Environment Research Facilities programme. MW acknowledges the support through a PhD scholarship by the German Academic Exchange Service (DAAD) and the Max-Planck-Society, Germany. The authors would like to thank Andrew Negri and three anonymous reviewers for constructive comments on this manuscript.

References

Alutoin S, Boberg J, Nyström M, Tedengren M (2001) Effects of the multiple stressors copper and reduced salinity on the metabolism of the hermatypic coral *Porites lutea*. Mar Environ Res 52:289–299

Babcock RC, Heyward AJ (1986) Larval development of certain gamete-spawning scleractinian corals. Coral Reefs 5:111–116

Babcock RC, Bull GD, Harrison PL, Heyward AJ, Oliver JK, Wallace CC, Willis BL (1986) Synchronous spawnings of 105 scleractinian coral species on the Great Barrier Reef. Mar Biol 90:379–394

Ball EE, Hayward DC, Reece-Hoyes JS, Hislop NR, Samuel G, Saint R, Harrison PL, Miller DJ (2002) Coral development: from classical embryology to molecular control. Int J Dev Biol 46:671–678

Bassim KM, Sammarco PW (2003) Effects of temperature and ammonium on larval development and survivorship in a scleractinian coral (*Diploria strigosa*). Mar Biol 142:241–252

Bassim KM, Sammarco PW, Snell TL (2002) Effects of temperature on success of (self and non-self) fertilization and embryogenisis in *Diploria strigosa* (Cnidaria, Scleractinia). Mar Biol 140:479–488

Brodie J, De'ath G, Devlin M, Furnas M, Wright M (2007) Spatial and temporal patterns of near-surface chlorophyll *a* in the Great Barrier Reef. Mar Freshwt Res 58:342–353

Chao SY (1988) Wind-driven motion of estuarine plumes. J Phys Oceanogr 18:1144–1166

Cox EF, Ward S (2002) Impact of elevated ammonium on reproduction in two Hawaiian scleractinian corals with different life history patterns. Mar Poll Bull 44:1230–1235

Crump BC, Baross JA (1996) Particle-attached bacteria and heterotrophic plankton associated with the Columbia River estuarine turbidity maxima. Mar Ecol Prog Ser 138:265–273

Devlin MJ, Brodie J (2005) Terrestrial discharge into the Great Barrier Reef Lagoon: nutrient behaviour in coastal waters. Mar Pollut Bull 51:9–22

Devlin M, Waterhouse J, Taylor J, Brodie J (2001) Flood plumes in the Great Barrier Reef: spatial and temporal patterns in composition and distribution. Great Barrier Reef Marine Park Authority, Research Publication No. 68, Townsville

Fabricius KE (2005) Effects of terrestrial runoff on the ecology of corals and coral reefs: review and synthesis. Mar Pollut Bull 50:125–146

Fabricius KE, De'ath G, McCook L, Turak E, Milliams DMcB (2005) Changes in algal, coral and fish assemblages along water quality gradients on the inshore Great Barrier Reef. Mar Pollut Bull 51:384–398

Furnas M (2003) Catchments and corals: Terrestrial runoff to the Great Barrier Reef. Australian Institute of Marine Science and CRC Reef Research Centre, Townsville

Furnas MJ, Mitchell AW (1999) Wintertime carbon and nitrogen fluxes on Australia's Northwest Shelf. Estuar Coast Shelf Sci 49:65–175

Furnas M, Mitchell AM, Skuza M (1995) Nitrogen and phosphorus budgets for the Central Great Barrier Reef Shelf. Great Barrier Reef Park Marine Authority, Research Publication No. 36, Townsville

Galbraith RV, MacIsaac EA, Macdonald JS, Farrell AP (2006) The effect of suspended sediment on fertilization success in sockeye (*Oncorhynchus nerka*) and coho (*Orcorhynchus kisutch*) salmon. Can J Fish Aquat Sci 63:2487–2494

Gilmour J (1999) Experimental investigation into the effects of suspended sediment on fertilisation, larval survival and settlement in a scleractinian coral. Mar Biol 135:451–462

Harrington L, Fabricius K, Eaglesham G, Negri A (2005) Synergistic effects of diuron and sedimentation on photosynthesis and survival of crustose coralline algae. Mar Pollut Bull 51:415–427

Harrison PL, Ward S (2001) Elevated levels of nitrogen and phosphorus reduce fertilisation success of gametes from scleractinian reef corals. Mar Biol 139:1057–1068

Harrison PL, Babcock RC, Bull GD, Oliver JK, Wallace CC, Willis BL (1984) Mass spawning in tropical reef corals. Science 223: 1186–1188

Hayashibara T, Ohike S, Kakinuma Y (1997) Embryonic and larval development and planula metamorphosis of four gamete-spawning *Acropora* (Anthozoa, Scleractinia). Proc 8th Int Coral Reef Sym 2:1231–1236

Haynes D, Johnson JE (2000) Organochlorine, heavy metal and polyaromatic hydrocarbon pollutant concentrations in the Great Barrier Reef (Australia) environment: a review. Mar Pollut Bull 41:267–278

Haynes D, Michalek-Wagner K (2000) Water quality in the Great Barrier Reef World Heritage Area: past perspectives, current issues and new research directions. Mar Pollut Bull 41:428–434

Hoegh-Guldberg O (1999) Climate change, coral bleaching and the future of the world's coral reefs. Mar Freshw Res 50:839–866

Hughes TP, Connell JH (1999) Multiple stressors on coral reefs: a long-term perspective. Limnol Oceanogr 44:932–940

Hughes TP, Baird AH, Bellwood DR, Card M, Connolly SR, Folke C, Grosberg R, Hoegh-Guldberg O, Jackson JBC, Kleypas J, Lough JM, Marshall P, Nystroem M, Palumbi SR, Pandolfi JM, Rosen B, Roughgarden J (2003) Climate change, human impacts, and the resilience of coral reefs. Science 301:929–933

Hutchings P, Haynes D (2005) Marine Pollution Bulletin special edition editorial. Mar Pollut Bull 51:1–2

Hutchings P, Haynes D, Goudkamp K, McCook L (2005) Catchment to reef: water quality issues in the Great Barrier Reef region - an overview of papers. Mar Pollut Bull 51:3–8

Jackson JBC, Kirby MX, Berger WH, Bjorndal KA, Botsford LW, Bourque BJ, Bradbury RH, Cooke R, Erlandson J, Estes JA, Hughes TP, Kidwell S, Lange CB, Warner RR (2001) Historical overfishing and the recent collapse of coastal ecosystems. Science 293:629–638

Kerswell AP, Jones RJ (2003) Effects of hypo-osmosis on the coral *Stylophora pistillata*: nature and cause of 'low-salinity bleaching'. Mar Ecol Prog Ser 253:145–154

Koop K, Booth B, Broadbent A, Brodie J, Bucher D, Capone D, Coll J, Dennison W, Erdmann M, Harrison P, Hoegh-Guldberg O, Hutchings P, Jones GB, Larkum AWD, O'Neill J, Steven A, Tentori E, Ward S, Williamson J, Yellowlees D (2001) ENCORE: The effect of nutrient enrichmenton coral reefs. Synthesis of results and conclusions. Mar Poll Bull 42:91–120

Loring DH, Rantala RTT (1992) Manual for the geochemical analyses of marine sediments and suspended matter. Earth Sci Rev 32:235–283

Luick JL, Mason L, Hardy T, Furnas MJ (2007) Circulation in the Great Barrier Reef Lagoon using numerical tracers and *in situ* data. Cont Shelf Res 27:757–778

Markey KL, Baird AH, Humphrey C, Negri AP (2007) Insecticides and a fungicide affect multiple coral life stages. Mar Ecol Prog Ser 330:127–137

Marshall DJ (2006) Reliably estimating the effect of toxicants on fertilization success in marine broadcast spawners. Mar Pollut Bull 52:734–738

McCulloch M, Fallon S, Wyndham T, Hendy E, Lough J, Barnes D (2003) Coral records of increased sediment flux to the inner Great Barrier Reef since European settlement. Nature 421:727–730

Moberg F, Nyström M, Kautsky N, Tedengren M, Jarayabhand P (1997) Effects of reduced salinity on the rates of photosynthesis and respiration in the hermatypic corals *Porites lutea* and *Pocillopora damicornis*. Mar Ecol Prog Ser 157:53–59

Muthiga NA, Szmant AM (1987) The effects of salinity stress on the rates of aerobic respiration and photosynthesis in the hermatypic coral *Siderastrea siderea*. Biol Bull 173:539–551

Negri AP, Heyward AJ (2000) Inhibition of fertilization and larval metamorphosis of the coral *Acropora millepora* (Ehrenberg, 1834) by petroleum products. Mar Pollut Bull 41:420–427

Negri A, Vollhardt C, Humphrey C, Heyward A, Jones R, Eaglesham G, Fabricius K (2005) Effects of the herbicide diuron on the early life history stages of coral. Mar Pollut Bull 51:370–383

Neil DT, Orpin AR, Ridd PV, Yu B (2002) Sediment yield and impacts from river catchments to the Great Barrier Reef lagoon. Mar Freshw Res 53:733–752

Okubu N, Motokawa T (2007) Embryogenesis in the reef-building coral *Acropora* spp. Zool Sci 24:1169–1177

Oliver J, Babcock R (1992) Aspects of the fertilization ecology of broadcast spawning corals: sperm dilution effects and *in situ* measurements of fertilization. Biol Bull 183:409–417

Pailles C, Moody PW (1992) Phosphorus sorption-desorption by some sediments of the Johnstone Rivers catchment, northern Queensland. Aust J Mar Freshw Res 43:1535–1545

Parker JG (1983) A comparison of methods used for the measurement of organic matter in marine sediments. Chem Ecol 1:201–210

R Development Core Team (2008) R: A language and environment for statistical computing. R Foundation for Statistical Computing, Vienna, URL http://www.R-project.org

Reichelt-Brushett AJ, Harrison PL (2005) The effect of selected trace metals on the fertilization success of several scleractinian coral species. Coral Reefs 24:524–534

Richmond RH (1993) Effects of coastal runoff on coral reproduction. In: Ginsburg RN (compiler) Proceedings of the colloquium on global aspects of coral reefs: health, hazards and history. Rosenthiel School of Marine and Atmospheric Science, University of Miami, Miami, pp 360–364

Ryle VD, Wellington J (1982) Reduction column for automated determination of nitrates. Analytical Laboratory Note No. 19. Australian Institute for Marine Science, Townsville

Ryle VD, Mueller HR, Gentien P (1981) Automated analysis of nutrients in tropical seawaters. AIMS Oceanography Series Technical Bulletin No. 3. Australian Institute of Marine Science, Townsville

Rogers CS (1990) Responses of coral reefs and reef organisms to sedimentation. Mar Ecol Prog Ser 62:185–202

Strickland JDH, Parsons TR (1972) A practical handbook of seawater analysis. Fisheries Research Board of Canada, Bulletin 167, Ottawa

Vaze J, Chiew HS (2004) Nutrient loads associated with different sediment sizes in urban stormwater and surface pollutants. J Environ Eng 130:391–396

Vermeij MJA, Fogarty ND, Miller MW (2006) Pelagic conditions affect larval behaviour, survival, and settlement patterns in the Caribbean coral *Montastraea faveolata*. Mar Ecol Prog Ser 310:119–128

Verstraeten G, Poesen J (2000) Assessments of sediment fixed nutrient export from small drainage basins in central Belgium using retention ponds. In: Stone M (ed) The role of erosion and sediment transport in nutrient and contaminant transfer. IHAS Publication No 263. IAHS Press, Wallingford, pp 243–249

Ward S, Harrison PL (1997) The effects of elevated nutrient levels on settlement of coral larvae during the ENCORE experiment, Great Barrier Reef, Australia. Proc 8th Int Coral Reef Symp 1:891–896

Ward S, Harrison PL (2000) Changes in gametogenesis and fecundity of acroporid corals that were exposed to elevated nitrogen and phosphorus during the ENCORE experiment. Exp Mar Biol Ecol 246:179–221

Weber M, Lott C, Fabricius KE (2006) Sedimentation stress in a scleractinian coral exposed to terrestrial and marine sediments with contrasting physical, organic and geochemical properties. J Exp Mar Biol Ecol 336:18–32

Wild C, Tollrian R, Huettel M (2004) Rapid recycling of coral mass-spawning products in permeable reef sediments. Mar Ecol Prog Ser 271:159–166

Wolanski E (1994) Physical oceanographic processes of the Great Barrier Reef. CRC Press, Boca Raton, Florida

Wolanski E, Fabricius K, Spagnol S, Brinkman R (2005) Fine sediment budget on an inner-shelf coral-fringed island, Great Barrier Reef of Australia. Estuar Coast Shelf Sci 65:153–158

Wolanski E, Fabricius KE, Cooper TF, Humphrey C (2008) Wet season sediment dynamics on the inner shelf of the Great Barrier Reef. Estuar Coast Shelf Sci 77:755–762

Woolfe KJ, Michibayashi K (1995) "Basic" entropy grouping of laser-derived grain-size data: an example from the Great Barrier Reef. Comput Geosci 21:447–462

Chapter 3

Sedimentation stress in a scleractinian coral exposed to terrestrial and marine sediments with contrasting physical, organic and geochemical properties

ELSEVIER

Journal of Experimental Marine Biology and Ecology 336 (2006) 18–32

Journal of EXPERIMENTAL MARINE BIOLOGY AND ECOLOGY

www.elsevier.com/locate/jembe

Sedimentation stress in a scleractinian coral exposed to terrestrial and marine sediments with contrasting physical, organic and geochemical properties

M. Weber [a,b,c,*], C. Lott [a,b,c], K.E. Fabricius [a]

[a] *Australian Institute of Marine Science, PMB No 3, Townsville, QLD 4810, Australia*
[b] *HYDRA Institute for Marine Sciences, Elba Field Station, Via del Forno 80, I-57034 Campo nell'Elba (LI), Italy*
[c] *Max Planck Institute for Marine Microbiology, Celsiusstrasse 1, 28359 D-Bremen, Germany*

Received 19 December 2005; received in revised form 14 March 2006; accepted 14 April 2006

Abstract

Terrestrial runoff increases siltation and nutrient availability on coastal coral reefs worldwide. However the factors determining stress in corals when exposed to short-term sedimentation, including the interactions between sediments and nutrients, are little understood. We exposed corals to ten different sediment types at environmentally relevant concentrations (33 to 160 mg DW cm^{-2}) and exposure times (12 to 60 h) in laboratory and field experiments. The sediments originated from 2 estuaries, 2 nearshore and one offshore locations and also included ground-up aragonite. For two of these sediments, three grain size fractions were used (silt <63 μm, fine sand: 63–250 μm, medium sand: 250–500 μm). Sediments were characterised by 19 parameters grouped into "physical", "organic and nutrient-related" and "geochemical" parameters. Changes in the photosynthetic yield of the coral *Montipora peltiformis* was measured by pulse–amplitude modulated chlorophyll fluorometry (PAM) as proxy for photophysiological stress from exposure, and to determine rates of recovery. Different sediments exerted greatly contrasting levels of stress in the corals. Our results show that grain size and organic and nutrient-related sediment properties are key factors determining sedimentation stress in corals after short-term exposure. Photophysiological stress was measurable after 36 h of exposure to most of the silt-sized sediments, and coral recovery was incomplete after 48 to 96 h recovery time. The four sandy sediment types caused no measurable stress at the same concentration for the same exposure time. Stress levels were strongly related to the values of organic and nutrient-related parameters in the sediment, weakly related to the physical parameters and unrelated to the geochemical parameters measured. *M. peltiformis* removed the sandy grain size classes more easily than the silt, and nutrient-poor sediments were removed more easily than nutrient-rich sediments. Anoxia developed on the sediment surfaces of the nutrient-rich silts, which had become slimy and smelled of hydrogen sulphide, suggesting increased bacterial activity. Our finding that silt-sized and nutrient-rich sediments can stress corals after short exposure, while sandy sediments or nutrient-poor silts affect corals to a lesser extent, will help refining predictions of sedimentation threats to coral reefs at given environmental conditions.

Keywords: Great Barrier Reef; Nutrient enrichment; Scleractinia; Sedimentation; Sediment properties; Terrestrial runoff

* Corresponding author. HYDRA Institute for Marine Sciences, Elba Field Station, Via del Forno 80, I-57034 Campo nell'Elba (LI), Italy. Tel.: +390565988027; fax: +390565988090.
E-mail address: m.weber@hydra-institute.com (M. Weber).

0022-0981/$ - see front matter © 2006 Elsevier B.V. All rights reserved.
doi:10.1016/j.jembe.2006.04.007

1. Introduction

Increasing terrestrial runoff of sediments, nutrients and chemical pollutants into coastal ecosystems has been identified as cause of degradation of some coastal corals reefs (Brodie et al., 2001; Devlin and Brodie, 2005). Of the various components of terrestrial runoff, sedimentation is reported to be among the most important agents of change (Roger, 1990; Fabricius, 2005). River plumes can discharge 5–300 mg L^{-1} of fine suspended solids rich in organics (Devlin et al., 2001), and sedimentation rates on some reefs have been found to exceed 300 mg DW cm^{-2} day^{-1} (Mapstone et al., 1989; Weber, 2003). The effects of sedimentation on stony corals have been studied for many years (reviews in Roger, 1990; Fabricius, 2005). What is known is that short-term sediment exposure affects corals by reducing their photosynthetic efficiency while increasing respiration, resulting in bleaching and necrosis (Riegl and Branch, 1995; Philipp and Fabricius, 2003). Sediment rejection activities through mucus production, polyp movement and tissue swelling further increase energy expenditure (Bak and Elgershuizen, 1976 and references therein). It is also known that rejection success varies between coral species and also between sediment types (Stafford-Smith and Ormod, 1992; Stafford-Smith, 1993). Furthermore, experimental studies have shown that sedimentation stress, and recovery after short-term sedimentation, are a linear function of the amount and duration of sediment deposited on the corals (Philipp and Fabricius, 2003).

Despite previous research efforts, the agents and mechanisms responsible for the damage on fauna and flora during sedimentation are still poorly understood. In this study we define sediment as "matter that settles to the bottom of a liquid" (Oxford English Dictionary), hence any matter including minerals, inorganic and organic matter. Studies on the effects of sedimentation often focus on the amount (weight) of sediment, ignoring that sediment consists of a vast and contrasting array of mineral particles varying in grain sizes, organic particles such as living organisms, detritus, mucus and exopolymeric particles, and that it can be a carrier of adsorbed or particulate nutrients and contaminants. Synergistic effects between sedimentation stress and nutrient concentrations in the sediments have been discussed before (Fabricius and Wolanski, 2000; Fabricius et al., 2003). Similarly, synergistic effects between sedimentation and herbicides have been found in crustose coralline algae, where sedimentation stress is greatly enhanced by the presence of traces of the herbicide diuron (Harrington et al., 2005). Such knowledge on synergistic effects between various sediment properties is needed to better understand the potential harm to corals from exposure to sedimentation.

In this study we investigated the effects of 10 different types of sediments of terrestrial, nearshore and offshore marine origin, with different properties, on corals in laboratory and field experiments. The study presents results on the photophysiological stress-responses in the scleractinian coral *Montipora peltiformis*, its ability to reject sediments and recover from exposure to varying periods of sedimentation by the different sediment types at varying but environmentally relevant concentrations. Measurements of 19 different sediment properties helped to better understand the relationships between sediment characteristics and extent of damage a coral may experience when exposed to re-suspended seafloor sediments compared with fine estuarine sediments from pristine or agriculturally used catchments.

2. Material and methods

2.1. Sediments: origin and analysis methods

Sediments were collected from the shores of two river estuaries and from sediments accumulated on three coral reefs. The upper 5 cm of sediment were collected from just below the water level at the estuarine shores of Herbert River (HR) (18° 31.5′ S, 146° 19.1′ E), the lower catchment of which is agriculturally used, and Normanby River (NR) (14° 55′ S, 144° 12.5′ E), a catchment in the Far Northern Queensland with little to no agriculture. The upper 5 cm of marine sediments were collected by SCUBA from 5 to 10 m depth from the leeward sides of the nearshore fringing reefs of High Island (NS2) (17° 09.6′ S, 146° 00.3′ E) and Wilkie Island (NS1) (13° 46.03′ S, 143° 38.07′ E), and the lagoon of the offshore Otter Reef (OS) (19° 23.5′ S, 148° 05.5′ E). The sixth sediment type was pure carbonate: we used aragonite saw-dust (AR), a by-product of slicing coral skeletons of massive *Porites sp*. for growth band analyses, kindly provided by Janice Lough (AIMS).

Three grain size classes were used of the estuarine Herbert River (HR) and offshore (OS) sediment. These were: silts (S) of <63 μm grain size, (henceforth called HR-S and OS-S); fine (F) sands of 63–250 μm grains (HR-F and OS-F); and medium (M) sands of 250–500 μm grains (HR-M and OS-M). Of the remaining four sediment types only the silt-sized class (<63 μm) was used: estuarine Normanby River (NR-S), nearshore 1 and 2 (NS1-S and NS2-S), and aragonite dust (AR-S). The sediments were wet-sieved with plastic sieves to obtain the desired grain

Table 1
List of the sediment parameters measured to characterise each of the ten sediments, and of the analytical methods used

Parameter	Method	Description
a) Physical parameters (PP)		
Grain size distribution (GSD)[a]	Laser defraction	Determined grain size frequency distribution with Masterseries X Malvern Particle Sampler (32 detector ranges); detector lens = 1000 μm for HR-S, HR-F and HR-M and 300 μm for HR-S, NR-S, NS1-S, NS2-S, OS-S and AR-S.
Settling volume (SV) Settling rate (SR) Compaction (Comp)[b, c]	Imhoff funnels	SV was determined by suspending 15 g DW of sediment in 1000 ml seawater in Imhoff funnels and expressed as proportion of total volume after 2 h settling time. SR was obtained by measuring the sediment volume after 15, 30, 60 and 90 min. Comp was determined by measuring the sediment volume after 0.5, 1, 1.5, 2, 18 and 38 h (after 2 h settling time), and calculated as proportion of SV.
Relative light transmission (RLT)	2π light sensor (Walz, Germany).	RLT was measured through a petri dish filled with an even layer of sediment (160 and 66 mg DW cm^{-2}), and compared with light transmission through a water-filled petri dish. An Intralux 5000 K-Lamp at constant distance was used as light source, providing 840 μmol m^{-2} s^{-1}.
b) Organic and nutrient-related parameters (ONP)		
Ash-free dry weight (AFDW)[d]	Combustion	Sediments dried at 100 °C for 24 h, weighed, heated at 500 °C for 1 h, and re-weighed.
Total organic carbon (TOC)[e]	Combustion	Shimadzu TOC-5000 carbon analyser (Shimadzu Corporation, Kyoto, Japan)
Total nitrogen (TN)[f]	Combustion	ANTEK Solid Auto Sampler (Antek Instruments, Inc., Houston, Texas, USA)
Total phosphorous (TP)[g]	Spectrometrically	Varian Liberty 220 ICP atomic emission spectrometer (ICP-AES)
Chlorophyll a (Chl a) and phaeophytin (Phaeo)[h]	Spectrophotometerically	UV-160l–Visible spectrophotometer (Shimadzu Corporation, Australia) after 24 h extraction in acetone in dark at 4 °C.
c) Geochemical parameters (GCP)		
Al, Ba, Cu, Fe, Mn, Ni, Pb, Zn and V[g]	Spectrometrically	Varian Liberty 220 ICP atomic emission spectrometer (ICP-AES)

The parameters are grouped into three categories: "physical parameters" (PP), "organic and nutrient-related parameters" (ONP), and "geochemical parameters" (GCP).
[a] Woolfe and Michibayashi, 1995.
[b] Folk, 1980.
[c] DIN 38409-H9.
[d] Parker, 1983.
[e] Furnas and Mitchell, 1999.
[f] Furnas and Skuza, 1995.
[g] Loring and Rantala, 1992.
[h] Lorenzen, 1967.

size fractions, and stored as stock solution in aerated seawater in 60 L bins until the experiments commenced.

Nineteen parameters were used to characterise the properties of the ten sediment types (Table 1). These parameters were grouped into three categories: here called "physical" parameters (PP), "organic and nutrient-related" parameters (ONP), and "geochemical" parameters (GCP). Sediment parameters were *z*-transformed and values summed for each sediment type to obtain specific coefficients for physical parameters (PP_{co}), organic and nutrient-related parameters (ONP_{co}), and geochemical parameters (GCP_{co}). PP_{co} was calculated as the sum of *z*-scores of the four parameters: sediment volume, settling rate after 15 min, compaction and light transmission. ONP_{co} was calculated as the sum of *z*-scores of the six parameters: chlorophyll a (Chl a) and phaeophytin (Phaeo) at the beginning (hence excluding the highly correlated values at the end of the exposure), ash-free dry weight (AFDW, a measure of organic matter), total organic carbon (TOC), total nitrogen (TN) and total phosphorous (TP). GCP_{co} was calculated as the sum of *z*-scores of the nine metals and trace elements (Table 1).

2.2. Coral stress measurements

The flat-foliose coral *M. peltiformis* that is abundant on northern nearshore reefs of the Great Barrier Reef was used for all experiments. For the tank experiments, fragments 50 cm^2 in size were collected from 5 to 7 m depth at Hannah Island (13° 52′ S, 143° 38′ E), and left to recover in 60 L flow-through aquariums for at least two days, whereas in the field experiments attached and undisturbed corals were used. Photosynthetic yields of photosystem II of the zooxanthellae were measured with a pulse–amplitude modulated chlorophyll fluorometer (PAM; Schreiber et al., 1986) as a proxy for photophysiological stress in the corals, as described in Philipp and Fabricius (2003). Briefly, F_0 was measured by applying a pulsed measuring beam (<1 μmol quanta m^{-2} s^{-1}), followed by a saturation pulse of white light to record F_m (>1000 μmol quanta m^{-2} s^{-1}). Maximal quantum yield was calculated as the ratio of variable to maximum fluorescence (F_v/F_m).

2.3. Tank experiments

Tank experiments where conducted at the Australian Institute of Marine Science (AIMS) in December 2002, and aboard the RV "The Lady Basten" in January/February 2003. The following protocol was common to the 3 tank experiments conducted: Ten coral pieces and four petri dishes were placed in 60 L plastic bins filled with seawater (29–30 °C), with constant flow-through of fresh seawater at a rate of 2 L min^{-1}. After 60 min of dark-adaptation, photosynthetic yields were measured by PAM. After the seawater flow-through was temporally turned off, sediment was applied to achieve final amounts of 33, 66, 100, 133 or 160 mg DW cm^{-2}. After 1 to 2 h of settlement time two coral fragments were added to each bin as controls (hence remaining free of sediments) and two petri dishes were removed to determine the sediment amount (DW), and concentrations of Chl a, Phaeo, TC, TOC, TN and TP. The latter was achieved by filtering subsamples onto precombusted GF/F glass fibre filters (0.2 μm nominal pore width), which were wrapped in aluminium foil and frozen at −20 °C until analysis. The seawater flow was turned on again, and after the water had cleared each coral fragment was photographed to determine the sediment-covered areas.

After exposure times of 12, 20, 36, 44 or 60 h, two to four coral fragments per bin were carefully removed and their sediment was washed off into a plastic jar with a gentle water jet for later determination of sediment DW in relation to the (photographically determined) area of coral covered by the sediment. The photosynthetic yields of the dark-adapted coral fragments were measured immediately by PAM. Fragments were returned into the flow-through tanks to determine recovery by measuring their dark-adapted yields every 24 h for up to two or four days. After the last fragments were sampled (longest exposure time: 44 or 60 h) the remaining two petri dishes were removed and their sediment was analysed as described above.

2.4. Experiment 1

The aim of experiment 1 was to investigate differences in the effects of sediment types of different grain sizes (silt, fine and medium sand). The sediments used were HR-M, HR-F, HR-S, OS-M, OS-F, OS-S, and AR-S. The nominal sediment cover was 160 mg DW cm^{-2}. For each sediment type, two tanks were set up, from each of which two to three coral fragments were sampled each after 12, 36 and 60 h. Recovery was measured for two to four days after the end of exposure.

2.5. Experiment 2

The aim of experiment 2 was to investigate the dose–response relationships of *M. peltiformis* exposed to low amounts and short duration of silty estuarine (HR-S) sediment. The nominal sediment cover was 33, 66, 100 and 133 mg DW cm^{-2}. Two to three fragments were sampled each after 12, 20, 36 and 44 h of exposure. Exposure was calculated as

$$E = \text{exposure time} \cdot \text{amount of sediment}[\text{h} \cdot \text{mgcm}^{-2}]$$

following Philipp and Fabricius (2003). Recovery was measured for two days.

2.6. Experiment 3

The aim of experiment 3 was to compare the effects of low-level sedimentation by six different types of silt (<63 μm) sediments at a nominal sediment cover of 66 mg DW cm^{-2}. The sediments used were HR-S, NR-S, NS1-S, NS2-S, OS-S, and AR-S. Two to three fragments were sampled after 20 h and 44 h. Recovery was measured for two days.

2.7. Field experiment

The aim of the field experiment was to determine the extent of photophysiological stress from different sediment types in situ at natural flow, wave and light conditions in otherwise undisturbed colonies of *M. peltiformis*. The field experiment was conducted at the front reef of Hannah Island (13°52′ S, 143°38′ E) at 4 to 6 m depth, in January 2003. The effects of three sediment types at a nominal

concentration of 66 mg DW cm^{-2} were compared: HR-S, OS-S and AR-S were applied to separate surface areas on each of 10 large colonies, and left for 24 h. PVC rings (height and diameter: 100 mm) were positioned onto flat colonies of *M. peltiformis*. A plastic bag with the right amount of sediment was attached to the ring and its contents released onto the coral. For the first hour, the plastic bag was left in place, with gaps between PVC ring and coral sealed by small sand bags. After 1 h of settling time the plastic bags were removed, and a digital photograph was taken to determine the size of the sediment-exposed area on the colony. After 24 h exposure, each sediment patch was sucked into a separate 20 L plastic bag with a hand-held battery-driven underwater vacuum pump for later determination of amount and final nutrient contents. The photosynthetic activity of the previously sediment-covered colony surfaces was measured instantly by PAM. Control PAM measurements were taken on light- and dark-adapted (covered by black plastic foil for 1 h) adjacent unexposed areas of the same colonies.

2.8. Calculation of sediment cleared area and sediment amount of coral pieces

The surface area of each coral fragment (A_{tot}), and the area of the fragment covered with sediment (A_{sed}) was determined from the digital photographs with the software NIH (NIH-Image 1.63, freeware © NIH).

$$\text{Freed Area}(\%) = [100-(100 \cdot A_{sed}/A_{tot})]$$

was calculated to determine the percent area cleared of sediment. The sediment samples retrieved from the corals and from the petri dishes were dried at 60 °C until constant dry weight (DW), and related to A_{sed} to determine the actual amount of sediment per unit surface area.

2.9. Statistical analysis

A principal component analysis on sediment property data (*z*-transformed) was used to compare and characterise the ten different sediments. Analyses of variance (ANOVA) were used to test for differences in photosynthetic yields after sediment removal (at 0 h recovery) between treatments (exposure to different sediment origins, grain sizes, amounts, and exposure times). The aim of the present study was to test for differences between sediment types. Since the fact that sedimentation reduces photosynthetic yields compared to control colonies had been shown previously (Philipp and Fabricius, 2003), yields of control colonies were excluded from the statistical analyses of all tank and field experiments (after having confirmed the existence of strong differences between sediment-treated and control colonies in our study; not shown). Differences between yields were expressed as proportion of maximum value observed, and arc sine square root transformed twice to reduce heteroscedasticy. However untransformed data are displayed in the figures for easier interpretation. A linear model was used to determine the relationship between yield and exposure (amount · duration of sediment application) in Experiment 2, and slopes were calculated for yields after 0 h, 24 h and 48 h of recovery. Results from Experiments 1 and 3 were combined to test whether the stress measured in the coral was related to any of the ONP_{co}, PP_{co} or GCP_{co} (sum of *z*-transformed data). For this, a multiple regression model was used, with yield as response variable, and the three coefficients, and exposure *E* as covariates. ANOVA was also used to test for differences in percentage of colony surface freed from sediment between treatments (exposure to different sediment origins, grain sizes, amounts, and duration) in 1, 2 and 3. All analysis where conducted with the software S-Plus (Statistical Science, 1999).

3. Results

3.1. Characterisation of the 10 sediments used

The physical (PP), organic and nutrient-related (ONP) and geochemical properties (GCP) of each of the ten sediments are listed in Table 2.

The coefficient PP_{co} was highest for AR-S and lowest for NS1-S. Median grain sizes of the silt-sized sediments ranged from 9 to 24 μm. The sediment volume (SV) of the fine sediments varied after 2 h settling time between 36.6 ml and 128.3 ml 15 g DW^{-1}. Settling rates (SR) of all 10 sediment types were fastest in the first 15 min and slowed afterwards. Within the first 15 min the 4 sandy sediments, OS-S and AR-S settled to 95–99% (of the 2 h SV), and no further compaction (Comp) occurred. The other 4 fine sediments settled to 71–88% after 15 min. After 38 h these 4 silt sediments were further compacted down to 46.3% of initial volume (SV). Five of 6 silt sediments showed relative light transmission of <0.2% at 66 mg DW cm^{-2}, whereas the bright white coral dust AR-S allowed a transmission of 7.7% at 66 mg DW cm^{-2}, and 1.2% at 160 mg DW cm^{-2}.

The coefficient ONP_{co} was highest for OS-S, and lowest for AR-S. Total organic carbon (TOC), total nitrogen (TN), total phosphorous (TP) chlorophyll a (Chl a) and phaeophytin (Phaeo) were generally higher in the silt sediments (except for AR-S) compared with the two sandy grain size fractions of HR and OS. The

Table 2
Results of the sediment parameters measured to characterise each of the ten sediments, and their coefficients "physical parameters" (PP_{co}), "organic and nutrient-related parameters" (ONP_{co}), and "geochemical parameters" GCP_{co})

		HR-M (Exp. I)	HR-F (Exp. I)	HR-S (Exp. I+II+III)	NR-S (Exp. III)	NS1-S (Exp. III)	NS2-S (Exp. III)	OS-M (Exp. I)	OS-F (Exp. I)	OS-S (Exp. III)	AR-S (Exp. III)
Nominal sediment amount	mg cm^{-2}	160	160	160+66	66	66	66	160	160	160+66	160+66
Freed area	%	52.45	66.13	26.17	68.40	38.47	25.73	65.32	75.11	35.38	78.31
Freed area (SE)		*4.29*	*4.72*	*4.93*	*4.38*	*3.93*	*4.83*	*5.48*	*3.75*	*4.45*	*3.80*
C/N ratio		34.26	27.69	10.49	11.04	7.03	6.98	6.43	6.18	5.54	6.03
Total carbon	%	1.03	0.77	2.30	1.81	3.23	3.89	11.13	11.62	9.94	10.60
TC (SE)		*0.20*	*0.08*	*0.08*	*0.078*	*0.16*	*0.20*	*0.47*	*0.14*	*0.18*	*0.28*
50% of sample volume=median of grain size distribution (GSD)	µm	507	129	10	9	10	9	528	214	17	24
25% of sample volume (GSD)	µm	355	91	4	4	5	5	414	163	7	10
75% of sample volume (GSD)	µm	659	181	22	20	20	18	660	276	40	40
Physical Parameters (PP)											
Relative light transmission	%	0.21	0.12	0.058	0.11	0.090	0.10	4.90	4.37	0.17	7.70
RTL (SE)		*0.023*	*0.007*	*0.011*	*0.004*	*0.008*	*0.006*	*0.15*	*0.16*	*0.017*	*0.25*
Sediment volume	ml 15 g DW^{-1}	14.00	13.00	115.83	50.00	148.33	101.67	11.83	11.33	36.67	12.83
SV (SE)		*<0.001*	*<0.001*	*2.50*	*<0.001*	*1.67*	*1.67*	*0.17*	*0.33*	*0.67*	*0.17*
Settling rate (15 min)	% $15\ min^{-1}$	1.43	1.50	25.17	12.17	25.17	18.83	1.18	1.13	5.00	1.53
SR (SE)		*0.017*	*0.029*	*0.66*	*0.17*	*0.17*	*0.60*	*0.017*	*0.033*	*<0.001*	*0.033*
Settling rate (1 h)	% h^{-1}	1.48	1.33	13.50	5.80	17.33	12.17	1.18	1.13	4.23	1.32
SR (SE)		*0.017*	*<0.001*	*0.17*	*0.10*	*0.17*	*0.17*	*0.017*	*0.033*	*0.033*	*0.017*
Compaction	%	99.00	98.90	49.70	50.00	46.28	51.81	99.10	99.20	70.42	98.67
Comp (SE)		*1.00*	*1.10*	*0.30*	*<0.001*	*0.38*	*0.19*	*1.00*	*1.12*	*0.97*	*1.33*
Organic and nutrient-related parameters (ONP)											
Ash-free dry weight	%	2.27	1.70	8.37	4.52	9.56	11.11	2.23	2.43	5.62	2.01
AFDW (SE)		*0.036*	*0.020*	*0.082*	*0.16*	*0.10*	*0.28*	*0.22*	*0.23*	*0.13*	*0.018*
Chlorophyll a begin	µg g DW^{-1}	4.16	3.82	11.46	4.63	19.76	22.29	9.19	4.34	23.36	2.87
Chl a begin (SE)		*0.35*	*1.39*	*1.75*	*1.26*	*6.31*	*3.78*	*3.30*	*0.17*	*13.64*	*2.18*
Chlorophyll a end	µg g DW^{-1}	24.46	8.33	20.09	6.73	43.31	47.51	20.99	14.40	34.50	7.50
Chl a end (SE)		*11.28*	*5.55*	*4.88*	*0.84*	*8.83*	*1.26*	*5.73*	*0.87*	*16.80*	*0.91*
Phaeophytin begin	µg g DW^{-1}	1.91	2.13	36.10	3.62	53.82	73.08	2.10	1.98	435.52	2.26
Phaeo begin (SE)		*0.14*	*0.29*	*6.03*	*0.50*	*5.72*	*13.29*	*0.02*	*0.56*	*372.37*	*2.78*
Phaeophytin end	µg g DW^{-1}	<0.001	4.18	38.43	3.87	128.58	80.23	7.55	2.85	516.51	2.85
Phaeo end (SE)		*3.61*	*1.61*	*6.58*	*1.51*	*12.95*	*6.56*	*3.63*	*0.83*	*450.41*	*1.25*
Total organic carbon	%	0.80	0.53	1.84	1.58	1.04	1.10	0.25	0.27	0.81	0.17
TOC (SE)		*0.14*	*0.084*	*0.043*	*0.041*	*0.037*	*0.052*	*0.006*	*0.008*	*0.023*	*0.019*
Total nitrogen	%	0.023	0.019	0.17	0.14	0.15	0.16	0.039	0.043	0.15	0.032
TN (SE)		*0.003*	*0.002*	*0.004*	*0.002*	*0.010*	*0.004*	*0.002*	*0.002*	*0.007*	*0.004*
Total phosphorus	%	0.010	0.009	0.036	0.041	0.037	0.041	0.017	0.017	0.033	0.004
TP (SE)		*<0.001*	*<0.001*	*<0.001*	*0.001*	*<0.001*	*<0.001*	*<0.001*	*<0.001*	*<0.001*	*<0.001*
Geochemical parameters (GCP)											
Aluminium	µmol g DW^{-1}	0.025	0.031	0.27	0.30	0.21	0.19	0.0018	0.0017	0.024	0.002

(continued on next page)

Table 2 (*continued*)

		HR-M (Exp. I)	HR-F (Exp. I)	HR-S (Exp. I+II+III)	NR-S (Exp. III)	NS1-S (Exp. III)	NS2-S (Exp. III)	OS-M (Exp. I)	OS-F (Exp. I)	OS-S (Exp. III)	AR-S (Exp. III)
Al (SE)		*0.004*	*0.004*	*0.009*	*0.007*	*0.010*	*0.007*	*<0.001*	*<0.001*	*<0.001*	*<0.001*
Barium	µmol g DW^{-1}	0.15	0.18	0.44	1.62	0.57	0.41	0.055	0.051	0.094	0.101
Ba (SE)		*0.018*	*0.021*	*0.0052*	*0.051*	*0.035*	*0.020*	*0.001*	*0.001*	*0.002*	*0.006*
Copper	µmol g DW^{-1}	0.067	0.083	0.32	0.31	0.15	0.20	0.076	0.016	0.053	0.074
Cu (SE)		*0.003*	*0.029*	*0.019*	*0.013*	*0.002*	*0.008*	*0.058*	*<0.001*	*0.003*	*0.004*
Iron	µmol g DW^{-1}	0.015	0.014	0.058	0.069	0.045	0.043	<0.001	<0.001	0.006	<0.001
Fe (SE)		*0.001*	*<0.001*	*0.002*	*0.002*	*0.002*	*0.002*	*<0.001*	*<0.001*	*<0.001*	*<0.001*
Manganese	µmol g DW^{-1}	3.35	3.92	6.74	1.97	4.53	7.97	0.17	0.13	0.73	0.11
Mn (SE)		*0.31*	*0.29*	*0.22*	*0.046*	*0.17*	*0.24*	*0.033*	*0.008*	*0.007*	*0.008*
Nickel	µmol g DW^{-1}	0.042	0.050	0.34	0.39	0.29	0.31	0.034	0.034	0.075	0.034
Ni (SE)		*0.003*	*0.007*	*0.006*	*0.009*	*0.007*	*0.014*	*<0.001*	*<0.001*	*0.003*	*<0.001*
Lead	µmol g DW^{-1}	0.031	0.034	0.13	0.11	0.060	0.074	0.014	0.014	0.014	0.014
Pb (SE)		*0.006*	*0.001*	*0.003*	*0.009*	*0.002*	*0.002*	*<0.001*	*<0.001*	*<0.001*	*<0.001*
Vanadium	µmol g DW^{-1}	0.19	0.21	0.86	1.65	0.74	0.72	0.040	0.039	0.13	0.039
V (SE)		*0.023*	*0.015*	*0.021*	*0.039*	*0.019*	*0.026*	*0.001*	*<0.001*	*0.014*	*<0.001*
Zinc	µmol g DW^{-1}	0.26	0.27	1.14	0.93	0.69	0.79	0.059	0.04	0.15	0.16
Zn (SE)		*0.020*	*0.019*	*0.013*	*0.023*	*0.016*	*0.022*	*0.006*	*0.005*	*0.006*	*0.001*
Coefficients											
PP_{co}		1.46	1.45	−0.33	−0.25	−1.08	−0.55	3.20	3.01	0.19	4.24
ONP_{co}		−4.60	−5.38	4.11	1.35	4.05	5.49	−4.13	−4.61	5.78	−6.15
GCP_{co}		−5.86	−5.27	8.55	12.09	3.72	5.59	−7.01	−7.57	−6.08	−6.70

(SE: standard error).

inorganic AR-S had two to four times lower ash-free dry weight (AFDW) than the other five silt sediments, associated with low TN, TP and TOC contents. AFDW, TOC, TN and TP concentrations in sediments collected from petri dishes before and after the experiments did not vary, but Chl a and Phaeo concentrations generally increased during the experimental exposure by up to 500%. Nutrient contents of the sediments recovered from the field experiments were indistinguishable from those recovered from the tank experiments (data not shown).

The coefficient GCP_{co} was highest in NR-S and lowest in OS-F. Metals and trace elements (Al, Ba, Cu, Fe, Mn, Ni, Pb, Zn, V) contents were generally higher in the silt fraction of the estuarine (HR-S and NR-S) and nearshore (NS1-S and NS2-S) sediments than in the offshore silt (OS-S) and AR-S as well as in the sandy grain size fractions HR-M, HR-F, OS-M and OS-F.

The principal component analysis comparing all sediment types (Fig. 1) showed that the four sandy sediments (HR-M, HR-F, OS-M, OS-F) and AR-S were overall quite similar in their properties, being characterised mainly by high values in PP and low values in ONP and GCP. The two nearshore sediments (NS1-S, NS2-S) displayed a contrasting pattern, with high ONP values and low PP values. OS-S was characterised by high concentrations of Chl a, Phaeo and TC, and low concentrations of metals, trace elements and TOC, whereas the two estuarine sediments (NR-S, HR-S) displayed opposite patterns: they had low concentrations of Chl a, Phaeo and TC, and high concentrations of metals, trace elements and TOC.

3.2. Exposure of corals

3.2.1. Experiment I: three different grain sizes

The amount of sediment settled in petri dishes was 160.4±18.1 (SD) mg DW cm^{-2} and similar to the nominal sedimentation amount of 160 mg DW cm^{-2}. Due to the corals′ sediment shifting and rejection activity, the amount of sediment actually remaining on the coral

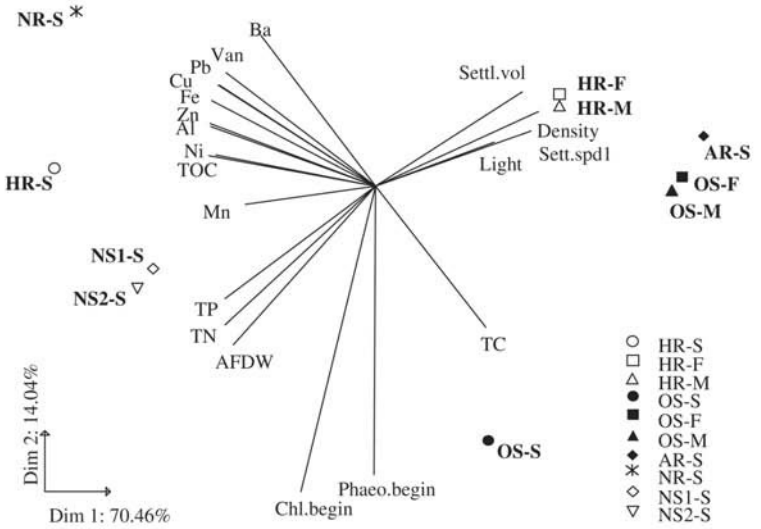

Fig. 1. Sediment parameters of ten different sediment types displayed in a principal component biplot (abbreviations in Table 2). Vectors representing the sediment parameter point towards sediment types with highest concentrations. The sediments used were: silts (grain sizes <63 μm) from Herbert River (HR-S), offshore (OS-S), Normanby River (NR-S), aragonite (AR-S), and nearshore 1 and 2 silt (NS1-S and NS2-S) and fine sand (63–250 μm) and medium–fine sand (250–500 μm) from Herbert River (HR-F, HR-M) and offshore (OS-F, OS-M).

surfaces for medium and fine sand 177.8±51.24 and for silt 148.9±24.9 mg DW cm^{-2}.

In control corals, the photosynthetic yield was 0.645 ±0.058 (representing the value for physiologically normal, healthy corals) during the whole experiment, and never dropped below 0.550. Yields of the corals exposed to the four sandy sediments (HR-M, HR-F, OS-M and OS-F) remained within the variation of the control measurements even at up to 60 h of exposure (Fig. 2), while yields of corals exposed to AR-S dropped slightly below control levels (0.520) after 60 h of exposure. For corals exposed to OS-S and HR-S, a drastic decrease in the fluorescence yield was measured after 36 h exposure: yields had dropped to 0.240 and 0.210 respectively, and were lower again at 60 h exposure. Grain size fraction and exposure time significantly influenced yield, F_0 and F_m, whereas the sediment origin only influenced F_0 and F_m (Table 3). Yields, F_0 and F_m did not increase substantially after 24, 48, 72, 96 or 120 h recovery times. After 120 h recovery time, yields were still reduced (~0.400) in corals that had been exposed to HR-S and OS-S for 36 or 60 h (not all data are shown in Fig. 2).

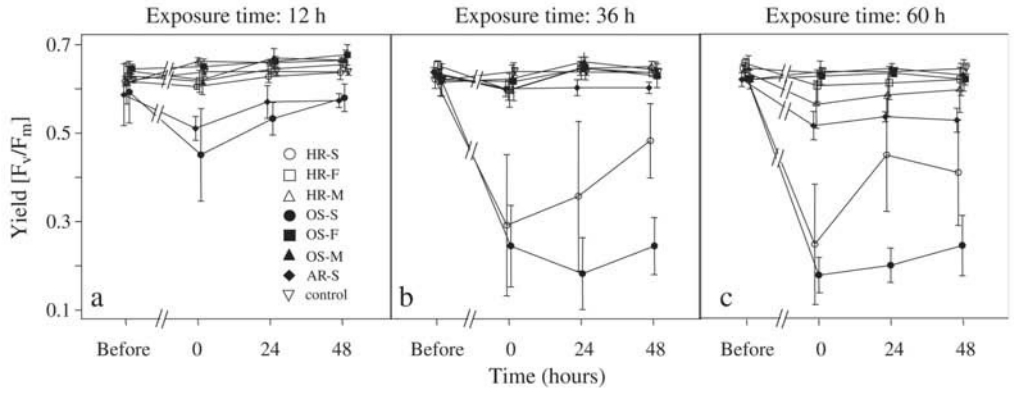

Fig. 2. Photosynthetic yields of *M. peltiformis* exposed for 12 h (a), 36 h (b) and 60 h (c) to seven sediment types: silt-sized (<63 μm) sediments from Herbert River, offshore and aragonite (HR-S, OS-S, AR-S,), and fine sands (63–250 μm) and medium sands (250–500 μm) from Herbert River and Offshore (HR-F, OS-F, and HR-M, OS-M,). The *x*-axis indicates observation times: "Before" = before sediment application, 0 h = time of sediment removal, 24 and 48 h are the number of hours of recovery time.

Table 3
Analyses of variance testing for differences in photosynthetic yields, F_0 and F_m of *M. peltiformis* of colonies directly after sediment removal (0 h recovery), after exposure to sediment types from 3 different origins, three different grain sizes, and 12–60 h exposure times (Experiment 1, Fig. 2)

Yield					F_0			F_m		
	Df	MS	*F*	Pr(*F*)	MS	*F*	Pr(*F*)	MS	*F*	Pr(*F*)
Origin	2	0.0516	2.83	0.0622	10753	4.17	0.0173	100907	4.84	0.00925
Grain size	2	2.07	114	<0.0001	113765	44.1	<0.0001	2045754	98.1	<0.0001
Exposure time	1	0.667	36.6	<0.0001	97157	37.7	<0.0001	1028493	49.3	<0.0001
Origin : grain size	2	0.0055	0.304	0.739	15145	5.88	0.00353	212524	10.2	<0.0001
Residuals	144	0.0182			2578			20853		

3.2.2. Experiment II: four different sediment amounts of estuarine silt

The nominated amounts of HR-S sediment were 33, 66, 100 and 133 mg DW cm^{-2}. Sediment amounts in the petri dishes were measured as 29.5±3.5, 60.7±9.2, 91.3±7.8 and 119.7±11.0 (SD) mg DW cm^{-2} respectively. Due to sediment rejection by the corals the actually remaining amount of sediment ranged from 20 to 97 mg cm^{-2} (31.7±12.9 SD for treatments with a nominal exposure of 33 mg DW cm^{-2}, 49.2±9.6 for the 66 mg DW cm^{-2} treatment, 70.0±12.7 for the 100 mg DW cm^{-2} treatment and 77.7±13.6 for the 133 mg DW cm^{-2} treatment).

Fluorescence yields of control corals were 0.628±0.02 (SD). Yields of corals exposed to sediments decreased from 0.600±0.083 to 0.180±0.107 as a linear function of exposure *E* (Fig. 3). Yields were strongly related to *E* even at very low levels of *E*, but did not change much between 0, 24 and 48 h of recovery time (Table 4).

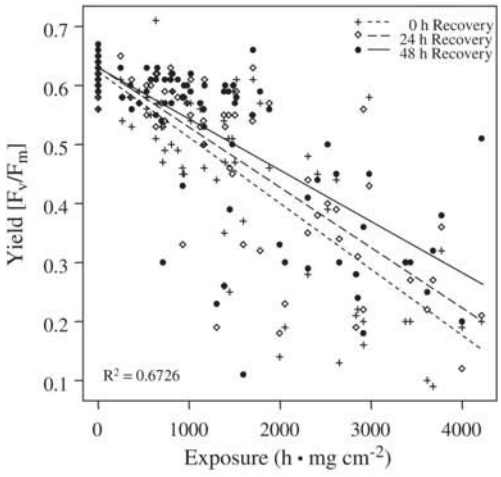

Fig. 3. Relationship between photosynthetic yields of *M. peltiformis* after 0, 24 and 48 h recovery time and exposure (amount · exposure duration) to Herbert River silt (HR-S,<63 μm). Nominal amounts were 33, 66, 100 and 133 mg DW cm^{-2}, the actual amount ranged from 20 to 97 mg cm^{-2}. Exposure times were 12, 20, 36 and 44 h.

3.2.3. Experiment III: six different silt types

The nominal sediment amount for this experiment was 66 mg DW cm^{-2}, wile actual sedimentation was 61.2 ±13.1 mg DW cm^{-2} in the petri dishes and 56.9 ±13.7 (66) mg DW cm^{-2} on corals. Yields of the control corals averaged 0.61±0.02 (SD). Yields of the sediment-exposed corals ranged from 0.62 to 0.26; yields and F_m differed significantly depending on sediment origin and exposure times (Table 5, Fig. 4). The strongest reduction in yields was measured in corals exposed to NS1-S with 0.33±0.141 after 20 h, and 0.26±0.151 after 44 h. No reduction in yields compared to controls was measured in corals exposed to NR-S and AR-S after 20 h and even after 44 h exposure. In the other four sediments, recovery was still incomplete after 48 h recovery time expressed by still lower yields (Fig. 4).

3.2.4. Field experiment: three silt sediments

The amount of sediment remaining on actually sediment-covered surfaces deviated considerably from the nominal 66 mg cm^{-2} after 24 h exposure in the field, due to the sediment shifting and rejection efforts by the corals: sediments coverage was 126.0±10.0 mg cm^{-2} for AR-S, 58.0±1.2 mg cm^{-2} for HR-S, and 80.6 ±20.2 mg cm^{-2} for OS-S. Generally, corals had moved and piled up the AR-S and OS-S sediments onto smaller but thicker patches than initially applied, whereas most of the HR-S sediment remained in place. After 24 h, yields and F_m

Table 4
Linear model testing for the effect of sediment exposure (amount [mg cm^{-2}] · duration of exposure [h]) to Herbert River silt (HR-S) on photosynthetic yields in *M. peltiformis* (Experiment 2, Fig. 3)

	Slope	SE of Slope	*t*	*P*
Exposure	−0.00012	<0.0001	−25.1613	<0.0001
0 h recovery	−0.0103	0.0148	−0.69662	0.48649
24 h recovery	0.0136	0.0149	0.91782	0.35932
48 h recovery	0.0341	0.0151	2.2929	0.02243

The relationship was strongly linear (R^2=0.6726, $F_{(4,363)}$=186.44, P<0.0001). Yields increased only little within the first 48 h after the end of sediment exposure.

Table 5
Analyses of variance testing for differences in photosynthetic yields, F_0 and F_m of *M. peltiformis* colonies directly after sediment removal (0 h recovery), after exposure to silt-sized sediments from 6 different origins, at 20 and 44 h exposure times (Experiment 3, see Fig. 4)

Yield					F_0			F_m		
	Df	MS	*F*	Pr(*F*)	MS	*F*	Pr(*F*)	MS	*F*	Pr(*F*)
Sediment origin	5	0.0572	4.747	0.0009	2051	2.023	0.0861	18958	2.525	0.0370
Exposure time	1	0.4267	35.39	<0.0001	53577	52.82	<0.0001	670091	89.24	<0.0001
Residuals	69	0.0121			1014			7508		

of the control areas differed between colonies. Thus the control data were not pooled, instead treatments and the two controls (light- and dark-adapted) were compared within each of the colonies. After 24 h exposure, yields, F_0 and F_m showed highly significant differences between the sediments and the control areas (Fig. 5), while yields and F_m also differed among the 3 sediments (yields: $F_{(2,17)}=5.580$, $P=0.0137$; F_m: $F_{(2,17)}=4.584$, $P=0.0256$; F_0: $F_{(2,17)}=0.222$, $P=0.804$).

3.2.5. Relationship between changes in yields and sediment properties

Linear models showed that the change in yields in exposed corals was strongly related to the ONP_{co}, weakly related to the PP_{co}, and unrelated to the GCP_{co} (Table 6, Fig. 6). Sediment exposure *E* was also a significant covariate explaining differences in yields. The model explained ~70% of the variation in the data ($R^2=0.702$, $F_{(4,21)}=12.393$, $P<0.0001$).

3.2.6. Rejection capability

Observations during the tank experiments showed that *M. peltiformis* had some capability to remove sediment from their surfaces: Convex areas of the colony were freed from sediment completely by tentacle action, tissue swelling and mucus release, while sediment accumulated in depressions. When rinsing the sediment off the coral, sediment removal by water jet was difficult after 44 h exposure to 66 mg DW cm^{-2} of HR-S, NS1-S or NS2-S, as it was bound to slimy and sticky coral mucus, and a strong smell of H_2S was noticed. After 30 h exposure to these sediments, black spots became visible on the sediment surfaces. When corals were exposed to a higher amount (160 mg DW cm^{-2}) of OS-S, black spots appeared on the sediment surface after 12 to 24 h. The sandy sediment types OS-M, OS-F, HR-M, HR-F and AR-S showed no signs of black spot development even after 60 h of exposure.

In the tank experiments, the proportion of colony surface area freed of sediment varied significantly as function of sediment origin, grain size and amount, but it was unrelated to exposure time in all three experiments (Table 7, Fig. 7). Overall, sandy sediments were more effectively removed than silt sediments (Experiment 1): Corals freed 50–70% of their surfaces from the fine or medium sand of HR and OS, but only ~18% from HR-S

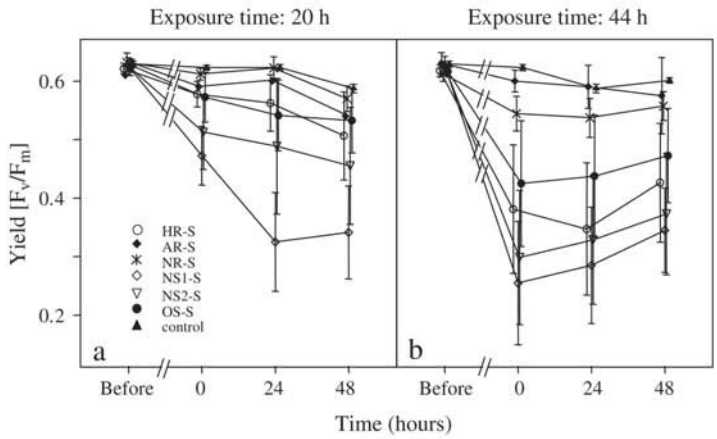

Fig. 4. Photosynthetic yields of *M. peltiformis* exposed for 20 h (a) and 44 h (b) to six silts: Herbert River (HR-S), aragonite (AR-S), Normanby River (NR-S), offshore (OS-S), nearshore 1 and 2 (NS1-S and NS2-S). The *x*-axis indicates observation times: "Before" = before sediment application, 0 h = time of sediment removal, 24 and 48 h are the number of hours of recovery time.

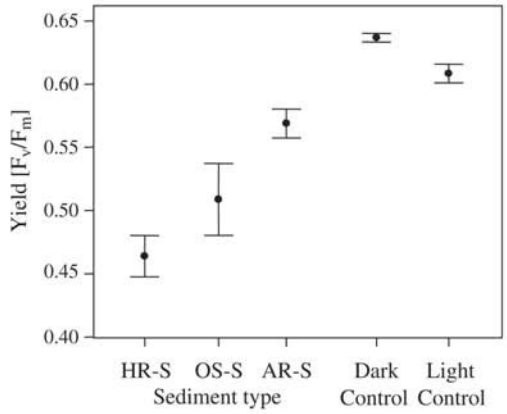

Fig. 5. Photosynthetic yields of *M. peltiformis* exposed in the field for 24h to three silts: Herbert River (HR-S), offshore (OS-S) and aragonite (AR-S). Control measurements where taken from light- and dark-adapted areas next to the sediment-exposed areas of the coral.

and OS-S. AR-S was removed as effectively as the fine and medium sands. The area freed of sediment also varied significantly between the four amounts of HR-S (Experiment 2): the corals freed 47% of their surface at the lowest sediment load of 32±13 (SD), but only 23 and 27%, respectively at the highest sediment loads of 70±13 and 77±14 mg DW cm^{-2}. Lastly, the area freed also varied significantly between the six fine sediment types (Experiment 3): Corals freed 78% of their surface from AR-S and 68% from NR-S, whereas only 26–38.5% were freed from the marine and Herbert River silts.

4. Discussion

Short-term sedimentation of some but not all of ten different sediment types at low levels exerted measurable photosynthetic stress in *M. peltiformis*. Highest stress levels resulted from short-term (20–44 h) exposure to nutrient-rich silts, whereas no effect was measurable after >2 days of exposure to fine and medium sand, and pure aragonite silt. We demonstrated that the effect of sediments on the photophysiological yield in corals increased with increasing concentrations of organic and nutrient-related matter in the sediment (namely: particulate nutrients, chlorophyll and ash-free dry weight). Changes in yields were to a lesser extent related to the physical sediment properties (compaction, light transmission rates, settlement volume and speed), and unrelated to the (very low) concentrations of trace elements and metals found in these sediments. It was impossible to separate the relative effects of the individual parameters within each of the three groups as they were highly correlated. Nevertheless, the findings suggest a fundamentally different outcome for corals exposed to sedimentation by sandy nutrient-poor sediments, such as storm-resuspended marine carbonate sediments as predominantly found in offshore environments, compared to sedimentation of silt-sized sediments rich in organic matter and nutrients (terrestrial and marine origin) that predominantly occur in nearshore environments.

4.1. Characterisation of the sediments used

Sediments differ widely in their mineral and organic composition reflecting geographic origin and genesis, and also differ in their contents of nutrients, contaminants, biopolymers (e.g., as mucus, carbohydrates, proteins) and biota. For example, high TC concentrations are a marker for the marine biogenic origin of the carbonates OS and AR-S, whereas high Ba and Al concentrations are a marker for terrestrial origin of the two river sediments (HR and NR-S). The presence of substantial amounts of Ba and Al in the two nearshore silts (NS1-S and NS2-S) suggests that these contained a significant proportion of terrigenous material (inshore GBR sediments can contain up to 80% terrigenous sediments; Maxwell, 1968).

The sediments with high values in physical parameters (PP) had fast settling rates, a small settling volume, almost no compaction and a high relative light penetration. PP-values differed mainly in regard of median grain size, especially between the four sediments with sandy grain sizes and all types of silt except AR-S. The sediments with high values of organic and nutrient-related parameters (ONP) contained relatively high concentrations of TN, TP, TOC, chlorophyll a, phaeophytin and AFDW. As expected, AFDW, TN, TP and TOC contents were much higher in the silt sediments (excluding AR-S) than the sandy sediments. Silt-sized minerals with greater surface area and reactivity bind more nutrients and contaminants and harbour more microorganisms (Pailles and Moody, 1992; Crump and Baross, 1996), making the sediment more sticky and fluffy (see below). Chlorophyll a, a proxy for photosynthetic productivity and the amount of organic matter in sediments, was high in OS-S, NS1-S,

Table 6
Multiple regression analysis (Experiments 1 and 3 combined) testing the relationship between photosynthetic yield of *M. peltiformis* after sediment removal, and the three coefficients (ONP_{co}, PP_{co}, and GCP_{co}) and sediment exposure *E*

	Slope	SE of slope	*t*	*P*
ONP_{co}	−0.02780	0.00641	−4.326	0.0003
PP_{co}	−0.00575	0.00289	−1.992	0.0596
GCP_{co}	0.00597	0.0051	1.171	0.255
E	−0.00003	0.00001	−3.197	0.00434

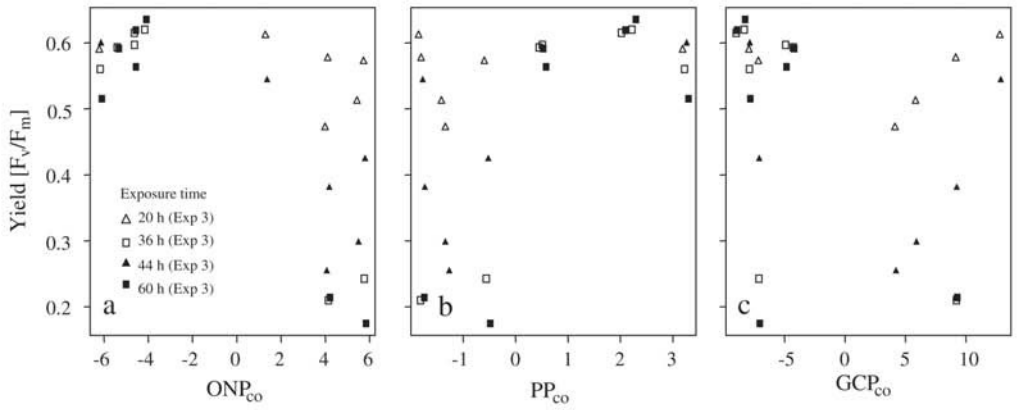

Fig. 6. Photosynthetic yields of *M. peltiformis* from Experiments 1 and 3 exposed for 20, 36, 44 and 60 h to ten different sediment types characterised by three calculated coefficients (sum of *z*-transformed data). a: ONP_{co} = six "organic and nutrient-related parameter", b: PP_{co} = four "physical parameter" and c: GCP_{co} = nine "geochemical parameter". Parameters are listed in Table 2.

NS2-S and HR-S, with concentrations being similar to those reported from highly productive coastal systems such as the North Sea (Boon et al., 1998) and a tropical lagoon in New Caledonia (Garigue, 1998). Chlorophyll a and phaeophytin concentrations further increased during exposure especially in the nutrient-rich sediments, indicating microphytobenthic activity in these sediments (Dell'Anno et al., 2002).

Concentrations of geochemical parameters (GCP), including diverse metals and trace elements, were overall low, as none of the sediments was collected at anthropogenically contaminated sites. However, as is expected for highly reactive small mineral particles (Gibbs, 1986) concentrations were naturally higher in the silt fractions of the estuarine (NR-S and HR-S) and nearshore (NS1-S and NS2-S) sediments than in the silty offshore and aragonite sediments (OS-S and AR-S) and in the sandy fractions from Herbert River and offshore.

4.2. Sedimentation effect on corals

Observations on nearshore coral communities showed that sediments from natural sedimentation events were predominantly found on concave or flat surface of corals, while no sediment was found on convex areas. For example, we occasionally observed fine sediment layers up to several mm thick (rarely sandy deposits) on nearshore reefs on flat-laminar coral species such as *Montipora spp.* and *Echinopora spp.*; coral surfaces underneath tended to be bleached or dead. Where it was difficult to re-suspend the sediment we found slimy black (anoxic) areas. On offshore reefs, layers of sandy carbonate sediments were occasionally observed on concave and flat corals, especially after storms and in areas heavily frequented by boats and divers.

Our results show that grain size is a key factor determining sedimentation stress in corals after short-term exposure. Sedimentation stress in *M. peltiformis* was measurable only when exposed to certain silt sediments, whereas the sandy fractions of two sediment types did not affect the corals in the short term. However we sometimes observed delayed bleaching after removal of the sandy sediments from the corals. This shows that even sandy sediments can cause some damage especially at high exposure levels.

Riegel and Branch (1995) showed that a 100 mg DW cm^{-2} layer of a mix of fine and medium sand reduced light transmission by 75% and at 400 mg DW cm^{-2} by 97%, and that coral photosynthesis was suppressed underneath such layer. In our study, all including the sandy sediments reduced light transmission by >92%, nevertheless photosynthetic stress did not develop in the sandy or low-nutrient silt sediments, suggesting that light limitation played only a minor role in the yield reduction measured in this study.

Table 7
Analysis of variance to test for differences in the percentage of colony surface freed from sediment after exposure to sediments from six different origins, three grain size fractions and five different amounts for varying exposure times (1, 2 and 3 combined)

	Df	MS	*F*	*P*
Sediment origin	5	6634	23.22	<0.0001
Grain size	2	25604	89.63	<0.0001
Sediment amount	1	14947	52.32	<0.0001
Exposure time	1	201.8	0.706	0.4014
Sediment type : grain size	2	744.7	2.607	0.0757
Residuals	263	285.7		

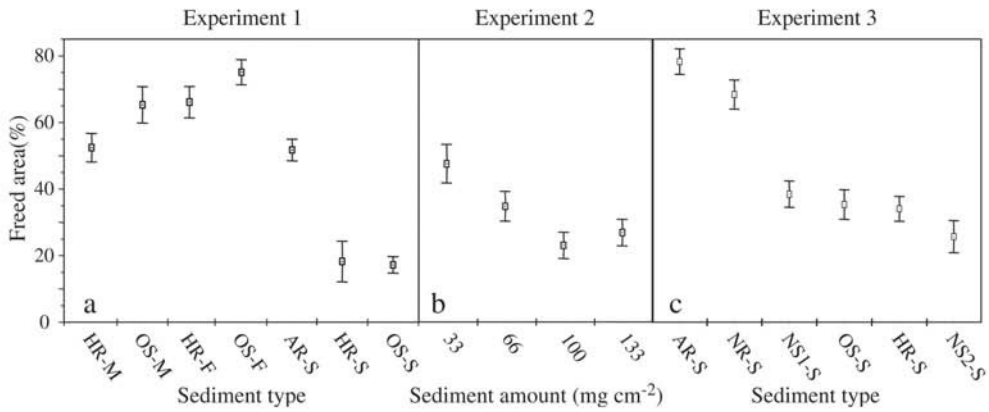

Fig. 7. Percent of surface area freed of sediment by *M. peltiformis* exposed to: (a) sediments with three different grain sizes from three origins (OS-F, OS-M, OS-S, HR-F, HR-M and AR-S) (Experiment 1), (b) four different nominal amounts of HR-S (33, 66, 100 and 100 mg DW cm^{-2}; Experiment 2), and (c) six silt sediments (HR-S, OS-S, NR-S, AR-S, NS1-S and NS2-S) from different origins (Experiment 3). Abbreviations as in Fig. 1.

The photophysiological stress in *M. peltiformis* was not only strongly related to grain size but also to the ONP_{co} concentrations in the sediments. ONP_{co} in sediments can derive from different sources, such as inorganic nutrients bound to minerals or nutrients incorporated in sediment-associated microorganisms. During the experiments a strong smell of hydrogen sulphide was observed after only 24 h of exposure to a thin layer (66 mg DW cm^{-2}) of HR-S, OS-S, NS1-S and NS2-S, and the corals were heavily stressed, while NR-S and AR-S did not create anoxia or stress after the same exposure time. Furthermore we observed anoxic areas on the surfaces of the high ONP_{co} sediments (HR-S, OS-S, NS1-S and NS2-S) but not of NR-S and AR-S, indicating high microbial densities and potentially harmful microbial activity in the former sediments. As differences in light penetration between the different silt sediments were small, we assume that darkness leading to low or no photosynthetic activity hence low oxygen concentration is not by itself the triggering factor for the observed anoxia in some of the sediments, and for the fast damage by short-term sedimentation. These observations suggest that sedimentation damage in corals is not only directly related to nutrient concentrations but also to increased microbial activity in sediments with high ONP_{co} values. The hypothesis is supported by a previous study where bleaching and necrosis in corals exposed to sedimentation was reduced by repeated tetracycline application to sediments (Hodgson, 1990).

4.3. Exposure, recovery and sediment rejection

Previous results showed that the level of stress after short-term sedimentation increased linearly with increasing amounts and duration of sediment exposure (Philipp and Fabricius (2003). Philipp and Fabricius (2003) had exposed the same coral species (*M. peltiformis*) to an average of 151±37 mg DW cm^{-2} of fine muddy coastal sediments (2.37% TC, 0.13% TN and 456 μg/g TP) for up to 36 h (E=1000 to 7000 h·mg cm^{-2}). In Experiment 2 we confirmed that this linear relationship also held at lower, hence environmentally more realistic amounts (E=266 to 4218 h · mg cm^{-2}).

Recovery potential and speed are key processes when assessing the damaging effect of sedimentation. Recovery was measured in laboratory experiments for up to four days after the sediment was washed off (not all data are shown in Fig. 2). After four days of recovery from exposure, recovery was still incomplete in all corals that were affected by short-term sedimentation. Similarly, Wessling et al. (1999) showed that after 20 to 68 h exposure to littoral sediment recovery was completed only after 3 to 4 weeks. As described above, some corals that initially appeared unaffected directly after sediment exposure developed visible signs of bleaching within 24 to 48 h of recovery, possibly from the expulsion of damaged zooxanthellae. Future studies may unravel a number of different types of physiological pathways causing sedimentation damage, possibly with contrasting recovery potentials.

One important mechanism to minimise sedimentation damage is sediment removal by the corals from their surfaces. In *M. peltiformis*, sediment removal rates depended on the sediment properties: sandy sediments were removed more efficiently than silty sediments, and among the 6 silts, AR-S and OS-S were easier removed than the 2 nearshore and 2 estuarine sediments. The

sandy grain size fractions were rejected about three to four times more effectively than the nutrient-rich silts, possibly due to the greater volume and stickiness of the latter (measured as compaction, settling rate and settling volume). Further, the copious mucus production by *M. peltiformis* appeared to trap the silt-sized sediments. A negative relation between rejection efficiency depending on stickiness has previously been shown in a pilot study, where coral-inhabiting barnacles and their host, *Acropora sp*., rejected nutrient-poor offshore sediment but not nutrient-rich nearshore sediment (Fabricius and Wolanski, 2000).

4.4. Hypothesis about the cause of coral death by short-term sedimentation

Increased terrestrial runoff is a problem for coastal coral reefs worldwide (Bryant et al., 1998; Spalding et al., 2001), and input of nutrient-rich silt into the GBR lagoon is stated as the most severe anthropogenic influence on nearshore ecosystems (Wolanski and Duke, 2002). Sediment input into the Great Barrier Reef in Australia has increased five- to ten-fold since European settlement ca. 200 years ago (McCulloch et al., 2003), nitrogen up to three-fold and phosphorous up to ten-fold (Furnas, 2003). The input of dissolved nutrients promotes higher phyto-, zoo- and bacterioplankton densities (Hagström et al., 2001). Newly imported or re-suspended silt particles can carry or bind nutrients and provide optimal substrata for additional microorganisms. The blooming of some of these plankton or particle-attached organisms can lead to an enhanced production of mucus and biopolymeric substances (Myklestad, 1995), in which re-suspended or newly imported mineral particles are trapped and larger aggregates called "marine snow" are formed. Such aggregates constitute a rich source of organic material (Alongi, 1998). Sedimentation velocity increases with flocculation (Burban et al., 1989; Posedel and Faganeli, 1991) and sedimentation of marine snow is a common occurrence on nearshore reefs (Wild, 2000; Fabricius et al., 2003). High microbial density on re-suspended and then settled particles can quickly lead to oxygen depletion, followed by sulphate oxidation and hydrogen sulphide development in sediments (Schulz and Zabel, 2000). Reduced circulation further reduces oxygen exchange and promotes anoxia and hydrogen sulphide development (Boudreau and Jørgensen, 2001).

During our experiments we observed increased mucus production by *M. peltiformis* in response to sedimentation. Coral mucus is a rich source of nutrients (mainly proteins and carbohydrate polymers) which, when bound with sediment particles as carriers of microbes, may further stimulate bacterial production, with flow-on effects into microbial food chains (Ducklow and Mitchell, 1979; Meikle et al., 1988). It remains to be tested whether the resulting anoxia, and microbial development of the cell toxin hydrogen sulphide may be major factors responsible for coral tissue poisoning, possibly accounting for the worsening (resulting in death) of photosynthetic stress in corals exposed to nutrient-rich compared with nutrient-poor sediments.

Acknowledgements

We gratefully acknowledge the help of Jeff Warbrick and Simon Talbot in the field, and of Isabelle Frese and Gunnar Hanebeck who assisted with the laboratory analyses, as well as the support by Omya SpA, Carrara, Italy (marble dust) and by Unimin Australia Limited (Snobrite 55 kaolonit) which provided sediment for control studies. MW acknowledges the supervision by Prof. M. Wolff, University of Bremen, Germany, and the support of a student scholarship by the German Academic Exchange Service (DAAD) and of the student award for the best Diploma thesis 2004 by the University of Bremen. The research was funded by the Cooperative Research Centre for the Great Barrier Reef World Heritage Area (CRC Reef) and the Australian Institute for Marine Science (AIMS). **[SS]**

References

Alongi, D.M., 1998. Coastal Ecosystem Processes. CRC Press, Boca Raton.

Bak, R.P.M., Elgershuizen, J.H.B.W., 1976. Patterns of oil-sediment rejection in corals. Mar. Biol. 37, 105–113.

Boon, A.R., Duineveld, G.C.A., Berghuis, E.M., Van der Weele, J.A., 1998. Relationships between benthic activity and the annual phytopigment cycle near-bottom water and sediments in the North Sea. Estuar. Coast. Shelf Sci. 46, 1–13.

Boudreau, B.P., Jørgensen, B.B., 2001. The Benthic Boundary Layer. Oxford University Press.

Brodie, J.E., Christie, C., Devlin, M., Haynes, D., Morris, S., Ramsay, M., Waterhouse, J., Yorkston, H., 2001. Catchment management and the Great Barrier Reef. Water Sci. Technol. 43 (9), 203–211.

Bryant, D.G., Burke, L., McManus, J., Spalding, M., 1998. Reefs at Risk: A Map-Based Indicator of Threats to the World's Coral Reefs. World Resources Institute, Washington DC.

Burban, P-Y., Lick, W., Lick, J., 1989. The flocculation of fine-grained sediments in estuarine waters. J. Geophys. Res. 94 (C6), 8323–8330.

Crump, B.C., Baross, J.A., 1996. Particle-attached bacteria and heterotrophic plankton associated with the Columbia River estuarine turbidity maxima. Mar. Ecol. Prog. Ser. 138, 265–273.

Dell'Anno, A., Mai, M.L., Pusceddu, A., Danovaro, R., 2002. Assessing the trophic state and eutrophication of coastal marine systems: a new approach based on the biochemical composition of sediment organic matter. Mar. Pollut. Bull. 44, 611–622.

Devlin, M.J., Brodie, J., 2005. Terrestrial discharge into the Great Barrier Reef Lagoon: nutrient behaviour in coastal waters. Mar. Pollut. Bull. 51, 9–22.

Devlin, M., Waterhouse, J., Taylor, J., Brodie, J., 2001. Flood Plumes in the Great Barrier Reef: Spatial and Temporal Patterns in Composition and Distribution. GBRMPA Research Publication No 68. Great Barrier Reef Marine Park Authority, Townsville, Australia.

DIN 38409-H9, Deutsches Institut für Normung e.V., 1980. Deutsche Einheitsverfahren zur Wasser-, Abwasser-und Schlammuntersuchung; Summarische Wirkungs-und Stoffkenngrößen (Gruppe h); Bestimmung des Volumenanteils der absetzbaren Stoffe in Wasser und Abwasser (H 9), Ausgabe:1980-07. http://www2.din.de/.

Ducklow, H.W., Mitchell, R., 1979. Bacterial populations and adaptations in the mucus layers on living corals. Limnol. Oceanogr. 4, 715–725.

Fabricius, K.E., 2005. Effects of terrestrial runoff on the ecology of corals and coral reefs: review and synthesis. Mar. Pollut. Bull. 50 (2), 125–146.

Fabricius, K.E., Wolanski, E., 2000. Rapid smothering of coral reef organisms by muddy marine snow. Estuar. Coast. Shelf Sci. 50, 115–120.

Fabricius, K.E., Wild, C., Wolanski, E., Abele, D., 2003. Effects of marine snow and muddy terrigenous sediments on the survival of hard coral recruits. Estuar. Coast. Shelf Sci. 56, 1–9.

Folk, R.L., 1980. Petrology of Sedimentary Rocks. Hemphill Publishing Company Austin, Texas.

Furnas, M., 2003. Catchments and Corals: Terrestrial Runoff to the Great Barrier Reef. Australian Institute of Marine Science and CRC Reef Research Centre, Townsville, Australia.

Furnas, M.J., Mitchell, A.W., 1999. Wintertime Carbon and Nitrogen Fluxes on Australia's Northwest Shelf. Estuar. Coast. Shelf Sci. 49, 165–175.

Furnas, M., Mitchell, A.M., Skuza, M., 1995. Nitrogen and Phosphorus Budgets for the Central Great Barrier Reef Shelf. Res. Publication No 36. Great Barrier Reef Park Marine Authority, Townsville, Australia.

Garigue, C., 1998. Distribution and biomass of microphytes measured by benthic chlorophyll-a in a tropical lagoon (New Caledonia, South Pacific). Hydrobiologia 835, 1–10.

Gibbs, R.J., 1986. Segregation of metals by coagulation in estuaries. Mar. Chem. 18, 149–159.

Hagström, A., Pinhassi, J., Zweifel, U.L., 2001. Marine bacterioplankton show bursts of rapid growth induced by substrate shifts. Aquat. Microb. Ecol. 24, 109–115.

Harrington, L., Fabricius, K., Eaglesham, G., Negri, A., 2005. Synergistic effects of diuron and sedimentation on photosynthesis and survival of crustose coralline algae. Mar. Pollut. Bull. 51, 415–427.

Hodgson, G., 1990. Tetracycline reduces sedimentation damage to corals. Mar. Biol. 104, 493–496.

Lorenzen, C.J., 1967. Determination of chlorophyll and phaeopigments: spectrophotometric equations. Limnol. Oceanogr. 12, 343–346.

Loring, D.H., Rantala, R.T.T., 1992. Manual for the geochemical analyses of marine sediments and suspended matter. Earth Sci. Rev. 32, 235–283.

Mapstone, B.D., Choat, J.H., Cumming, R.L., Oxley, W.G., 1989. The Fringing Reefs of Magnetic Island: Benthic Biota and Sedimentation — A Baseline Study. Research Publication, vol. 13. Great Barrier Reef Marine Park Authority, Townsville, Australia. 134 pp.

Maxwell, W.G.H., 1968. Atlas of Great Barrier Reef. Elsevier, Amsterdam.

McCulloch, M., Fallon, S., Wyndham, T., Hendy, E., Lough, J., Barnes, D., 2003. Coral record of increased sediment flux to the inner Great Barrier Reef since European settlement. Nature 421, 727–730.

Meikle, P., Richards, G.N., Yellowlees, D., 1988. Structural investigations on the mucus from six species of corals. Mar. Biol. 99, 187–193.

Myklestad, S.M., 1995. Release of extracellular products by phytoplankton with special emphasis on polysaccharides. Sci. Total Environ. 165, 155–164.

NIH-Image 1.63, freeware © National Institute of Health. USA. http://rsb.info.nih.gov/nih-image/.

Pailles, C., Moody, P.W., 1992. Phosphorous sorption–desorption by some sediments of the Johnstone River catchment, Northern Queensland. Aust. J. Mar. Freshw. Res. 43, 1535–1545.

Parker, J.G., 1983. A comparison of methods used for the measurement of organic matter in marine sediments. Chem. Ecol. 1, 201–210.

Philipp, E., Fabricius, K., 2003. Photophysiological stress in scleractinian corals in response to short-term sedimentation. J. Exp. Mar. Biol. Ecol. 287, 57–78.

Posedel, N., Faganeli, J., 1991. Nature and sedimentation of suspended particulate matter during density stratification in shallow waters (Gulf of Trieste, northern Adriatic). Mar. Ecol. Prog. Ser. 77, 135–145.

Riegl, B., Branch, G.M., 1995. Effects of sediment on the energy budget of four scleractinian (Bourne 1900) and five alcyonacean (Lamouroux 1816) corals. J. Exp. Mar. Biol. Ecol. 186, 259–275.

Roger, C.S., 1990. Responses of coral reefs and reef organisms to sedimentation. Mar. Ecol. Prog. Ser. 62, 185–202.

Schreiber, U., Schliwa, U., Bilger, W., 1986. Continuous recording of photochemical and non-photochemical chlorophyll fluorescence quenching with a new type of modulation fluorometer. Photosynth. Res. 10, 51–62.

Schulz, H.D., Zabel, M., 2000. Marine Geochemistry. Springer-Verlag, Berlin.

Spalding, M.D., Ravillious, C., Green, E.P., 2001. World Atlas of Coral Reefs. University of California Press, Berkley.

Stafford-Smith, M.G., 1993. Sediment-rejection efficiency of 22 species of Australian scleractinian corals. Mar. Biol. 115, 229–243.

Stafford-Smith, M.G., Ormod, R.F.G., 1992. Sediment-rejection mechanisms of 42 species of Australian scleractinian corals. Aust. J. Mar. Freshw. Res. 43, 683–705.

Statistical Science, 1999. S-PLUS, Version 2000 for Windows. A division of Mathsoft Inc. Seattle.

Weber, M., 2003. Synergismuseffekte von Sedimentation und Nährstoffen auf Steinkorallen. University of Bremen, Germany. Diplomarbeit (Master Thesis).

Wessling, I., Uychiaoco, A.J., Alino, P.M., Aurin, T., Vermaat, J.E., 1999. Damage and recovery of four Philippine corals from short-term sediment burial. Mar. Ecol. Prog. Ser. 176, 11–15.

Wild, C., 2000. Effekte von "marine-snow"—Sedimentation auf Steinkorallen (Hexacorallia, Scleractinia) des Great Barrier Reef, Australia. University of Bremen, Germany. Diplomarbeit (Master Thesis).

Wolanski, E.D., Duke, N.C., 2002. Mud threat to the Great Barrier Reef of Australia. In: Healy, T.R., Wang, W., Healy, J.A. (Eds.), Muddy Coasts of the World: Process, Deposits and Function. Elsevier Science B.V, Amsterdam. 533–542 pp.

Woolfe, K.J., Michibayashi, K., 1995. "Basic" entropy grouping of laser-derived grain-size data: an example from the Great Barrier Reef. Comput. Geosci. 21, 447–462.

ELSEVIER

Journal of Experimental Marine Biology and Ecology 341 (2007) 151

Journal of EXPERIMENTAL MARINE BIOLOGY AND ECOLOGY

www.elsevier.com/locate/jembe

Corrigendum

Corrigendum to "Sedimentation stress in a scleractinian coral exposed to terrestrial and marine sediments with contrasting physical, organic and geochemical properties" [Journal of Experimental Marine Biology and Ecology 336 (2006) 18–32]

M. Weber [a,b,c,*], C. Lott [a,b,c], K.E. Fabricius [a]

[a] *Australian Institute of Marine Science, PMB No 3, Townsville, QLD 4810, Australia*
[b] *HYDRA Institute for Marine Sciences, Elba Field Station, Via del Forno 80, I-57034 Campo nell'Elba (LI), Italy*
[c] *Max Planck Institute for Marine Microbiology, Celsiusstrasse I, 28359 D-Bremen, Germany*

The authors regret that when the above article was printed, there were a series of errors in Table 2. Table 2 contained an error in the sediment data on aluminium and iron concentrations. The correct units and values are displayed here. These changes do not alter any of the statistical analyses and other results, and do not alter the conclusion of greatly different levels of stress in corals in response to exposure to sediments with contrasting concentrations of organic and nutrient-related parameters.

Table 2

		HR-M	HR-F	HR-S	NR-S	NS1-S	NS2-S	0S-M	0S-F	0S-S	AR-S
		(Exp. I)	(Exp. I)	(Exp. I+II+III)	(Exp. III)	(Exp. III)	(Exp. III)	(Exp. I)	(Exp. II)	(Exp. III)	(Exp. III)
Aluminium	mmol g DW^{-1}	0.254	0.307	2.702	3.046	2.102	1.877	0.018	0.017	0.243	0.025
Al (SE)		*0.036*	*0.040*	*0.086*	*0.066*	*0.096*	*0.067*	*0.003*	*0.002*	*0.008*	*0.003*
Iron	mmol g DW^{-1}	0.145	0.143	0.576	0.690	0.445	0.429	0.006	0.006	0.055	0.008
Fe (SE)		*0.007*	*0.005*	*0.017*	*0.016*	*0.021*	*0.016*	*0.001*	*0.001*	*0.001*	*0.001*

DOI of original article: 10.1016/j.jembe.2006.04.007.

* Corresponding author. HYDRA Institute for Marine Science, Elba Field Station, Via del Forno 80, I-57034 Campo nell'Elba (LI), Italy. Tel.: +390565988027; fax: +390565988090.

E-mail address: m.weber@hydra-institute.com (M. Weber).

doi:10.1016/j.jembe.2006.10.007

Chapter 4

A cascade of microbial processes kills sediment-covered corals

A cascade of microbial processes kills sediment-covered corals

Weber, M.*[,1,2], Lott, C.[1,2], Kohls, K.[1], Polerecky, L.[1], Abed, R. M. M.[1,4], Ferdelman, T.[1], Fabricius, K. E.[3], and de Beer, D.[1]

[1] Max Planck Institute for Marine Microbiology, Celsiusstrasse 1, 28359 Bremen, Germany

[2] HYDRA Institute for Marine Sciences, Elba Field Station, Via del Forno 80, 57034 Campo nell'Elba (LI), Italy

[3] Australian Institute of Marine Science, PMB No 3, Townsville, QLD 4810, Australia

[4] Sultan Qaboos University, College of Science, Biology Department, P.O. Box 36, Muscat 123, Sultanate of Oman

* Corresponding author phone: +390565988027; fax: +498913060132; e-mail: m.weber@hydra-institute.com

This chapter will be submitted to a peer-reviewed international journal.

1. Abstract

We investigated how microbial activity mediated physiological stress and subsequent death of corals covered with sediment having contrasting organic matter content. Measurements were conducted in mesocosm experiments and supporting data were obtained from microsensor profiles in naturally accumulated sediment layers on corals in the field. On corals covered with organic-rich sediments first necrotic areas were detected within 1 day, whereas organic-poor sediments had no effect after 6 days. Sediments suppressed coral photosynthesis by preventing ambient light from reaching the corals, however this did not affect coral survival. Microsensor profiles showed that in the organic-rich but not in organic-poor sediment, pH and oxygen started to decrease immediately, while very little sulfide was detected after one day. Sulfide concentrations increased substantially afterwards. Sulfate reduction played a minor role in the sulfide generation, which mainly originated from the degradation of sulfur compounds of the coral mucus and dead tissue. In a series of dark incubations corals were exposed separately to anoxia, low pH and sulfide. They showed that anoxia at the pH of ambient seawater does not lead to coral mortality within four days, while the combination of anoxia and low pH lead to death within one day. Corals died even earlier when first exposed 12 h to anoxia and low pH and then, already stressed, to sulfide. We conclude that sedimentation can kill corals within less than one day through a cascade of microbial processes. This chain reaction is triggered locally via microbial activity of anaerobic organic matter degradation in the sediment, immediately lowering the pH. Then the decay of coral tissue leads to an increase in sulfide, which diffuses to the neighboring, already stressed, polyps. The entire sediment-covered coral is so killed within hours. The experiments confirmed previous findings that coral damage by the sediments tested was positively correlated to their content of organic matter. For coastal management it is important to know that sedimentation enriched with organic matter is particularly dangerous for coral reefs.

2. Introduction

Worldwide coral reefs are threatened by sedimentation induced via import from terrestrial runoff and by resuspension from the seafloor (Wilkinson 2002). The discharge of fine nutrient-rich sediment is the most important direct anthropogenic impact to nearshore coral reef ecosystems (Wolanski & Duke 2002). This sediment eventually covers corals, leading to their damage or death (Fabricius et al. 2007). The negative impacts of smothering on corals are studied, and the resulting effects like necrosis and bleaching are documented (Fabricius 2005, Roger 1990, and references therein). Earlier studies did not specify the applied sediments or used unnaturally high sediment loads and large grain size fractions such as sand

(Rogers 1983, Stafford-Smith 1993, Wessling et al. 1999). Resuspension of sand occurs during big storms (Bothner et al. 2006), whereas runoff or resuspension induced by moderate winds transport smaller grain size fractions such as silt (Larcombe et al. 2001).

Furthermore, earlier studies regarded sediment mainly as mineral particles (Peters & Pilson 1985, Vargas-Ángel et al. 2006, Sofonia & Anthony 2008), and disregarded that sediment includes much more. Here we use as a broader definition for sediment: "matter that settles to the bottom of a liquid" (Oxford English Dictionary). Sediment consists of mineral particles with variable size, organic particles such as faecal pellets, detritus, mucus, and exopolymeric substances (Ayukai & Wolanski 1997). It can carry adsorbed or particulate nutrients and contaminants (Gibbs 1983). Sedimenting particular matter forms aggregates (Edzwald et al. 1974) called marine-snow (Alldredge & Silver 1988). They harbour highly active phytoplankton (Passow 2002) and microbial communities (Grossart & Ploug 2001, Kaltenböck & Herndl 1992). A pilot study showed that estuarine silt enriched with marine snow smothered and killed reef organisms within hours, whereas silt without enrichment was rejected by the organisms (Fabricius & Wolanski 2000). Another study showed that the grain size and the quality of the sediment determines the effect on corals: fine sediments rich in organic matter lead to death within one to two days, whereas fine organic matter-poor or coarse sediments did not kill the coral (Weber et al. 2006). The damage on the corals correlates with the sediment amount multiplied the exposure time (Philipp & Fabricius 2003).

However, what happens within or under the sediment layer covering the coral remains unknown. It is assumed that reduced light excludes photosynthesis, and that the subsequent lack of oxygen damages the coral (Peters & Pilson 1985, Philipp & Fabricius 2003). Based on observations, Weber et al. (2006) suggested that the protonated form of sulfide, hydrogen sulfide (H_2S), which is well known for its toxicity (Bagarinao 1992), leads to the damage of the coral. It was suggested by Carlton & Richardson (1995), that the coral black band disease resulted in tissue lysis because of sulfide exposure. Sulfate reduction (SR) is the prevailing microbial process in anoxic sediments (Jørgensen 1982) and leads to the formation of sulfide. Sorokin (1978) and Dubinsky & Stambler (1996) suggested that in reef sediments SR, enhanced by eutrophication, could kill corals in the vicinity.

The objective of this study was to investigate microbial processes within organic matter-rich sediments that cover corals, and to test the putative damaging compounds individually. We proposed that the coral damage is not due to the exclusion of photosynthesis induced by the lack of light, but the damage is mediated by a rapid depletion of oxygen due to respiration by the microbial community in the sediment. The death of the coral is then caused by sulfide from sulfate reduction in the sediment layer on the coral.

This study presents the results of the photophysiological stress responses in the scleractinian coral *Montipora peltiformis* to the coverage with organic matter-rich sediment and to the exposure to putative damaging compounds, namely darkness, anoxia, pH and sulfide. Here we provide data on the changing environment and the microbial community within the sediment layer once settled on the coral. By modelling we discriminated the sources of the measured sulfide. Experiments were done in controlled mesocosms and were further supported by microsensor measurements in naturally accumulated sediment layers on corals in the field. In the discussion we describe the cascade of microbial processes killing corals upon sediment coverage.

3. Material and Methods

3.1 Coral and sediment collection

The flat-foliose coral *Montipora peltiformis* is an abundant species along nearshore reefs in the Great Barrier Reef (GBR) of Australia. For laboratory experiments coral fragments were collected by SCUBA diving at Hannah Island (13° 52' S, 143° 43' E) from 4-5 m water depth. Fragments of 10-25 cm^2 were kept in flow-through aquaria until they resumed growth. For the field measurements *Montipora peltiformis*, *Montipora* sp., *Pachyseris* sp., *Porites* sp., and *Turbinaria reniformis* were chosen because they were often observed to be covered by naturally accumulated sediment.

To obtain test sediments the first 5 cm of the seafloor (5-10 m water depth) were sampled at Wilkie Island (13° 46' S, 143° 38' E), another nearshore reef in the GBR. The sediment was wet-sieved with plastic sieves to obtain the desired silt grain size fraction of <63 μm. Silt is most often accumulating on corals or sampled in sediment traps in the reef (Bothner et al. 2006, Brooks et al. 2007).

3.2 Sediment exposure experiment I

In this experiment we tested the photophysiological stress response of *Montipora peltifomis* to sediment with and without enrichment with organic matter. The changing environmental parameters in the sediment layer covering the coral were measured and the microbial community of the sediment monitored.

Sediments with four different levels of organic matter content were prepared by adding a plankton mixture. The plankton has been collected with a net. Subsequently the mixture has been minced with a blender and sieved to remove large fragments. The sediment was enriched with three concentrations of plankton mixture, expressed in percent C_{org} of the dry weight of the sediment: a) + 0%, b) + 0.06%, c) + 0.3% and d) + 0.6% C_{org}. The untreated sediment had

1.25% C_{org}. The four test sediments were then incubated for 24 h in 2 l seawater on a rotor shaker to assure mixing.

3.2.1 Experimental procedure

The mesocosm experiment was conducted at the outdoor aquaria facilities of the Australian Institute of Marine Sciences (AIMS). Petridishes were used to collect control sediment. Ten coral fragments and petridishes were placed in a 60 l tank with constant flow-through of 2 l min^{-1} seawater of 24-25°C. Maximum illumination was 400 µmol photons m^{-2} s^{-1}. The amount of sediment necessary to obtain a load of 66 mg dry weight (DW) cm^{-2}, was suspended in each of the eight (two per treatment) tanks at no-flow conditions. The sediment load was chosen based on results obtained by Weber et al. (2006). The flow was turned on again 2 h later. Two coral fragments were added as controls and remained free of sediment. Four coral fragments and four petridishes with sediment were removed after 3 h, 1, 2, 3, and 4 or 6 days.

As a proxy for the health status of the corals the photosynthetic yield of the photosystem II of the corals' zooxanthellae was measured. The non-invasive pulse-amplitude modulated (PAM) chlorophyll fluorometer (Schreiber et al. 1986) was used as described in Philipp and Fabricius (2003). After two days of acclimatisation in the tank and 60 min of dark-adaptation of the corals, between 10-15 PAM readings were taken to obtain the initial health status of the coral fragments. At each sampling time, coral health measurements (PAM) were performed on control corals and on four treated corals after the sediment was removed. Samples of the sediment from the corals and of the control sediment (petridishes) were taken for microbial community analysis (§ 3.2.3) and geochemical analysis (§ 3.2.4). The coral fragments were photographed prior and after sediment removal, and the necrotic area of the coral fragments was determined photogrammetrically using the free software ImageJ (http://rsb.info.nih.gov/ij/).

3.2.2 Microsensor measurements

At each sampling time microsensor measurements were conducted in the sediment layers of two coral fragments. Oxygen, hydrogen sulfide, pH, and light microsensors were prepared as described previously (Revsbech 1989, Lassen & Jørgensen 1994, de Beer et al. 1997, Kühl et al. 1998). The pH sensors were modified for field measurements by combining the pH-reference electrode into the sensor as described in Weber et al. (2007). All microsensors had a tip diameter of 10-30 µm and a stirring sensitivity of <1.5%. The O_2 microsensors were calibrated using air- and nitrogen-flushed seawater at in situ temperature and salinity. The

sulfide microsensor was calibrated by adding increments of 100 µl of a 500 mM sulfide (Na_2S) stock solution to a nitrogen-flushed 200 mM phosphate buffer (pH 7.5) at in situ temperature. Subsamples from the calibration solution were immediately fixed in 2% zinc-acetate and the total sulfide concentration was determined spectrophotometrically with the methylene blue method (Cline 1969). The hydrogen sulfide concentration in the calibration buffer was calculated using the pK_1 6.9, which was determined as described in Weber (2009). Total sulfide in the sediment layer on the coral was calculated with the H_2S and pH profile (Jeroschewski et al. 1996), and the temperature and salinity corrected pK_1 6.6 (Millero, 1988). The pH microsensors were calibrated using standard buffers with pH 7.02 and 9.21 (Mettler Toledo, Germany) at in situ temperature. The light microsensor was calibrated against a LI-250 light-meter (LI-COR, USA).

Vertical profiles in the sediment layer covering the coral were measured after the coral was transferred into a small flow chamber. The flow conditions were the same as in the experimental tanks. The microsensors were first carefully positioned at the sediment surface and then moved through the sediment layer until the surface of the coral skeleton was reached. Using a motorized system controlled by a computer, the microprofiles where then measured upwards in 100 µm steps. The microsensors were mounted on a motorized micromanipulator (Faulhaber Group and MM33 from Märzhäuser, Germany) and connected to amplifiers. A DAQ-Card (National Instruments, Germany) connected the amplifiers to a computer. Measurements were automated with the software m-Profiler (http://www.mpi-bremen.de/en/Lubos_Polerecky.html). On each coral three profiles were measured at different spots. Oxygen, sulfide and pH were measured in the dark. During the light profiles 370 µmol photons m^{-2} s^{-1} were applied using a KL 1500 electronic Schott lamp (Zeiss, Germany).

The field measurements were conducted during AIMS research cruises in 2005-2006. Four corals were chosen in 4-5 m water depth at two nearshore reefs (High Island, 17° 09' S, 146° 00' E; Bedarra Island, 17° 96'S, 146° 09' E) and four corals at two offshore reefs (Gilbey, Reef 17° 34' S, 146° 34' E; Wardle Reef, 17° 27', 146° 32' E). Nearshore to offshore reflects a gradient of anthropogenic impact. River discharge imports increased sediment and nutrient loads to the nearshore reefs. Thus we expect the sediment accumulated on nearshore corals to have a higher organic content than the sediments on corals at offshore reefs. Consequently we expect different O_2 and pH conditions in the sediment layer on the corals. Three microsensor profiles were measured at random spots in the naturally accumulated sediments on corals. O_2, pH and light profiling was conducted during the day at natural illumination. Average light was 486 ± 116 SE µmol photons m^{-2} s^{-1}, continuously measured with submersible Odyssey light loggers (Dataflow Systems Pty Ltd, New Zealand). pH profiles were measured only

once at High Island. Profiling was conducted similar to the laboratory measurements with an underwater microsensor system (Weber et al. 2007). Sediment samples were collected for further molecular and geochemical analyses.

3.2.3 Molecular analyses

The structure of the bacterial communities within the 0, 0.3 and 0.6% C_{org}-enriched sediment covering the corals and from control sediment (petridishes) was determined. Nineteen samples were chosen for denaturing gradient gel electrophoresis (DGGE) DNA fingerprinting. From those, six samples were then analyzed constructing 16S rRNA clone libraries. The nucleic acid extraction, the polymerase chain reaction (PCR), the DGGE of the sediment samples, the phylogenetic analysis and the calculation of diversity and richness indices from the obtained sequences were conducted as previously described (Ludwig et al., 1998, Abed & Garcia-Pichel 2001, Abed et al. 2007). Modifications were the following: The PCR for the DGGE samples and for the excised bands was done with 10 ng DNA using the primers GM5F (with GC clamp) and 970RM. For subsequent sequencing of the bands the primer GM5F (with GC clamp) at 58°C, GM1F and 907RM at 56°C annealing temperature were used (Muyzer et al. 1995). The obtained partial sequences were transformed to consensus sequences using the Sequencher DNA sequence assembly and analysis software (http://www.genecodes.com/).

3.2.4 Sediment, plankton mixture and coral tissue analysis

The listed parameters of the sieved Wilkie Island sediment were determined as previously described (Weber et al. 2006 and references therein): grain size distribution, settling volume, settling rate, compaction, organic matter (ash-free dry weight), total organic carbon (TOC), total nitrogen (TN), total phosphorous (TP), chlorophyll a (Chl a) and phaeophytin (Phaeo), Calcium, Magnesium, Aluminium, Iron, Manganese, Barium, Zinc, Vanadium, Copper, Cobalt, Lead, Nickel, Cadmium, Molybdenum, Selenium, and the Aluminium-Calcium ratio. TOC, TN, TP, Chl a and Phaeo were measured in samples from the sediment exposure experiment I and of the plankton mixture.

Total carbon (TC), total nitrogen (TN) and total sulfur (TS) were measured from the coral tissue by combustion with a CNS analyser (NA 1500 Series 2, Fisons Instruments, Germany). Prior to the analysis, corals were frozen in liquid nitrogen. The tissue was airbrushed off the skeleton with 60-100 ml of filtered seawater, washed 3 times, freeze dried and grinded.

3.3 Sediment exposure experiment II

In this experiment we tested whether the sulfate reduction rate (SRR) in sediments covering the corals increases upon enrichment with the plankton mixture. The SRR data where then used for modeling. With the modeling approach we discriminated whether the sulfide concentrations measured with microsensors could have been derived from the SRR in the sediment covering the coral or from another source.

3.3.1 Sulfate Reduction rates

Each coral fragment (10-15 cm^2) was put in a beaker. A gentle stirring of the water was achieved by water-saturated airflow over the water surface. Evaporation of the seawater in the beaker was limited and the salinity was 35-36 ppt and the temperature was 26-27°C. Light with an intensity of 450 µmol m^{-2} s^{-1} was applied for 12 h daily. The sediment was enriched by 0.6% C_{org} with the plankton mixture and pre-incubated for 24 h. Radiolabeled $^{35}SO_4^{2-}$ (Amersham) was added to an end concentration of 25 kBq ml^{-1} into the seawater. Then the reef sediment was suspended in the beaker and left to settle onto the coral (66 mg DW cm^{-2}). After 6, 22, and 45 h in two beakers the sediment from the coral fragment and the remaining sediment in the beaker (laying beside the coral) were fixated separately in 20% zinc-acetate. To measure radiolabeled sulfide, samples were processed according to the cold chromium distillation procedure (Kallmeyer et al. 2004). Porewater sulfate concentration in the 2-3 mm thin sediment layer was assumed to be 28 mmol per liter seawater because the sediment had just settled. Porosity of the sediment was calculated after 6, 22 and 45 h from the weight loss of a known wet sediment volume after drying to constant weight at 60°C.

3.3.2 Modeling

Modeling was used to identify the source of the measured sulfide, assuming that the sample was laterally homogenous and transport of sulfide in the sediment was governed by diffusion. First, to check whether sulfate reduction in the sediment covering the coral was the source for sulfide, we assumed a homogenously distributed sulfate reduction rate (SRR) in the sediment layer of thickness z_s. Thus, a one-dimensional diffusion reaction equation could be used to calculate the steady state sulfide concentration profile, $c(z)$ above the coral tissue:

$$0 = D_{S_{tot}^{2-}}\left(\frac{\partial^2 c}{\partial z^2}\right) + SRR, \qquad (1)$$

where z is depth and $D_{S_{tot}^{2-}} = 1.82 \times 10^{-9} m^2 s^{-1}$ is the temperature- and salinity corrected diffusion coefficient of sulfide, which was assumed to be equal both in the sediment and overlaying water. $D_{S_{tot}^{2-}}$ was calculated with the diffusion coefficients D_{H_2S} and D_{HS^-} (Schulz

2006) assuming 40% H_2S and 60% HS^-. We further assumed that both the sulfide concentration at the top of the diffusive boundary layer ($z = -z_{DBL}$; Jørgensen 2001) and the sulfide flux at the bottom of the sediment layer ($z = z_s$) were zero. The latter condition corresponded to the assumption that sulfide could not diffuse into the coral skeleton and that no sulfide production occurred in the coral tissue. Using these boundary conditions, the solution to Eq. (1) is (see SI. Fig. S5, solid line)

$$c(z) = -\left(\frac{SRR}{2D_{S_{tot}^{2-}}}\right)\left(z^2 - 2zz_s - 2z_s z_{DBL}\right). \quad (2)$$

Thus, the sulfide concentration and diffusive flux ($J = -D_{S_{tot}^{2-}}\left(\frac{\partial c}{\partial z}\right)$) at the sediment-water interface ($z = 0$), and the sulfide concentration at the coral tissue ($z = z_s$), were calculated as

$$c(0) = \left(\frac{SRR}{D_{S_{tot}^{2-}}}\right) z_s z_{DBL}, \quad (3a)$$

$$J(0) = SRR z_s, \quad (3b)$$

$$c(z_s) = \left(\frac{SRR}{2D_{S_{tot}^{2-}}}\right) z_s\left(z_s + 2z_{DBL}\right). \quad (3c)$$

Second, to check whether the decomposition of the coral tissue was the sulfide source, we assumed that the sulfide flux at the bottom of the sediment layer was equal to the areal tissue decomposition rate ($J(z_s) = -J_d$), and that sulfide concentration at the top of the diffusive boundary layer as well as SRR in the sediment was zero. Under these boundary conditions, the solution to Eq. (1) is (see SI. Fig. S5, dotted line)

$$c(z) = -\left(\frac{J_d}{D_{S_{tot}^{2-}}}\right)\left(z + z_{DBL}\right), \quad (4)$$

and the flux J_d is calculated as

$$J_d = \frac{-D_{S_{tot}^{2-}} c(z_s)}{\left(z_s + z_{DBL}\right)}, \quad (5)$$

where $c(z_s)$ is the sulfide concentration at the bottom of the sediment layer.

3.4 Anoxia, pH and sulfide exposure experiment

To differentiate between the effects of anoxia, pH and sulfide exposure on *Montipora peltiformis*, coral fragments (10-15 cm^2) were exposed to each of the treatments listed in table 1 (n = 3-5). We conducted three consecutive experiments to reveal: A) the effect of anoxia and of anoxia combined with pH 7; B) the effect of increasing sulfide concentration and

exposure time; and C) the additive affect of exposure to anoxia at pH 7 followed by additional sulfide exposure. The light conditions, sulfide concentrations and pH 7 were chosen based on the microsensor data of the sediment exposure experiment I.

Salinity was 34-35 ppt and temperature was 26-27°C. O_2 concentrations were measured by the Winkler titration method (Winkler 1888) and the total sulfide concentration was determined spectrophotometrically (Cline 1969). The sulfide concentration in the seawater was calculated using the pK_1 6.5, corrected for salinity and temperature (Millero 1988). The pH was measured with a sulfide tolerant pH-sensor (IntLab 412/170, Mettler Toledo, Germany). The pH was adjusted by adding drops of concentrated HCl. Very slow stirring prevented stratification, and imitated the zero flow conditions the corals experienced during sediment coverage. The anoxia and sulfide treatments were conducted in a glove box flushed with N_2. O_2 and temperature sensors constantly monitored the ambient conditions. Coral stress measurements were done with the PAM instrument as described above. After the experiment the corals were transferred back into a large tank. All specimens were further observed in case long-term recovery would be successful.

Table 1. List of treatments of the anoxia, pH and hydrogen sulfide (H_2S) exposure experiments (#). Coral health status measurements were made according to the listed exposure (exp) and recovery (rec) time points.

#	Treatment	Light conditions	O_2 [µM]	H_2S [µM]	pH	Exposure and recovery times [h]: PAM measurements
NC	Negative control	12 h light/dark	207	0	8.2	exp 6, 12, 24, 48, 72, 96 rec 5, 12, 17, 24, 48
PC1	Positive control 1	24 h dark	207	0	8.2	exp 6, 12, 24, 48, 72, 96 rec 5, 12, 17, 24, 48
PC2	Positive control 2	24 h dark	207	0	7	exp 6, 12, 24, 48, 72, 96 rec 5, 12, 17, 24, 48
A1	Anoxia 1	24 h dark	0	0	8.2	exp 24, 48, 72, 96 rec 5, 24, 48
A2	Anoxia 2	24 h dark	0	0	7	exp 6, 12, 24, 48, 72, 96 rec 5, 24, 48
B1	H_2S 1	24 h dark	0	10	7	exp 6, 12, 24, 48 rec 5, 17, 24, 48
B2	H_2S 2	24 h dark	0	20	7	exp 6, 12, 24, 48 rec 5, 17, 24, 48
C	12 h anoxia, then 3 h H_2S	24 h dark	0	20	7	exp 3 rec 12, 24, 48
C	12 h anoxia, then 12 h H_2S	24 h dark	0	20	7	exp 12 rec 12, 24, 48

4. Results

4.1 Sediment exposure experiment I

4.1.1 Coral stress and necrosis measurements

The photosynthetic yield of the control corals was 0.656 ± 0.052 (SD) at the beginning, and 0.652 ± 0.049 at the end of the sediment exposure experiment I, indicating that they remained healthy during the entire experiment. Corals exposed to sediment with + 0% and + 0.06% C_{org} were not affected. Corals exposed to sediment with + 0.3% and + 0.6% C_{org} showed a continuous decrease in photosynthetic yield and an increase in necrotic coral tissue during the experiment. The first killed areas of a size of square millimetres were observed after one (Fig. 1) and two days. The extent of decrease of the coral health status proxy, and the increase of necrosis correlated with the amount of C_{org}-enrichment and exposure time (Fig. 2).

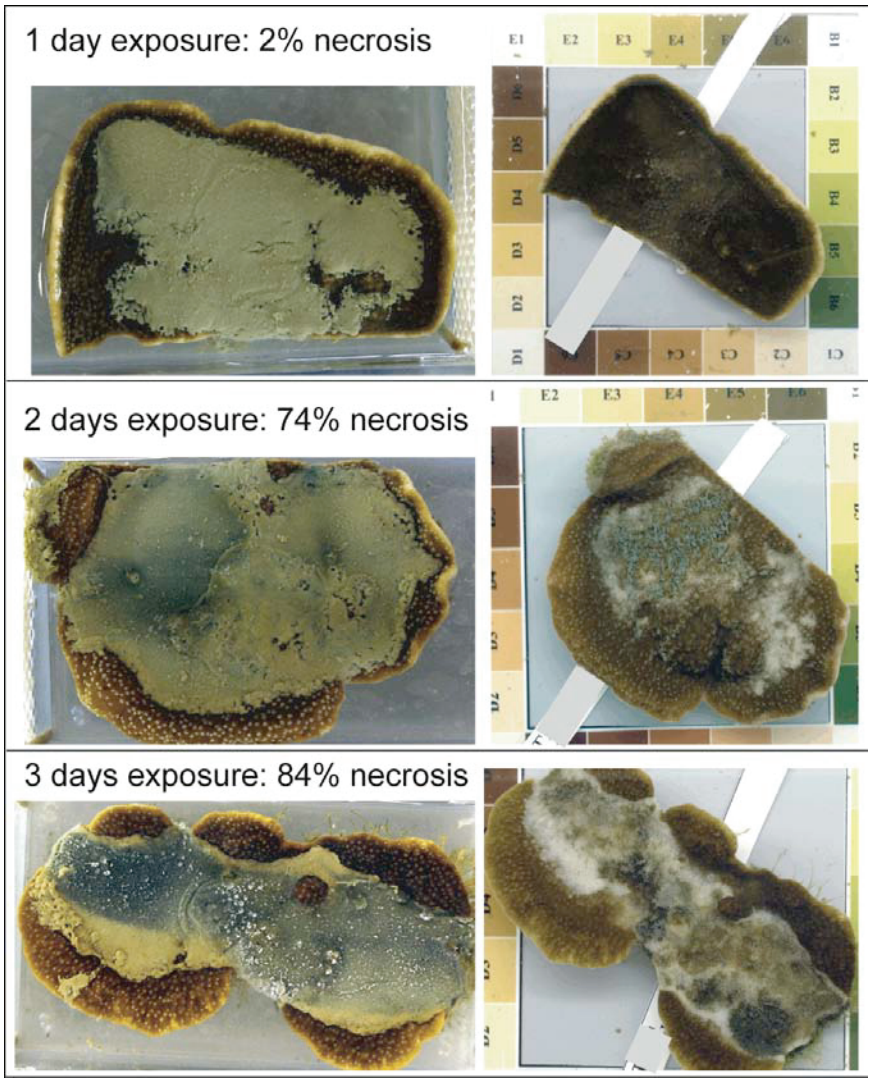

Figure 1. Fragments of the coral *Montipora peltiformis* covered with sediment, which was enriched with + 0.6% C_{org}, and after the sediment was removed. Exposure times were 1, 2 and 3 days, and first necrotic areas were detected after one day.

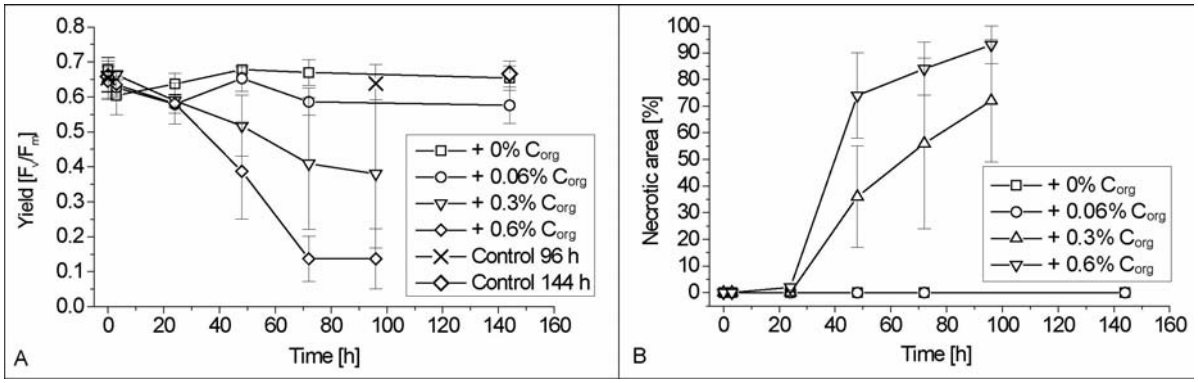

Figure 2. A) The coral health status measured as photosynthetic yield of *Montipora peltiformis* covered by fine reef sediment, and of the coral control pieces. B) The percentage of necrotic coral tissue of the entire sediment-covered area. The sediment (<63 μm) was enriched with three concentrations of plankton mixture, expressed in percent C_{org} of the dry weight of the sediment: + 0%, + 0.06%, + 0.3% and + 0.6% C_{org}. Error bars represent the standard deviation of 4 replicate measurements (n=4).

4.1.2 Mesocosm microsensor measurements

The thickness of the sediment layer covering the coral fragments varied between 2.1-2.6 mm. O_2 concentrations in the sediment layer decreased with increasing exposure time and C_{org}-concentration (Fig. 3). Sediments with + 0% and + 0.06% C_{org}-concentration were depleted in oxygen, but never anoxic. The exposure to sediments enriched with + 0.3% C_{org} and + 0.6% C_{org} caused anoxia at the coral surface after only 3 h. In sediments enriched with + 0.3% C_{org} anoxia was reached in 2 mm sediment depth, whereas in sediments enriched with + 0.6% C_{org} already in 1 mm.

The pH at the coral surface decreased with increasing exposure time and C_{org}-concentration (Fig. 3). In sediments with + 0% and + 0.06% C_{org} pH initially decreased to 8 ± 0.02 (SD) at the coral surface, but afterwards increased to 8.1 ± 0.01 again. A pronounced decrease in pH was measured in sediments enriched with + 0.3% and + 0.6% C_{org}. The pH reached 6.6 and 6.9 respectively.

The hydrogen sulfide (H_2S) concentrations increased with increasing exposure time and C_{org}-concentration (Fig. 4). 1-2 μM H_2S was measured after 48 h of exposure to sediment enriched with + 0.3% C_{org} and after 24 h of exposure to sediment enriched with + 0.6% C_{org}. One day later a substantial increase occurred and the H_2S concentrations were by two orders of magnitudes higher. Total sulfide (S^{2-}_{tot}) concentrations followed initially the same pattern as the H_2S concentration, but after the large increase in sulfide a decrease was observed (Fig. 4).

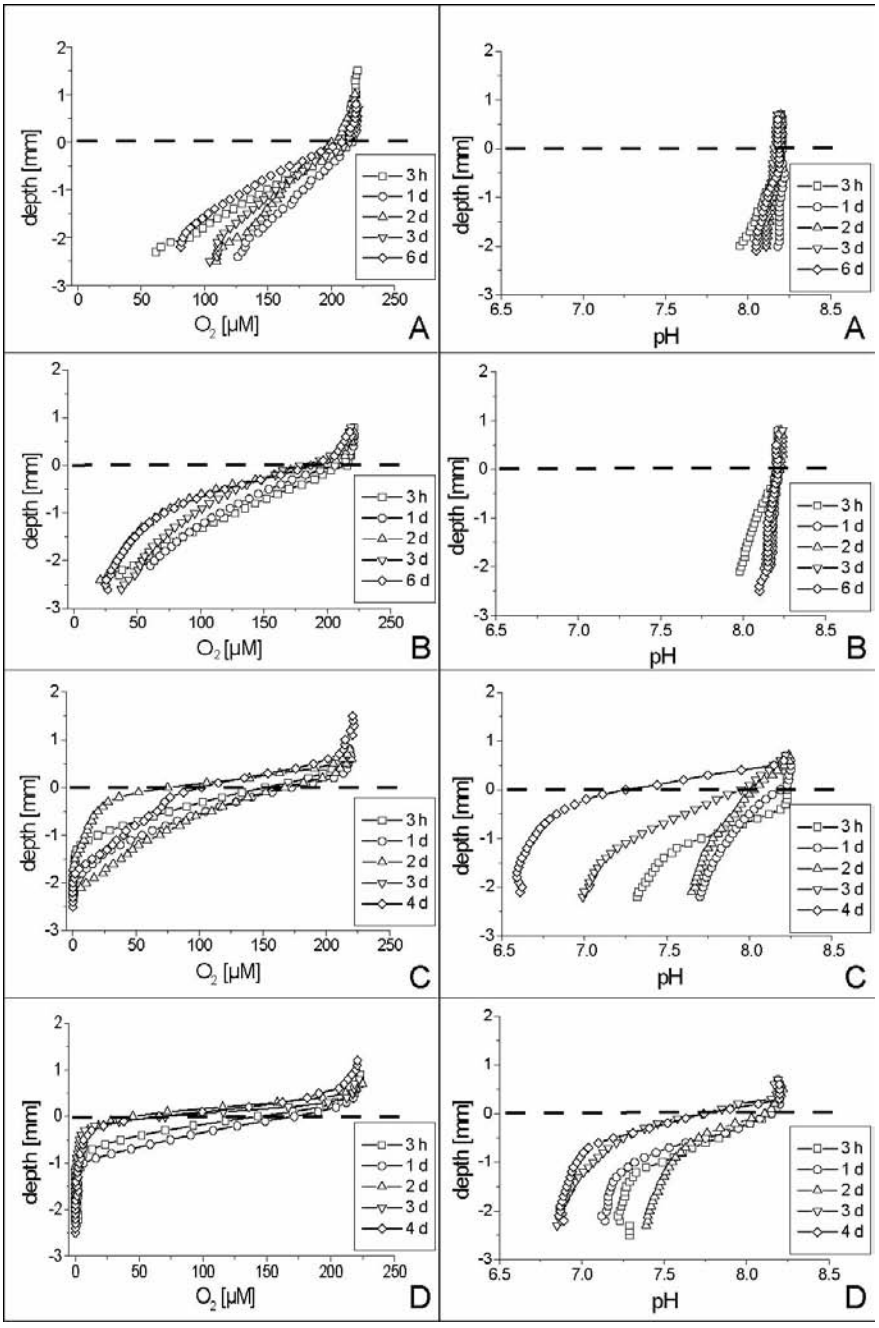

Figure 3. Oxygen concentrations and pH in sediment layers covering *Montipora peltiformis*. Exposure times were 3 hours, 1, 2, 3 and 4 or 6 days. The sediment was enriched with three concentrations of plankton mixture, expressed in percent C_{org} of the dry weight of the sediment: A) + 0%, B) + 0.06%, C) + 0.3% and D) + 0.6% C_{org}. Error bars are omitted for clarity. Each profile represents the average of 3-6 profiles measured at random points (n = 3-6).

Light decreased exponentially in the sediment layer, irrespectively of the C_{org}-concentration. 43% of the surface light reached 0.5 mm sediment depth, 9% reached 1 mm, and <1% reached 1.5 mm. The sediment cover hindered light form reaching the coral surface in all cases.

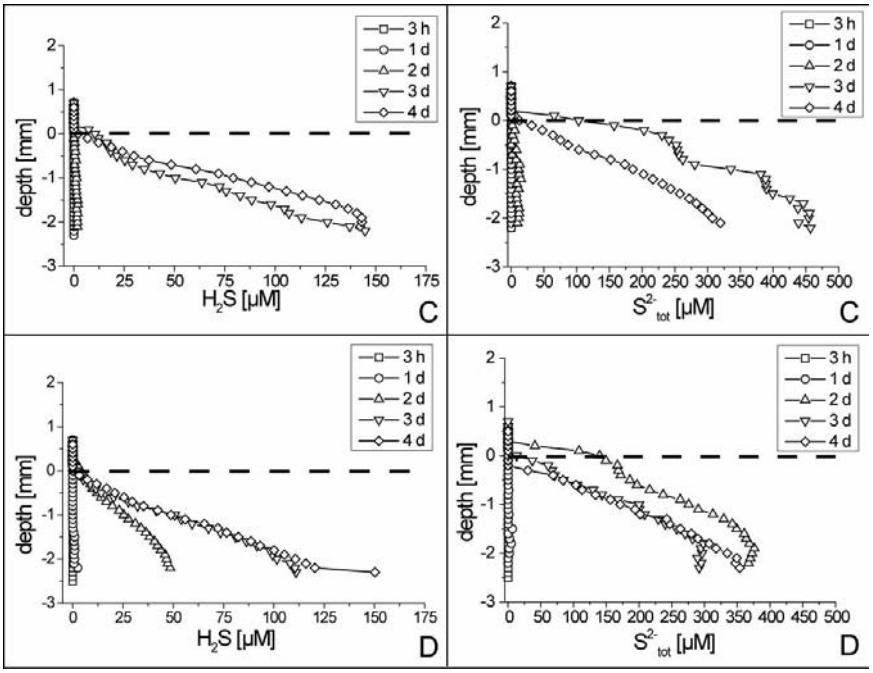

Figure 4. Hydrogen sulfide (H_2S) and total sulfide (S^{2-}_{tot}) concentrations in sediment layers covering *Montipora peltiformis*. Exposure times were 3 hours, 1, 2, 3 and 4 or 6 days. The sediment was enriched with three concentrations of plankton mixture, expressed in percent C_{org} of the dry weight of the sediment: + 0%, + 0.06%, C) + 0.3% and D) + 0.6% C_{org}. Error bars are omitted for clarity. Each profile represents the average of 3-6 profiles measured at random points (n = 3-6). Note that in the + 0% and + 0.06% C_{org}-enrichments no H_2S and S^{2-}_{tot} was measured, so that the graphs are not shown.

4.1.3 Field microsensor measurements

The thickness of the sediment covering the corals varied between 2.5-5 mm. At the offshore sites none of the O_2 profiles measured indicated anoxia at the coral surface under the covering sediment (Fig. 5B1). At the nearshore sites in three out of four corals O_2 was depleted at the coral surface under the sediment layer (Fig. 5A1). At the coral surface pH dropped to 7.6-7.7 in all three replicate profiles (Fig. 5A3). Light intensity had decreased to <1% of the ambient intensity in all samples at 1.5 mm sediment depth (Fig. 5A+B2). During profiling the ambient light recorded was 548 ± 186 (SE) at offshore reefs and 281 ± 62 µmol photons m^{-2} s^{-1} at nearshore reefs.

The microsensor measurements in the field showed similar profiles as in the mesocosm sedimentation exposure experiment I. Although ambient light conditions prevailed, no light reached the coral surface. Reduced pH and oxygen depletion were observed in the sediments with higher concentrations in organics (TOC, TN and TP), but not in the sediments with lower organic matter content (details in § 4.1.5). This supports that the mesocosm experiments realistically mimicked the situation *in situ*.

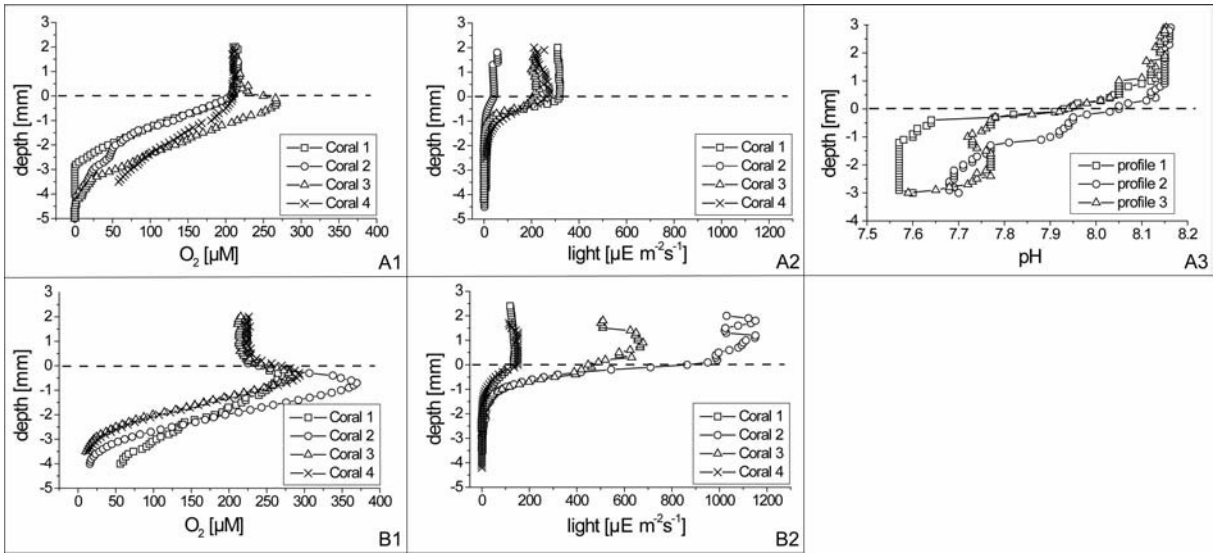

Figure 5. Oxygen, light and pH microprofiles at haphazardly chosen points in natural sediment layers covering corals. O_2 (A1 and B1) and light (A2 and B2) profiles were done on four corals at nearshore (A) and on four at offshore (B) reefs. One coral was chosen for pH profiles at a nearshore (A3) reef site. Each profile represents the average of 3 profiles measured at random points (n = 3).

4.1.4 Molecular analysis

The bacterial community structure within the sediments was investigated using denaturing gradient gel electrophoresis (DGGE) and 16S rRNA cloning. The comparative 16S rRNA sequence analysis showed that most sequences grouped to the bacterial groups *Bacteriodetes, α-, δ-, ε-, γ-Proteobacteria, Firmicutes,* and *Fusobacteria* (Fig. 6 and 7). The dominant bacteria species (DGGE-banding pattern) in the control sediment compared to the sediment covering the corals were the same in all treatments (Fig. 6). This shows that the microbial community was independent from the presence of the coral underneath. After plankton addition to the sediment an immediate increase of microbial activity has been measured with microsensors (Fig. 3 and 4), and within 1-2 days first necrotic areas were detected on the coral (Fig. 2B). The microbial community was similar prior and at the end of the sediment exposure experiment I, and no drastic shift in the bacterial diversity was observed (Fig. 7 and S1). The high number of bacterial groups in clone library III resulted possibly from the long exposure time of 6 days and the nutrient-limited aerobic conditions in the sediment (Fig. 3 and 4). Details on the 16S rRNA clone libraries are in the supporting information (SI. Tab. S1, Fig. S1, S2 and S3 A-F).

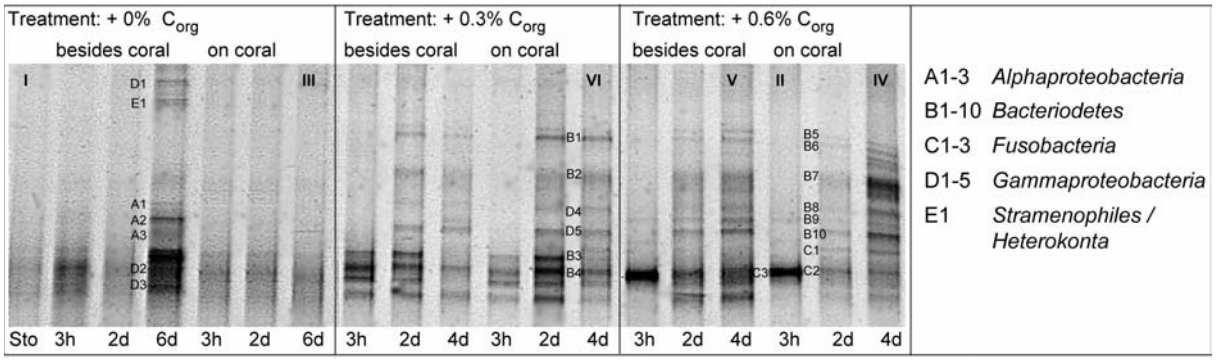

Figure 6. Denaturing gradient gel electrophoresis fingerprints from PCR-amplified 16S rRNA gene fragments of sediments covering the coral *Montipora peltiformis* or control sediments in petridishes. Exposure times were 3 hours, 2, and 4 or 6 days. (Sto) stands for the stock sediment prior to the start of the sediment exposure experiment I. The sediment was enriched with three concentrations of plankton mixture, expressed in percent C_{org} of the dry weight of the sediment: + 0, + 0.3% and + 0.6%. Sequenced bands are indicated according to the legend. Roman numerals (I-VI) indicate the samples from which also 16S rRNA clone libraries were obtained in this study.

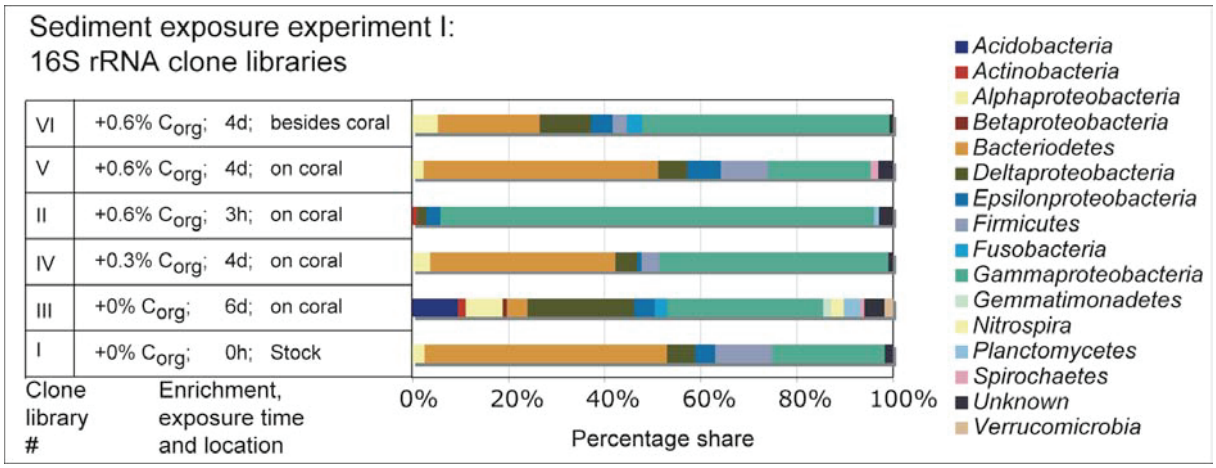

Figure 7. Bacterial community composition obtained from 16S rRNA cloning of six sediment samples covering the coral *Montipora peltiformis* or from control sediment in petridishes (besides coral). Clone library I was from sediment prior to the start of the experiment (stock). Exposure times were 3 hours, and 4 or 6 days. The sediment was enriched with three concentrations of plankton mixture, expressed in percent C_{org} of the dry weight of the sediment: + 0, + 0.3% and + 0.6%. Percentage share refers to the total number of clones obtained in each library (about 120 clones per library (SI. Tab. S1)).

4.1.5 Sediment, plankton mixture and coral tissue analysis

The sediment used for the sediment exposure experiments I and II had a TOC content of 12.5 ± 1 µg DW mg^{-1} before the experiment started. More details on the sediments characteristics, the plankton mixture, and on the coral tissue can be found in the supporting information (SI. Tab. S2 and S3).

TOC, TN, TP, Chl a and Phaeo increased in the sediment enriched with + 0.3% and + 0.6% C_{org} covering the corals. These increases correlated with the death of the corals, and reflected the release from the underlying decaying coral tissue. Sediments with lower C_{org} did not show increased TOC, TN and TP, and the corals survived the experiment. Also in the control sediments (petridishes) these chemical parameters remained constant. The increased Chl a and

Phaeo content in the lower C_{org}-enriched sediment and the control sediments were correlating with algae growth on the sediment surface (personal observation), and therefore regarded as an artifact of the experiment. Graphic illustrations on the temporal changes of TOC, TN, TP, Chl a and Phaeo during the experiment can be found in the supporting information (SI. Fig. S4).

The TOC, TN, and TP analyses of the sediments collected from on top of corals after microsensor profiling in the field, revealed clear differences between the near- and offshore sites. Concentrations were one fourth to twice as high in the sediments from nearshore reefs than in the sediments from offshore reefs (SI. Fig. S5). This indeed corresponds to the *in situ* microsensor measurements where anoxia and reduced pH was measured in the sediment with higher TOC content (details in §4.1.3).

4.2 Sediment exposure experiment II

4.2.1 Sulfate Reduction Rates (SRR)

The SRR of the sediments not C_{org}-enriched remained very low. Some increase in SR in the sediment covering corals was measured after 2 days, however remained below 1. The C_{org}-enrichment of the sediment increased SRR with approximately three orders of magnitude in 2 days. The same rates were measured in sediments covering the corals and the inert surface of the beaker bottom. Interestingly, during the first day of coverage on the corals, the SRR in the sediment seemed to be repressed (Fig. 8).

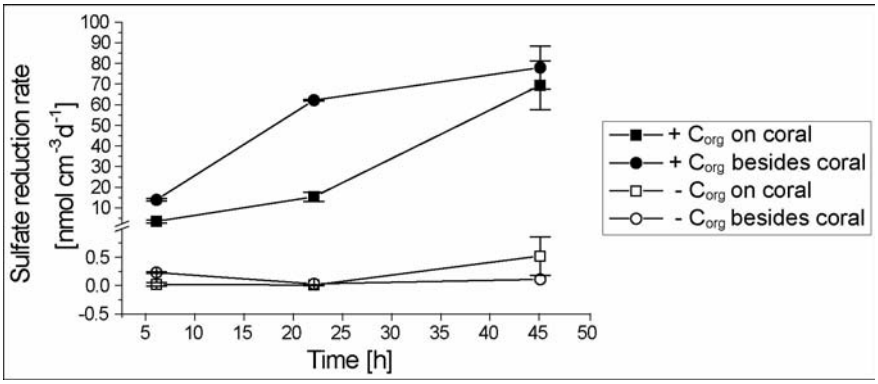

Figure 8. Sulfate reduction rates in sediments covering corals and besides corals. The exposure times were 6, 22, and 45 h. The sediment was enriched with plankton mixture (+C_{org}) or was not enriched (-C_{org}). The error bars represent the standard deviation of 2 replicate measurements (n=2).

4.2.2 Modeling

The observed sulfide profiles were linear inside the sediment layer covering the coral. This implies that no detectable sulfide production occurred in the sediment, but that all sulfide originated from the coral surface. This conceptual conclusion was confirmed by modeling,

which showed that the shape of the measured profiles resembled those derived from Eq. (4) rather than those derived from Eq. (2) (compare Fig. 4 and SI S6). Furthermore, when the measured sulfate reduction rates (Fig. 8) were applied in Eqs. (3a-c), the calculated sulfide concentrations at the top and at the bottom of the sediment layer, as well as the sulfide flux at the sediment surface, were at least an order of magnitude lower than those measured with microsensors (Tab. 2).

Table 2. Sulfide (S^{2-}_{tot}) concentrations and fluxes from microsensor profiles, and from calculations based on measured sulfate reduction rates (SRR) in the sediment layer covering the coral *Montipora peltiformis*. Measurements were conducted as described in sediment exposure experiment I and II. Calculation information and equations see §3.3.2.

Profiles	S^{2-}_{tot} flux	S^{2-}_{tot} concentration sediment surface	coral surface
time [h]	Flux [nmol $m^{-2}s^{-1}$]	c S^{2-}_{tot} [nmol cm^{-3}]	c S^{2-}_{tot} [nmol cm^{-3}]
3	0.00	0.00	0.00
24	-1.97	0.00	2.17
48	-336.35	109.60	369.62
72	-267.64	44.64	294.11
SRR	S^{2-}_{tot} flux	S^{2-}_{tot} concentration sediment surface	coral surface
time [h]	Flux [nmol $m^{-2}s^{-1}$]	c S^{2-}_{tot} [nmol cm^{-3}]	c S^{2-}_{tot} [nmol cm^{-3}]
6	-0.08	0.01	0.05
22	-0.36	0.04	0.23
45	-1.61	0.18	1.06

4.3 Anoxia, pH and sulfide exposure experiment

The corals exposed in the dark to oxic water with pH 8.2 or 7 remained healthy (Fig. 9C). The corals also survived anoxia at pH 8.2 for four days (Fig. 9A1). The exposure to anoxia and reduced pH at the same time resulted in irreversible coral damage after 24 h of exposure (Fig. 9A2). When exposed to anoxia, pH 7 and sulfide, irreversible damage correlated with exposure time and sulfide concentration. At 10 μM sulfide corals were harmed after 48 h and at 20 μM sulfide after 24 h (Fig. 9B1 and B2). Coral death occurred very fast (within 15 h) when they were first exposed to anoxia at pH 7, and then to 20 μM sulfide (Fig. 9C).

5. Discussion

This study showed that the coral damage, which occurred quickly after the accumulation of organic-rich sediment on corals, is microbially mediated. Our hypothesis that sulfide, originating from sulfate reduction, triggered the killing of the sediment-covered coral was falsified. The death of corals could be induced within 15 to 48 hours, and the microbial mechanisms with the causal links to biogeochemical processes turned out to be more complex than anticipated.

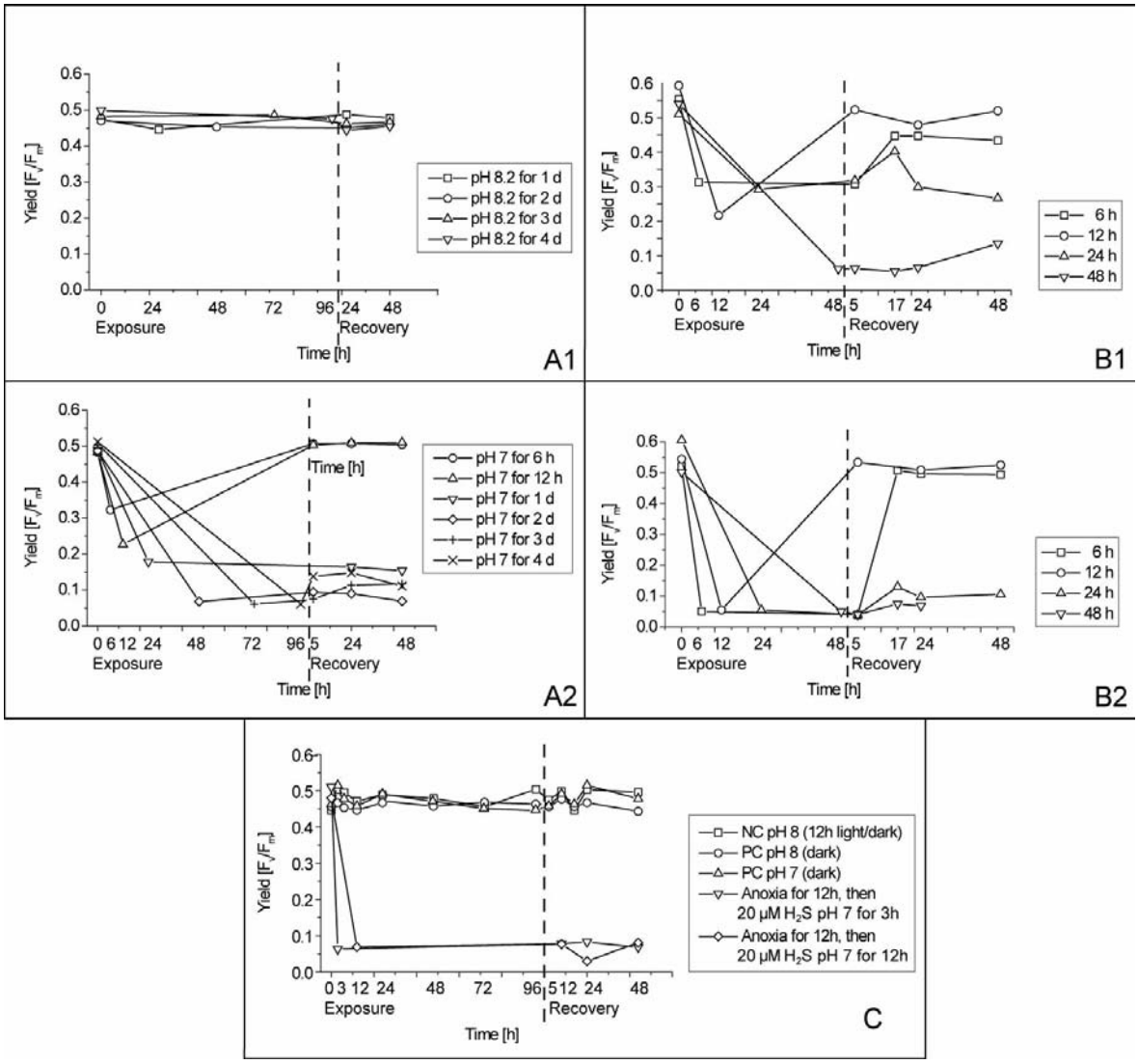

Figure 9. The coral health status measured as photosynthetic yields of *Montipora peltiformis* exposed to anoxia, reduced pH and sulfide. All treatments are listed in table 1 (§ 3.4). The exposure times and recovery times are separated by a dotted line. A1) shows the anoxia treatment at pH 8.2 and A2) shows the anoxia treatment at pH 7. B1) shows the 10 µM sulfide treatment, and B2) shows the 20 µM sulfide treatment. C) shows the positive and negative controls (PC and NC) and the additive exposure treatment. Error bars are omitted for clarity (n = 3-5).

The death of the coral depended on the amount of organic matter in the sediment covering the coral, which led to a combination of microbially induced anoxia, reduced pH and increased sulfide content. We showed that at anoxic conditions low pH alone triggered the initial dying of distinct spots of coral tissue of only few square millimeters in size (Fig. 1, 2 and 10). In the exposure experiment without sediment, but under exclusion of light, oxygenated seawater at pH 7 or anoxic seawater at pH 8.2 did not kill corals. But in anoxic seawater at pH 7 (without sulfide and light) corals were dead within one day (Fig. 9 and 10). Sulfide is not needed for initiating coral death; low pH alone kills corals during anoxia. In fact 20 µM H_2S was needed to kill the coral within one day, whereas only 1-2 µM H_2S were measured in the sediment layer after one day of sediment covering a dying coral. Toxic concentrations of sulfide were

not detected until later in the decay process. The sulfate reduction rates in the sediment layer on the coral were too low to generate sulfide concentrations that were actually measured, and certainly too low to kill the coral. Sulfide could therefore be excluded being the initial trigger for tissue death. But as discussed further below, it did play an important role in speeding up the killing process after little areas of coral tissue had died.

We could falsify a few mechanisms that had previously been suggested to cause coral death. The exclusion of light by covering with sediment did not affect coral health within six days. The coral can survive without photosynthesizing for several days. Also oxygen depletion did not lead to damage of corals within exposure times of four days. Thus we can exclude suffocation and energy shortage as direct cause for the coral demise. It is well documented that corals regularly experience hypoxia or anoxia (Kühl et al. 1995, Ulstrup et al. 2005), and it has been shown that they can survive several days of anoxia (Yonge et al. 1932, Sassaman & Mangum 1973). So it was not surprising that corals were able to handle anoxic conditions at seawater pH for up to six days (Fig. 3 and 9). Also sea anemones, close relatives of corals, can survive anoxia for several days to weeks (Sassaman & Mangum 1973, Mangum 1980). Thus they must be able to sustain energy shortage and then survive on fermentation, as an adaptation to anoxia. Indeed, sea anemones ferment during hypoxic and anoxic conditions (Ellington 1977, 1980). This can lead to a pronounced acidification within the cell (Hochachka et al. 1973), eventually causing severe cell damage (Busa 1986, Grieshaber et al. 1994). We cannot exclude that during the initial killing process, end products from anaerobic metabolic activity, such as succinate, fumarate and lactate, may accumulate in the coral tissue due to the diffusional barrier of the covering sediments. They could exert additional stress, by reducing internal pH or because such end products may be more harmful at pH 7 than at pH 8.2.

Also an infectious disease process, e.g. by fungi and pathogenic bacteria, may be considered. *Alpha-, Beta-, Gamma-, Deltaproteobacteria, Bacteriodetes,* and *Cyanobacteria* have been reported as potential pathogens causing the Black Band Disease of corals (Carlon & Richardson 1995, Sekar et al. 2006). During this study molecular investigations revealed that in the sediments, which damaged the corals, no shifts in the bacterial groups upon enrichment with organic matter and with exposure time were observed (Fig. 7). On the other hand, the microsensor profiles showed that the microbial activity was clearly increased (Fig. 3 and 4). Hence the death of the coral occurred due to increased microbial activity of the dominant bacteria in the sediment on the coral, and possibly not due to specific pathogens. For the successful infection of the host tissue a quorum is needed, which might however be present in the sediments covering corals. Such a hypothesis of classical pathogenesis could only

convincingly be tested using Koch's postulate. The infectious agent must be isolated from diseased individuals and able to induce the disease in otherwise healthy corals. Such an experiment would only be needed if our findings of the direct effects of low pH at anoxic conditions can be disproven.

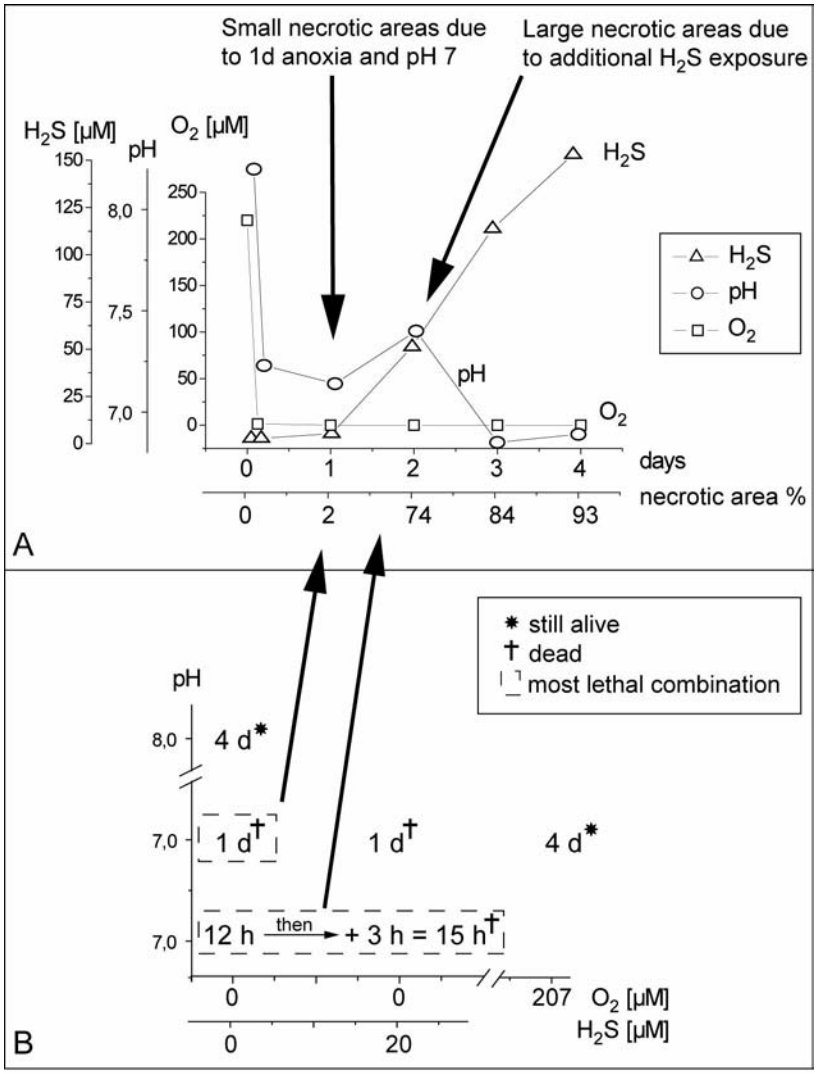

Figure 10. A) Overview of the oxygen, pH, and hydrogen sulfide concentrations at the coral-sediment interface in the sediment enriched with + 0.6% C_{org}. Measuring points were after 3 hours, 1, 2, 3, and 4 days of sediment exposure time. The percentage necrotic coral tissue of the entire sediment-covered coral area is listed to the corresponding measuring times (§ 4.1.2, Fig. 3 and 4). B) Summary of the simulated exposure experiment, where the corals were exposed to anoxia, pH and sulfide. The exposure times and the life status of the coral are listed (§ 4.3, Fig. 9). The arrows indicate that one day of anoxia combined with pH 7 was enough to kill small areas of coral tissue, and that sulfide from decaying tissue accelerated the damage to the neighboring polyps, so that the entire sediment-covered coral was quickly killed.

During the sediment exposure experiment, oxygen scavenging and pH decreasing degradation processes dominated in the layer of sediment enriched with fresh organic matter. After accumulation of the sediment on the coral surface oxygen became rapidly depleted due to respiration of the microbial community in the sediment, and of the coral underneath.

Degradation of the plankton mixture in the sediment led to an accumulation of acidic end products and decreased the pH in the sediment. In the sediment not enriched with the plankton mixture anoxia or a pH below 8.1 was not detected. The mucus of the coral alone was apparently insufficient to induce degradation processes as observed in the enriched sediments, or the coral mucus could have had to a certain extent biocidal effects. The sediment covering live coral had a sulfate reduction rate of only 25% of identical sediment that did not cover the corals. Thus corals seemed to be able to repress sulfate reduction rates and thereby possibly prevent high sulfide concentrations. Indeed it was previously shown that fresh coral mucus inhibits sulfate reduction in sediments (Werner et al. 2006).

The high H_2S concentrations of 50 to >100 μM in the sediment layer on the coral, were measured only 24 h after the first signs of coral death and sulfide detection (Fig. 4 and 10). Although sulfate reduction rates increased upon enrichment with plankton mixture, they were too low to account for the sudden large sulfide fluxes measured with microsensors (Fig. 8, Tab. 2). Moreover, the shape of the sulfide profiles indicated that the source of the sulfide was not in the 2 mm sediment layer, but at the coral-sediment interface. Most of the observed sulfide therefore originated from microbially degraded coral tissue and coral mucus, both known to contain substantial amounts of organic sulfur compounds (Hill et al. 1995, Brown & Bythell 2005). The rapid consumption of the sulfur-rich tissue and mucus locally increased the sulfide concentrations at the coral surface. The concentration of hydrogen sulfide (H_2S) in the sediment layer on the coral increased due to continuously decreasing pH, as the sulfide (S^{2-}_{tot}) equilibrium of H_2S, HS^- and S^{2-} is influenced by pH (Kühl & Steuckart, 2000). H_2S is known to easily penetrate tissues (Jacques 1936), and is thus probably more poisonous than HS^- and S^{2-}. So sulfide poisoning killed the surrounding living tissue, already stressed by the exposure to anoxia and reduced pH, speeding up the killing process substantially. The result was the rapid death of the whole sediment-covered area of several square centimeters size (Fig. 10). In our exposure experiment without sediment, the negative effect on the coral was enhanced when the coral was first exposed for 12 h to anoxia at pH 7 and then additionally for 3 h to sulfide (§ 4.3, Fig. 9). This confirmed that the defense mechanisms of the coral against sulfide were impacted by previous anoxia and low pH exposure. However, we cannot exclude that also products from e.g. proteolytic processes, such as biogenic amines, phenolic compounds, or ammonia could have added stress during sediment-coverage and speeding up the killing process.

The observed almost linear sulfide profiles showed that in the sediment mainly diffusive sulfide transport occurred. The sulfide profiles gradually developed over hours to days, and thus a true steady state was not reached. However, for the quantitative analyses the production

rates were sufficiently slow to assume a steady state for each profile. The decrease of sulfide in the sediment layer after three days (Fig. 4) indicates that the sulfur pool of the coral tissue was depleted. Black spots on the sediment surface as well as white filamentous bacteria were observed during the experiment after the third and fourth day respectively. This indicated a sulfur cycle within this 2 mm sediment layer, including chemical and biological sulfide oxidation (Cline & Richards 1969, Kelly 1988).

Related to coastal development it has been reported that after flood plumes and resuspension events organic-rich sediment covers reef organisms (Nemeth & Nowlis 1999, Nugues & Robertes 2003, Fabricius et al. 2007). This organic matter-rich sediment largely consists of labile high- and low-molecular-weight compounds (Santschi et al. 1995), similar to the fresh plankton mixture we added. From fresh plankton it is known that it releases dissolved organics, which are extremely bioreactive (Ohnishi et al. 2004), and that they immediately enhance the microbial activity (Harvey et al. 1995). Hydrolyzing, fermenting and respiring bacteria, such as *Gammaproteobacteria*, *Bacteriodetes*, and *Fusobacteria* are well-known to respond quickly to input of organics and to decompose polymers also under anoxic conditions (Jørgensen 2006). As shown in this study, consecutive microbial processes can kill corals within less than one day after the sediment accumulated on the coral, depending on organic matter content of the sediment. For coastal management it is therefore important to know that sedimentation of organic-rich material is particularly dangerous for coral reefs.

6. Acknowledgements

We thank Craig Humphrey (AIMS) and Tim Cooper (AIMS) for lab and field assistance and Steven Boyle (AIMS), Raphael Wust (James Cook University), Thomas Max (MPI MM) and Astrid Rohwedder (MPI MM) for analytical support. We gratefully acknowledge all technicians of the Microsensor Department for providing the microsensors. Many thanks also to Claudio Richter (at that time ZMT Bremen), Dieter Hanelt (at that time AWI Helgoland) and Kai Bischof (University of Bremen) for kindly lending measuring instruments. MW acknowledges the support through a PhD scholarship by the German Academic Exchange Service (DAAD) and the Max Planck Society.

7. Supporting Information Available

One phylogenetic reconstruction of 16S rRNA gene sequences recovered from denaturing gradient gel electrophoresis of the sediment exposure experiment I (SI. Fig. S1), six phylogenetic reconstructions of 16S rRNA gene sequences from cloning of sediment samples of the sediment exposure experiment I (SI. Fig. S3 A-F), the diversity-richness calculations from the clone libraries of the six sediment samples (SI. Tab. S1), the calculated rarefaction

curves of the observed operational taxonomic units richness among the six clone libraries (SI. Fig. S2), data on the characteristics of the sediment used in the sediment exposure experiment I and II (SI. Tab. S2), the TOC, TN, TP, Chla a and Phaeo content in the plankton mixture used for the enrichment of the Wilkie Island sediment in the sediment exposure experiment I and II, and the TC, TN and TS content in the tissue of the coral *Montipora peltiformis* (SI. Tab. S3), the graphic illustrations on changes of TOC, TN, TP, Chl a and Phaeo with exposure time in the sedimentation exposure experiment I (SI. Fig. S4), data on the characteristics of the natural sediment on the corals at the nearshore and offshore reefs in Australia (SI. Tab. S4), and the graphic illustration for the modeling approach (SI. Fig. S5).

8. References

Abed RMM, Garcia-Pichel F (2001) Long-term compositional changes after transplant in a microbial mat cyanobacterial community revealed using a polyphasic approach. Environ. Microbiol. 3:53-62

Abed RMM, Kohls K, de Beer D (2007) Effect of salinity changes on the bacterial diversity, photosynthesis and oxygen consumption of cyanobacterial mats from an intertidal flat of the Arabian Gulf. Environ. Microbiol. 7:593-601

Alldredge A, Silver, MW (1988) Characterstics, dynamics and significance of marine snow. Prog. Oceanogr. 20:41-82

Ayukai T, Wolanski E (1997) Importance of biologically mediated removal of fine sediments from the Fly River plume, Papua New Guinea. Estuar. Coast. Shelf Sci. 44:629-639

Bagarinao T (1992) Sulfide as an environmental factor and toxicant: tolerance and adaptations in aquatic organisms. Aquat. Toxicol. 24:21-62

Bothner M, Reynolds RL, Casso MA, Storlazzi CD, Field ME (2006) Quantity, composition, and source of sediment collected in sediment traps along the fringing coral reef off Molokai, Hawaii. Mar. Poll. Bull. 52:1034-1047

Brooks G, Devine B, Larson RA, Rood BP (2007) Sedimentary development of Coral Bay, St. John, USVI: A shift from natural to anthropogenic influences. Carib. J. Sci. 43:226-243

Brown BE, Bythell JC (2005) Perspectives on mucus secretion in reef corals. MEPS 296:291-309

Busa WB (1986) Mechanisms and consequences of cell regulation. Ann. Rev. Physiol. 48:389-402

Carlton RG, Richardson LL (1995) Oxygen and sulfide dynamics in a horizontally migrating cyanobacterial mat: Black band disease of corals. FEMS Microbiol. Ecol. 18:155-162

Cline JD (1969) Spectrophotometric determination of hydrogen sulfide in natural waters. Limnol. Oceanogr. 14:454-458

Cline JD, Richards FA (1969) Oxygenation of hydrogen sulfide in seawater at constant salinity, temperature and pH. ES&T 3:838-843

de Beer D, Glud A, Epping E, Kühl M (1997) A fast-responding CO_2 microelectrode for profiling sediments, microbial mats, and biofilms. Limnol. Oceanogr. 42:1590-1600

Dubinsky Z, Stambler, N (1996) Marine pollution and coral reefs. Global Change Biology 2:511-526

Edzwald JK, Upchurch JB, O'Melia CR (1974) Coagulation in estuaries. ES&T 8:58-63

Ellington WR (1977) Aerobic and anaerobic degradation of glucose by the estuarine sea anemone, *Diadumene leucolena*. Comp. Biochem. Physiol. 58B:173-175

Ellington WR (1980) Some aspects of the metabolism of the sea anemone *Haliplanella luciae* (Verrill) during air exposure and hypoxia. Mar. Biol. Lett. 1:255-262

Fabricius KE (2005) Effects of terrestrial runoff on the ecology of corals and coral reefs: review and synthesis. Mar. Poll. Bull. 50:125-146

Fabricius KE, Golbuu Y, Victor S (2007) Selective mortality in coastal reef organisms from an acute sedimentation event. Coral Reefs 26:69-69

Fabricius KE, Wolanski E (2000) Rapid smothering of coral reef organisms by muddy marine snow. Estuar. Coast. Shelf Sci. 50:115-120

Gibbs RJ (1983) Effect of natural organic coatings on the coagulation of particles. ES&T 17:237-240

Grieshaber M, Hardeig I, Kreutzer U, Pörtner H-O (1994) Physiological and metabolic responses to hypoxia in invertebrates. Rev. Physiol. Biochem. Pharmacol. 125:43-147

Grossart HP, Ploug H (2001) Microbial degradation of organic carbon and nitrogen on diatom aggregates. Limnol. Oceanogr. 46:267-277

Harvey H, Tuttle JH, Bell JT (1995) Kinetics of phytoplankton decay during simulated sedimentation: Changes in biochemical composition and microbial activity under oxic and anoxic conditions. Geochim. Cosmochim. Acta. 59:3367-3377

Hill R, Dacey JWH, Krupp, DA (1995) Dimethylsulfoniopropionate in reef corals. Mar. Bull. Mar. Sci. 57:489-494

Hochachka PW, Fields J, Mustafa T (1973) Animal life without oxygen: Basic biochemical mechanisms. Amer. Zool. 13:543-555

Jacques AG (1936) The kinetics of penetration: XII. Hydrogen sulfide. J. Gen. Physiol. 19:397-418

Jeroschewski P, Steuckart C, Kühl M (1996) An amperometric microsensor for the determination of H_2S in aquatic environments. Analyt. Chem. 68:4351-4357

Jørgensen BB (1982) Mineralization of organic matter in the sea bed - the role of sulphate reduction. Nature 296:643-645

Jørgensen BB (2001) Life in the diffusive boundary layer. In: Boudreau PB, Jørgensen BB (eds) The benthic boundary layer. Oxford University Press, Oxford, pp 348-373

Jørgensen BB (2006) Bacteria and marine biogeochemistry. In: Schulz HD, Zabel M (eds) Marine Geochemistry. Springer Verlag, Berlin, pp 173-208

Kallmeyer J, Ferdelman TG, Weber A, Fossing H, Jørgensen BB (2004) A cold chromium distillation procedure for radiolabeled sulfide applied to sulfate reduction measurements. Limnol. Oceanogr. Methods 2:171-180

Kaltenböck E, Herndl GJ (1992) Ecology of amorphous aggregations (marine snow) in the Northern Adriatic Sea. IV. Dissolved nutrients and the autotrophic community associated with marine snow. MEPS 87:147-159

Kelly DP (1988) Oxidation of sulfur compounds. In: Cole AS, Ferguson SJ (eds) The nitrogen and sulfur cycles. Soc. Gen. Microbiol., pp 65-98

Kühl M, Cohen Y, Dalsgaard T, Jørgensen BB, Revsbech NP (1995) Microenvironment and photosynthesis of zooxanthellae in scleractinian corals studied with microsensors for O_2, pH and light. MEPS 117:159-172

Kühl M, Steuckart C (2000) Sensors for in situ analysis of sulfide in aquatic systems. In: Buffle J, Horvai G (eds) In situ monitoring of aquatic systems. Chemical analysis and speciation. Wiley-VHC Verlag, pp 121-159

Kühl M, Steuckart C, Eickert G, Jeroschewski P (1998) A H_2S microsensor for profiling biofilms and sediments: Application in an acidic lake sediment. Aquatic Microbial Ecology 15:201-209

Larcombe P, Costen A, Woolfe KJ (2001) The hydrodynamic and sedimentary setting of nearshore coral reefs, central Great Barrier Reef shelf, Australia: Paluma Shoals, a case study. Sedimentology 48:811-835

Lassen C, Jørgensen BB (1994) A fiberoptic irradiance microsensor (cosine collector) - Application for *in situ* measurements of absorption-coefficients in sediments and microbial mats. FEMS Microbiol. Ecol. 15:321-336

Ludwig W, Strunk O, Klugbauer S, Klugbauer N, Weizenegger M, Neumaier J, Bachleitner M, Schleider K-H (1998) Bacterial phylogeny based on comparative sequence analysis. Electrophoresis 19:554–568.

Magnum DC (1980) Sea anemone neuromuscular responses in anaerobic conditions. Science 208:1177-1178

Millero FJ, Plese T, Fernandez M (1988) The dissociation of hydrogen sulfide in seawater. Limnol. Oceanogr. 33:269-274

Muyzer G, Teske A, Wirsen CO, Jannasch HW (1995) Phylogenetic relationships of *Thiomicrospira* species and their identification in deep-sea hydrothermal vent samples by Denaturing Gradient Gel-Electrophoresis of 16S rDNA fragments. Arch. Microbiol. 164:165-172

Nemeth RS, Nowlis JS (2001) Monitoring the effects of land development on the near-shore reef environment of St. Thomas, USVI. Bull. Mar. Sci. 69:759-775

Nugues MM, Roberts CM (2003) Coral mortality and interaction with algae in relation to sedimentation. Coral Reefs 22:507-516

Ohnishi Y, Minoru F, Murashige S, Yuzawa A, Miyasaka H, Suzuki Y (2004) Microbial decomposition of organic matter derived from phytoplankton cellular compounds in seawater. Microbes Environ. 19:128-136

Passow U (2002) Transparent exopolymer particles (TEP) in aquatic environments. Progr. Oceanogr. 55:287-333

Peters EC, Pilson MEQ (1985) A comparative study of the effects of sedimentation on symbiotic and asymbiotic colonies of the coral *Astrangia danae*. JEMBE 92:215-230

Philipp E, Fabricius K (2003) Photophysiological stress in scleractinian corals in response to short-term sedimentation. JEMBE 287:57-78

Revsbech NP (1989) An oxygen microsensor with a guard cathode. Limnol. Oceanogr. 34:474-478

Rogers CS (1983) Sublethal and lethal effects of sediments applied to common Caribbean Reef corals in the field. Mar. Poll. Bull. 14:378-382

Rogers CS (1990) Responses of coral reefs and reef organisms to sedimentation. MEPS 62:185-202

Santschi PH, Guo L, Baskaran M, Trumbore S, Southon J, Bianchi TS, Honeyman B, Cifuentes L (1995) Isotopic evidence for the contemporary origin of high-molecular weight organic matter in oceanic environments. Geochim. Cosmochim. Acta 59:625-631

Sassaman C, Mangum CP (1973) Relationship between aerobic and anaerobic metabolism in estuarine anemones. Comp. Biochem. Physiol. 44A:1313-1319

Schreiber U, Schliwa U, Bilger W (1986) Continuous recording of photochemical and non-photochemical chlorophyll fluorescence quenching with a new type of modulation fluorometer. Photosynth. Res. 10:51-62

Schulz H, Zabel M. (2006) Marine Geochemistry. Springer-Verlag, Berlin

Sekar R, Mills DK, Remily ER, Voss JD, Richardson LL (2006) Microbial communities in the surface mucopolysaccharide layer and the black band microbial mat of Black Band-diseased *Siderastrea siderea*. Appl. Environ. Microbiol. 72:5963-5973

Sofonia J, Anthony KRN (2008) High-sediment tolerance in the reef coral *Turbinaria mesenterina* from the inner Great Barrier Reef lagoon (Australia). Estuar. Cost. Shelf Sci. 78:748-752

Sorokin YI (1978) Microbial production in the coral-reef community. Arch. Hydrobiol. 83:281-323

Stafford-Smith MG (1993) Sediment-rejection efficiency of 22 species of Australian scleractinian corals. Mar. Biol. 115:229-243

Ulstrup KE, Ross H, Peter J (2005) Photosynthetic impact of hypoxia on in hospite zooxanthellae in the scleractinian coral *Pocillopora damicornis*. MEPS 286:125-132

Vargas-Ángel B, Riegl B, Gilliam D, Dodge RE (2006) An experimental histopathological rating scale of sediment stress in the Caribbean coral Montastrea cavernosa. 10th International Coral Reef Symposium. Proceedings of the 10th International Coral Reef Symposium, Okinawa, pp 1168-1173

Weber M (2009) How sediment damages corals. PhD thesis. University of Bremen

Weber M, Färber P, Meyer V, Lott C, Eickert G, Fabricius KE, De Beer D (2007) In situ applications of a new diver-operated motorized microsensor profiler. ES&T 41:6210-6215

Weber M, Lott C, Fabricius KE (2006) Sedimentation stress in a scleractinian coral exposed to terrestrial and marine sediments with contrasting physical, organic and geochemical properties. JEMBE 336:18-32

Werner U, Bird P, Wild C, Ferdelman T, Polerecky L, Eickert G, Jonstone R, Hoegh-Guldberg O, de Beer D (2006) Spatial patterns of aerobic and anaerobic mineralization rates and oxygen penetration dynamics in coral reef sediments. MEPS 309:93-105

Wessling I, Uychiaoco AJ, Alino PM, Aurin T, Vermaat JE (1999) Damage and recovery of four Philippine corals from short-term sediment burial. MEPS 176:11-15

Wilkinson C (2002) Status of coral reefs of the world: 2002. Australian Institute of Marine Science, Townsville

Winkler LW (1888) Die Bestimmung des in Wasser gelösten Sauerstoffs. Ber. dtsch. chem. Ges.:2843-2854

Wolanski E, Duke N. (2002) The threat mud poses to the Great Barrier Reef of Australia. In: Healy T, Wang Y, Healy JA (eds) Muddy coasts of the world: Process, Deposits and Function. Elsevier Science, Amsterdam, pp 533-542

Yonge C, Yonge MJ, Nicholls AG (1932) Studies on the physiology of corals - VI. The relationship between respiration in corals and the production of oxygen by their zooxanthellae. Great Barrier Reef Expedition 1928-29 Science Reports 1:213-251

9. Supporting Information

A cascade of microbial processes kills sediment-covered corals

Weber, M.*[1,2], Lott, C.[1,2], Kohls, K.[1], Polerecky, L.[1], Abed, R. M. M.[1,4], Ferdelman, T.[1], Fabricius, K. E.[3], and de Beer, D.[1]

[1] Max Planck Institute for Marine Microbiology, Celsiusstrasse 1, 28359 Bremen, Germany
[2] HYDRA Institute for Marine Sciences, Elba Field Station, Via del Forno 80, 57034 Campo nell'Elba (LI), Italy
[3] Australian Institute of Marine Science, PMB No 3, Townsville, QLD 4810, Australia
[4] Sultan Qaboos University, College of Science, Biology Department, P.O. Box 36, Muscat 123, Sultanate of Oman

The supporting information provides:

1. The phylogenetic reconstruction of 16S rRNA gene sequences recovered from denaturing gradient gel electrophoresis of the sediment exposure experiment I – page 28 (SI. Fig. S1)
2. The diversity-richness calculations from the clone libraries of the six sediment samples – page 29 (SI. Tab. S1)
3. The calculated rarefaction curves of the observed operational taxonomic units richness among the six clone libraries – page 29 (SI. Fig. S2)
4. Six phylogenetic reconstructions of 16S rRNA gene sequences from cloning of sediment samples of the sediment exposure experiment I – pages 30-36 (SI. Fig. S3 A-F)
5. Data on the characteristics of the sediment used in the sediment exposure experiment I and II – page 36 (SI. Tab. S2)
6. The TOC, TN, TP, Chla a and Phaeo content in the plankton mixture used for the enrichment of the Wilkie Island sediment in the sediment exposure experiment I and II, and the TC, TN and TS content in the tissue of the coral *Montipora peltiformis* – page 36 (SI. Tab. S3)
7. Data on the characteristics of the natural sediment on the corals at nearshore and offshore reefs in Australia – page 37 (SI. Tab. S4)
8. The graphic illustrations on changes of TOC, TN, TP, Chl a and Phaeo with exposure time in the sedimentation exposure experiment I – page 38 (SI. Fig. S4)
9. The graphic illustration of the curved and linear steady-state diffusive profiles of the sulfide concentrations used for the modeling approach – page 39 (SI. Fig. S5)

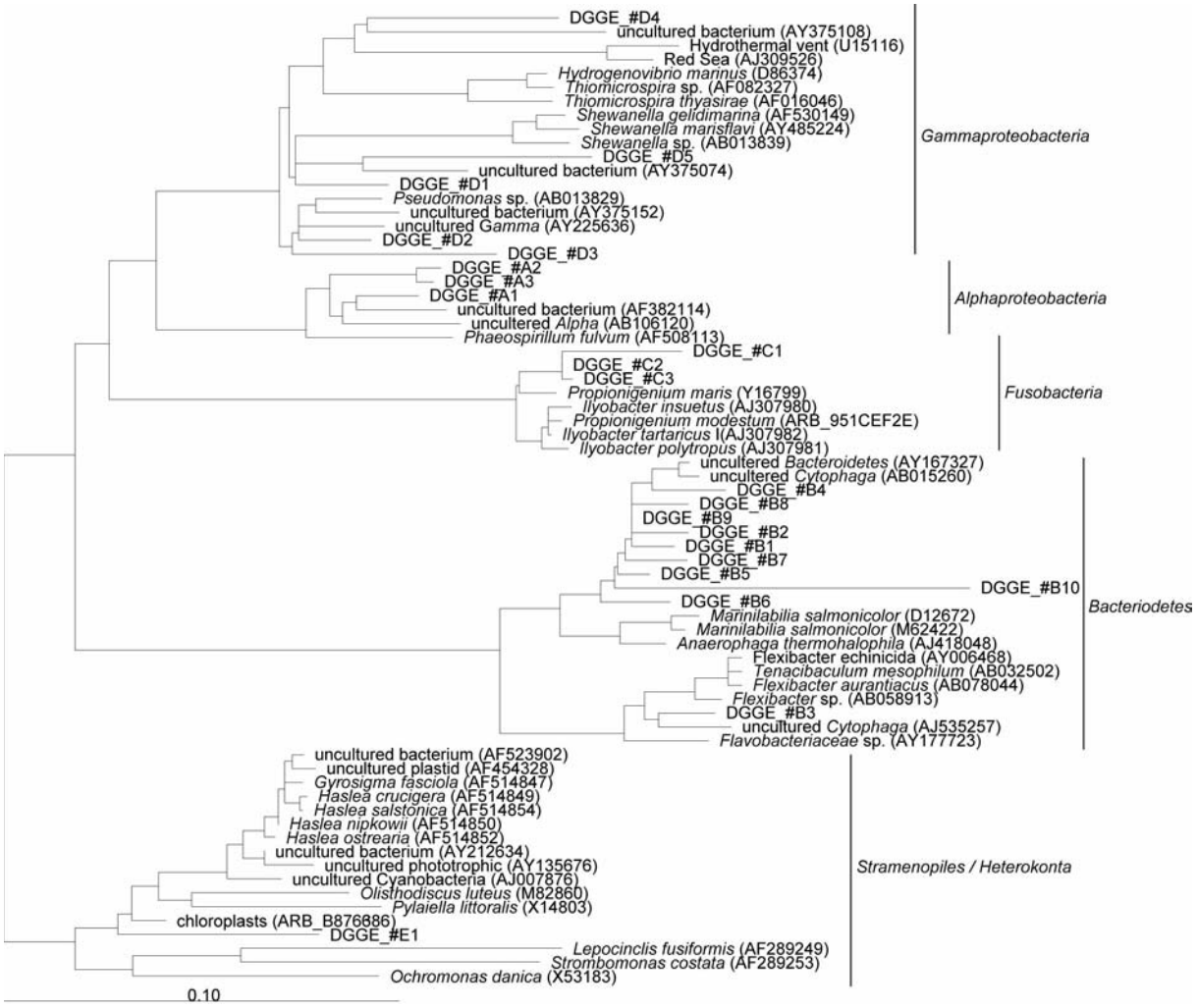

Figure S1. Phylogenetic reconstruction of 16S rRNA gene sequences recovered from denaturing gradient gel electrophoresis of sediment samples. These were exposed on the coral *Montipora peltiformis* or besides corals on petridishes (control) for 3 hours and 4 or 6 days. The numbers in the sequence name refer to the DGGE gel bands (fig. 6). The sequences were compared against sequences obtained from public databases and the phylogenetic placement was carried out using parsimony criteria without changing topology of the pre-established tree using ARB software. The bar indicates 10% sequence divergence.

Table S1. Diversity-richness calculations from 16S rRNA clone libraries of six sediment samples covering the coral *Montipora peltiformis* or from control sediment in petridishes (besides coral). Clone library I was from sediment prior to the start of the experiment (stock). Exposure times were 3 hours, and 4 or 6 days. The sediment was enriched with three concentrations of plankton mixture, expressed in percent C_{org} of the dry weight of the sediment: + 0, + 0.3% and + 0.6%.

Clone library #	I	III	II	V	IV	VI
C_{org}-enrichent	+ 0%	+ 0%	+ 0.6%	+ 0.6%	+ 0.6%	+ 0.3%
Exposure time	-	6 d	3 h	4 d	4 d	4 d
Location	Stock	on coral	on coral	besides coral	on coral	on coral
Number of clones	119	117	103	132	131	109
Number of total OTUs	56	86	14	46	51	48
Number of unique OTUs	35	72	9	27	32	27
Number of classes	7	15	6	8	8	7
Coverage (%)	71	38	91	80	76	75
Species richness	26.50	41.10	6.50	21.20	23.60	23.10
Spieces evenness	1.50	2.10	-2.10	1.10	1.20	1.50
Shannon-Weaver index	2.65	4.06	-2.38	1.77	2.11	2.54

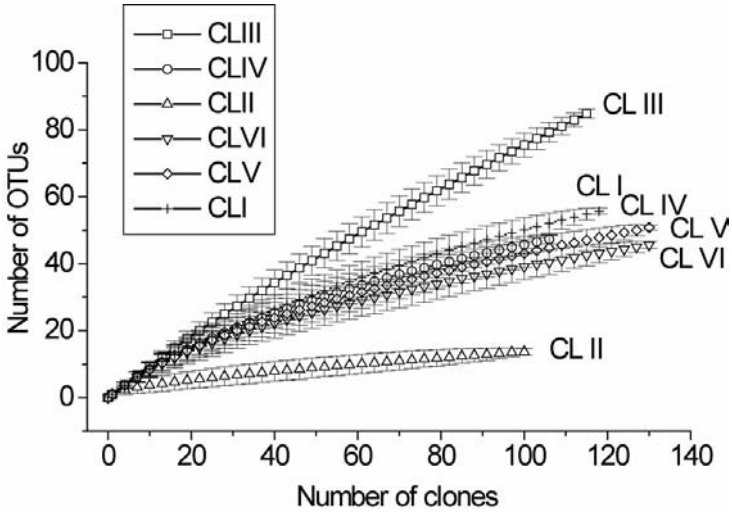

Figure S2. Calculated rarefaction curves of the observed operational taxonomic units (OTU) richness among the six clone libraries I-VI. For details see table S1.

Fig. S3 A: Clone library I = stock sediment with + 0% C_{org} (figure legend page 97)

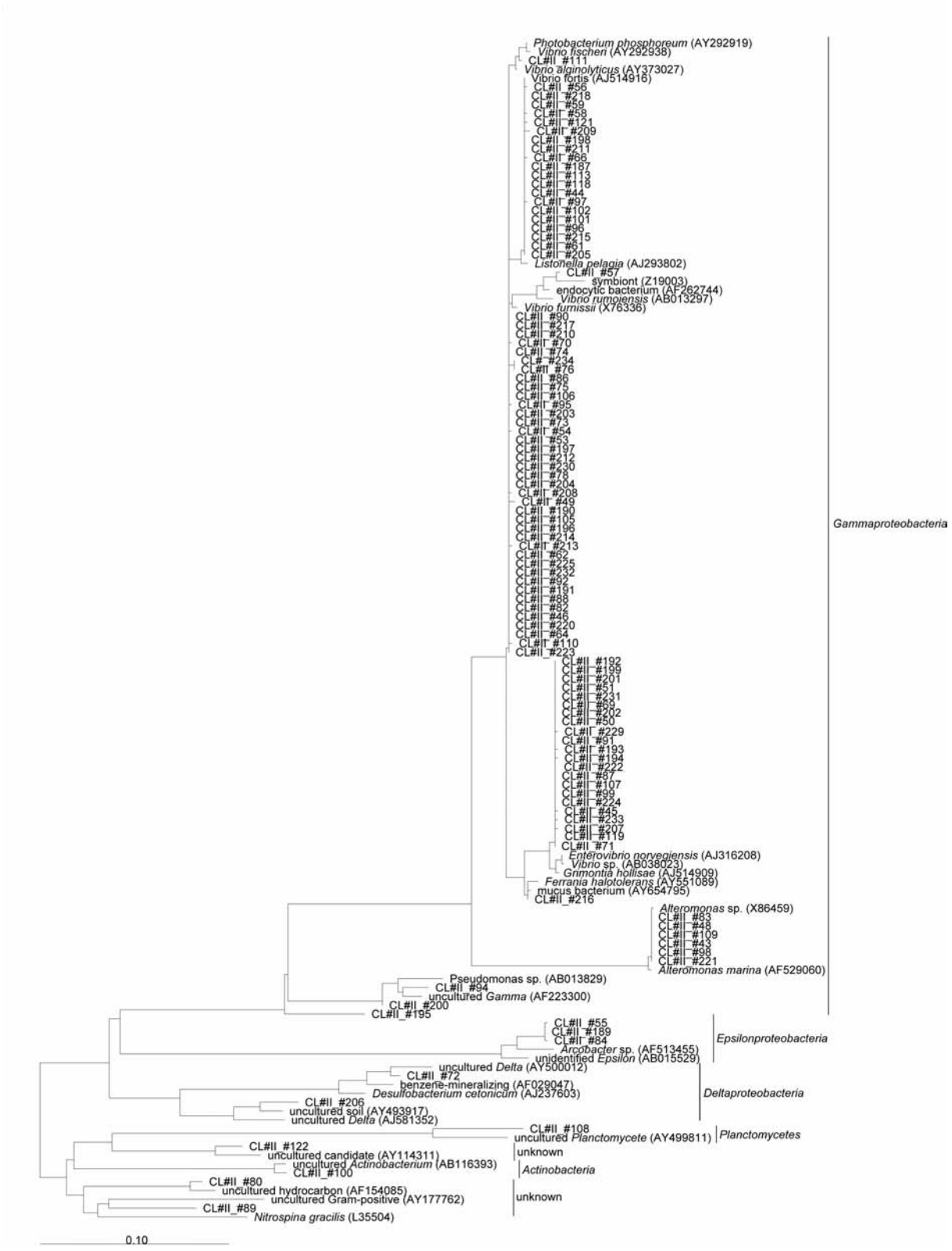

Fig. S3 B: Clone library II = + 0.6% C_{org}, 3 h, on coral (figure legend page 97)

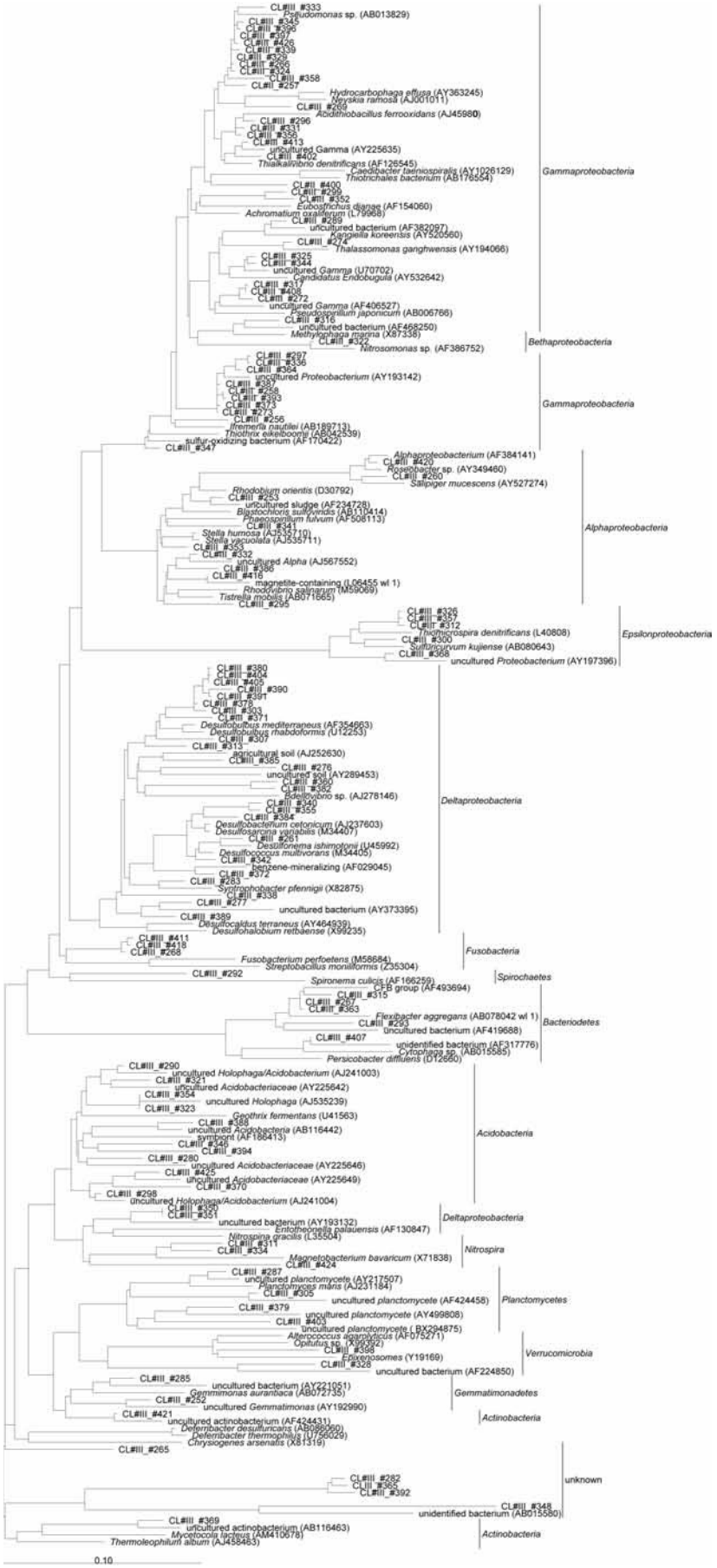

Fig. S3 C: Clone library III = + 0.6% C_{org}, 6 d, on coral (figure legend page 97)

Fig. S3 D: Clone library IV = + 0.6% C_{org}, 4 d, on coral (figure legend page 97)

Fig. S3 E: Clone library V = + 0.6% C_{org}, 4 d, besides coral (figure legend page 97)

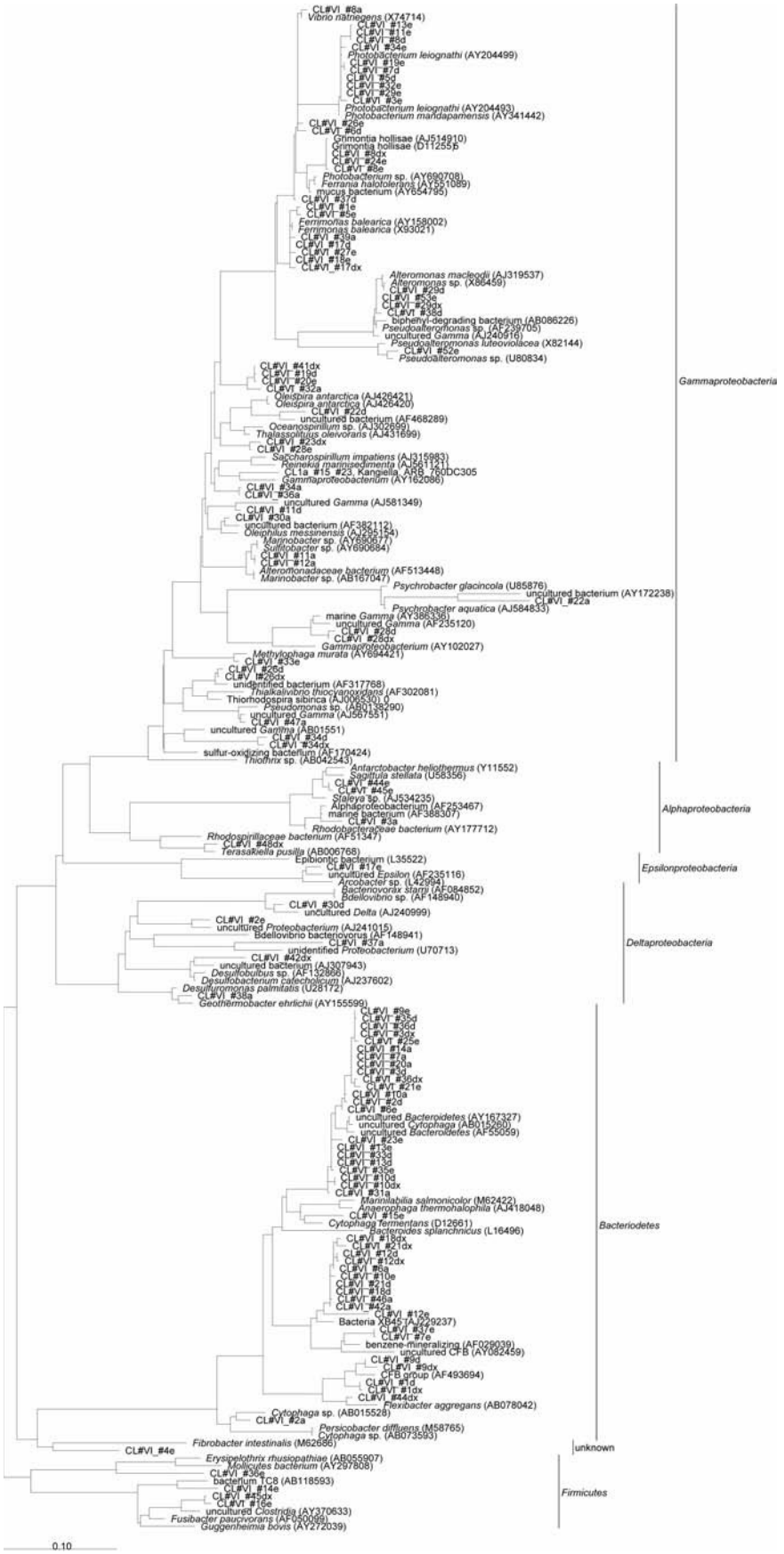

Fig. S3 F: Clone library VI = + 0.3% C_{org}, 4 d, on coral (figure legend page 97)

Fig. S3 A-F. Phylogenetic reconstruction of 16S rRNA gene sequences recovered from cloning of sediment samples from the sediment exposure experiment I. These were exposed on the coral *Montipora peltiformis* or on petridishes (besides coral = control) for 3 hours and 4 or 6 days. The sediment was enriched with three concentrations of plankton mixture, expressed in percent C_{org} of the dry weight of the sediment: + 0, + 0.3% and + 0.6%. A) Clone library I: was the sediment prior to the start of the experiment (stock), B) clone library II: + 0.6% C_{org}, 3 h on coral, C) clone library III: + 0% C_{org}, 6 d on coral, D) clone library IV: + 0.6% C_{org}, 4 d on coral, E) clone library V: + 0.6% C_{org}, 4 d besides coral, F) clone library VI: + 0.3% C_{org}, 4 d on coral. The sequences were compared against sequences obtained from public databases and the phylogenetic placement was carried out using parsimony criteria without changing topology of the pre-established tree using ARB software. The bar indicates 10% sequence divergence.

Tab. S2. Characteristics of the Wilkie Island sediment used in the sediment exposure experiment I and II prior to the experiment start. SD = standard deviation (n=3).

Wilkie Island Sediment	Unit	Mean	SD
Grain size distribution data			
Mean	[µm]	15.2	17.4
Skewness		2.5	
Kurtosis		7.1	
1st quartil	[µm]	4	
2nd quartil (median)	[µm]	9	
3rd quartil	[µm]	19	
Settling rate within the first 15 minutes	%	37	2.6
Settling rate within the first hour	%	18	0.7
Settling volume after 2 h	[ml]	145	6
Compaction during 24 h after settlement	%	56	1.5
Compaction during 48 h after settlement	%	48	1.7
Compaction during144 h after settlement	%	41	2
Organic matter (ash-free dry weight)	%	12.4	0.9
Total organic carbon (TOC)	[µg g^{-1} DW]	12.5	1.0
Total nitrogen (TN)	[µg g^{-1} DW]	2.1	0.1
Total phophorous (TP)	[µg g^{-1} DW]	0.4	0.0
Chlorophyll a (Chl a)	[µg g^{-1} DW]	2.2	0.0
Phaeophytin (Phaeo)	[µg g^{-1} DW]	13.9	0.9
Trace elements and metals			
Calcium (Ca)	[mmol g^{-1} DW]	1.86	0.01
Magnesium (Mg)	[mmol g^{-1} DW]	0.89	0.02
Aluminium (Al)	[mmol g^{-1} DW]	1.86	0.08
Iron (Fe)	[mmol g^{-1} DW]	0.46	0.01
Manganese (Mn)	[µmol g^{-1} DW]	5.61	0.10
Barium (Ba)	[µmol g^{-1} DW]	0.51	0.02
Zinc (Zn)	[µmol g^{-1} DW]	0.71	0.01
Vanadium (V)	[µmol g^{-1} DW]	1.08	0.19
Copper (Cu)	[µmol g^{-1} DW]	0.14	0.01
Cobalt (Co)	[µmol g^{-1} DW]	0.11	0.01
Lead (Pb)	[µmol g^{-1} DW]	0.08	0.00
Nickel (Ni)	[µmol g^{-1} DW]	0.22	0.02
Cadmium (Cd)	[µmol g^{-1} DW]	0.00	0.00
Molybdenum (Mo)	[µmol g^{-1} DW]	0.01	0.00
Selenium (Sn)	[µmol g^{-1} DW]	0.08	0.00
Aluminium / Calcium (Al/Ca)	ratio	1.00	0.04

Table S3. Characteristics of the plankton mixture, which was used to enrich the Wilkie Island sediment in the sediment exposure experiment I and II, and the total carbon, total nitrogen and total sulfur content in the tissue of the coral *Montipora peltiformis*. SD = standard deviation (n=3).

Sample		Plankton mixture		Coral	
	Unit	Mean	SD	Mean	SD
Total organic carbon	µg ml^{-1}	856	60		
Total nitrogen	µg ml^{-1}	210	12.4		
Total phosphorous	µg ml^{-1}	5.5	0.5		
Chlorophyll a	µg ml^{-1}	0.36	0.004		
Phaeophytin	µg ml^{-1}	0.6	0.001		
Total carbon	%			27.27	0.34
Total nitrogen	%			2.87	0.03
Total sulfur	%			1.3	0.05

Table S4. Characteristics of the natural sediment on the corals at different nearshore and offshore reefs of the Great Barrier Reef in Australia. SD = standard deviation (n=6-8). Bold numbers represent the higher average value of the both sites.

Sites		Nearshore		Offshore	
	Unit	Mean	SD	Mean	SD
Chlorophyll a (Chl a)	[µg g^{-1} DW]	14.1	9.46	**18.5**	15.72
Phaeophytin (Phaeo)	[µg g^{-1} DW]	**60.5**	25.21	48.2	25.83
Total nitrogen (TN)	[µg g^{-1} DW]	**1.18**	0.41	1.14	0.24
Total organic carbon (TOC)	[µg g^{-1} DW]	**7.57**	2.42	6.28	1.61
Total phosphorous (TP)	[µg g^{-1} DW]	**0.35**	0.14	0.23	0.02
Aluminium	[mg g^{-1} DW]	**0.24**	0.10	0.01	0.00
Calcium (Ca)	[mg g^{-1} DW]	1.54	0.54	**2.84**	0.34
Aluminium/Calcium ratio (Al/Ca)		**0.157**		0.005	
Iron (Fe)	[mg g^{-1} DW]	**0.14**	0.06	0.01	0.00
Manganese (Mn)	[mg g^{-1} DW]	**0.32**	0.07	0.02	0.01
Grain size mean	[µm]	142.5	34.34	**149.8**	29.14
Grain size 2^{nd} quartil (median)	[µm]	93.7	23.25	**121.7**	41.08

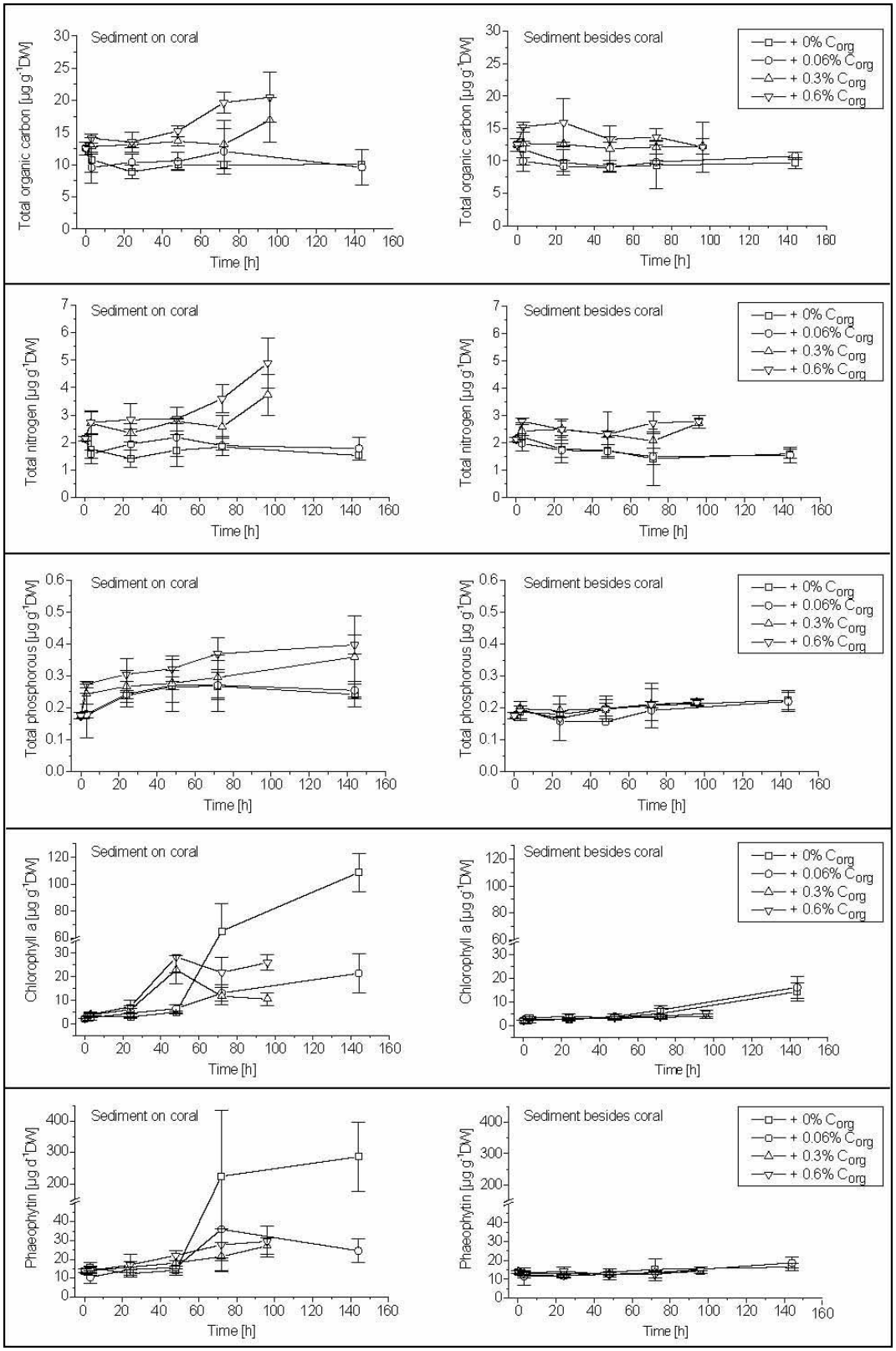

Fig. S4. Total organic carbon, total nitrogen, total phosphorous, chlorophyll a and phaeophytin concentrations in sediments covering corals and in control sediments (besides coral) during the sediment exposure experiment I. Exposure times were 3 hours, 1, 2, 3 and 4 or 6 days. The sediment was enriched with three concentrations of plankton mixture, expressed in percent C_{org} of the dry weight of the sediment: + 0%, + 0.06%, + 0.3% and + 0.6% C_{org}. Error bars represent the standard deviation of 4 replicate measurements (n=4).

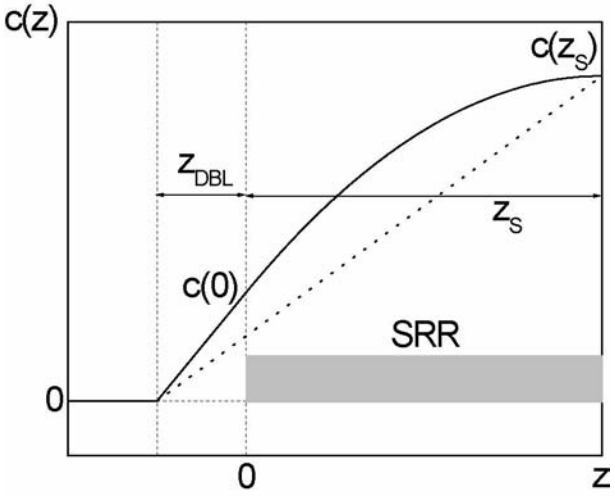

Fig. S5. Steady-state diffusive profiles of H_2S concentrations, c(z), calculated from Eq. (2) (solid line), assuming zero concentration at the top of the diffusive boundary layer ($z=-z_{DBL}$), zero flux at the bottom of the sediment layer ($z=z_S$), and homogeneously distributed sulfate reduction rate in the sediment (SRR), and from Eq. (4) (dotted line), assuming zero concentration at the top of the diffusive boundary layer, zero sulfate reduction rate in the sediment, and fixed flux at the bottom of the sediment layer. In the curved profile all sulfide is produced in the sediment (between x=o and x=z). In the linear profile the entire sulfide flux originates from the coral surface (below x=z) and must be fed by decomposing coral tissue.

Chapter 5

In Situ Applications of a New Diver-Operated Motorized Microsensor Profiler

In Situ Applications of a New Diver-Operated Motorized Microsensor Profiler

MIRIAM WEBER,*,†,‡ PAUL FAERBER,† VOLKER MEYER,† CHRISTIAN LOTT,†,‡ GABRIELE EICKERT,† KATHARINA E. FABRICIUS,§ AND DIRK DE BEER†

Max-Planck-Institute for Marine Microbiology, Celsiusstrasse 1, 28359 Bremen, Germany, HYDRA Institute for Marine Sciences, Elba Field Station, Via del Forno 80, 57034 Campo nell'Elba (LI), Italy, and Australian Institute of Marine Science, PMB No 3, Townsville, Queensland 4810, Australia

Microsensors are powerful tools for microenvironment studies, however their use has often been restricted to laboratory applications due to the lack of adequate equipment for in situ deployments. Here we report on new features, construction details, and examples of applications of an improved diver-operated motorized microsensor profiler for underwater field operation to a water depth of 25 m. The new motorized profiler has a final precision of 5 μm, and can accommodate amperometric Clark-type microsensors for oxygen and hydrogen sulfide, potentiometric microsensors (e.g., for pH, Ca^{2+}), and fiber-optic irradiance microsensors. The profiler is interfaced by a logger with a signal display, and has pushbuttons for underwater operation. The system can be pre-programmed to autonomous operation or interactively operated by divers. Internal batteries supply power for up to 24 h of measurements and 36 h of data storage (max. 64 million data points). Two flexible stands were developed for deployment on uneven or fragile surfaces, such as coral reefs. Three experimental pilot studies are presented, where (1) the oxygen distribution in a sand ripple was 3-D-mapped, (2) the microenvironment of sediment accumulated on a stony coral was studied, and (3) oxygen dynamics during an experimental sedimentation were investigated. This system allows SCUBA divers to perform a wide array of in situ measurements, with deployment precision and duration similar to those possible in the laboratory.

Introduction

On water−solid interfaces (surfaces of sediment, organisms, etc.), high conversion rates by microorganisms or chemical processes combined with mass transfer resistance often lead to steep concentration gradients of metabolic substrates and products. High spatial resolution techniques are needed to investigate these gradients on the surfaces of sediments, biofilms, and benthic organisms. Microsensors have the required spatial resolution (5−100 μm) and are widely used to study such chemical and physical microenvironments. The accuracy of flux and conversion measurements in benthic microlayers depends on minimal disturbance of systems under investigation. A significant advantage of microsensors is that they are minimally invasive because of their small tip diameters (1−20 μm). However, the transport of samples to the laboratory may change their fluxes and metabolic rates. For example, sediment retrieval leads to altered oxygen uptake because of changed pressure, flow, or advective transport conditions (*1*, *2*), and stress due to retrieval can potentially alter metabolic rates in macro-organisms. Therefore, laboratory measurements should preferably be compared against field measurements.

Previously microsensor field applications were conducted either close to the water surface where a laboratory microsensor profiler could be used without submersion or using submersible systems. Autonomous microsensor profiling systems were mounted on free-falling landers or deployed by remotely operated vehicles (*3*−*5*). Diver-operated microsensor submersible systems have also been used before. For example the MiniProfiler (Unisense, Denmark), a portable unit for field measurements to a depth of 50 m, was previously used for seagrass studies (*6*, *7*), while others placed laboratory instruments into custom-made housings to study the oxygen dynamics in sediment burrows of a mud shrimp (*8*, *9*). Further, a commercial profiler (Unisense, Denmark) was used by divers to study wave-induced hydrogen sulfide fluxes around a sessile ciliate colony, oxygen profiles in seagrass, and Antarctic microbial mats (*6*, *10*, *11*). In these studies the microsensor was fixed to a micromanipulator on a monopod, positioned manually (description see ref *10*) and left stationary for up to 4 h. To investigate algae below sea ice a buoyant up-side-down tripod was used under water and connected by cable to the control and data acquisition instruments which were put onto the ice surface (*12*). All previously described in situ systems so far lacked the possibility to interact with the measuring procedure, to be deployed on uneven fragile surfaces, and depended on external storage capabilities and power supplies either by extra battery packs or from a power source, e.g., on a boat.

We have built a system that overcomes the limitations described above. Our purpose was to investigate the effects of sedimentation by different types of sediment on scleractinian corals, which required detailed in situ measurements of microenvironments and fluxes within the coral−sediment interface. None of the previously used profilers was suitable for our studies. The purpose of our developments was to extend the capabilities of in situ microsensor applications, by providing for (1) manual and very precise micropositioning, to avoid breakage of the microsensor on the coral skeleton, (2) choice of motorized and autonomous profiling operation, in order to avoid disturbance by the diver as well as allowing measurements beyond diving times, (3) control by a diver over all functions in order to react to the natural setting such as, e.g., sediment depth, and (4) deployment on uneven and fragile environments by flexible stands.

Various features of the equipment, e.g., the flexibility of our two new stands, the motorized profiling of the amperometric oxygen and potentiometric pH microsensors, and the ability of the diver to interact with the system during measurements are shown by three examples of field applications. We addressed the following hypothesis that (1) oxygen concentration in a sand ripple differs among peak, slope, and trough due to wave-induced differential porewater flow; (2) oxygen is depleted and pH is reduced in muddy

* Corresponding author phone: +390565988027; fax: +390565-988090; e-mail: m.weber@hydra-institute.com.
† Max-Planck-Institute for Marine Microbiology.
‡ HYDRA Institute for Marine Sciences.
§ Australian Institute of Marine Science.

10.1021/es070200b CCC: $37.00
Published on Web 07/1 /2007

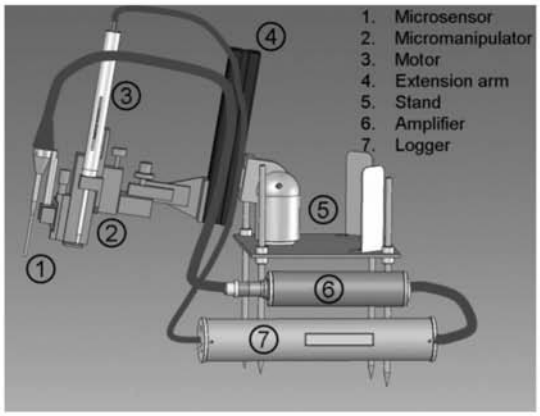

FIGURE 1. Schematic diagram of the diver-operated motorized microsensor profiler with the small stand.

sediment accumulated on corals as consequence of microbial activity, harming corals irreversibly; and (3) oxygen at the surface of an alga is depleted immediately after a sedimentation event. We also demonstrate that this profiler is highly suitable for other underwater studies.

Experimental Section

The profiler consists of a microsensor, a micromanipulator with motor, the stand, the amplifier, and the logger. The microsensor is mounted onto a 3-D-micromanipulator and connected to an amplifier by a cable. The motor is also mounted onto the micromanipulator and connected by a cable to the logger, the control and data acquisition unit of the system. Another cable connects the logger to the amplifier. The micromanipulator is fixed onto an extension arm, which is mounted onto a ball-head onto the stand. The flexible stands have individually adjustable legs, with holders for lead weights to stabilize the profiler (Figures 1 and 2).

Microsensors. Amperometric Clark-type oxygen and spherical fiber-optic irradiance microsensors were prepared as described previously (*13*, *14*). Liquid ion-exchange membrane pH microsensors (*15*) were modified by combining a pH-reference electrode into the sensor (Figure S1; for detailed description see Supporting Information). All microsensors had a tip diameter of 10−50 μm and a stirring sensitivity of <1.5%. After the top end of the microsensor was sealed with epoxy, the sensing cathode, guard cathode, and the reference were soldered to a miniature high-density plug (MHDG-5-OF + MDHG-CCF of adaptor PDM Neptec Limited, UK). A conical waterproof holder fitting exactly the plug, sealed with an O-ring, held the microsensor. To connect the microsensor to the amplifier a PDM Neptec manufactured cable harboring double-shielded coaxial RS 367-280 cables (RS Components, UK) was used. The glass fiber of the light microsensor was directly connected to the photomultiplier via a waterproof plug (D.G. O'Brien, UK).

Before and after the dive the oxygen microsensor was calibrated using air- and nitrogen-flushed seawater at the in situ temperature and salinity. The pH microsensors were calibrated using standard pH buffers (7.02, 9.21) and seawater at pH 8.2 at in situ temperature.

Measuring Devices. The amplifier housings are made of titanium (50 × 200 mm), and the photomultiplier housing is made of polyoxymethylene (100 × 240 mm). All instruments are turned on and off via magnetic switches. NiMH rechargeable batteries (150 mAh) ensure 24 h operation time. As input stage for the potentiometric amplifier a standard boosting electrometer as impedance transformer and for the amperometric amplifier a high impedance current-to-voltage converter is used. The amplifier is able to transmit signals up to 30 Hz (5.31 ms), 20 times faster than the microsensors. To minimize the signal noise, the amplifier separates fast changing signal rates from background signal by using a microcontroller. The background signal is recorded directly while the fast changing signal rates become amplified and filtered, before being digitized.

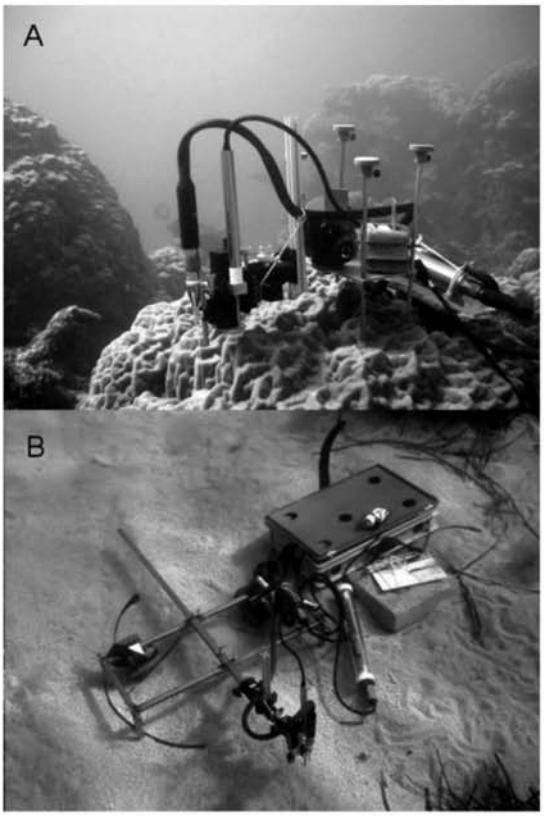

FIGURE 2. Diver-operated motorized microsensor profiler. (A) Use of the small stand on the massive stony coral *Porites* sp., Great Barrier Reef, Australia measuring oxygen profiles in sediment accumulated on the coral (scale: the coral head is ca. 1 m in diameter). (B) Use of the large stand measuring oxygen profiles within the peak, slope, and trough of a ripple of silicate sand, Elba, Italy.

An H5702-50 photomultiplier (Hamamatsu Photonics, Germany) is used to measure the incoming light from the scalar irradiance microsensor. The instrument includes a scaling mode to adjust the measuring sensitivity to the ambient light conditions. Activated via a magnetic switch, the acceleration voltage changes and therefore the gain of the photomultiplier. A microprocessor varies the amplification of the instrument until an opportune reference value is reached.

Logger. The custom-made housing (64 × 442 mm) consists of a clear polycarbonate tube, so that the LCD-display is visible, and two titanium lids with four pushbuttons for operation under water. Two NiMH rechargeable batteries (7.2 V 2.1 Ah and 700 mAh) deliver electric power for 36 h. An integrated circuit driver (Allegro Microsystems, USA) controls the motor. The driver includes an emergency stop to prevent electrical overload or overheating. A 64 MB compact flash card (Reichelt Elektronik, Germany) is used for data storage of a maximum of 64 million data points. The minimum sampling rate is 0.01 s. Data transfer and pro-

gramming is done via a serial interface using an integrated circuit driver. The CPU microchip (Microchip, USA) contains the software for operating and controlling the measuring procedure. Ten different measuring programs, written by the researcher, can be downloaded and accessed any time. Interactive operation and functions of the software are shown in Figure S2. The software and the pushbuttons on the housing allow the diver to change step size, data points, and waiting time during the measuring procedure. Further commands including "emergency stop", "continue", "move back to starting point", "take the actual position as zero", and various display options including background light are available. A clock is integrated and the UTC-time is saved with each measuring point, allowing the synchronization with other measuring devices. The logger can also be used manually as a data acquisition instrument; the motor is then controlled via pushbuttons. For detailed information for the initial programming, on the mechanics, and the electronical circuit see Supporting Information Figures S3−S14.

Motor. A DC-motor with gearbox and encoder (RE10 6V, Maxon motor AG, Switzerland) is used to precisely move the microsensors. On the titanium housing (16 × 125 mm) a M6 × 0.5 threaded spindle (maximum travel distance 8 cm) is fixed, moving the *y*-axes of the micromanipulator onto which the microsensor is mounted. The final precision of the positioning is equal or better than 5 μm while moving in one direction. Upon changing direction the hysteresis is 5 μm.

Stands. Two new micromanipulator stands were developed for stable deployment of the microsensors. The small stand (stainless steel 22 × 27 cm) has four independently adjustable 31 cm long legs with pointed feet. These can be covered with discs of polyoxymethylene to obtain flat feet if needed. Two holders for 8−16 kg of diving lead weights were used for stabilization. A 488RC2 Midi ball-head (Manfrotto, Italy) is mounted onto the stand, holding a manufacturer-modified MM33 3-D-micromanipulator (Märzhäuser, Germany; Dec. 1998 order number 15241) mounted onto an extension arm (Paletti Profilsysteme GmbH, Germany). This construction ensured complete flexibility to move the microsensor to the measuring point (Figure 2a).

The large stand (stainless steel 76 × 32 cm) has four adjustable 52 cm long legs with flat feet. The stabilizing weights are hooked onto the rack. The ball-head is fixed onto the 110 cm long extension arm of the stand, allowing measurements within an area of 70 × 100 cm without moving the system (Figure 2b).

Additional Equipment and Underwater Deployment Procedure. Accessories, such as a magnifying glass, an underwater torch, a tool board with magnet, paintbrush, screwdriver, elastic band, and syringe needle as well as the logger, amplifiers, motor, micromanipulator, and microsensor are brought to the measuring site in a plastic suitcase (UTZ, Germany). First the stand is placed in a stable position. Then the ball-head and micromanipulator are positioned close to the measuring point. The logger and the amplifier are placed close to the stand. To reduce induction noise by water motion, the cables are fixed to the stand with ties. A split polycarbonate tube held together with two rubber bands protects the microsensor. After the tube is removed the microsensor is fixed with the adapter to the micromanipulator. If two microsensors are to be used, both are put on the same ball-head of the stand 1 cm apart. The magnification glass and torch helped to precisely position the microsensor tip to the measurement starting point. The usual profiling design was to measure in steps of 100 or 500 μm, to wait at each point for 20 s before data acquisition and to then acquire 15 data points with 0.5 s interval. The logger starts the measuring procedure and allows the diver to interactively control procedures as the data are continuously displayed on the logger (Figure 1).

Study I: 3-D-Mapping of the Oxygen Distribution in a Sand Ripple. Oxygen profiles were measured with the motorized profiling system, the large stand, and the interactive logger, along a sand ripple in Sant' Andrea, Elba, Italy (N 42° 49′; E 010° 09′) at 6 m depth. The silicate sand had a median grain size of 406 μm, a porosity of 46%, and a permeability of 51 × 10^{-12} m^2 (*16*). The sand ripples were 6 cm high and the distance between two ripple peaks was 40 cm. The oscillating flow due to wave action was v_{max} = 8 cm s^{-1} and the phase length was 5−10 s. We measured three oxygen profiles each along the peak of the ripple, its slope, and within the trough. The distance between replicate profiles was 5 cm and the depth of the profiles was 4−6 cm, with a step size of 100 μm.

Study II: Microenvironment of Sediment Accumulated on a Stony Coral. The small stand with variable leg length and pointy feet, stabilized with 12 kg of dive weights, was deployed on uneven fragile corals at 5 m depth at the coastal coral reef High Island, Great Barrier Reef, Australia (S 17° 09′; E 146° 00′). pH and oxygen profiles were measured on foliose stony corals at haphazardly chosen points in patches of naturally accumulated mixed muddy terrestrial and marine sediments. The microsensors penetrated through the sediment layer, stopping precisely on the hidden surface of the coral skeleton.

Study III: Experimental Sedimentation Event. Oxygen dynamics were measured during a sedimentation experiment on the coralline red algae *Lithophyllum sp.* in the Bay of Fetovaia, Elba, Italy (N 42° 44′; E 010° 10′) at 8 m depth. The experiment was conducted on a rock overgrown with various turf and red algae. The sediment was collected from a nearby creek that discharges muddy terrestrial sediment into the bay during flash floods after heavy rain. We positioned the microsensor on the algal surface, deployed a sedimentation chamber (described in ref *17*) and added sediment with a syringe to obtain 66 mg dw cm^{-2} coverage. After settlement, the sedimentation chamber was removed to expose the alga to ambient hydrodynamic conditions. Oxygen was measured on the algal surface for 2 h, after which a profile was measured back in the water.

Results and Discussion

Environmental Conditions. Both stands remained stable in 2 m water depth at wave heights up to 0.8 m. The system operated at all water temperatures used (11−31 °C). By tracking particles around the measurement tips of the sensors, equal flow data (not shown here) were obtained at the same spot before and after the stands and other equipment were deployed, thus the microsensor tip does not significantly change hydrodynamics.

Study I. In the sand ripple, the first profiles showed that oxygen penetrated only 3 cm into the sediment. The diver was able to react to this measurement, and changed the profiling range from 6 to 4 cm under water. Without repositioning the large stand and disturbing the setting, the oxygen microsensor was positioned at different locations, providing the opportunity to study oxygen profiles at both macro- and microscale around the sand ripple. The profiles and oxygen penetration depth were comparable to those of profiler measurements in coastal sandy sediments at the Wadden Sea, Germany (*18*) and Heron Island, Australia (*19*). However, our data show that oxygen penetration depth is highly variable at the peak, more consistent in the slope area, and again variable within the trough (Figure 3). Our field data also confirm previous flume studies that found significant in-bed porewater flow is generated by water flowing over a sand ripple (*20*). Interestingly photosynthetic activity was detected at the trough of the sand ripple (Figure 3c), but not at the peak or the slope. This heterogeneity was not described before, indicating the value of such in situ studies.

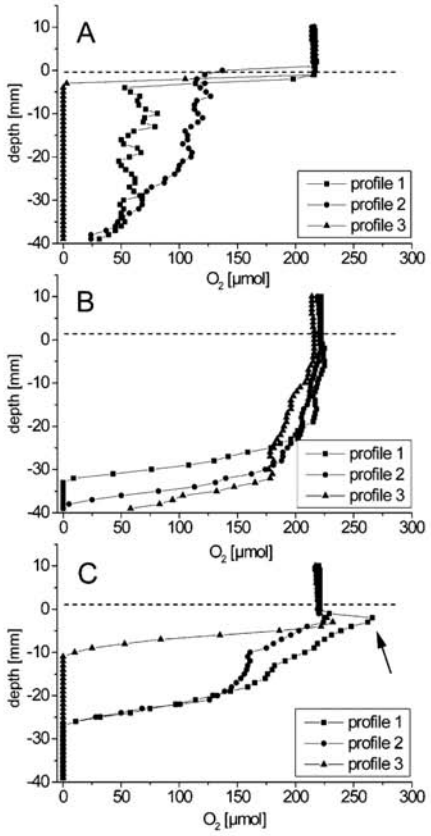

FIGURE 3. Oxygen profiles measured with a diver-operated motorized microsensor profiler around a sand ripple (Study I). Three profiles were measured with 5 cm distance at the ripple peak (A), the ripple slope (B), and the trough (C). Arrow in (C) indicates oxygen production due to benthic photosynthetic activity. Dashed line shows sediment surface. Error bars are omitted for clarity.

Our data show that in situ oxygen concentrations are variable along a sand ripple presumably mainly caused by wave action and the resulting porewater flow, but also by a heterogenic pattern of photosynthetically active organisms.

Study II. The small stand proved to be suitable for microsensor studies on corals, and to work on fragile and uneven surfaces (Figure 2A). The adjustable leg length, the pointy feet, and the stabilization with dive weights allowed deploying microsensors even in quite shallow water. The ball-head with the extension arm including micromanipulator and the additional equipment (magnification glass and torch) allowed the diver to position the delicate microsensors precisely on hard surfaces such as stony corals. This was the only way to study the microenvironment in such sediment layers, which naturally accumulate on stony corals in coastal environments, because it was not possible to recover undisturbed samples for laboratory studies. The oxygen profiles were reproducible and showed low variability, whereas the pH profiles varied up to 0.3 of a pH unit (Figure 4). In the 4 mm thin sediment layer, pH decreased gradually by about 0.5 units within the uppermost ~2 mm, while some oxygen penetrated to 3 mm, similar to other muddy sediments (*21*−*23*). The hypothesis that no oxygen is available to coral surfaces covered with muddy sediment was confirmed. The sediment was rich in organic matter. The steep pH and oxygen profiles indicate high microbial respiration activity. A previous experimental study showed that corals are irreversibly harmed after <24 h exposure to sediments with high N-, P-,

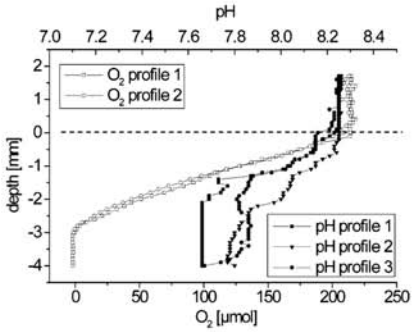

FIGURE 4. Two oxygen and three pH profiles in muddy sediment patches accumulated on a stony coral, measured with a diver-operated motorized microsensor profiler (Study II). Dashed line shows sediment surface. Error bars are omitted for clarity.

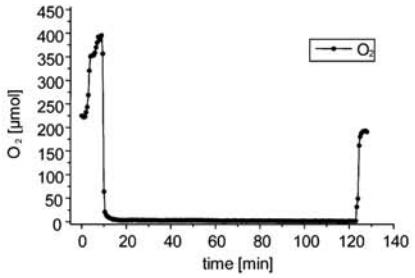

FIGURE 5. Oxygen dynamics during a sedimentation experiment on the red algae *Lithophyllum sp.* measured with a diver-operated motorized microsensor profiler (Study III). The microsensor was positioned on the algal surface at time 0. Sediment was applied into the sedimentation chamber after 10 min. A profile back into the water was measured after 120 min of exposure. Error bars are omitted for clarity.

and C_{org}-content (*17*), but not by sterile organic-poor sediment. Our profiles and the previous studies suggest that sedimentation stress in corals is due to microbial activity, as previously hypothesized (*24*), possibly worsened by the mud and organic content of the sediments.

Study III. The small stand proved to be suitable also for use in combination with a small sedimentation chamber where a defined amount of sediment could be deposited on the organism while the motorized microsensor was already positioned. After removal of the chamber in situ hydrodynamic conditions prevailed. Oxygen concentrations peaked at the surface of the uncovered photosynthesizing alga *Lithophyllum sp.* but rapidly dropped to zero upon experimental coverage with muddy sediments (Figure 5). Oxygen disappeared from the algal surface due to reduced exchange with seawater (*25*), stopped photosynthesis by the alga, and oxygen consumption by the alga and microorganisms in the sediment (*26*) (see also Study II). Previous studies showed that muddy sediments high in organic matter have been more harmful to algae and corals than sediments low in organics, and coarser sediments (*17*, *27*−*30*). However, a sediment analysis was not included in this study.

Strengths and Limitations. In contrast to a benthic profiler and other diver-operated profilers, our 3-D-micromanipulator in combination with the ball-head allows for total flexible (including up-side-down) positioning of the microsensor. Furthermore, the small Maxon DC-motor in connection with the logger enables continuous motorized measurements on a micromanipulator, which is far more precise than manual profiling. The battery lifetime of 24 h was sufficient for our needs, but can be extended to 5 days

by using Li-Ion rechargeable batteries. However it will not outlast power supplied from a boat or additional battery packs (*12*). In contrast to that, our profiler is carried in a small compact suitcase giving the diver autonomy and flexibility to find the best study site. The new stands enabled deployment on uneven and fragile surfaces. Deep deployments are theoretically possible as all parts of the profiler are pressure tested to 20 bar. However we did not test the profiler deeper than 25 m. The interactive capacities of the logger allow efficient use of limited dive time. The high-speed measuring amplifiers enable measuring rapid dynamics (<0.5 s), useful for the Eddy correlation technique (*31*) and for gross photosynthesis studies (*32*). The new profiler can also be used with other microsensors, e.g., Ca^{2+} (*15*) and N_2O (*33*). Underwater electromagnetic noise levels are low, so that the signal-to-noise ratio is maximized. However, movement of the connecting cables by wave action and currents can induce noise, which we solved by fixing the cables to the stand, or at the commercially available profiler by connecting the microsensors directly to the amplifier (*11*). A further limitation of diver-operated systems is, apart from the physiological constraints, that the user must be an experienced diver and well trained in using microsensors.

Acknowledgments

We thank Alexandra Stein, Caterina Adams, Craig Humphrey, Duygu Sevilgen, Felix Hahn, Lorenzo Bramanti, Martina Neher, Silke Dahms, and Stephan Pfannschmidt for their field assistance and Boris Unger for technical support. We gratefully acknowledge all technicians of the Microsensor Department for providing the microsensors, and engineers of the Max-Planck-Institute for Marine Microbiology and the Australian Institute of Marine Sciences for the construction of the profiler. Many thanks also to Hans Røy for his constructive comments during the developmental period, and Felix Janβen for valuable comments to the manuscript. M.W. acknowledges the support through a PhD scholarship by the German Academic Exchange Service (DAAD) and the Max-Planck-Society. We also thank three anonymous reviewers, who greatly helped in improving the manuscript.

Supporting Information Available

Drawings of the modified liquid ion-exchange membrane pH microsensor, a flow-chart of the interactive operation and functions of the software, information on the programming of the logger, the electrical circuit of the logger, and the mechanical details of the motor. This material is available free of charge via the Internet at http://pubs.acs.org.

Literature Cited

(1) Altmann, D.; Stief, P.; Amann, R.; de Beer, D. Distribution and activity of nitrifying bacteria in natural stream sediment versus laboratory sediment microcosms. *Aquat. Microb. Ecol.* **2004**, *36*, 73−81.

(2) Sauter, E. J.; Schlüter, M.; Suess, E. Organic carbon flux and remineralization in surface sediments from the northern North Atlantic derived from pore-water oxygen microprofiles. *Deep-Sea Res., Part I* **2001**, *48*, 529−553.

(3) Viollier, E.; Rabouille, C.; Apitz, S. E.; Breuer, E.; Chaillou, G.; Dedieu, K.; Furukawa, Y.; Grenz, C.; Hall, P.; Janssen, F.; Morford, J. L.; Poggiale, J.-C.; Roberts, S.; Shimmield, T.; Taillefert, M.; Tengberg, A.; Wenzhöfer, F.; Witte, U. Benthic biogeochemistry: state of the art technologies and guidelines for the future of in situ survey. *J. Exp. Mar. Biol. Ecol.* **2003**, 5−31.

(4) Luther, G. W.; Reimers, C. E.; Nuzzio, D. B.; Lovalvo, D. In situ deployment of voltammetric, potentiometric, and amperometric microelectrodes from a ROV to determine dissolved O_2, Mn, Fe, S^{-2}, and pH in porewaters. *Environ. Sci. Technol.* **1999**, *33*, 4352−4356.

(5) Tercier-Waeber, M. L.; Belmont-Hebert, C.; Buffle, J. Real-time continuous Mn(II) monitoring in lakes using a novel voltammetric in situ profiling system. *Environ. Sci. Technol.* **1998**, *32*, 1515−1521.

(6) Sand-Jensen, K.; Pedersen, O.; Binzer, T.; Borum, J. Contrasting oxygen dynamics in the freshwater isoetid *Lobelia dortmanna* and the marine seagrass *Zostera marina*. *Ann. Bot.* **2005**, *96*, 613−623.

(7) Borum, J.; Pedersen, O.; Greve, T. M.; Frankovich, T. A.; Zieman, J. C.; Fourqurean, J. W.; Madden, C. J. The potential role of plant oxygen and sulphide dynamics in die-off events of the tropical seagrass, *Thalassia testudinum*. *J. Ecol.* **2005**, *93*, 148−158.

(8) Ziebis, W.; Forster, S.; Huettel, M.; Jørgensen, B. B. Complex burrows of the mud shrimp *Callianassa truncata* and their geochemical impact in the sea bed. *Nature* **1996**, *382*, 619−622.

(9) Ziebis, W.; Pillen, T.; Unger, B. A diver observatory for in-situ studies in sublittoral sediments. *Underwat. Technol.* **1998**, *23*, 63−69.

(10) Vopel, K.; Hawes, I. Photosynthetic performance of benthic microbial mats in Lake Hoare, Antarctica. *Limnol. Oceanogr.* **2006**, *51*, 1801−1812.

(11) Vopel, K.; Thistle, D.; Ott, J.; Bright, M.; Røy, H. Wave-induced H_2S flux sustains a chemoautotrophic symbiosis. *Limnol. Oceanogr.* **2005**, *50*, 128−133.

(12) Kühl, M.; Glud, R. N.; Borum, J.; Roberts, R.; Rysgaard, S. Photosynthetic performance of surface-associated algae below sea ice as measured with a pulse-amplitude-modulated (PAM) fluorometer and O_2 microsensors. *Mar. Ecol.-Prog. Ser.* **2001**, *223*, 1−14.

(13) Revsbech, N. P. An oxygen microsensor with a guard cathode. *Limnol. Oceanogr.* **1989**, *34*, 474−478.

(14) Lassen, C.; Jørgensen, B. B. A fiberoptic irradiance microsensor (cosine collector) - Application for in-situ measurements of absorption-coefficients in sediments and microbial mats. *FEMS Microbiol. Ecol.* **1994**, *15*, 321−336.

(15) De Beer, D.; Glud, A.; Epping, E.; Kühl, M. A fast-responding CO_2 microelectrode for profiling sediments, microbial mats, and biofilms. *Limnol. Oceanogr.* **1997**, *42*, 1590−1600.

(16) Werner, A. R. Vergleich von Abundanzen und Tiefenverteilung der Meiofauna, im Speziellen der Harpacticoida (Copepoda, Crustacea), in sublitoralen Kalk- und Quarzsedimenten (Mittelmeer). Master Thesis, Carl von Ossietzky University Oldenburg, 2006, 72 pp (in German).

(17) Weber, M.; Lott, C.; Fabricius, K. E. Sedimentation stress in a scleractinian coral exposed to terrestrial and marine sediments with contrasting physical, organic and geochemical properties. *J. Exp. Mar. Biol. Ecol.* **2006**, *336*, 18−32.

(18) De Beer, D.; Wenzhöfer, F.; Ferdelman, T. G.; Boehme, S. E.; Hüttel, M.; van Beusekom, J. E. E.; Böttcher, M. E.; Musat, N.; Dubilier, N. Transport and mineralization rates in North Sea sandy intertidal sediments, Sylt-Rømø Basin, Wadden Sea. *Limnol. Oceanogr.* **2005**, *50*, 113−127.

(19) Werner, U.; Bird, P.; Wild, C.; Ferdelman, T.; Polerecky, L.; Eickert, G.; Jonstone, R.; Hoegh-Guldberg, O.; de Beer, D. Spatial patterns of aerobic and anaerobic mineralization rates and oxygen penetration dynamics in coral reef sediments. *Mar. Ecol.-Prog. Ser.* **2006**, *309*, 93−105.

(20) Thibodeaux, L. J.; Boyle, J. D. Bedform-generated convective-transport in bottom sediment. *Nature* **1987**, *325*, 341−343.

(21) Böttcher, M. E.; Hespenheide, B.; Llobet-Brossa, E.; Beardsley, C.; Larsen, O.; Schramm, A.; Wieland, A.; Böttcher, G.; Berninger, U. G.; Amann, R. The biogeochemistry, stable isotope geochemistry, and microbial community structure of a temperate intertidal mudflat: an integrated study. *Cont. Shelf Res.* **2000**, *20*, 1749−1769.

(22) De Beer, D.; Sauter, E.; Niemann, H.; Kaul, N.; Foucher, J. P.; Witte, U.; Schlüter, M.; Boetius, A. In situ fluxes and zonation of microbial activity in surface sediments of the Hakon Mosby Mud Volcano. *Limnol. Oceanogr.* **2006**, *51*, 1315−1331.

(23) Brinkhoff, T.; Santegoeds, C. M.; Sahm, K.; Kuever, J.; Muyzer, G. A polyphasic approach to study the diversity and vertical distribution of sulfur-oxidizing Thiomicrospira species in coastal sediments of the German Wadden Sea. *Appl. Environ. Microbiol.* **1998**, *64*, 4650−4657.

(24) Hodgson, G. Tetracycline reduces sedimentation damage to corals. *Mar. Biol.* **1990**, *104*, 493−496.

(25) Hüttel, M.; Røy, H.; Precht, E.; Ehrenhauss, S. Hydrodynamical impact on biogeochemical processes in aquatic sediments. *Hydrobiologia* **2003**, *494*, 231−236.

(26) Koster, M.; Dahlke, S.; Meyer-Reil, L. A. Microbial colonization and activity in relation to organic carbon in sediments of hypertrophic coastal waters (Nordrugensche Bodden, Southern Baltic Sea). *Aquat. Microb. Ecol.* **2005**, *39*, 69−83.

(27) Fabricius, K. E.; Wolanski, E. Rapid smothering of coral reef organisms by muddy marine snow. *Estuar. Coast. Shelf Sci.* **2000**, *50*, 115−120.
(28) Fabricius, K. E.; Wild, C.; Wolanski, E.; Abele, D. Effects of transparent exopolymer particles and muddy terrigenous sediments on the survival of hard coral recruits. *Estuar. Coast. Shelf Sci.* **2003**, *57*, 613−621.
(29) Fabricius, K. E. Effects of terrestrial runoff on the ecology of corals and coral reefs: review and synthesis. *Mar. Pollut. Bull.* **2005**, *50*, 125−146.
(30) Harrington, L.; Fabricius, K.; Eaglesham, G.; Negri, A. Synergistic effects of diuron and sedimentation on photosynthesis and survival of crustose coralline algae. *Mar. Pollut. Bull.* **2005**, *51*, 415−427.
(31) Berg, P.; Røy, H.; Janssen, F.; Meyer, V.; Jørgensen, B. B.; Huettel, M.; de Beer, D. Oxygen uptake by aquatic sediments measured with a novel non-invasive eddy-correlation technique. *Mar. Ecol.-Prog. Ser.* **2003**, *261*, 75−83.
(32) Revsbech, N. P.; Jørgensen, B. B. Photosynthesis of benthic microflora measured with high spatial-resolution by the oxygen microprofile method - capabilities and limitations of the method. *Limnol. Oceanogr.* **1983**, *28*, 749−756.
(33) Revsbech, N. P.; Nielsen, L. P.; Christensen, P. B.; Sørensen, J. Combined oxygen and nitrous-oxide microsensor for denitrification studies. *Appl. Environ. Microbiol.* **1988**, *54*, 2245−2249.

Received for review January 25, 2007. Revised manuscript received May 22, 2007. Accepted June 8, 2007.

ES070200B

Supporting Information

In situ applications of a new diver-operated motorised microsensor profiler.

Miriam Weber, *, [1,2] Paul Faerber, [1] Volker Meyer, [1] Christian Lott, [1,2] Gabriele Eickert, [1] Katharina E. Fabricius, [3] and Dirk de Beer [1]

[1] Max-Planck-Institute for Marine Microbiology, Celsiusstrasse 1, 28359 Bremen, Germany

[2] HYDRA Institute for Marine Sciences, Elba Field Station, Via del Forno 80, 57034 Campo nell'Elba (LI), Italy

[3] Australian Institute of Marine Science, PMB No 3, Townsville, QLD 4810, Australia

The supporting information provides:

1. Drawings of the modified liquid ion-exchange membrane pH microsensor - page S1
2. A flow-chart of the interactive operation and functions of the software - page S2
3. Information on the programming of the logger - page S3
4. The mechanics of the motor and the electrical circuits of the logger - page S4 –S14

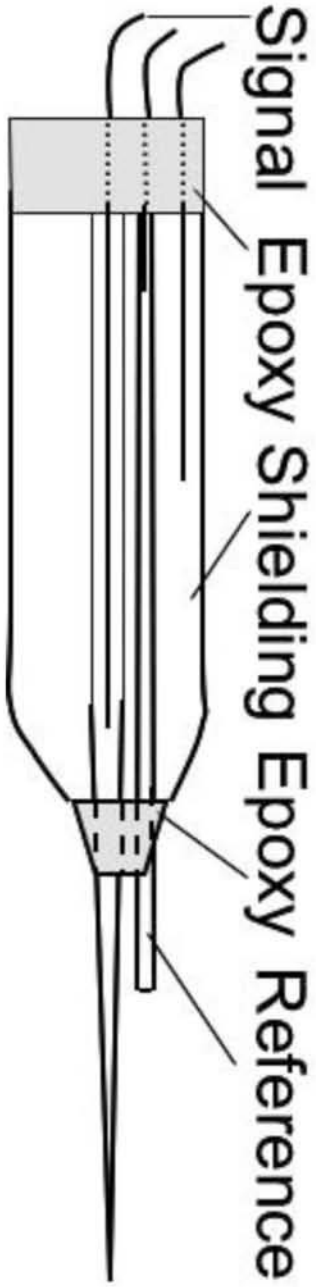

Figure S1: Modified liquid ion-exchange membrane pH microsensor. The reference is a thin rubber tube filled with 1% agar containing 0.35% KCl, which passes through the shielding, fixed with epoxy resin.

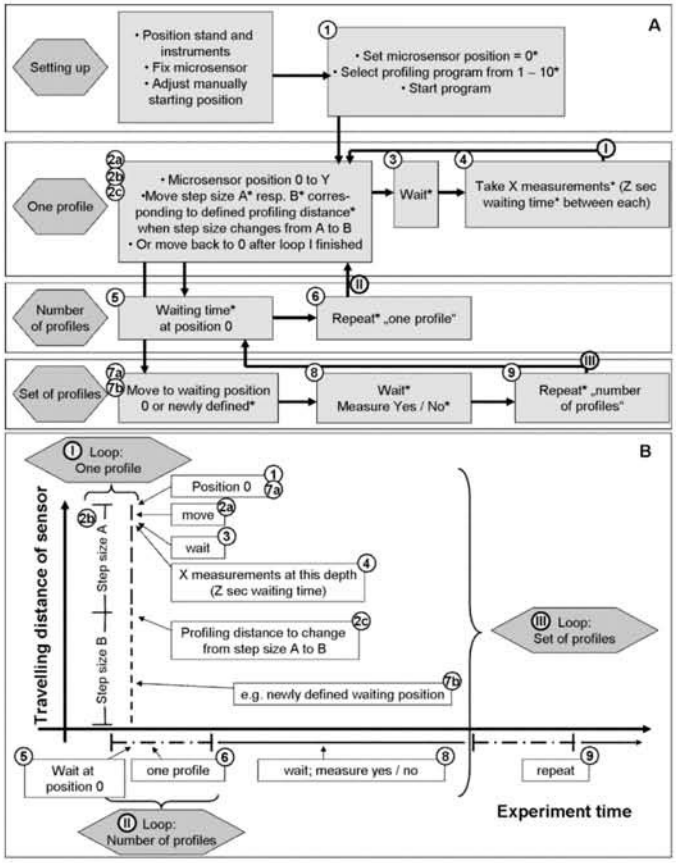

Figure S2: Interactive operation and functions of the software. All possible functions and measuring procedure of the diver-operated motorized microsensor profiler. The deployment in the field explained by a graphical display (A) is linked to a flow-chart (B). The part called „setting up" explains steps involved in getting started; and the three loops (I-III) show how the logger moves the motor and acquires microsensor data. *Functions are pre-programmable in the laboratory.

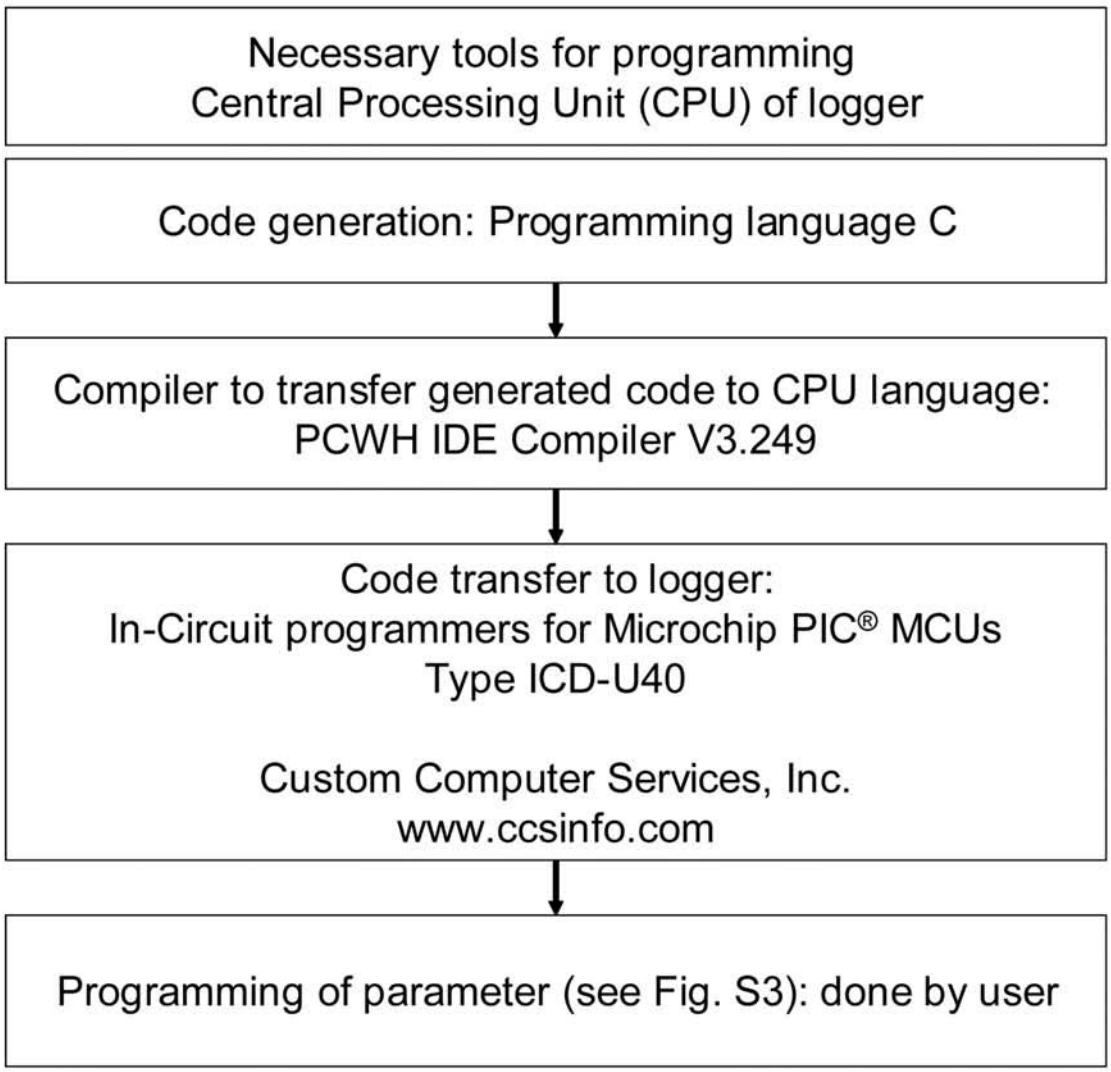

Figure S3: Detailed information for the initial programming of the logger of the new diver-operated motorized microsensor profiler.

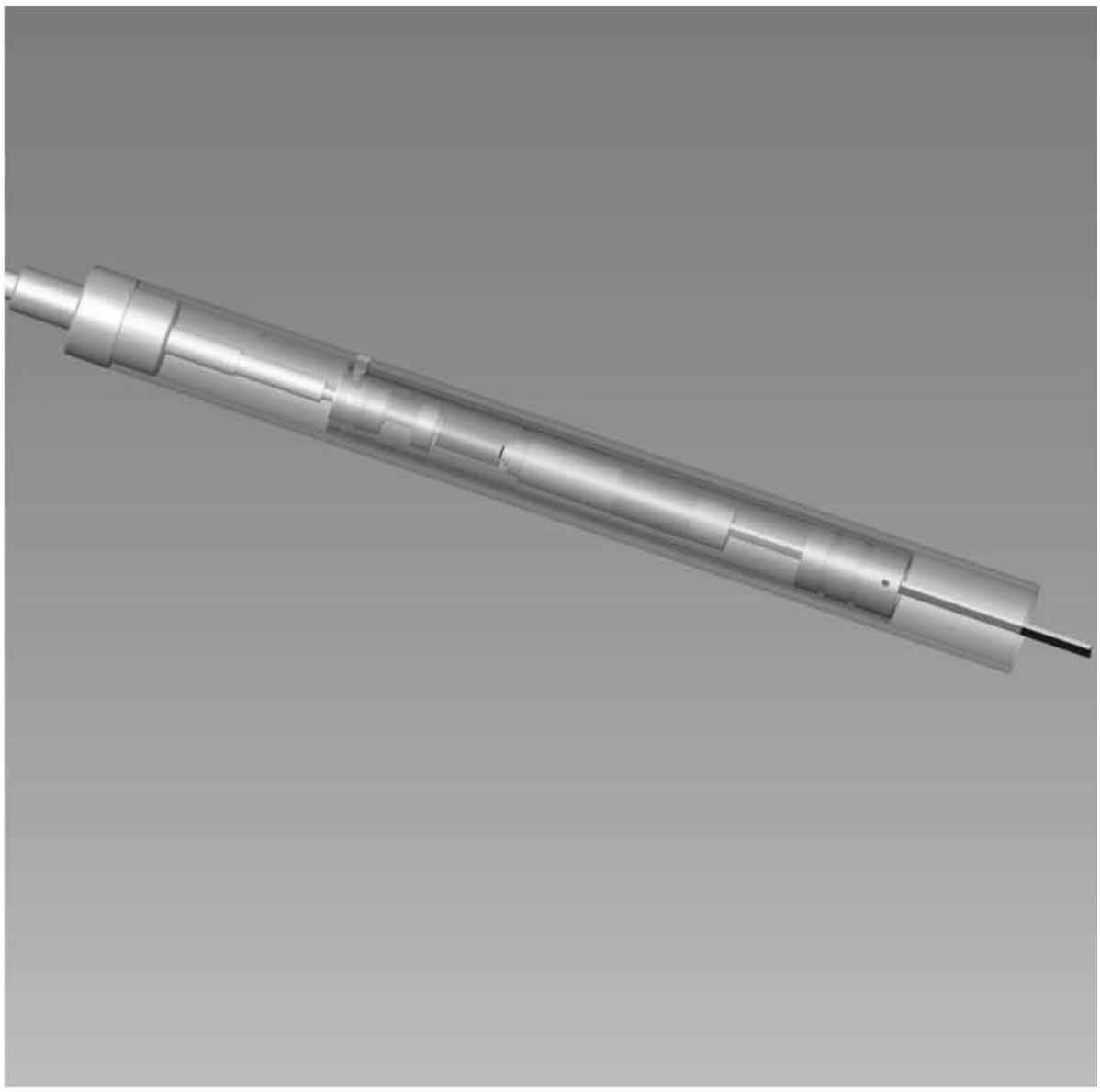

Figure S4 – S14: Overview and details of the motor mechanics, and electronical details of the logger.

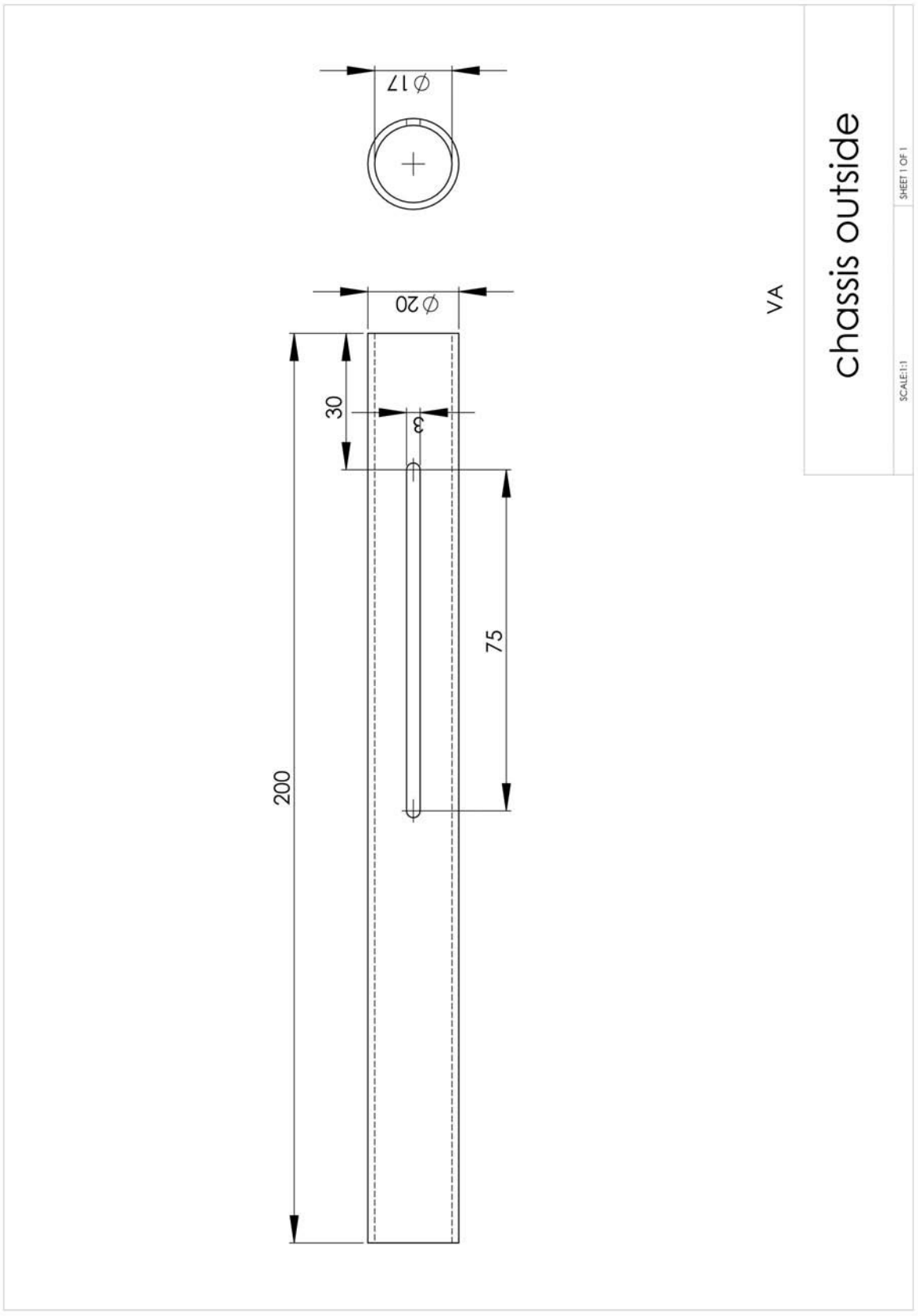
Ø17
Ø20
30
3
75
200
VA
chassis outside
SCALE:1:1
SHEET 1 OF 1

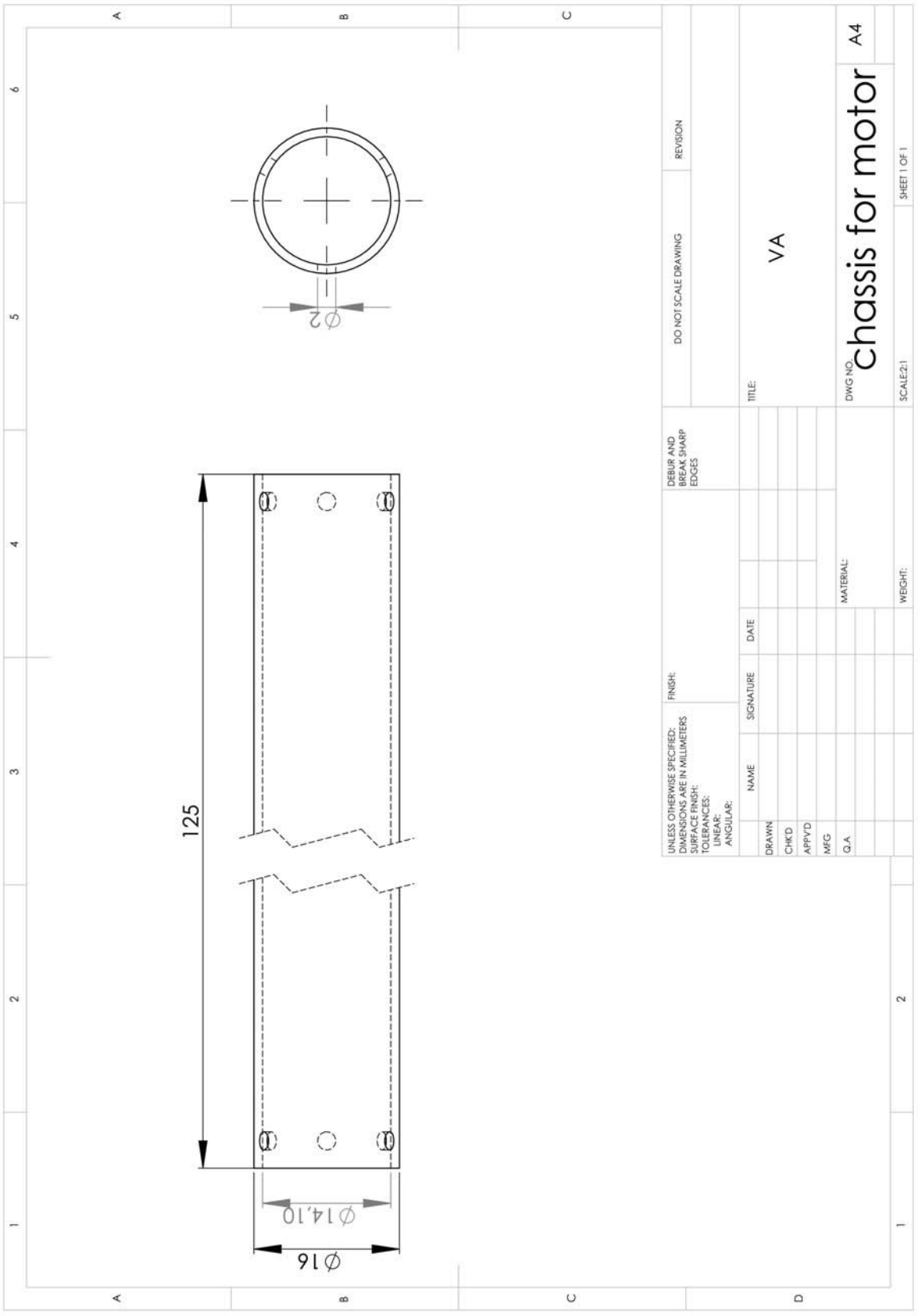
Ø2
125
Ø14,10
Ø16
UNLESS OTHERWISE SPECIFIED:
DIMENSIONS ARE IN MILLIMETERS
SURFACE FINISH:
TOLERANCES:
LINEAR:
ANGULAR:
FINISH:
DEBUR AND BREAK SHARP EDGES
NAME
SIGNATURE
DATE
DRAWN
CHK'D
APP'VD
MFG
Q.A
MATERIAL:
WEIGHT:
DO NOT SCALE DRAWING
REVISION
TITLE:
VA
DWG NO.
chassis for motor
A4
SCALE:2:1
SHEET 1 OF 1

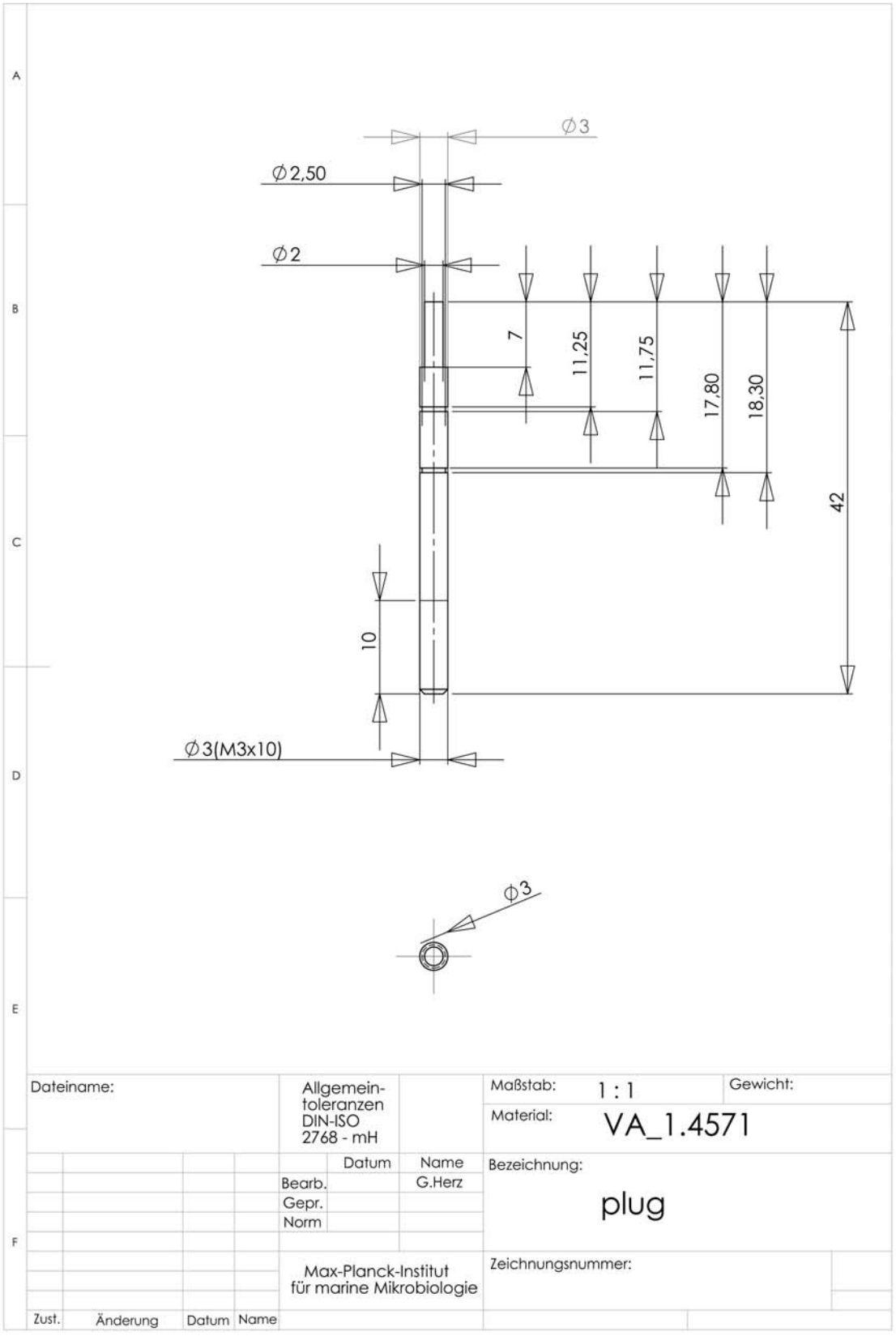
A
B
C
D
E
F
Ø3
Ø2,50
Ø2
7
11,25
11,75
17,80
18,30
42
10
Ø3(M3x10)
Ø3
Dateiname:
Allgemein-
toleranzen
DIN-ISO
2768 - mH
Maßstab: 1 : 1
Gewicht:
Material: VA_1.4571
Datum
Name
Bearb.
G.Herz
Gepr.
Norm
Bezeichnung:
plug
Max-Planck-Institut
für marine Mikrobiologie
Zeichnungsnummer:
Zust.
Änderung
Datum
Name

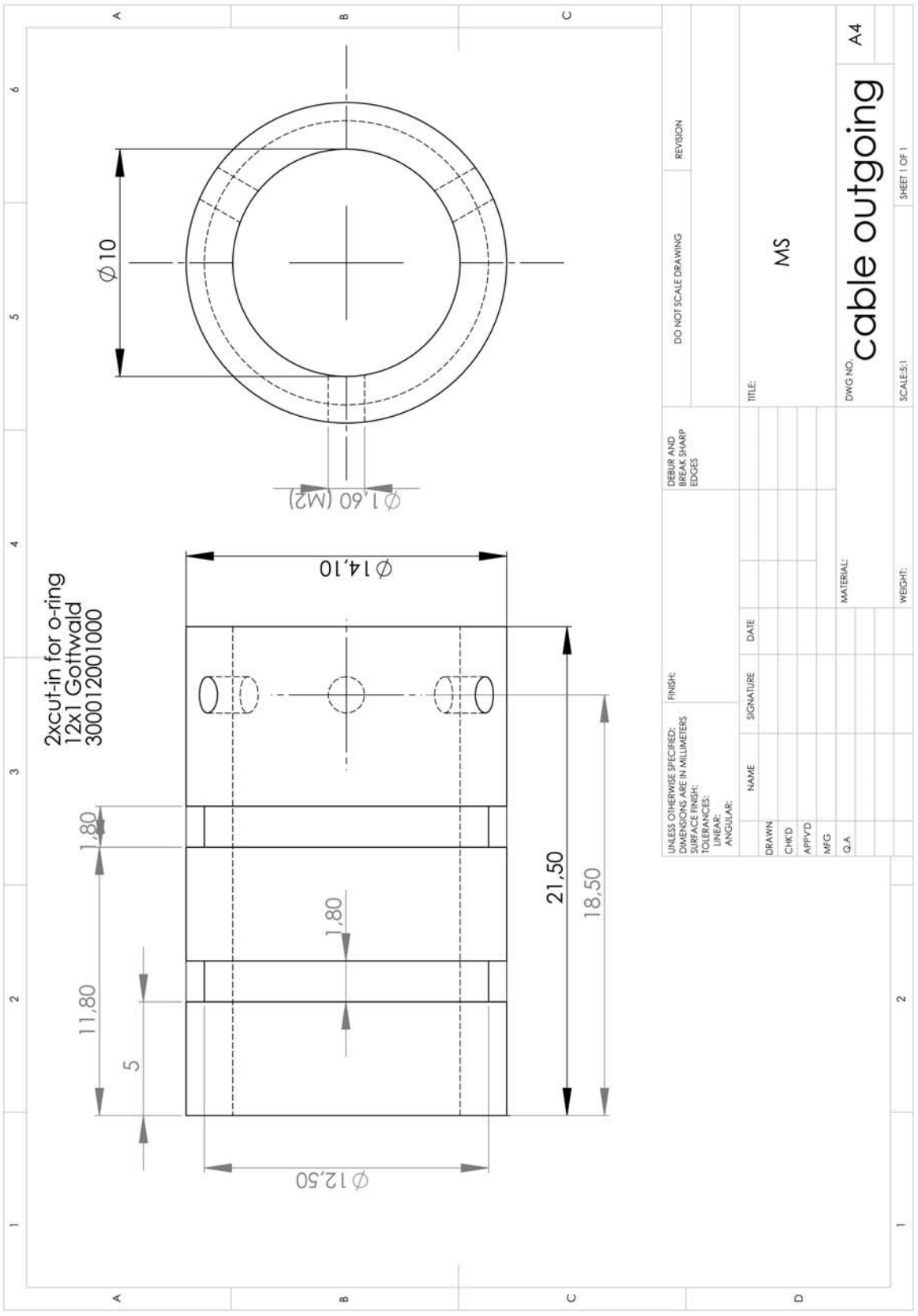
Ø10
Ø1,60 (M2)
Ø14,10
2xcut-in for o-ring
12x1 Gottwald
300012001000
1,80
11,80
5
1,80
21,50
18,50
Ø12,50
UNLESS OTHERWISE SPECIFIED:
DIMENSIONS ARE IN MILLIMETERS
SURFACE FINISH:
TOLERANCES:
LINEAR:
ANGULAR:
FINISH:
DEBUR AND BREAK SHARP EDGES
DO NOT SCALE DRAWING
REVISION
NAME
SIGNATURE
DATE
DRAWN
CHK'D
APPV'D
MFG
Q.A
MATERIAL:
WEIGHT:
TITLE:
MS
DWG NO.
cable outgoing
A4
SCALE:5:1
SHEET 1 OF 1

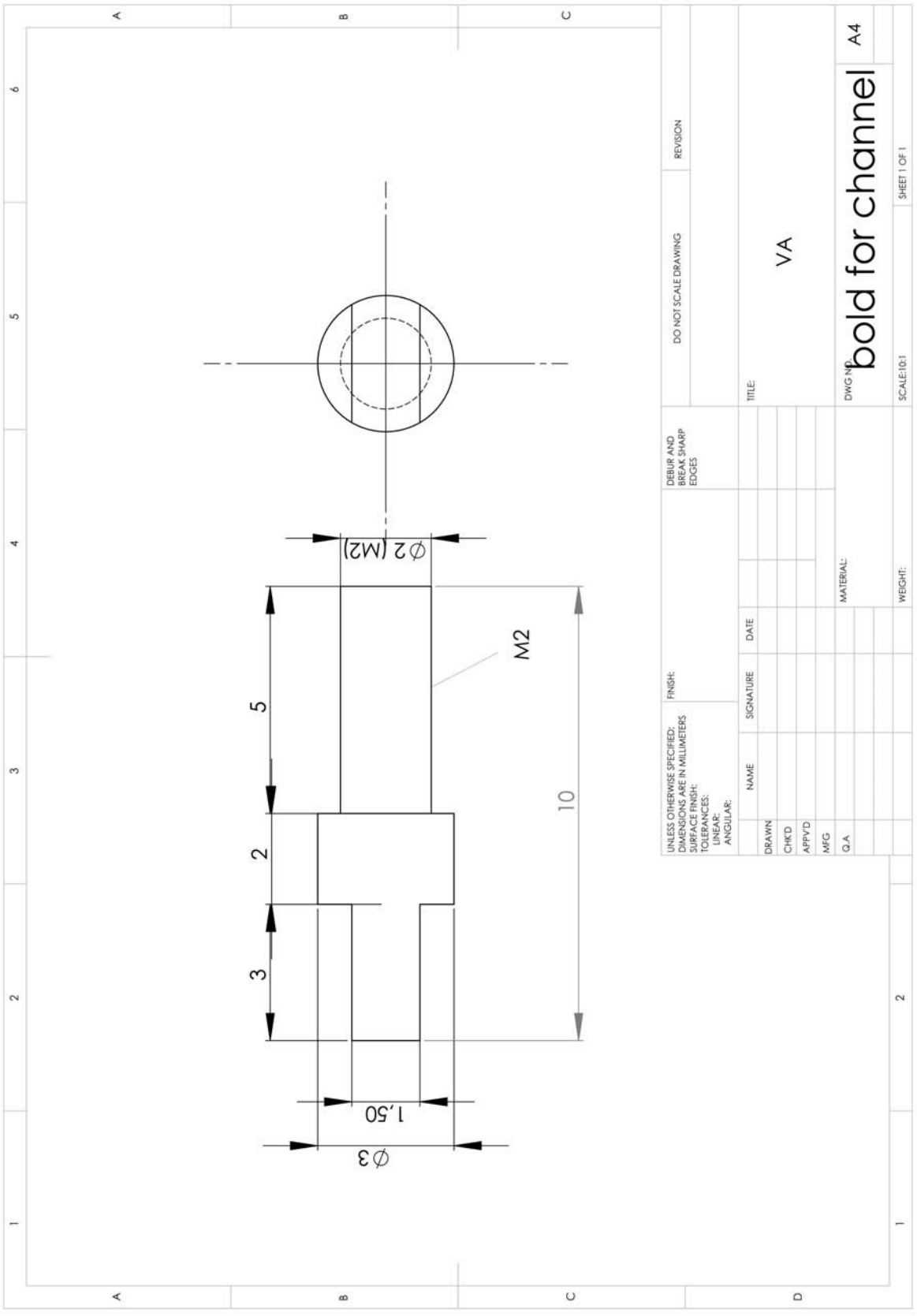
Ø2 (M2)
M2
5
2
3
10
1,50
Ø3
UNLESS OTHERWISE SPECIFIED:
DIMENSIONS ARE IN MILLIMETERS
SURFACE FINISH:
TOLERANCES:
LINEAR:
ANGULAR:
FINISH:
DEBUR AND BREAK SHARP EDGES
DO NOT SCALE DRAWING
REVISION
NAME
SIGNATURE
DATE
DRAWN
CHK'D
APPV'D
MFG
Q.A
MATERIAL:
TITLE:
VA
DWG NO.
bold for channel
A4
WEIGHT:
SCALE:10:1
SHEET 1 OF 1

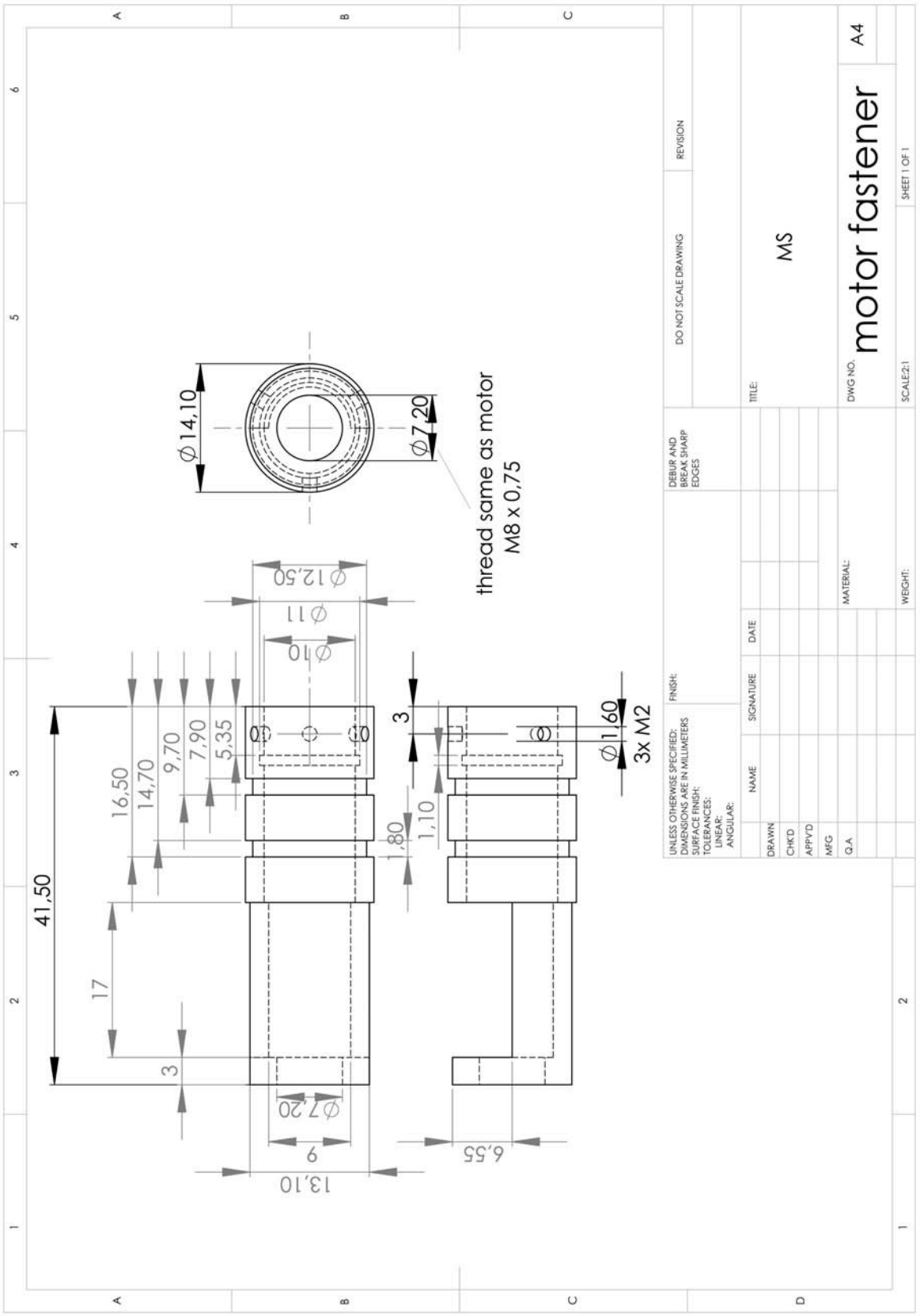
Ø14,10
Ø7,20
thread same as motor
M8 x 0,75
Ø12,50
Ø11
Ø10
16,50
14,70
9,70
7,90
5,35
41,50
17
3
Ø7,20
9
13,10
3
1,80
1,10
Ø1,60
3x M2
6,55
DO NOT SCALE DRAWING
REVISION
DEBUR AND BREAK SHARP EDGES
FINISH:
UNLESS OTHERWISE SPECIFIED:
DIMENSIONS ARE IN MILLIMETERS
SURFACE FINISH:
TOLERANCES:
LINEAR:
ANGULAR:
NAME
SIGNATURE
DATE
DRAWN
CHK'D
APP'VD
MFG
Q.A
MATERIAL:
WEIGHT:
TITLE:
MS
DWG NO.
motor fastener
A4
SCALE:2:1
SHEET 1 OF 1

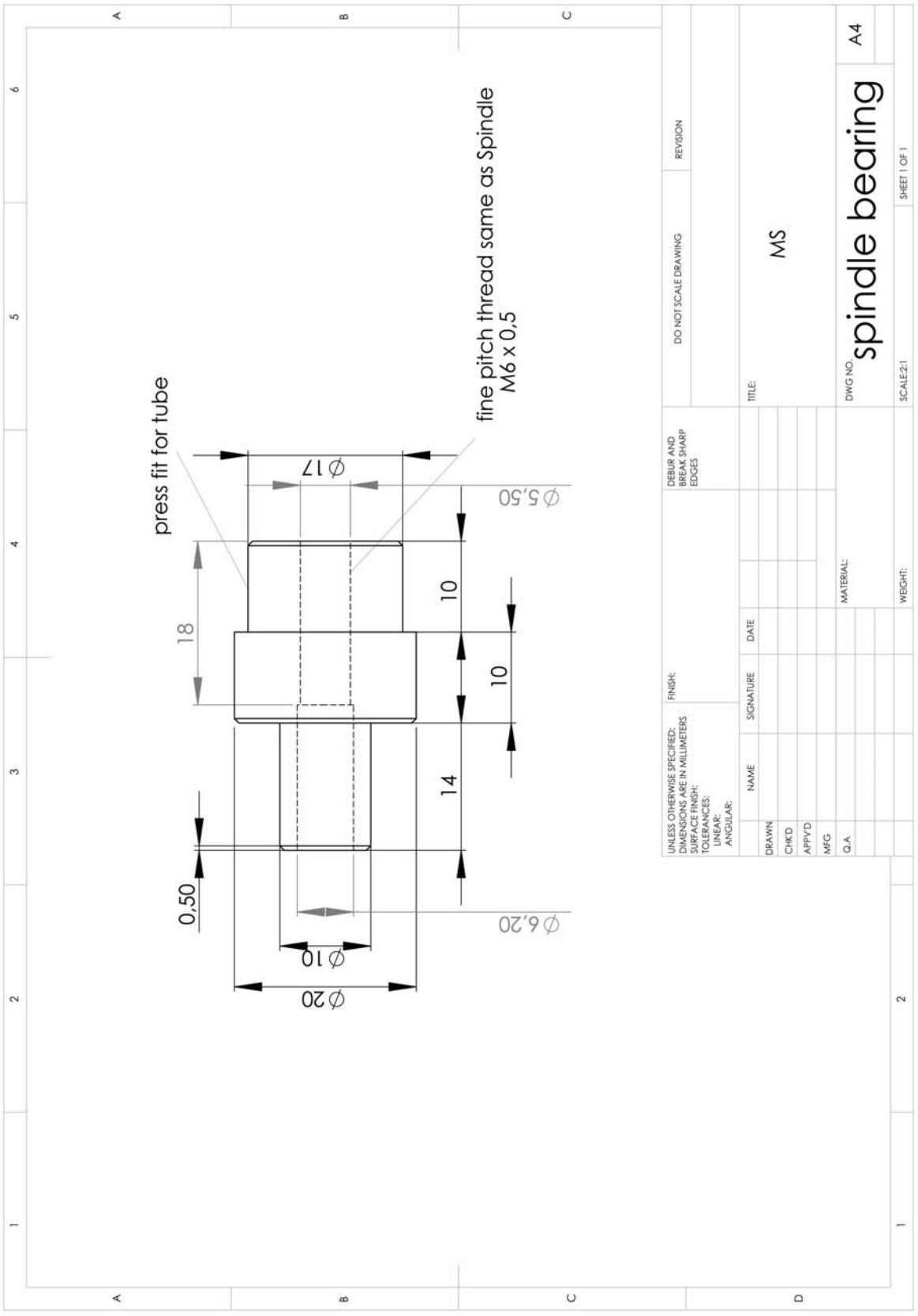
press fit for tube
fine pitch thread same as Spindle
M6 x 0,5
Ø17
Ø5,50
10
18
10
14
0,50
Ø6,20
Ø10
Ø20
DEBUR AND BREAK SHARP EDGES
FINISH:
DO NOT SCALE DRAWING
REVISION
UNLESS OTHERWISE SPECIFIED:
DIMENSIONS ARE IN MILLIMETERS
SURFACE FINISH:
TOLERANCES:
LINEAR:
ANGULAR:
NAME
SIGNATURE
DATE
DRAWN
CHK'D
APP'VD
MFG
Q.A
MATERIAL:
TITLE:
MS
DWG NO.
spindle bearing
A4
WEIGHT:
SCALE:2:1
SHEET 1 OF 1

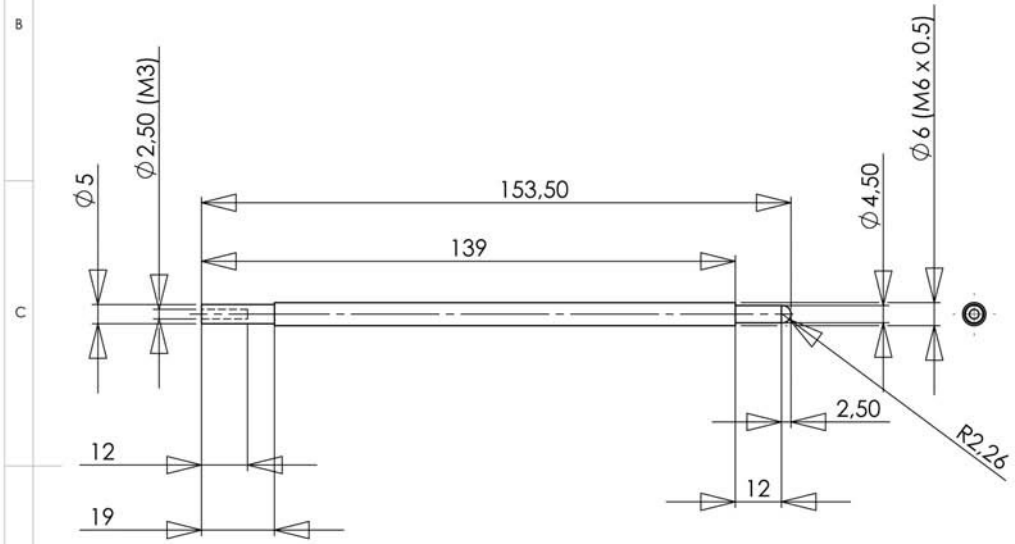

Dateiname:	Allgemeintoleranzen DIN-ISO 2768 - mH	Maßstab: 1 : 1	Gewicht:
		Material: VA-1.4571	
	Datum / Name	Bezeichnung:	
Bearb.	G.Herz	spindle	
Gepr.			
Norm			
Max-Planck-Institut für marine Mikrobiologie		Zeichnungsnummer:	

Zust. | Änderung | Datum | Name

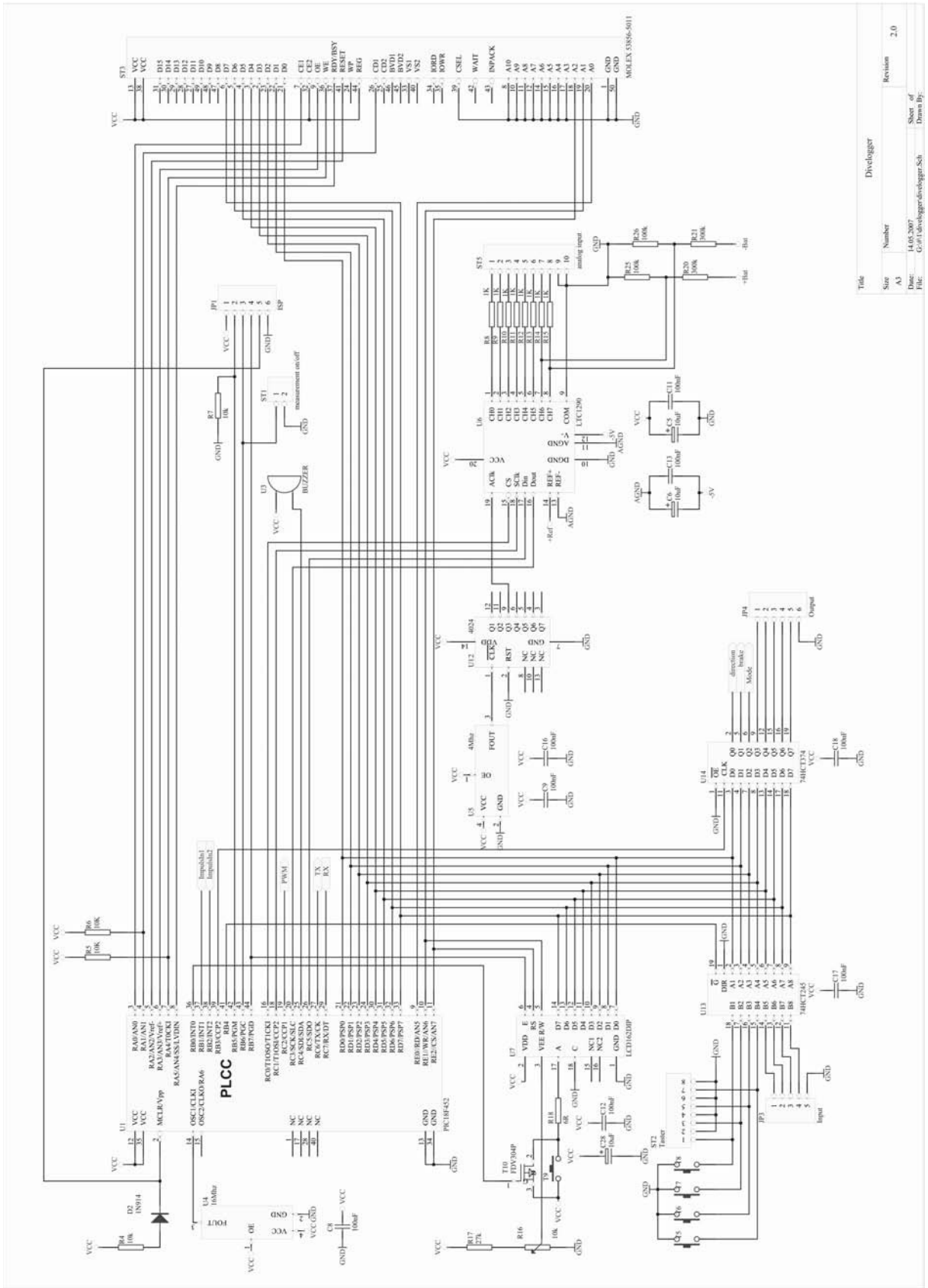
PLCC
Title
Divelogger
Size
A3
Number
Revision
2.0
Date:
14.05.2007
Sheet of
File:
G:\#11\divelogger\divelogger.Sch
Drawn By:

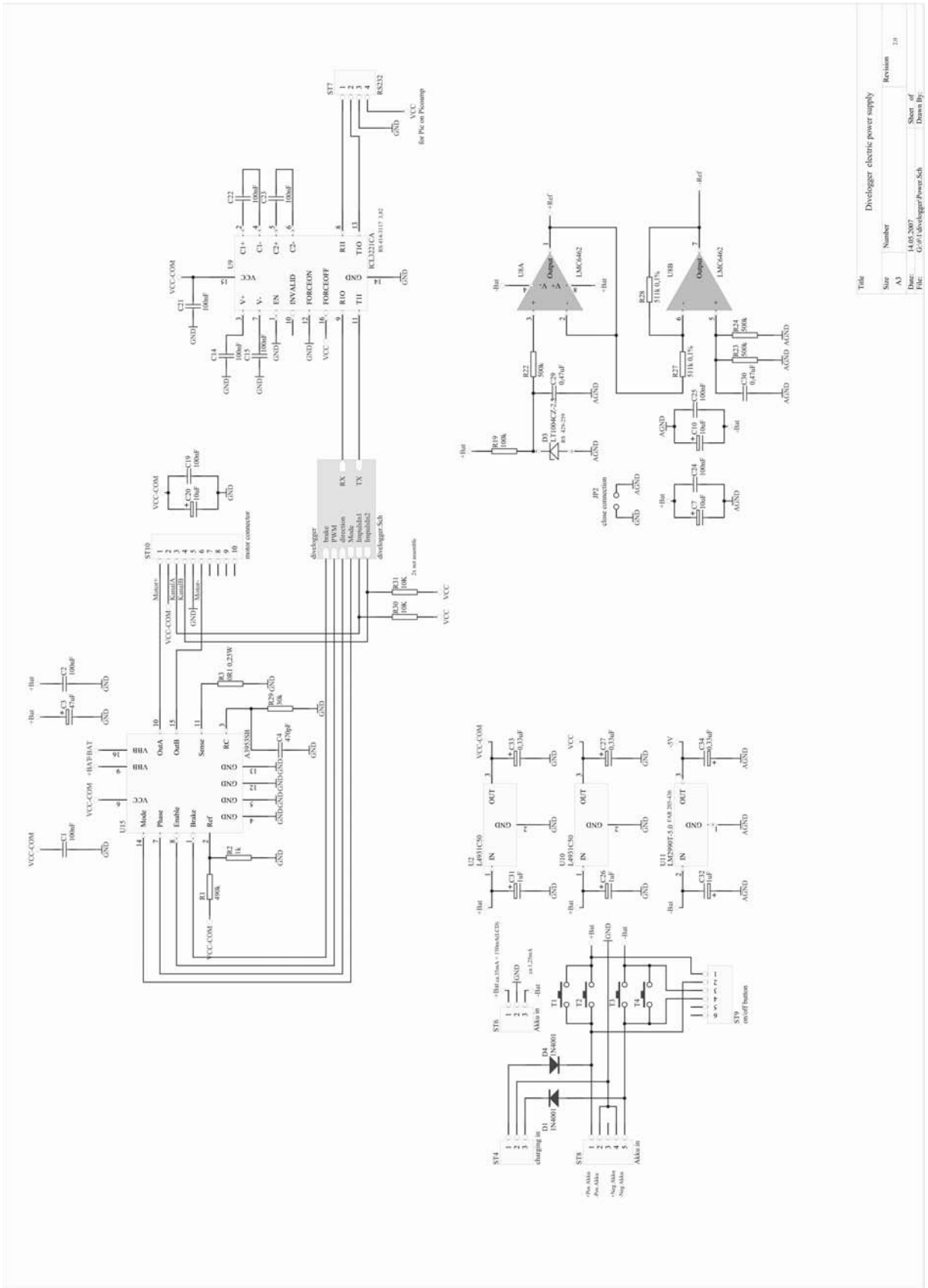
Divelogger electric power supply
Size
A3
Number
Revision
Date:
14.05.2007
Sheet of
File:
G:\#1\divelogger\Power.Sch
Drawn By:
divelogger
brake
PWM
direction
Mode
Impulse1
Impulse2
RX
TX
divelogger.Sch
motor connector
Motor+
Motor-
KontrA
KontrB
VCC-COM
GND
+Bat
-Bat
+Ref
-Ref
AGND
VCC
-5V
U15
U2
U10
U11
U8A
U8B
LMC6462
L4931C50
LM2990T-5.0
A3953SB
ICL3221CA
RS232
VCC
for Pic on Picomp
charging in
Akku in
on/off button
JP2
close connection
not assembly

Chapter 6

In situ measurement of gross photosynthesis using a microsensor- based light-shade shift method

LIMNOLOGY
and
OCEANOGRAPHY: METHODS

Limnol. Oceanogr.: Methods 6, 2008, 373–383

In situ measurement of gross photosynthesis using a microsensor-based light-shade shift method

Lubos Polerecky[1]*, *Christian Lott*[1,2], *and Miriam Weber*[1,2]
[1]Max Planck Institute for Marine Microbiology, Celsiusstrasse 1, 28359 Bremen, Germany
[2]HYDRA Institute for Marine Sciences, Elba Field Station, Via del Forno 80, 57034 Campo nell'Elba (LI), Italy

Abstract

We present a measuring procedure that allows the quantification of gross photosynthesis at the ambient light intensity, P(I), from light transition measurements similar to those employed in the light-dark shift method but without the necessity of achieving complete darkness. The method is thus more readily applicable in situ, where, during daylight, complete sample darkening is very difficult or even impossible to achieve. The procedure involves rapid microsensor-based monitoring of oxygen in the sample during a series of light transitions from ambient light intensity to a few intermediate levels, and determination of the initial rates of oxygen decrease during each partial darkening (shading) period. P(I) is then recovered by fitting the measured rates with a function derived from the model describing the change in photosynthesis rate with light intensity (P-I curve) and extrapolating it to the full light-to-dark transition. We validated this approach in the lab on coral and microbial mat samples and found that a satisfactory estimate of P(I) can be obtained with as few as 4-5 shade levels. We also applied the procedure in situ and showed that the gross photosynthesis rate at the ambient sunlight in the microbial mat and in the coral reached, respectively, approximately 50% to 65% and 94% to 97% of the saturated rate.

Introduction

The microsensor-based light-dark shift method, introduced more than two decades ago by Revsbech and Jørgensen (1983, 1986), has been widely used to quantify with submillimeter spatial resolution the primary production in densely stratified biological systems, such as microbial mats (e.g., Camacho and De Wit 2003; Jonkers et al. 2003; Wieland et al. 2003; Benthien et al. 2004; Fourçans et al. 2004; Ludwig et al. 2005, 2006; Pringault et al. 2005; Wieland and Kühl 2006; Abed et al. 2006), biofilms (Kühl et al. 1996; Hancke and Glud 2004), coral zooxanthellae (Kühl et al. 1995; De Beer et al. 2000; Al-Horani et al. 2003), and sponges (Schönberg et al. 2005). It involves rapid monitoring of oxygen concentrations in the sample during its prolonged exposure to constant photosynthetically active radiation (PAR) followed by a short (2-3 s) period of complete darkness. Oxygen concentration in the measured sample point, denoted as c, which reaches steady state during the prolonged PAR exposure, will start to decrease immediately after PAR is switched off, as a result of the disturbed balance between photosynthesis, respiration, and diffusive transport in and around the measuring point. Assuming that respiration rates in the sample in the light and during the few seconds of darkness succeeding the light period do not change, the volume-specific rate of gross photosynthesis, P, in the sample point during the illumination period equals the initial rate of O_2 decrease measured during the dark period (Revsbech and Jørgensen 1983, 1986):

$$P(I) = -[dc/dt]_0, \quad (1)$$

where subscript 0 refers to the light transition I→0.

This approach has been widely used under laboratory conditions, where the light-dark transitions can easily be achieved either by blocking the light source (e.g., a lamp) illuminating the sample with an opaque object (e.g., Revsbech and Jørgensen 1983), or by rapidly switching the light on/off electronically (e.g., Polerecky et al. 2007). Such "luxury" of a complete control

*Corresponding author: E-mail: lpolerec@mpi-bremen.de

Acknowledgments

We thank Ines Schröder, Gaby Eickert, and Anja Niclas for the preparation of excellent oxygen microelectrodes, and the 2007 HYDRA team for their support during field measurements. Valuable comments from Henk M. Jonkers and Andrew Bissett, as well as the continuous support from Bo Barker Jørgensen and Dirk de Beer are also greatly appreciated. We are grateful to the reviewers, especially to Olivier Pringault, whose comments and suggestions helped improve the manuscript. Financial support was provided by the European Union project ECODIS (Contract No. 518043), the German Academic Exchange Service (DAAD), and the Max Planck Society.

over the illuminating light is, however, very difficult or even impossible to achieve in situ, where the sample is illuminated by the sunlight. Since rapid and complete darkening of the sample, i.e., the transition I→0, is a fundamental prerequisite for the light-dark shift method to give accurate values of P at the given illumination intensity I, implementation of this method is not straightforward outside a lab.

Using a standard laboratory microsensor system, which typically comprises a fast Clark-type oxygen microelectrode attached to a (motorized) micro-manipulator mounted on a heavy stand, a pA-meter, and a data recording unit (see, e.g., Polerecky et al. 2007), one can readily measure physico-chemical gradients not only in the lab but also in shallow-water systems, such as microbial mats and biofilms found in shallow ponds or rivers (Jonkers et al. 2003; Fourçans et al. 2004; Bissett et al. 2008). A recent technical development of a diver-operated submersible microsensor system (Weber et al. 2007) made it possible to conduct delicate microsensor measurements that can be fully controlled by the operator (e.g., to accurately position the microsensor tip to a selected point in the sample) also under water. Thus, one logical application of such systems would be to quantify the rates of gross photosynthesis in situ. However, considering the difficulties associated with the need of a complete sample darkening mentioned above, a new approach is required to allow such measurements.

As an immediate solution to this practical problem, one may propose using partial darkening (shading) of the sample, i.e., decreasing the ambient PAR intensity I to an intermediate level $0 < I_j < I$, and calculating the gross photosynthesis rate as a linear extrapolation of the measured initial rate of the O_2 concentration decrease $[dc/dt]_j$ to the full I→0 transition, i.e.,

$$P(I) \approx -[dc/dt]_j \times I/(I-I_j). \quad (2)$$

This procedure is, obviously, correct only under the assumption that the relation between the gross photosynthesis rate, P, and the PAR intensity, I, is linear. Such an assumption is valid, and thus this measurement principle is applicable, only over a limited range of intensities. It is well documented that as a result of finite rates of electron transfer in the photosynthetic apparatus of a phototrophic cell, the increase of P with I slows down above a certain intensity level, and photosynthesis eventually reaches some saturated rate P_{max}. This saturation of photosynthesis with increasing light intensity can be modeled by several suitable functions (Jassby and Platt 1976), one of which is the mono-exponential function proposed by Webb et al. (1974):

$$P(I) = P_{max}\,[1 - \exp(-I/E_a)], \quad (3)$$

where E_a is the onset of photosynthesis saturation. Thus, a correct approach for the estimation of P(I) should emerge by combining the idea of partial sample darkening (shading) with the knowledge of the nonlinear behavior of P versus I.

Here we present a measuring procedure that allows the quantification of gross photosynthesis at any ambient PAR intensity but does not require achieving complete darkening of the sample. The procedure involves rapid microsensor-based monitoring of O_2 in the sample during a series of light transitions from the ambient light intensity to a few intermediate levels (shades), and determination of the initial rates of O_2 decrease during each partial darkening (shading) period. Since rapid shading of the measured sample, e.g., by moving an opaque obstacle above or next to the sample so as to partially block the illuminating PAR (e.g., the ambient sunlight), is much easier than complete darkening, the method is more readily applicable for in situ measurements. We validate this new approach under laboratory conditions using a lamp as the source of PAR, and apply it to quantify gross photosynthesis rates in microbial mats and coral zooxanthellae under in situ and natural light conditions.

Materials and procedures

Theoretical basics—The new method is based on the assumption that the dependence of the gross photosynthesis rate (P) on the ambient PAR intensity (I) is described by some generally nonlinear function P(I), referred to as the P-I curve. Although the method is, in general, independent of the actual form of the function, we chose the exponential function described by Eq. 3. Based on this assumption, it is straightforward to realize that by measuring gross photosynthesis at several light levels, one can reconstruct the P-I curve, determine the parameters P_{max} and E_a in Eq. 3, and thus allow prediction of P at any given light intensity I.

Typically, the P-I curve in dense microbial systems is determined by measuring gross photosynthesis using the traditional microsensor-based light-dark shift approach at gradually increasing intensities of the ambient light (e.g., Wieland and Kühl 2006). Here, we propose a different approach, which does not require manipulation of the ambient light. Namely, we propose to maintain the ambient light intensity constant and, instead, use shading to decrease the light intensity illuminating the sample.

When the sample is illuminated by the full ambient light intensity, I, photosynthesis operates at a full rate, P(I). When the illumination is decreased, e.g., by shading the sample with a filter of transmission T_j, photosynthesis will operate at a decreased rate, $P(T_jI)$. Using Eq. 3, it is easy to see that for a given ambient light intensity, I, the decrease in the gross photosynthesis rate, denoted as $\Delta P_j = P(I) - P(T_jI)$, decreases exponentially with T_j:

$$\Delta P_j(T_j) = P_{max}\,[\exp(-T_jI/E_a) - \exp(-I/E_a)]. \quad (4)$$

In the same way the initial rate of the O_2 decrease upon sample darkening corresponds to the local gross photosynthesis rate in the traditional light-dark shift method (Eq. 1; Revsbech and Jørgensen 1983), the initial rate of the O_2 decrease upon sample *shading* represents the *decrease* in the local gross photosynthesis rate, i.e.,

$$\Delta P_j(T_j) = -[dc/dt]_j, \quad (5)$$

where subscript j refers to the light transition I→T_jI. Note that

the quantification of $\Delta P_j(T_j)$ does not require that the steady state O_2 concentration at the measured point has been fully reached. When the O_2 concentration is slowly increasing or decreasing before shading, e.g., due to slowly increasing or decreasing ambient light intensity, the decrease in photosynthesis rate, $\Delta P_j(T_j)$, can be evaluated as the difference between the rates of O_2 decrease immediately before and after shading. This follows from the same mass balance considerations as those thoroughly described by Revsbech and Jørgensen (1983).

At this point, it is useful to note that shading, i.e., $0 < T_j < 1$, is not the only possible way of altering the sample illumination. In the same way as shading leads to a decrease in photosynthesis rate, $\Delta P_j > 0$, addition of light to the sample, e.g., by illuminating it with an extra lamp, will increase the photosynthesis rate, i.e., $\Delta P_j < 0$. Assuming that the increase in photosynthesis from the rate at the ambient light level to that at the increased light intensity is immediate (within ~1 s), this approach will provide additional experimental points on the P-I curve, and may thus further increase confidence of the P-I curve prediction, especially in the high intensity range.

Samples—Two types of microbial mat samples and one coral species were used in this work. The first microbial mat sample originated from the hypersaline lake La Salada de Chiprana (NE Spain). It was collected in September 2005 and stored in an aquarium filled with in situ water (salinity 80 g L^{-1}, temperature 20°C) under a 16 h light/8 h dark illumination regime (250-300 μmol photons m^{-2} s^{-1}) for many months prior to the measurements. The composition and a more detailed functional description of the mat are given elsewhere (Jonkers et al. 2003). This mat was used only in the laboratory measurements.

The second mat sample originated from the Island of Elba (Italy) and was found in a rockpool, approx. 50 cm above the mid-water line. The mat has not yet been characterized in greater detail, but was dominated by *Rivularia atra*, a filamentous, sheath-forming cyanobacterium that can form dense irregular crusts up to 8 mm thick. The mat also contains carbonate precipitates at depth of ~2 mm, presumably as a result of calcification coupled to photosynthesis (Bissett et al. 2008). The salinity and temperature of the pool water varies greatly during the day (38-50 g L^{-1}, 23-35°C), as a result of exposure to intense sunlight (2000-2700 μmol photons m^{-2} s^{-1} on a sunny day) and, depending on the wind, frequent or sporadic flushing with the water from the sea. The investigated coral *Cladocora caespitosa* was found several meters off-shore of Elba Island at depth of ~5 m (salinity 39 g L^{-1}, temperature 23°C, in situ scalar irradiance on a sunny day of 1300-1500 μmol photons m^{-2} s^{-1}), which was also the location of the in situ measurements conducted on the coral. For laboratory measurements, small samples of the rockpool mat and the coral were collected in a Petri dish together with the in situ water, and brought to a nearby field station, where they were stored under in situ light conditions until the measurements.

Measurement setup—A fast Clark-type oxygen microelectrode (tip size ~2 μm, response time <0.5 s, stirring sensitivity <1.5%) with a guard cathode (Revsbech 1989) was used to measure oxygen concentrations inside the mat/coral tissue. For the laboratory and ex situ measurements, the microelectrode was assembled in a laboratory microsensor system, comprising a heavy stand, motorized stage, motorized micromanipulator, sensitive pA-meter, data acquisition device, and a portable computer (see, e.g., Polerecky et al. 2007). In situ measurements were conducted using a recently developed diver-operated microsensor system (Weber et al. 2007), comprising an adjustable stand, a motorized micromanipulator, a microsensor connected to an amplifier, and a data logger, all powered by a battery. Two-point linear sensor calibration was based on the readings in the water used in the measurements, which was bubbled with air and N_2 gas.

Light during the laboratory measurements used for method validation was provided by a fiber-optic halogen light source (KL 2500, Schott AG) equipped with a short-pass NIR filter, while all the remaining measurements were conducted in direct sunlight. Shading of the light produced by the lamp was done manually using gray filters (10 × 10 cm), which were made by laser-printing various shades of gray on standard transparency foils (Lexmark). Shading of the sunlight, both in air and under water, was done by placing gray neutral density foils (LEE filters #209, 210, 211, 298, and 299) attached to frames (~50 × 50 cm) between the sun and the sample, ~40 cm above the sample. Enhanced illumination was provided by underwater video lights (HID, Multitec). The scalar irradiance at the sample surface, at full light (I) or at the various shade/enhanced levels (I_j), was quantified using a spherical micro quantum sensor (US-SQS/L, Walz), which was connected to a light meter (LI-250A, LI-COR Biosciences) and positioned a few centimeters from the measuring point. Transmission coefficients were then calculated as $T_j = I_j/I$.

Rate measurements—The measuring protocol for the light-shade shift method is essentially the same as for the light-dark shift method (Revsbech and Jørgensen 1983). Namely, the microsensor was positioned in the point of interest inside the sample, and O_2 concentrations were recorded every 0.2-0.3 s. The sample was illuminated by ambient light intensity until the O_2 concentration in the measuring point reached steady state. Then the sample was shaded for a short period (2-3 s), during which the initial slope of O_2 decrease was determined, giving the value of ΔP_j (Eq. 5). This was repeated for as many different shade levels as possible (see below), so as to increase the confidence with which the P-I curve would eventually be reconstructed and thus the gross photosynthesis at the ambient PAR intensity predicted. The 2-3 s duration of the shading period was employed to limit the spatial resolution of the measured slopes $[dc/dt]_j$ to ~100 μm, as discussed by Revsbech and Jørgensen (1983). Each shading was carried out in triplicates to assess measurement's reproducibility.

To validate the concept of the proposed light-shade shift method, measurements were conducted in a dark laboratory, using a lamp as the source of PAR. Each sample was placed

separately in a small aquarium filled with in situ water bubbled with air. A pump was used to induce defined water flow above the sample surface. The measurements were realized using two protocols, each simulating a different quality of ambient light illumination that can be encountered in situ. In the first protocol, applied in the rockpool mat and coral measurements, the illumination intensity was adjusted to the peak value measured in situ during the day of the measurement, and a total of 5 transmission filters were used for shading (Table 1, lines 1-2). Two enhanced light levels were additionally used in the coral measurement (Table 1; $T_j > 1$). This protocol was employed to simulate the first and preferred measuring strategy, whereby the light-shade shift measurements are carried out during midday when the ambient illumination is maximum and approximately constant for a few hours, and with as many filters and enhanced light levels as possible. In contrast, the measurements in the Chiprana mat were conducted at 3 different ambient light intensities and using only 3 filters (Table 1, line 3). This was done to simulate the second possible strategy, whereby the measurements are done earlier or later in the day, when the ambient light intensity changes relatively fast, and the number of shadings performed when the illumination is approximately constant is limited.

Immediately after these measurements, traditional light-dark shift measurements were conducted at several defined intensities (corresponding to the intermediate light intensities during the light-shade shift measurements) to determine the true P-I curve. To facilitate direct comparison, the light-shade and light-dark shift measurements were conducted in the same point of the sample and with the same data acquisition timing protocol (see above).

Ex situ and in situ measurements were conducted during a clear day in July 2007 on Elba Island. On the measuring day, the disturbance of the rockpool by waves from the sea was frequent, which posed a high risk of damage to the microsensor system. Therefore, a small mat sample was collected in a glass beaker together with the in situ water (salinity 39 g L^{-1}, temperature 23°C), and the measurements were performed ex situ, ~5 m away from the site, immediately after the collection. Ambient sunlight intensity during the measurement and the applied transmissions are summarized in Table 1, lines 4-6. The light-shade shift measurements were conducted in 100 μm steps from the mat surface down to the carbonate precipitate layer (depth interval of 0-2 mm), always starting with the shading of the lowest transmission at each depth. Only when the lowest transmission resulted in a detectable change in oxygen concentrations were the shades with the higher transmission applied. Afterward, steady state O_2 profiles were measured at the ambient light intensity and in the dark (after sunset). All measurements were conducted in the same spot to allow comparative estimation of areal rates of gross and net photosyntheses and respiration, which were calculated as described previously (Kühl et al. 1996; Polerecky et al. 2007).

The in situ measurements in the coral tissue were performed while diving. One diver controlled the microsensor setup and gave instructions, while the other diver, when instructed, carefully shaded the sample with a filter and/or illuminated the sample with additional light, taking care to not disturb the water flow above the sample. The in situ scalar irradiance was monitored and recorded by a third person from a boat above (Table 1, lines 7-8). The measurements were conducted in several points in the coral tissue but only at a single depth to avoid sensor breakage by the coral skeleton.

Data analysis—For the data obtained at constant ambient light intensity, the measured pairs $[T_j, \Delta P_j]$ were fitted by Eq. 4, giving the best estimates of P_{max} and E_a together with their 95% confidence intervals δP_{max} and δE_a. These values were subsequently used to extrapolate Eq. 4 to $T_j = 0$, giving the best estimate of the predicted gross photosynthesis at the ambient light intensity, P(I), (note that $\Delta P[0] = P[I]$) and its 95% confidence interval δP(I). The measured values of ΔP_j were subsequently subtracted from the predicted value of P(I), giving the best estimates of the gross photosynthesis rate P_j at intensity T_jI. Similarly, the best estimate of the reconstructed P-I curve was calculated by subtracting the fitted curve $\Delta P_j(T_j)$ from the predicted value P(I), as follows from Eq. 4. The 95% prediction

Table 1. Summary of the experimental conditions during the laboratory (used for method validation), ex situ and in situ light-shade shift measurements, together with the parameters characterizing the P-I curve (Eq. 3) recovered for each measurement.*†

	Location	Sample	Light source	I	Transmission coefficients, T_j							P_{max}	E_a	Position
1	lab	rockpool mat	lamp	2630	0.04	0.06	0.09	0.21	0.38	–	–	5.67±0.10	950±108	–
2	lab	coral	lamp	1350	0.24	0.50	0.64	0.78	0.87	1.13	1.28	32.0±6.6	1771±692	–
3	lab	Chiprana mat	lamp	40, 130, 310	0.26	0.55	0.74	–	–	–	–	11.1±1.1	250±35	–
4	ex situ	rockpool mat	sunlight	1900	0.10	0.22	0.31	0.56	0.68	1.25	1.5	6.91±0.42	1425±211	1.8 mm
5				=	=	=	=	=	=	=	=	13.3±1.6	2726±536	1.9 mm
6				=	=	=	=	=	=	=	=	6.55±0.27	1529±154	2.0 mm
7	in situ	coral	sunlight	1000	0.10	0.20	0.4	0.50	0.75	1.8–2.6	–	11.2±0.6	488±77	spot 1
8				600	=	=	=	=	=	2–2.8	3.3–3.8	8.5±0.3	393±33	spot 2

*The parameters are shown as the best estimate ± the 95% confidence interval. Ambient scalar irradiance above the sample surface, I, at which the measurements were conducted, and E_a are given in μmol photons $m^{-2}s^{-1}$, P_{max} is in mmol $m^{-3}s^{-1}$.
†Symbols = and – refer to the same value as on the preceding line of the table and to no value, respectively.

confidence interval of the reconstructed P-I curve, shown in Figs. 1-3 below by dash-dotted lines, was calculated as a sum of the 95% confidence interval of the fitting curve $\Delta P_l(T_l)$ and $\delta P(I)$. Alternatively, the lower and upper 95% confidence band of the predicted P-I curve, shown in Figs. 1-3 below by dotted lines, was estimated as the minimum and maximum photosynthesis rate calculated from Eq. 3, using all combinations of fitted parameters $P_{max} \pm \delta P_{max}$ and $E_a \pm \delta E_a$, respectively. Nonlinear fitting and predictions, including the 95% confidence intervals, were done in Matlab (version 7.0; Mathworks) using functions 'fit' and 'predint'. Fitting of the data obtained at variable ambient light intensity I, i.e., triplets [I, T_l, ΔP_l], was done using Matlab's function 'fminsearch', which, unlike function 'fit', supports fitting by a function with more than one independent variable (I and T_l in this case). The Matlab source codes of the fitting programs are available as supplementary material (LSShift.zip; http://www.mpi-bremen.de/Lubos_Polerecky.html). Statistical significance of the fitting parameters was evaluated in SigmaPlot (version 10.0; Systat Software Inc.). Prediction of the photosynthesis rate at the ambient light intensity, P(I), was considered statistically significant if both estimates of the fitting parameters P_{max} and E_a were statistically significant ($p < 0.05$).

Assessment

Method validation—The oxygen concentration at the measured point started to decrease immediately after the sample was shaded. It returned to the steady state level (i.e., that which had been reached before the shading) within 1-2 min after the shading was removed and the original ambient light level was restored (data not shown). In general, the rate of the O_2 decrease was higher when a darker shade (i.e., lower T_l) was used, as expected from Eq. 4. The situation was opposite when additional light was shined onto the sample, resulting in an immediate increase in local O_2 concentration. This indicated that the microsensor tip was located at a point where the gross photosynthesis was non-zero and exhibited dependence on light intensity. In contrast, if the measured change in the rate of O_2 evolution after shading or light-addition was not immediate but delayed for a few seconds, it was concluded that the local gross photosynthesis was zero and the delayed change occurred as a result of diffusive transport between the measured point and a photosynthetically active volume located in close proximity (Revsbech and Jørgensen 1983). This happened, for example, when the sensor tip was in the diffusive boundary layer or in the photosynthetically inactive zones in the sample.

The experiments conducted at constant illumination show that the measured decrease in photosynthesis, ΔP_l, decreased exponentially with the filter transmission, T_l, in both the rockpool mat and coral experiments (circles in Figs. 1A and 1B, top-right axes). The data were fitted with Eq. 4, from which the best estimates of P_{max} and E_a were obtained (Table 1, lines 1-2). Both estimates were statistically significant ($p < 0.05$). The measured data and the fit were subtracted from the estimate of P(I), which was calculated by extrapolating the fit to $T_l = 0$. This resulted in predicted rates of gross photosynthesis (squares) and in the best estimate of the reconstructed P-I curve (solid curve, both in Figs. 1A and 1B, bottom-left axes). When the gross photosynthesis rates were measured directly by the light-dark shift method, the values for all measured intensities closely followed this reconstructed P-I curve and fell within the 95% confidence intervals (compare crosses with solid, dash-dotted, and dotted lines in Figs. 1A–B). In particular, the rates predicted for the rockpool mat and coral tissue at the ambient illumination of 2630 and 1350 μmol photons m^{-2} s^{-1} were 5.3 ± 0.3 and 16.4 ± 2.4 mmol m^{-3} s^{-1}, respectively, while the rates measured by the light-dark shift method at the same point and light intensity were 5.5 ± 0.4 and 17.1 ± 0.7 mmol m^{-3} s^{-1}, respectively.

In the measurements conducted at three defined light intensities in the Chiprana mat (Fig. 1C), the ΔP_l values decreased approximately linearly with T_l for the two lowest light intensities (40 and 130 μmol photons m^{-2} s^{-1}), whereas a trend of exponential decrease was apparent at the highest PAR intensity (310 μmol photons m^{-2} s^{-1}). The data did not lie on a single exponential curve, but rather followed three distinct trends (shown by dashed lines in Fig. 1C). This was expected from Eq. 4, which predicts that both the rate of decrease as well as the offset of the ΔP_l versus T_l curve are parameterized by the ambient light intensity I. However, after the complete dataset was processed as described in *Data analysis* section, a single P-I curve was recovered (squares and solid line in Fig. 1C), characterized by statistically significant ($p < 0.05$) values of P_{max} and E_a (Table 1, line 3). The gross photosynthesis rates measured by the light-dark shift method at the three ambient light intensities closely followed this predicted P-I curve (compare crosses with solid, dash-dotted, and dotted lines in Fig. 1C).

Thus, it can be concluded that the new light-shade shift approach and the traditional light-dark shift method give equivalent results regarding the light dependence of the gross photosynthesis rate. This was confirmed for all photosynthetic systems studied in this work and over the range of illumination intensity typically encountered naturally in these systems. This finding is important, and it needs to be verified before quantifying gross photosynthesis rates in full sunlight to validate the applicability of the light-shade shift procedure for such measurements in the studied system.

Method application—After successful validation of the method, light-shade shift measurements were conducted in the full sunlight. The ex situ measurements in the rockpool mat showed that the decrease in photosynthesis with the transmission coefficient (Fig. 2A), and thus the reconstructed P-I curve (Fig. 2B), varied with depth in the mat. This was due to a significant variation of P_{max} with depth, which changed between 6.55 ± 0.27 and 13.3 ± 1.6 mmol m^{-3} s^{-1} (Table 1) and was most likely related to a variation in biomass of the phototrophic cells. The best-fit values of E_a were similar for the

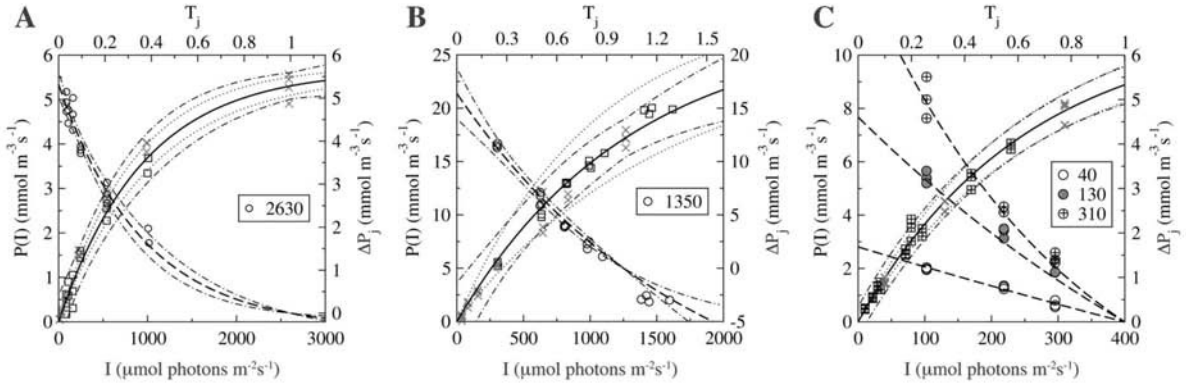

Fig. 1. Raw data obtained from the light-shade shift measurements (ΔP_j vs. T_j; circles), and the light dependence of the gross photosynthesis rate (P vs. I, squares) recovered from them using Eqs. 3–4, measured (A) in a rockpool microbial mat (dominated by *Rivularia atra*), (B) in the tissue of coral *Cladocora caespitosa*, and (C) in a Chiprana microbial mat, using a laboratory lamp as the illuminating light source (PAR intensity in μmol photons $m^{-2}s^{-1}$ is specified in legend). Note that the measuring points with $T_j > 1$ were obtained by temporarily increasing the sample illumination using an additional lamp, as opposed to shading it with a neutral density filter ($T_j < 1$). Top-right axes: dashed lines represent the best fits of the experimental data by Eq. 4, with the 95 % confidence interval indicated by the dash-dotted line. Bottom-left axes: solid line represents the predicted P-I curve (Eq. 3), with the 95% confidence interval, calculated in two alternative ways, shown by the dash-dotted and dotted lines (see text for more details). Gross photosynthesis values measured in the same point of the sample by the conventional light-dark shift method at varying PAR intensities are depicted by crosses for comparison.

two depths with lower P_{max} (~1500 μmol photons m^{-2} s^{-1}), which suggests similar light adaptation, but they were substantially lower than that corresponding to the highest P_{max} (~2700 μmol photons m^{-2} s^{-1}; Table 1). Although the estimates of both parameters were statistically significant ($p < 0.05$) for all depths, this difference was probably due to the reconstructed P-I curve being insufficiently constrained at the high-intensity end. This is also suggested by the relatively large uncertainty of the E_a estimate, which was related to the fact that even the highest intensity applied during the measurement (~3000 μmol photons m^{-2} s^{-1}) did not result in close-to-saturating photosynthesis rate. At all measured depths, the value of E_a was very high and comparable to the maximum intensities experienced by the mat during a clear summer day. This suggests that the photosynthetic activity in the mat is limited by light throughout the day. For example, the photosynthesis rate at the ambient PAR intensity of 1900 μmol photons m^{-2} s^{-1} reached only 50% to 65% of the maximum (saturated) value of P_{max} (Fig. 2B). Similar light limitation was observed in other photosynthetic systems such as microphytobenthic

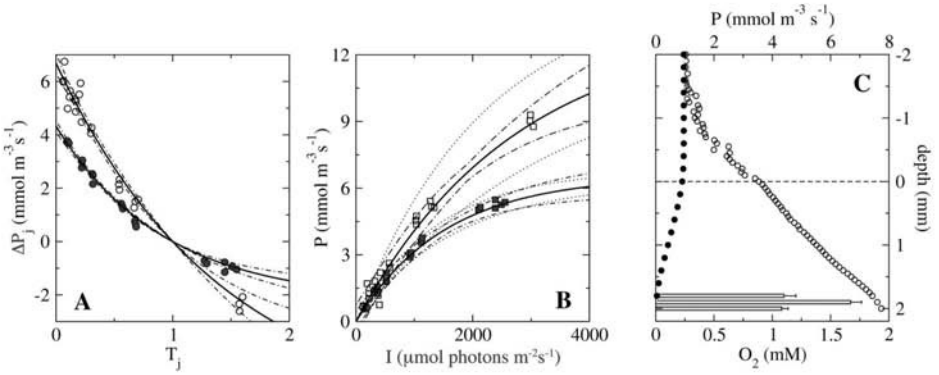

Fig. 2. Measurements in a rockpool microbial mat (dominated by *Rivularia atra*) conducted in a glass beaker at full sunlight (scalar irradiance above the mat surface 1900 μmol photons $m^{-2}s^{-1}$) a few meters away from the site from which the mat was collected. Examples of (A) the raw data fitted with Eq. 4 and (B) the recovered P-I curves, obtained at selected depths (1.8 mm = filled symbols; 1.9 mm = open symbols) are shown. The 95% confidence intervals are depicted in the same way as explained in Fig. 1. Panel C shows a vertical profile of the gross photosynthesis rate in the mat, as predicted from the light-shade shift measurements exemplarily shown in panels A-B for the light intensity 1900 μmol photons $m^{-2}s^{-1}$. Error bars represent the 95% confidence intervals. Light (open circles) and dark (filled circles) profiles of O_2 concentrations in the same spot are shown for completeness.

assemblages (Lassen et al. 1997; Dodds et al. 1999) or microbial mats (Wieland and Kühl 2006).

The gross photosynthesis rates predicted for the ambient light intensity ranged from 4.3 to 6.7 mmol m^{-3} s^{-1} and were localized over a depth interval 1.8-2.0 mm (Fig. 2C). Photosynthetic activity outside this interval was either not detectable (<1.8 mm) or was not measured (>2.0 mm) because of the risk of breaking the sensor. Thus, the photic zone that could be investigated in our measurements was 0.3 mm thick. The oxygen profile in the mat measured at the same light intensity showed enormous concentration values in the photic zone, reaching approximately 10 times the air-saturated values, or ~2 times the ambient atmospheric pressure. This result was not an artifact, as the sensor was carefully calibrated after the measurements using in situ water saturated with nitrogen, air, and pure oxygen, as well as checked for possible cross-sensitivity to temperature. Although this observation is interesting, its explanation and possible implications are beyond the aims of this work.

Owing to the limited dataset available for the oxygen concentrations and gross photosynthesis rates, only an incomplete oxygen budget in the mat could be estimated. Areal rate of gross photosynthesis, obtained by depth-integrating the volumetric rates over the photic zone thickness, amounted to $P_{a,ph}$ ~ 1.5 μmol m^{-2} s^{-1}, whereas the total oxygen flux into the overlying water in the light was $NP_{a,l}$ ~ 1.0 μmol m^{-2} s^{-1}. Considering the relatively constant oxygen gradient and complete absence of photosynthesis at depths 0-1.8 mm, respiration activity was comparatively very low or absent in this zone. Assuming that the decrease from the gross oxygen production rate $P_{a,ph}$ to the net production rate $NP_{a,l}$ occurred in the photic zone, which is equivalent to the assumption that the oxygen flux at depth 2.0 mm was zero, the areal respiration rate in the photic zone in the light would be $R_{a,l} = P_{a,ph} - NP_{a,l}$ ~ 0.5 μmol m^{-2} s^{-1}. In the dark, oxygen penetrated down to the top boundary of the photic zone, again suggesting that it was consumed only at depths below 1.8 mm. The dark oxygen flux at the mat-water interface amounted to $R_{a,d}$ ~ 0.3 μmol m^{-2} s^{-1}, suggesting that the respiration in the photic zone between 1.8 and 2.0 mm was enhanced in the light by a factor of ~1.67 compared to the respiration in the dark. This enhancement was possibly underestimated because the flux at 2.0 mm depth was assumed to be zero. Although it could not be determined more accurately due to the insufficient amount of data points at depths around 2 mm, the oxygen gradient seemed to change only minimally between depths 1.8 and 2.0 mm (Fig. 2C), suggesting lower net photosynthesis $N_{a,l}$, i.e., higher respiration $R_{a,l}$, and thus even more intensive oxygen recycling in the photic zone in the mat under illumination. As suggested in other studies (e.g., Kühl et al. 1996), this enhancement of respiration in the light was most likely due to the release of photosynthesis products which stimulate respiration by heterotrophic microorganisms, or may have been partly due to an increased depth of O_2 penetration in the light.

The in situ measurements in the coral showed that the decrease in photosynthesis with the transmission coefficient (Fig. 3A), and thus the reconstructed P-I curve (Fig. 3B), varied across the coral tissue. This was due to a significant variation of P_{max}, which decreased from 11.2 ± 0.6 mmol m^{-3} s^{-1} inside the polyp to 8.5 ± 0.3 mmol m^{-3} s^{-1} between the polyps (Table 1) and was probably related to different densities of algal symbionts in the coral tissue. The value of E_a was relatively low and similar for both locations, suggesting similar light adaptation (Table 1). The gross photosynthesis rates in the coral tissue determined for the maximum light intensity encountered by the coral during a sunny day (1350 μmol photons m^{-2} s^{-1}) amounted to 8.2-10.5 mmol m^{-3} s^{-1} (Fig. 3C). In contrast to the microbial mat (see above), these values were 94% to 97% of the maximum rate P_{max}, indicating that the symbiotic zooxanthellae operated at close to saturated rates at typical daylight intensities.

The areal rate of net photosynthesis in the light, determined ex situ from the profiles measured at a similar PAR intensity (Fig. 3C), amounted to 0.7 μmol m^{-2} s^{-1}, whereas the respiration in the dark was ~0.5 μmol m^{-2} s^{-1}. Since the gross photosynthesis was measured only at a single depth in the coral tissue, no information about its depth variation and extent is available. Thus, no comparison between the areal respiration rates in the light and dark is possible.

Minimum and optimum requirements—To assess the sensitivity of the light-shade shift method to the amount and combination of the shade levels, the fitting procedure described in the *Data analysis* section was conducted for all possible combinations of at least two shades employed in the coral laboratory experiment. The results of this assessment are summarized in Table 2 and Fig. 4.

Overall, the proportion of statistically significant predictions of P(I) (i.e., those based on the estimates of P_{max} and E_a derived from the fit of the measured data pairs $[T_j, \Delta P_j]$ with $p < 0.05$) increased with increasing number of shades (Fig. 4). Both of the fitted values of P_{max} and E_a were usually statistically significant when the combination included shades with low or both low and high transmission coefficients (values marked with an asterisk in Table 2, data points with small error bars in Fig. 4). This was possible even with 2-3 shades combined. On the other hand, when the transmissions of the combined shades were close to each other or did not include the darkest shade, the p value of at least one of the parameters P_{max} and E_a was > 0.05, leading to statistically insignificant predictions of P(I). These were typically marked with an unacceptably large 95% confidence interval (values not marked with an asterisk in Table 2, data points with large error bars in Fig. 4), and often underestimated the real P(I) value. This happened relatively often for the combination of 2-4 shades, but was possible also for 5-6 shades (e.g., lines 16 and 18 in Table 2). All statistically significant predictions of P(I) were accurate, i.e., fell within the 95% confidence interval of the photosynthesis rate measured by the light-dark shift method. The 95% confidence

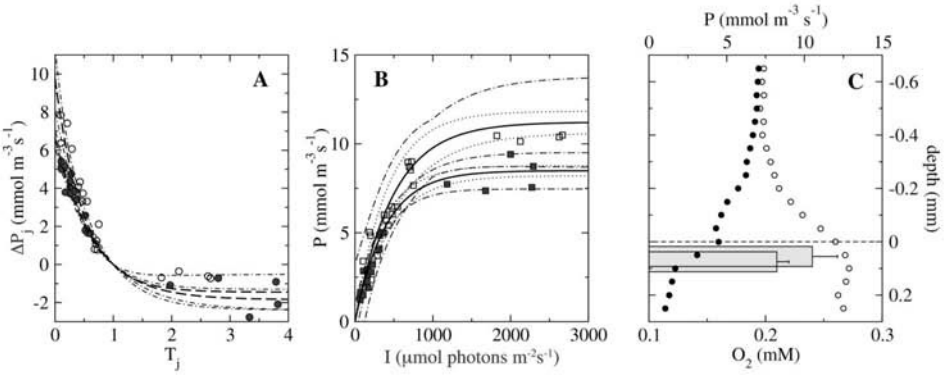

Fig. 3. Measurements in the tissue of the coral *Cladocora caespitosa* conducted in situ at full sunlight using a diver-operated microsensor system. Examples of (A) the raw data fitted with Eq. 4, and (B) the recovered P-I curves, obtained in a point inside the coral polyp (open symbols) and between two polyps (filled symbols) at ambient light intensities 1000 and 600 μmol photons $m^{-2}s^{-1}$, respectively, are shown. The 95% confidence intervals are depicted in the same way as explained in Fig. 1. Panel C shows the gross photosynthesis rates in the two points predicted for the maximum ambient light measured in situ during a sunny day (1350 μmol photons $m^{-2}s^{-1}$). Error bars represent the 95 % confidence intervals. Examples of light (open circles) and dark (filled circles) profiles of O_2 concentrations in another spot in the coral polyp (measured ex-situ at the same ambient light intensity and in the dark) are also shown.

Table 2. Examples of gross photosynthesis rates (P[I] in mmol $m^{-3}s^{-1}$) at the ambient light intensity and the parameters characterizing the recovered P-I curve (P_{max} in mmol $m^{-3}s^{-1}$, E_a in μmol photons $m^{-2}s^{-1}$), predicted from the light-shade shift measurements using selected combinations of shades.†

	N	T_1	T_2	T_3	T_4	T_5	T_5	T_6	Predicted				
Line		(0.24)	(0.50)	(0.64)	(0.78)	(0.87)	(1.13)	(1.28)	P(I)	P_{max} (*p*)		E_a (*p*)	
1	2	*	*						17.3 ± 3.2 (*)	28.0 ± 3.8	(0.002)	1318 ± 483	(0.035)
2	2	*						*	16.5 ± 0.5 (*)	35.0 ± 2.2	(<0.0001)	1993 ± 207	(<0.0001)
3	2		*			*			24.5 ± 25.2	28.4 ± 7.4	(0.01)	637 ± 388	(0.41)
4	2			*				*	11.6 ± 0.7	115 ± 53	(0.0756)	11916 ± 6150	(< 0.0001)
5	3	*	*		*				17.7 ± 2.1 (*)	26.6 ± 2.0	(<0.0001)	1159 ± 259	(0.0036)
6	3	*		*		*			18.5 ± 0.8 (*)	24.8 ± 0.4	(<0.0001)	923 ± 60	(< 0.0001)
7	3	*		*				*	16.8 ± 1.3 (*)	29.8 ± 2.5	(<0.0001)	1523 ± 269	(0.0002)
8	3		*	*	*				22.6 ± 11.0	27 ± 3.0	(<0.0001)	715 ± 234	(0.1139)
9	3			*	*			*	11.3 ± 2.2	156 ± 379	(0.6002)	16962 ± 44257	(0.0011)
10	4	*	*	*			*		16.8 ± 1.4 (*)	29.5 ± 2.4	(<0.0001)	1500 ± 268	(< 0.0001)
11	4	*		*	*		*		16.4 ± 3.1 (*)	33.2 ± 11.4	(0.0135)	1871 ± 1120	(0.0302)
12	4	*			*	*		*	16.9 ± 1.1 (*)	30.1 ± 2.4	(< 0.0001)	1542 ± 252	(< 0.0001)
13	4			*	*	*	*		11.7 ± 11.6	>100	(0.9820)	>5000	(0.4367)
14	4			*		*	*	*	11.7 ± 6.6	>100	(0.9030)	>5000	(0.1078)
15	5	*	*		*	*		*	16.9 ± 1.2 (*)	29.6 ± 2.3	(< 0.0001)	1504 ± 249	(< 0.0001)
16	5		*	*	*		*	*	13.2 ± 4.0	81 ± 148	(0.5902)	7123 ± 15358	(0.0205)
17	6	*	*	*	*	*		*	17.1 ± 1.3 (*)	28.1 ± 1.6	(< 0.0001)	1353 ± 190	(< 0.0001)
18	6		*	*	*	*	*	*	13.3 ± 3.8	66 ± 86	(0.4510)	> 5000	(0.0125)
19	7	*	*	*	*	*	*	*	16.3±1.9 (*)	32.4±5.1	(<0.0001)	1811±540	(0.0001)

†The different shades are characterized by transmission coefficients T_j, and those selected for the prediction of P(I) for a given line are marked by asterisks. Calculations were based on the raw data shown by circles in Fig. 1B. Numbers after ± represent the 95% confidence interval of the predictions. N = number of selected shades. The gross photosynthesis rate at the same light intensity, determined by the traditional light-dark shift method, was 17.1 ± 0.7 mmol $m^{-3}s^{-1}$. Statistical significance of the fitting parameters P_{max} and E_a are shown by *p* values.
*Indicates statistically significance (see text for further explanation).

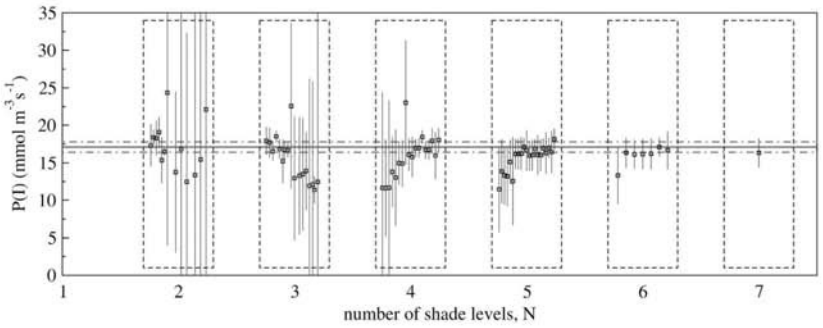

Fig. 4. Gross photosynthesis rates in a coral tissue at ambient light intensity of 1350 μmol photons $m^{-2}s^{-1}$, predicted from a combination of *N* different shade levels using data points in Fig. 1B. Values selected randomly from predictions determined from *all* possible shade combinations for a given *N* ($7!/N!(7-N)!$, $N=2,\ldots,7$) are shown. Error bars indicate the 95% confidence interval. Predictions from selected shade combinations are listed in Table 2. Gross photosynthesis rate measured by the traditional light-dark shift method (replicate measurements displayed by crosses at light intensity 1350 μmol photons $m^{-2}s^{-1}$ in Fig. 1B) is depicted here by horizontal lines (solid = mean, dash-dotted = 95% confidence interval).

interval of these predictions was lower for fits characterized by lower *p* values of the fitted parameters P_{max} and E_a, and was typically 2-3 times larger than the 95% confidence interval of the P(I) value measured directly by the light-dark shift method (Fig. 4). The precision of the P(I) prediction did not improve beyond this level even when 6-7 shades were applied.

This result is a direct consequence of the P-I curve shape (Fig. 1B), and the relative position of the ambient and shaded light intensities on the curve. Specifically, shades which are insufficiently dark ($T_j > 0.5$) probe only the leveling-off part of the P-I curve, missing its (possibly) steeper gradient at lower intensities and thus generally leading to underestimated P(I) predictions based on the model given by Eq. 4. On the other hand, the combination of similar shade levels probes only a narrow region on the P-I curve, which generally results in a poorly constrained prediction of the P-I curve, leading to P(I) estimates with unacceptably large 95% confidence intervals.

Thus, taking into account the accuracy of P(I) prediction, we conclude that 2-4 shade levels can be sufficient to accurately estimate the gross photosynthesis rate at ambient light intensity, provided that these shades are selected so as to cover as wide an intensity range on the P-I curve as possible, especially toward the low-intensity end. Considering also the precision of the prediction and the practical aspects (e.g., measurement time and experimental effort), 4-5 properly selected shade levels seem to be optimal for satisfactory P(I) estimation. The optimum choice of the shade levels should include as dark a shade as possible, and the transmission coefficients should be spread relatively evenly between the lowest and highest value, covering as wide a range of the illumination intensity as possible. Whether or not the choice of shades leads to satisfactory P(I) estimates based on the model given by Eq. 4 can be checked by evaluating the *p* values of the fitting parameters P_{max} and E_a. For example, in our case, a combination of shades and light additions with corresponding transmission coefficients around 0.25, 0.5, 0.6-0.8, and 1.2 allowed satisfactory reconstruction of the P-I curve, i.e., with both P_{max} and E_a statistically significant ($p < 0.05$), and thus accurate estimation of the gross photosynthesis rate over the entire range of light intensities experienced by the studied system in situ (see Fig. 1B).

Comments and recommendations

The presented method allows high spatial resolution quantification of volumetric gross photosynthesis rates in a sample exposed to ambient light. In contrast to the microsensor-based light-dark shift method that has been traditionally used for such measurements under laboratory conditions, our new method does not require full darkening of the sample. Therefore, it is suitable for in situ applications conducted at full sunlight. The execution of the light-shade shift measurement is straightforward: using an oxygen microelectrode and a calibrated light sensor, one needs to accurately and rapidly (at least every 0.5 s) monitor the oxygen concentration and illuminating light intensity in the studied system, while placing objects with different transmissions (e.g., neutral density transmission foils) between the sample and the sun for a few seconds in a few minutes intervals (usually every 1-2 min). From the rate of oxygen decrease measured during the short shading period, and by applying several different shade levels, one can essentially reconstruct the light-dependence of the gross photosynthesis rate (the so-called P-I curve) and thus predict the rate at the measured point in the sample at the ambient light level. Additional information about the P-I curve, in particular at the high-intensity end, can be obtained by illuminating the sample with additional light instead of shading.

From the practical point of view, an accurate and reasonably precise estimate of gross photosynthesis at one measuring point can be accomplished within 15-30 min, considering that 4-5 different shade levels are applied in triplicates and that a typical "recovery" phase after the shade removal lasts 1-2 min. Thus, the measurements should preferably be carried out during

midday of a clear or very cloudy day, when the ambient light intensity practically does not change. In such case, the data analysis is simple, as one only needs to fit the measured pairs $[T_i, \Delta P_i]$ with Eq. 4, without considering its explicit dependence on the ambient light intensity I (see Figs. 1A–B). When the ambient light intensity is not stable over such long time periods, e.g., in the morning or later in the afternoon, it is recommended that the measurements are carried out with as many shade levels and as fast as possible, e.g., by decreasing the number of replicate measurements at each shade level to 2 or 1. In such case, data analysis must be slightly modified, as the explicit dependence of the fitting Eq. 4 on I must be considered when fitting the complete dataset $[I, T_i, \Delta P_i]$.

The measurements are easy to handle when done in the air where the sensor and filter positioning as well as the communication is simple. Underwater measurements are more difficult, but possible when done by experienced divers and with a well thought-through measuring protocol. Because of the higher friction, filter positioning under water is not as simple as in the air but can be done without disturbing the water flow conditions above/in the sample.

Because the method employs microsensor-based monitoring of O_2 concentrations in the sample and its temporal variation induced by the change in illumination, it is very important that the changes in O_2 concentration are not disturbed by other factors, such as sudden changes in water flow in or above the sample, which may be difficult to control. Thus, the method is best suited for systems found in habitats with well-defined and relatively constant flow conditions, such as microbial mats or biofilms in lakes or slow rivers, corals in areas sheltered against too high water currents, intertidal sediments at low or high tide, etc. Using the newly developed diver-operated microsensor system (Weber et al. 2007), the measurements are not restricted to shallow waters but can be relatively easily conducted completely under water, as practically demonstrated in this work.

Although the primary aim of the light-shade shift measurement is to quantify gross photosynthesis, P(I), at the ambient light intensity, I, we showed that the measurement also leads to a useful byproduct, namely to the P-I curve characterizing the response of the studied photosynthetic system to light intensity in the range from 0 to at least I. The 95% confidence interval of the P-I curve recovered from the light-shade shift measurement is generally larger than that recovered from the light-dark shift measurements, typically by a factor 2-3. This is because the photosynthesis rates at variable light intensities are not measured directly, as with the light-dark shift method, but determined indirectly from a model that fits the decrease in photosynthesis measured at variable shade levels. Nevertheless, considering that such estimation is possible from data collected in situ, the light-shade shift method may be useful also for in situ studies of light adaptation. Here, the use of light addition (as opposed to shading) may be particularly useful, especially for the assessment of the P-I curve at the high-intensity end, if the studied system is not light adapted or if the ambient light intensity happens to be too low at the time of the measurement. However, the validity of this conceptual approach over the intensity range intended for the P-I curve assessment should be checked ex situ under controlled laboratory conditions before it is applied in situ.

References

Abed, R. M. M., L. Polerecky, M. Al-Najjar, and D. De Beer. 2006. Effect of temperature on photosynthesis, oxygen consumption and sulfide production in an extremely hypersaline cyanobacterial mat. Aquat. Microb. Ecol. 44:21-30.

Al-Horani, F. A., S. M. Al-Moghrabi, and D. De Beer. 2003. Microsensor study of photosynthesis and calcification in the scleractinian coral, *Galaxea fascicularis*: active internal carbon cycle. J. Exp. Mar. Biol. Ecol. 288:1-15.

Benthien, M., A. Wieland, T. G. De Oteyza, J. Grimalt, and M. Kühl. 2004. Oil contamination on a hypersaline microbial mat community (Camargue, France) as studied with microsensors and geochemical analysis. Ophelia 58:135-150.

Bissett, A., D. De Beer, R. Schoon, F. Shaaishi, A. Reimer, and G. Arp. (2008). Microbial mediation of tufa formation in karst-water creeks. Limnol. Oceanogr. 53(3):1159-1168.

Camacho, A., and R. De Wit. 2003. Effect of nitrogen and phosphorus additions on a benthic microbial mat from a hypersaline lake. Aquat. Microb. Ecol. 32:261-273.

De Beer, D., M. Kühl, N. Stambler, and L. Vaki. 2000. A microsensor study of light enhanced Ca2+ uptake and photosynthesis in the reef-building hermatypic coral *Favia* sp. Mar. Ecol. Progr. Ser. 194:75-85.

Dodds, W. K., B. J. F. Biggs, and R. L. Lowe. 1999. Photosynthesis-irradiance patterns in benthic microalgae: variations as a function of assemblage thickness and community structure. J. Phycol. 35:42-53.

Fourçans, A., and others. 2004. Characterization of functional bacterial groups in a hypersaline microbial mat community (Salins-de-Giraud, Camargue, France). FEMS Microbiol. Ecol. 51:55-70.

Hancke, K., and R. N. Glud. 2004. Temperature effects on respiration and photosynthesis in three diatom-dominated benthic communities. Aquat. Microb. Ecol. 37:265-281.

Jassby, A. D., and T. Platt. 1976. Mathematical formulation of relationship between photosynthesis and light for phytoplankton. Limnol. Oceanogr. 21(4):540-547.

Jonkers, H. M., and others. 2003. Structural and functional analysis of a microbial mat ecosystem from a unique permanent hypersaline inland lake: 'La Salada de Chiprana' (NE Spain). FEMS Microbiol. Ecol. 44:175-189.

Kühl, M., Y. Cohen, T. Dalsgaard, B. B. Jørgensen, and N. P. Revsbech. 1995. Microenvironment and photosynthesis of Zooxanthellae in Scleractinian corals studied with microsensors for O-2, pH and light. Mar. Ecol. Progr. Ser.

117:159-172.

———, R. N. Glud, H. Ploug, and N. B. Ramsing. 1996. Microenvironmental control of photosynthesis and photosynthesis-coupled respiration in an epilithic cyanobacterial biofilm. J. Phycol. 32:799-812.

Lassen, C., N. P. Revsbech, and O. Pedersen. 1997. Macrophyte development and resuspension regulate the photosynthesis and production of benthic microalgae. Hydrobiologia 350:1-11.

Ludwig, R., F. A. Al-Horani, D. De Beer, and H. M. Jonkers. 2005. Photosynthesis-controlled calcification in a hypersaline microbial mat. Limnol. Oceanogr. 50:1836-1843.

———, O. Pringault, R. De Wit, D. De Beer, and H. M. Jonkers. 2006. Limitation of oxygenic photosynthesis and oxygen consumption by phosphate and organic nitrogen in a hypersaline microbial mat: a microsensor study. FEMS Microbiol. Ecol. 57:9-17.

Polerecky, L., A. Bachar, R. Schoon, M. Grinstein, B. B. Jørgensen, D. de Beer, and H. M. Jonkers. 2007. Contribution of *Chloroflexus* respiration to oxygen cycling in a hypersaline microbial mat from Lake Chiprana, Spain. Environ. Microbiol. 9(8):2007-2024.

Pringault, O., R. De Wit, and G. Camoin. 2005. Irradiance regulation of photosynthesis and respiration in modern marine microbialites built by benthic cyanobacteria in a tropical lagoon (New Caledonia). Microb. Ecol. 49:604-616.

Revsbech, N. P. 1989. An oxygen microsensor with a guard cathode. Limnol. Oceanogr. 34:474-478.

——— and B. B. Jørgensen. 1983. Photosynthesis of benthic microflora measured with high spatial-resolution by the oxygen microprofile method - capabilities and limitations of the method. Limnol. Oceanogr. 28:749-756.

——— and ———. 1986. Microelectrodes – their use in microbial ecology. Adv. Microb. Ecol. 9:293-352.

Schönberg, C. H. L., D. De Beer, and A. Lawton. 2005. Oxygen microsensor studies on zooxanthellate clionaid sponges from the Costa Brava, Mediterranean Sea. J. Phycol. 41:774-779.

Weber, M., P. Faerber, V. Meyer, C. Lott, G. Eickert, K. Fabricius and D. de Beer. 2007. In situ applications of a new diver-operated motorized microsensor profiler. Environ. Sci. Technol. 41(17):6210-6215.

Webb, W. L., M. Newton, and D. Starr. 1974. Carbon dioxide exchange of *Alnus rubra*: a mathematical model. Oecologia 17:281-291.

Wieland, A., and others. 2003. Microbial mats on the Orkney Islands revisited: Microenvironment and microbial community composition. Microb. Ecol. 46:371-390.

——— and M. Kühl. 2006. Regulation of photosynthesis and oxygen consumption in a hypersaline cyanobacterial mat (Camargue, France) by irradiance, temperature and salinity. FEMS Microbiol. Ecol. 55:195-210.

Submitted 19 October 2007
Revised 6 June 2008
Accepted 27 June 2008

Chapter 7

Heterogeneous oxygenation resulting from active and passive flow in two Mediterranean sponges

Heterogeneous oxygenation resulting from active and passive flow in two Mediterranean sponges

Schläppy, M-L[1*], Weber M.[1,3], Mendola, D.[2], Hoffmann F.[1], de Beer D.[1]

[1] Max-Planck-Institute for Marine Microbiology, Celsiusstr. 1, 28359 Bremen, Germany, mlschlae@mpi-bremen.de

[2] Wageningen University, Food and Bioprocess Engineering Group, P.O. Box 8129, 6700 EV Wageningen, The Netherlands

[3] HYDRA Institute for Marine Sciences, Elba Field Station, Via del Forno 80, 57034 Campo nell'Elba (LI), Italy.

This chapter is submitted to Limnol. Oceanogr.

1. Abstract

The oxygen dynamics and ventilation behaviour in *Dysidea avara* and *Chondrosia reniformis* (Porifera, Demospongiae) were investigated using oxygen micro-electrodes hot-bead thermistors. Both field and laboratory experiments proved the occurrences of anoxia in the sponge tissue that lasted up to approximately 1 h. Before and after the anoxic events, the sponge body was well aerated and contained similar oxygen concentrations as the ambient water. The onset of anoxia was not caused by the insertion of the micro-electrode into the sponge's body but started at various times after insertion (1 min to 6 h). Strong temporal and spatial heterogeneity of oxygen concentrations was observed with replicate oxygen profile series across the sponge surface, though tissue close to an osculum was generally better oxygenated. The oscular outflow velocities in *Dysidea avara* were in the range of 0 – 0.6 mm s^{-1}. The state of oxygenation of sponge tissue could only be partially attributed to its ventilating activity. Complex oxygenation patterns indicate a mosaic of different ventilation activities in the sponge. Ambient flow also influenced oxygenation patterns of sponges. Individuals with a functional aquiferous system regulated their pumping activity according to the ambient flow regime, while a small individual without osculum was passively influenced by ambient flow and became anoxic 39 minutes after ambient flow was stopped. Our findings show that temporal and spatial anoxic niches are found within sponges both in captivity and in the field, and are regulated by active (pumping) and passive (ambient flow) ventilation events. The variable oxygen concentrations inside the sponges will have great consequences for sponge metabolism, as well as for community composition and processes of sponge-associated microbes.

2. Introduction

Sponges are sessile marine filter-feeders. They possess an aquiferous system, which allows them to draw water into their body, filter food particles from the water and expel waste water through their oscula, their outflow siphon. Sponges in nature have been shown to have various ventilating behaviors. Some species, such as *Mycale* sp., ventilates continuously whereas others sponges, such as *Verongia gigantean*, periodically stop pumping at random intervals (Reiswig 1971), possibly following an endogenous rhythm. Some species respond to physical disturbances. For example, *Verongia lacunose* reduces its ventilating activity to avoid damage to its aquiferous system in the presence of high sediment loads in the water (Gerrodette and Flechsig 1979). *Microciona prolifera* explants ceased ventilating in response to lower salinities and their aquiferous system was reduced (Fell 1998).

Through the ability of sponges to pump large amounts of water through their bodies, it has been assumed that the water within the body is oxygen saturated or close to it. However, anoxia has now been reported in several sponge species kept in captivity. Examples include *Geodia baretti*, a cold water bacteriosponge (Hoffmann et al. 2005a, b), its explants (Hoffmann et al. 2005a), *Aplysina aerophoba* (Hoffmann et al. 2008), *Dysidea avara* (Schläppy et al. 2007) and *Chondrosia reniformis* (Hoffmann and Schläppy submitted).

Oxygen is supplied to the sponge tissue by active ventilation and by advection driven by seawater currents (ambient flow), as the aquiferous system gives the tissue a certain permeability. This passive flow is driven by pressure differences and will be influenced by the sponge topography and of water current velocity. Passive ventilation is of zero metabolic cost to the sponge (Vogel 1974). Pile et al. (1997) found that *Baikalospongia bacillifera* ventilated less when ambient current was high. In the absence of ventilation or passive flow, diffusion is the only oxygen transport mechanism. Anoxia in sponges is probably due to several factors, most of which are still unknown. Absence of ventilation and low ambient flow are presumably important factors. Intuitively, the sponge should become anoxic if the combined demand of sponge cells and sponge-associated microbes' respiration exceeds the input of oxygen through active ventilation, diffusion and passive flow (see Hoffmann et al. 2008).

The presence of anoxic niches within a sponge is likely to influence microbial community structure and processes within sponges. The oxygen levels are a strong regulator for anaerobic processes. Typically, organic matter is degraded by the energetically most favorable process, which is aerobic respiration. The use of alternative electron acceptors, such as nitrate and sulfate occurs usually only under anoxic conditions. However, nitrate reducers and many sulfate reducers can nevertheless be active at low oxygen concentrations (Canfield and Marais 1991). Facultative anaerobic microbes and obligate anaerobic microbes have been found in several species of sponges (Schumann-Kindel et al. 1997, Webster et al. 2001), suggesting the presence of either temporal or spatial anoxic niches within sponges. Fermenting bacteria were found in *Ceratoporella nicholosni* (Santavy et al. 1990), sulfate reducing bacteria in tetractinellid sponges (Schumann-Kindel et al. 1997), and methanogenic euryarchaeotes may also be present (Webster et al. 2001).

Ventilation in sponges has been described in several species in the field or in laboratory conditions but how the temporal and spatial oxygen distribution in sponges is influenced by ventilation and ambient flow has not yet been documented. Microelectrode measurements of oxygen on sponges have been, to date, restricted to laboratory experiments. Therefore, we investigated the oxygen dynamics and ventilation behaviour of *Dysidea avara* and

Chondrosia reniformis both in the laboratory and in the field, and in the presence or absence of ambient flow.

3. Material and Methods

3.1 Methodologies

3.1.1 Microsensors

Clark-type oxygen electrodes (Revsbech 1989) with a 20 µm tip diameter were made at the Max-Planck-Institute for Marine Microbiology, Bremen, Germany and calibrated with a two point calibrations using oxygen-saturated seawater and oxygen depleted seawater made anoxic by the addition (to saturation) of an oxygen scavenger (sodium sulfite). Care was taken to obtain the zero value as quickly as possible as a protracted stay in the anoxic solution would have 'poisoned' the sensor, making it unusable.

For laboratory measurements the sensors were mounted on a motorized micromanipulator (Fig. 1). The oxygen microsensor penetrated the surface of *D. avara*'s body easily, but the cortex of *C. reniformis* had to occasionally be pre-pierced before a microsensor could be inserted. Thermistor and oxygen measurement were carried out simultaneously and in a range of conditions: in an aquarium with flow-through natural seawater and in a well-aerated 8 L flow-cell, at a temperature of 20 ^{o}C. For static measurements (not profiles) unidirectional flow was produced using a standard aquarium pump, which re-circulated the seawater. The water in the flow-cell was aerated with an air stone, kept at a constant temperature. The sponges were not fed during the experiments. The micro-electrode was attached to a computer-controlled micro-manipulator (Fig. 1). Static oxygen measurements were performed either in the tissue or in the osculum while profiles were always carried out in the tissue. A laminar flow-cell with a re-circulating mixture of artificial and natural seawater was used for experiments involving the manipulation of ambient flow.

For field measurements, a diver operable setup microsensor equipment was used as described in Weber et al. (2007). In both laboratory and in the field 4 sponges were used to make oxygen profiles by lowering the sensor 3 times to 3 mm inside the target sponges. Those profiles were performed along a transect going from a haphazardly chosen osculum and away from it in 2 mm steps (i.e. first set of 3 profiles was made at 2 mm from osculum, the 2nd and 3rd set at 4 and 6 mm from the osculum, respectively). Additionally, static oxygen measurements were conducted within the chosen osculum of the same individuals used for the oxygen profiles and the microsensor was left overnight. Only a selection of oxygen

measurements are shown here. They were chosen for their representativeness of a range of tissue oxygenation.

3.1.2 Thermistor

A hot bead thermistor (temperature sensitive electrical resistor) and recorder were built at the Max-Planck-Institute for Marine Microbiology according to LaBarbera and Vogel (1976). Its design allowed measurement of water flow speed in sponges' osculum. The non-directional flow probe comprised a 1 mm diameter glass-bead-covered thermistor and an additional temperature compensation thermistor was sealed onto the distal end of a 2 mm diameter stainless steel tube in which the electrical connection led to the recorder. The apparatus functions according to the following principle: the bead is heated electrically and the heat is removed by the water flow created by the sponge. The energy needed to keep the bead heated is measured by the recorder and stored in the computer. To calibrate the thermistor, a cylindrical PVC block with a 10 cm deep circular grove (30 cm long) was made to rotate at a known speed with a motor. The grove was filled with seawater and the thermistor was held stationary inside the groove while the block moved in circles. Error was estimated to range between 2 and 15 %.

3.2 Sampling sites

Sponge specimens of *Dysidea avara* and *Chondrosia reniformis* were collected at several sites by SCUBA diving:

1. from a coralliferous community (20 m depth) on the Montgri Coast (Catalan coast; NW Mediterranean Sea, 42º 3' N, 3º 13' E, Spain).
2. at 10-15 m depth in Cala Montgo (Catalan coast, West Mediterranean Sea, 42º06.863' N 03º10.116' E Spain). The microsensor applications in the field also took place at this site.

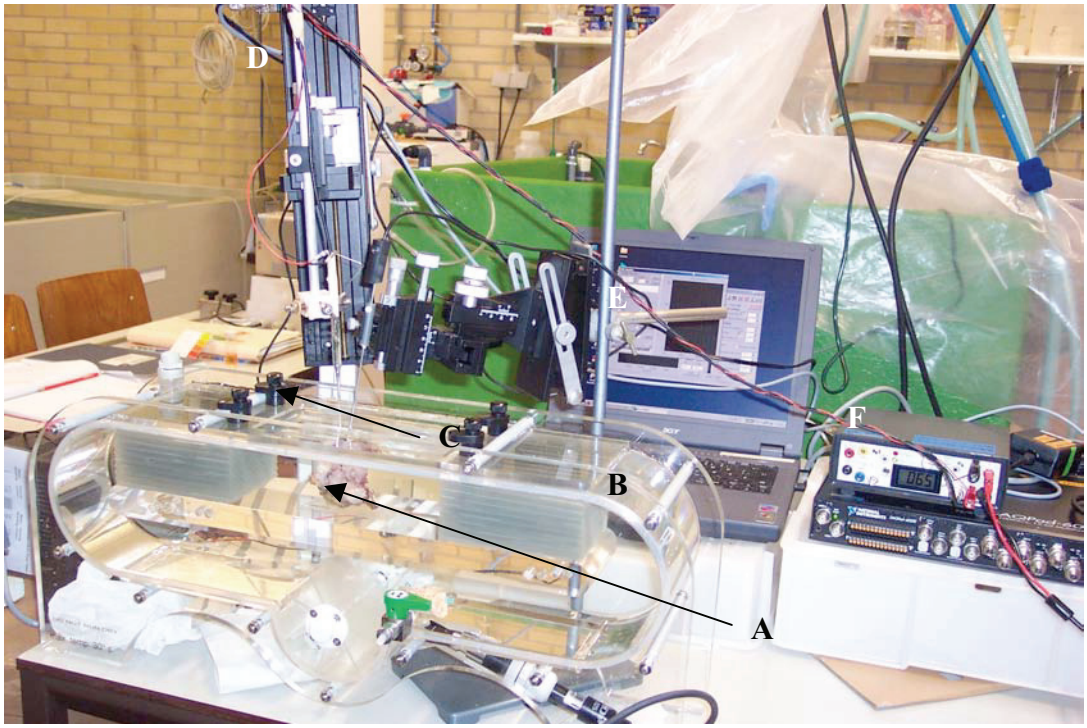

Figure 1. Microsensor and flow cell set up, showing a specimen of *D. avara* (A) in the flow-cell (B) and an oxygen microsensor (C) controlled by a micromanipulator (D) connected to a computer (E) and a pico-ampere meter (F)

3.3 Study species

Dysidea avara is a small sponge with well defined conuli and inter-dispersed oscula (exhalant siphons) (Fig. 2). This species is a common Mediterranean sponge (Uriz et al. 1992), easily available (in shallow water of 4 – 40 m) and has desirable morphological characteristics for micro-electrode work such as a body made of a soft spongin skeleton (Galera et al. 2000). This species is of commercial interest due to its ability to produce avaraol and anti-inflammatory compounds (see Chapter 1). *Chondrosia reniformis* is a Mediterranean sponge commonly found in shallow water and has a cushion-like appearance, with a smooth body surface and few oscula (Fig. 3). The body of the sponge lacks spicules but has high amounts of collagen fibers (Boury-Esnault 2002), which make the species of interest for commercial production of collagen for cosmetics or as nano-particle carrier (Swatschek et al. 2002) (see Chapter 1). A dense cortex sometimes precluded the insertion of the micro-electrode directly into the sponge body so a hole was pre-pierced in the sponge's surface.

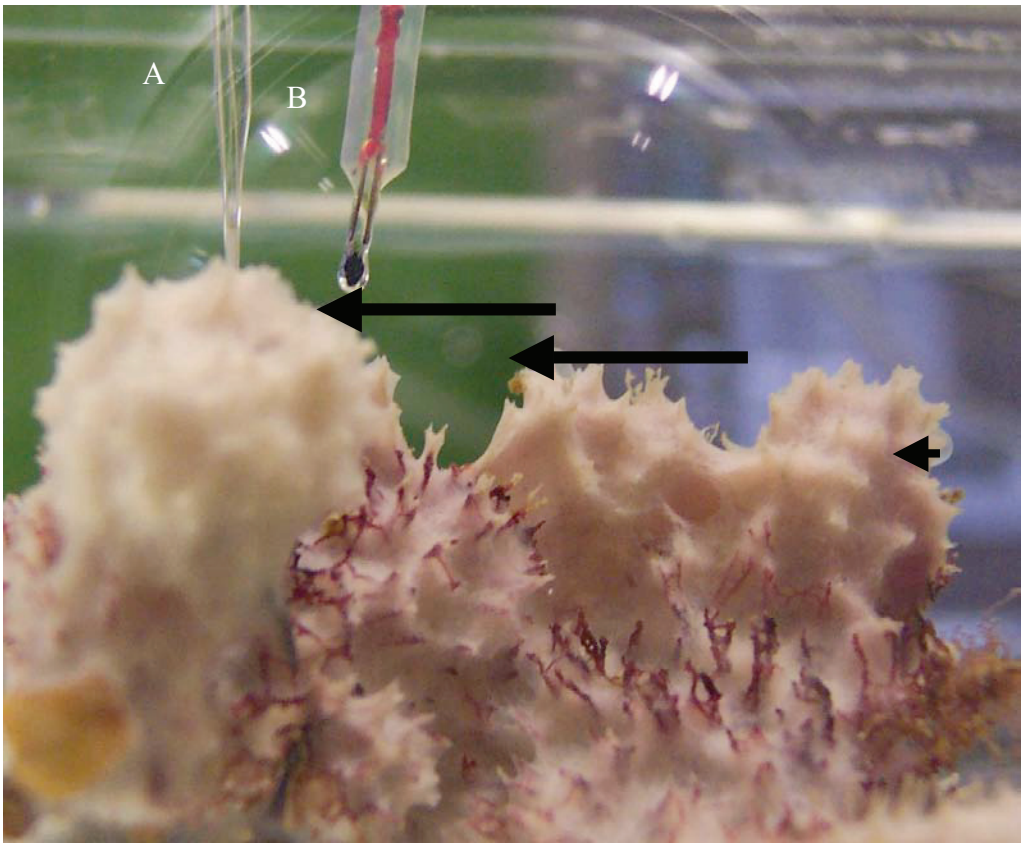

Figure 2. *Dysidea avara* with oxygen microsensor (A) in its body and a hot bead thermistor (B) above one of its oscula. The arrows point to the oscules

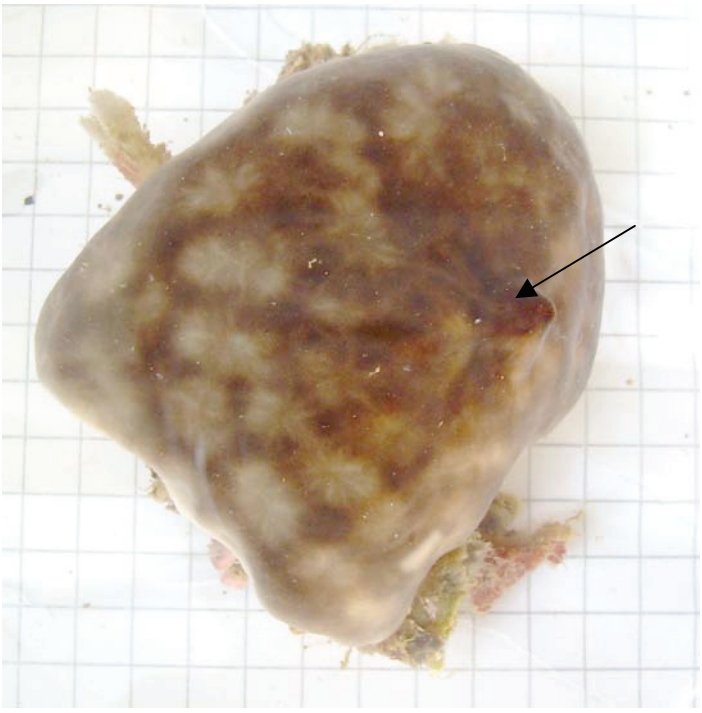

Figure 3. *Chondrosia reniformis*, specimen with one (semi-closed) oscule (arrow)

4. Results

4.1 Anoxia

The field measurements of oxygen dynamics in the osculum of *D. avara*, using a SCUBA diver-operated micro-electrode system, showed periods of tissue anoxia of 1 h (Fig. 4 a) and of 6 min (Fig. 4 b) in 2 out of the 4 studied specimens. Before and after the anoxic events the water exiting the osculum was close to saturated between 200-250 µM (Fig. 4 a, b). For 2 other *D. avara* specimens in the field, oxygen in water stream exiting the osculum fluctuated between 120 and 225 µM and never approached anoxia (Fig. 4 c, d).

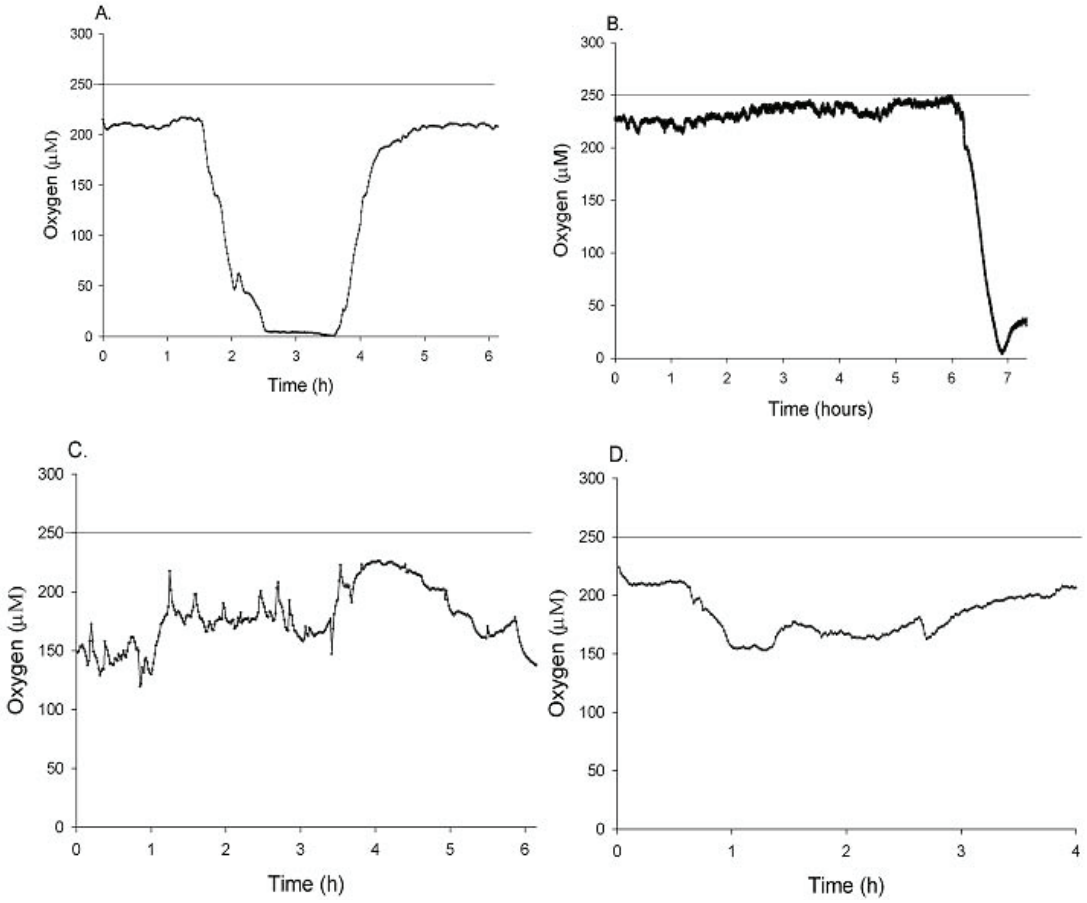

Figure 4. Field static oxygen micro-electrode measurement in the osculum of four different *D. avara* individuals. The upper line indicates the oxygen content in the ambient water. Each data point represents a minute. A) showing anoxia for 1 h 04 minutes B) showing anoxia for 6 minutes C, D) showing fluctuating oxygen concentrations but without anoxia

Under laboratory conditions tissue anoxia was found in 4 out of 12 specimens of *D. avara* and in 2 out of 10 specimens of *C. reniformis* kept in captivity under a variety of conditions. In *D. avara*, anoxic conditions were observed for 6 min (Fig. 5 a) and 41 min periods (Fig. 5 b). In another two specimens, suddenly decreasing oxygen levels followed by quickly increasing oxygen levels were also observed (Fig. 5 c, d). These sharp changes in oxygen concentration

where of ephemeral nature but occurred several times over 7 h (Fig. 5 c) and 17 h (Fig. 5 d). In *C. reniformis* anoxic events were observed for 1 hour and 42 minutes (Fig. 5 e, f). The rest of the time the water exiting *C. reniformis*' osculum remained stable (150 – 200 µM). Anoxia started at random times after insertion of the sensor (1 min – 6 h).

When profiles where carried out on captive *C. reniformis* (Fig. 6 a, b) and *D. avara* (Fig. 6 c, d) a clear differentiation was observed between well-aerated (Fig. 6 a, c) and poorly-aerated (Fig. 6 b, d) individuals. Poorly-aerated sponges showed diffusive oxygen concentration profiles with a boundary layer of 0.5 – 1 mm, and an oxygen penetration of 1 and 2 mm into the sponge's body (Fig. 6 b, d). Conversely, well aerated sponges had no boundary layer and the sponge tissue oxygenation was close to those levels found in ambient water up to 1 mm into the sponge tissue. At 3 mm, oxygen was approximately 200 µM in both species (Fig. 6 a, c).

4.2 Spatial oxygen heterogeneity

4.2.1 Oxygenation and distance from target osculum

Spatially heterogeneous oxygenation patterns were found in field measurements made on 4 *D. avara* individuals (only 2 shown here, Fig. 7). These replicate profiles showed some variability in the oxygen levels in the sponge, within the 3 - 6 min required to measure a single profile. Replicate profiles on the same location on the same sponge were sometime highly variable (Fig. 7 a, c). Nonetheless, a pattern emerged which showed that in proximity of the osculum the tissue was better oxygenated than in areas far from the target osculum (Fig. 7).

Under laboratory conditions, the high temporal and spatial variability in oxygen levels was even more pronounced than in the field (Fig. 8). Particularly near the osculum the variability was prevailing, whereas in areas remote from the osculum more reproducible oxygen profiles were measured (Fig. 8). High oscular flow speed (0.6 mm s^{-1}) did not always correlate with profiles of well-oxygenated sponge tissue (Fig. 8 c, e). The reverse was also true: at low oscular flow speeds the profiles were not always approaching anoxia (Fig. 8 a, f).

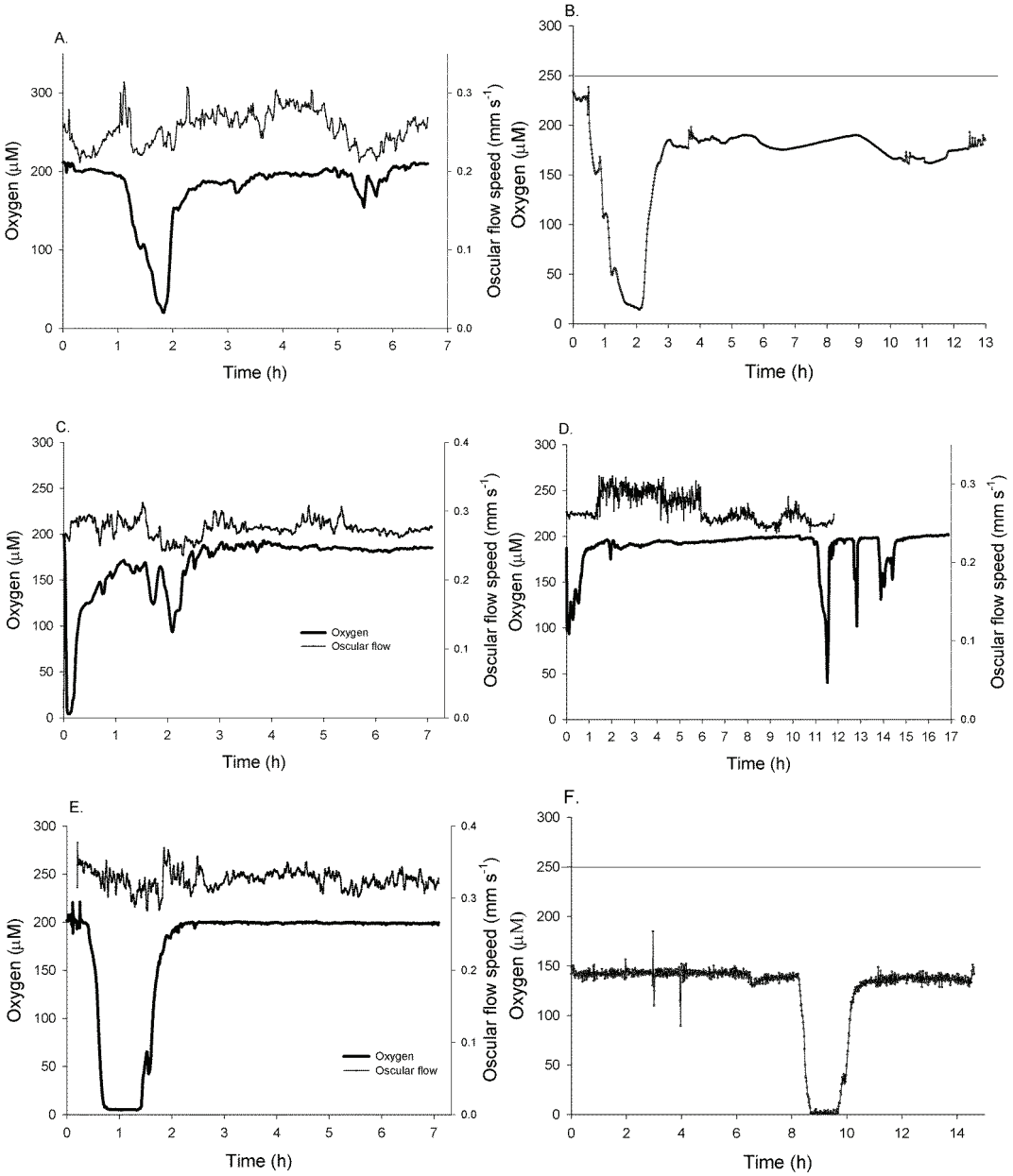

Figure 5. Laboratory static oxygen micro-electrode measurement in the osculum of *D. avara* (A, B, C, D) *and C. reniformis* (E, F). Each data point represents a minute. The upper line indicates the oxygen content in the ambient water. A, B) *D. avara* showing conditions close to anoxia for 6 and 41 min, respectively B, C) *D. avara* showing repeatedly fluctuating oxygen conditions approaching anoxia E, F) in two freshly sampled *C. reniformis* individuals, showing anoxia for 60, 42 minutes, respectively

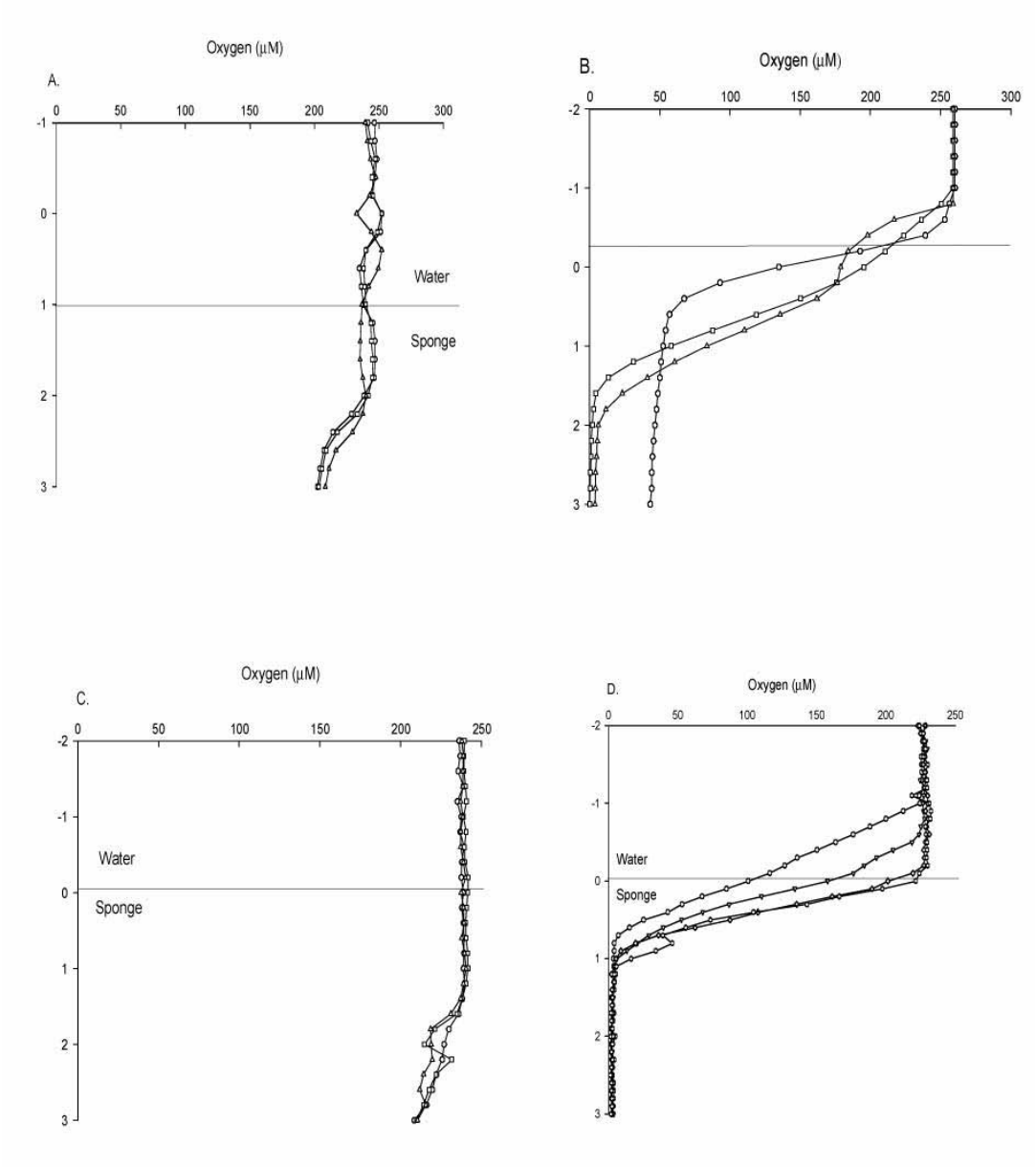

Figure 6. Oxygen profiles (replicated 3x) in the body of *C. reniformis* A) when the sponge was well oxygenated B) when the sponge was anoxic. In the body of *D. avara* C) when it was well oxygenated D) when the sponge was anoxic

At a distance of 4 mm (midway) from the osculum, the most oxygen depleted tissue was found (Fig. 8 b, e). At this location, a steep diffusion boundary layer was occasionally observed (Fig. 8 b). In two sets of profiles, a lag-time between the oscular flow speed and the oxygenation occurred (Fig. 8 b, f). When the first profile midway from the osculum was made (Fig. 8 b), the sponge had already stopped pumping (oscular flow 0 mm s^{-1}), but the sponge had still had oxygen for about 6 minutes, the time required to carry out all three profiles. In another case, the oscular flow was high during the first two profiles near the osculum (Fig. 8 f), but the effect of strong ventilation on oxygenation was only shown 2 minutes later in the last profile, which showed highly oxygenated sponge tissues.

4.2.2 Oxygenation and ambient flow

Oxygen concentration in the osculum of a *D. avara* specimen decreased at lower ambient flow (Fig. 9). Exposed to unidirectional flow, the average oxygen content of the sponge oscular water was 5 μM (± 0.37 SEM) below the seawater concentration (227 μM). Approximately once every two minutes, stronger deoxygenated water (150 μM) exited the osculum during approximately 30 seconds (see Fig. 9). Without ambient flow, the frequency of pulses of deoxygenated water increased to approximately one per minute, and the oxygen content of the sponge oscular water fluctuated in peaks between 105 and 218 μM (i.e. 9 – 122 μM below seawater) (Fig. 9). Thus ambient flow increased the oxygen supply in the sponge. In an experiment with another specimen (*D. avara*) and when the flow velocity in the flow-cell was increased, the oxygenation remained in the same range as originally but upon decreasing ambient flow, oxygenation in the sponge decreased until ambient flow was stopped (Fig. 10). At that point, oxygen concentrations in the sponge showed fluctuations but returned to approximately in the range of original levels (Fig. 10).

When the influence of ambient flow on tissue oxygenation of a small individual was repeated, another result was apparent. This individual lacked an osculum (and presumably a functional aquiferous system) and became completely anoxic in stagnant water. Upon switching off the flow the tissue became anoxic in 39 minutes. When flow was re-established, the tissue oxygenation recovered in 15 minutes to steady state levels (50 - 100 μM). When this was repeated several times with various ambient flow levels it became apparent that the flow velocities above 0.9 cm s^{-1} did not further increase the oxygen level in the tissue (Fig. 11).

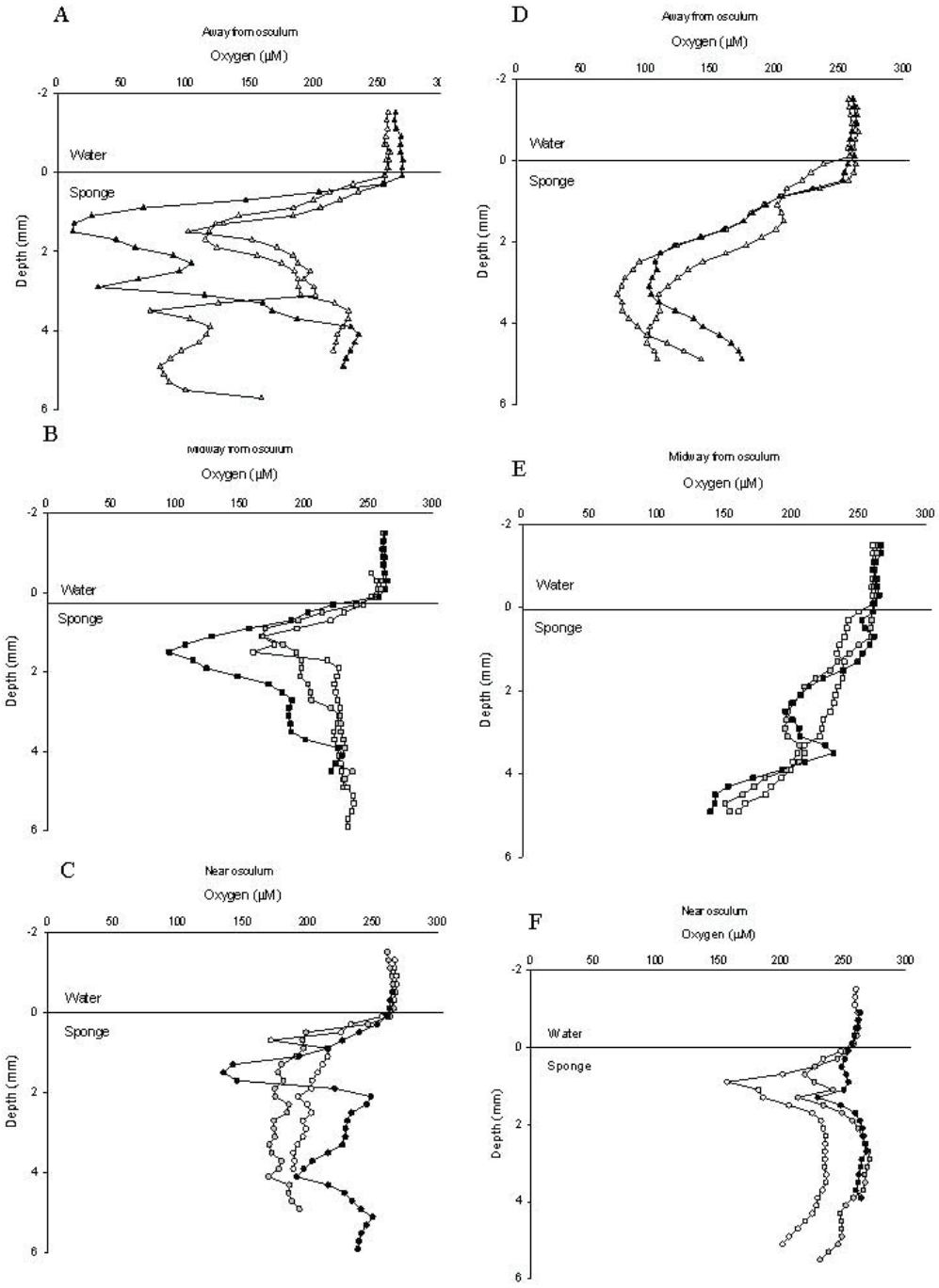

Figure 7. Field profiles in two *D. avara* individuals (Individual 1 = A, B, C; Individual 2 = D, E, F). A, D) away, B, E) midway and C, F) near an osculum. Open symbols = 1st profile; grey symbols = 2nd profile and black symbols = 3rd profile

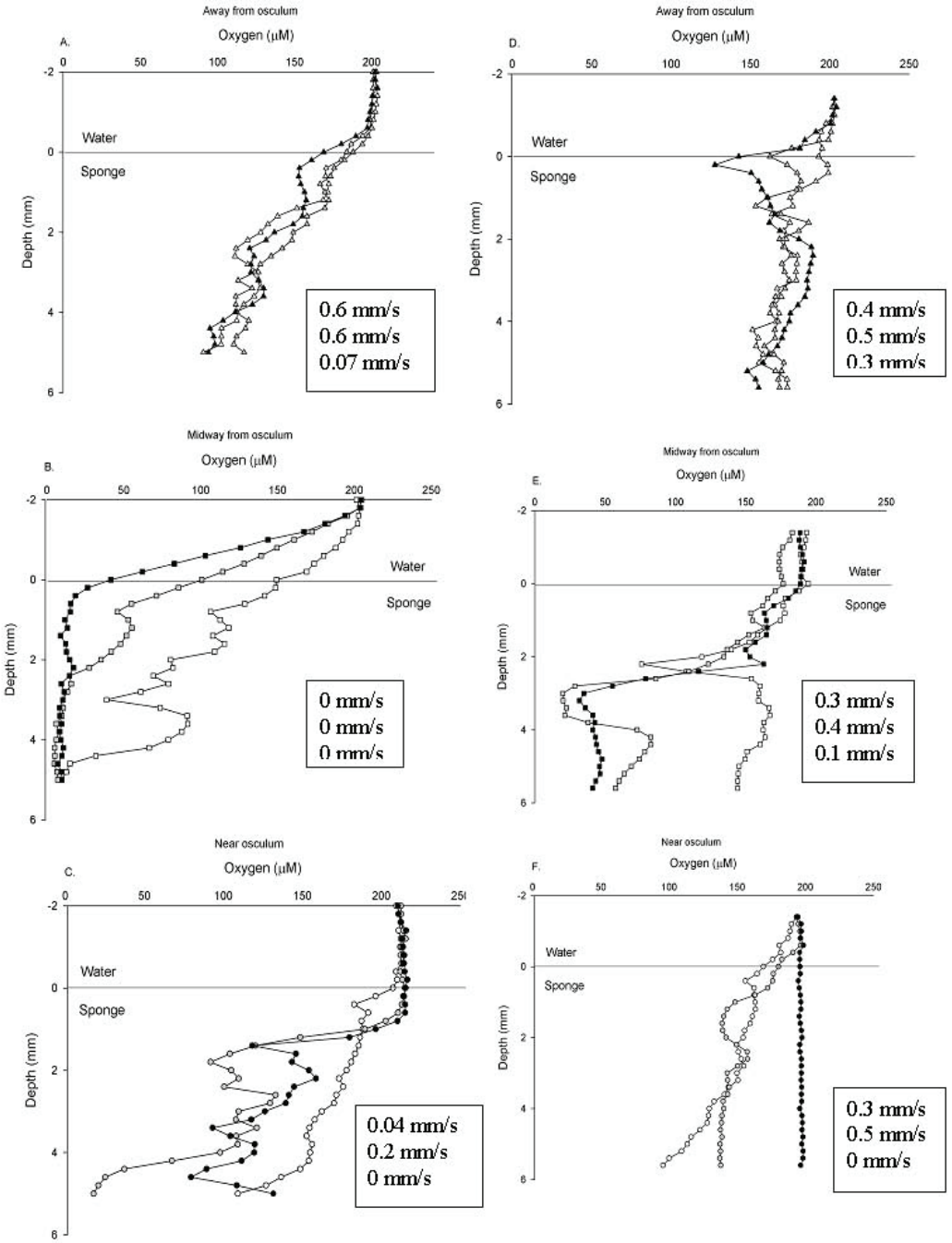

Figure 8. Laboratory profiles in two *D. avara* individuals (Individual 1 = A, B, C; Individual 2 = D, E, F). A, D) away, B, E) midway and C, F) near an osculum. Open symbols = 1st profile, grey symbols = 2nd profile and black symbols = 3rd profile. The values in the box represent the oscular flow measured at the closest osculum to the micro-electrode. The first value correspond to the first profile, second value to second profile and third value to the third profile

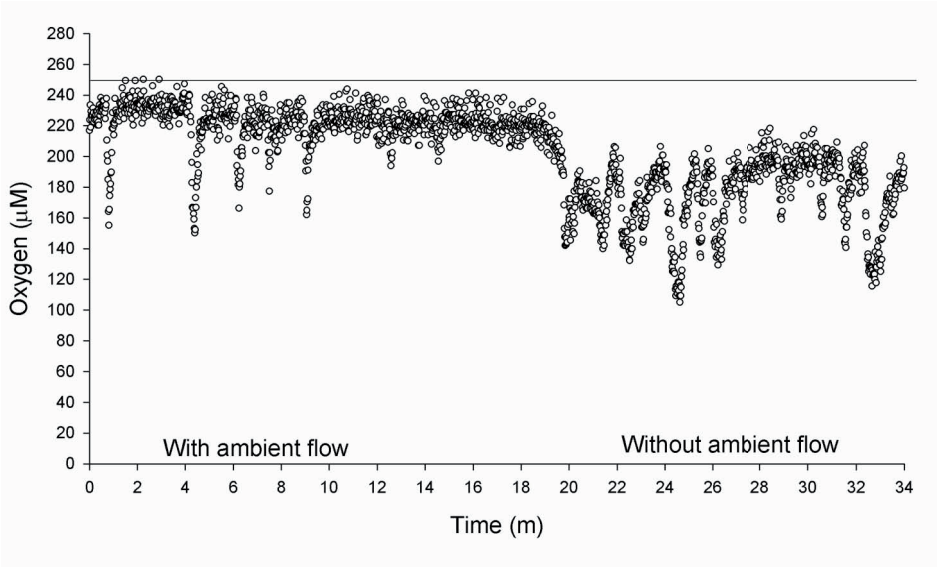

Figure 9. Oxygen micro-electrode measurement in the osculum of *D. avara* in a flow-cell with re-circulating seawater, with the presence and absence of ambient flow. The vertical bar indicates oxygen content in the water

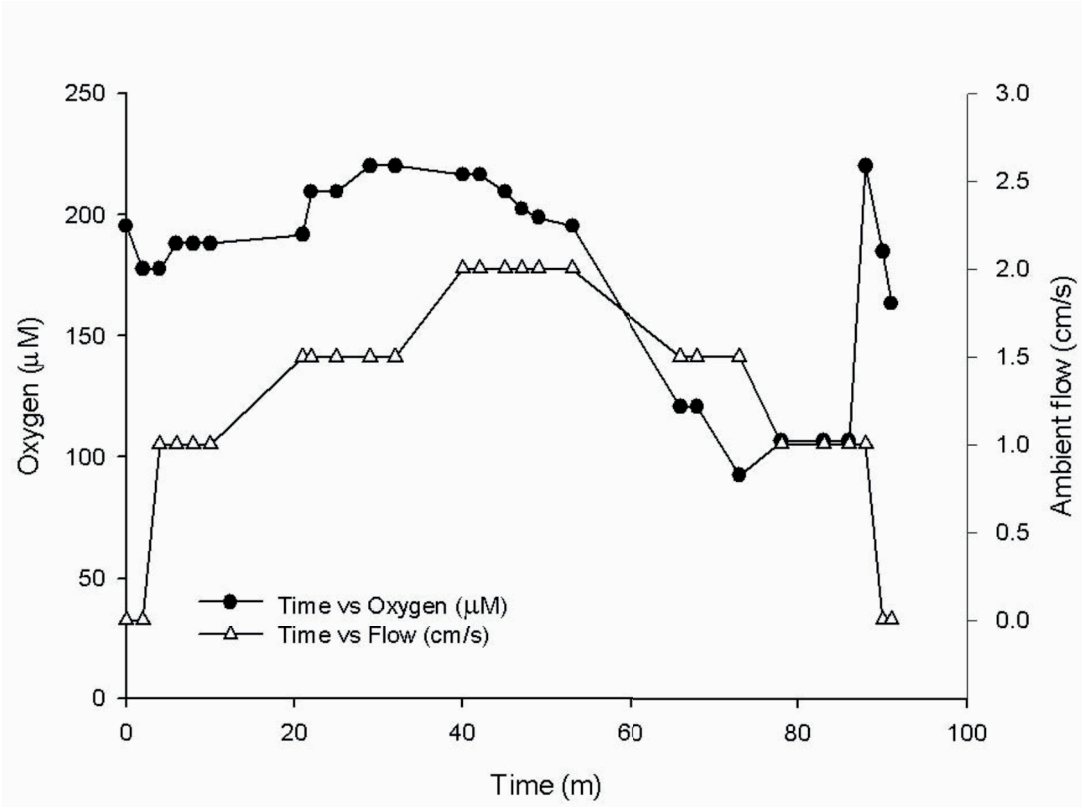

Figure 10. Oxygen micro-electrode measurement in sponge in relation to ambient flow velocities in a large *D. avara* with oscula

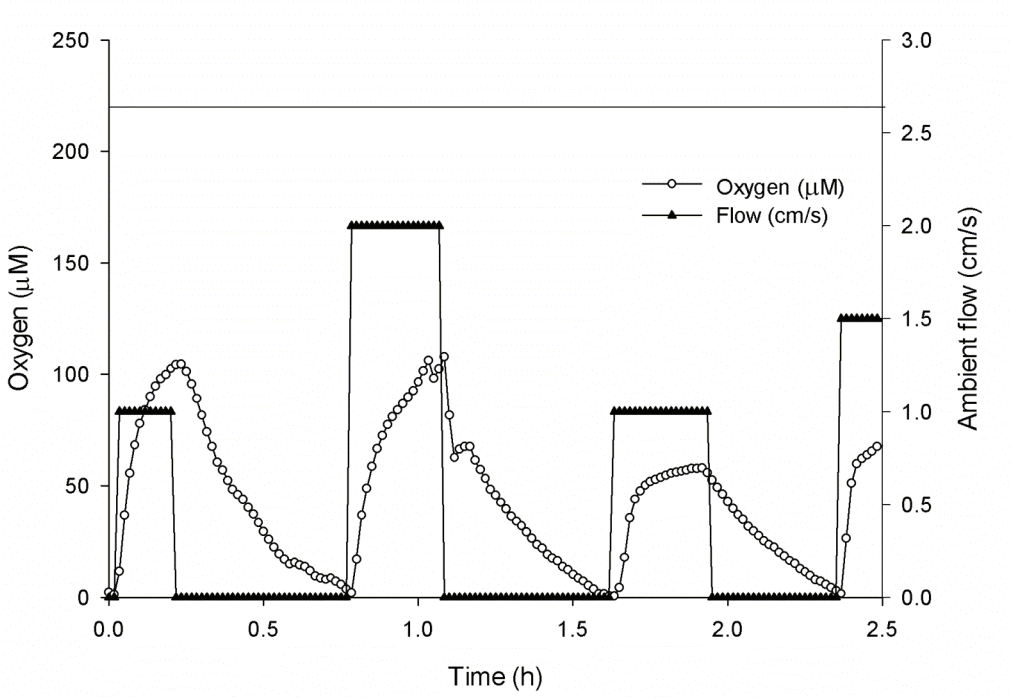

Figure 11. Oxygen micro-electrode measurement in sponge in relation to ambient flow velocities in a small *D. avara* without oscula. The straight line indicated oxygen concentration in the seawater

5. Discussion

5.1 Anoxia

Field and laboratory static oxygen measurements within the tissue of both *D. avara* and *C. reniformis* specimens revealed that those sponges underwent periods of anoxia. The anoxia was therefore not a consequence of potentially unfavorable sponge laboratory conditions, as *D. avara* showed the same pattern of oxygen dynamics and oxygen distributions in both the laboratory and in undisturbed field conditions (Fig. 4, 5). The onset of anoxia was not induced by the sensor measurements, but occurred random times after insertion (Fig. 4, 5). For these reasons, we feel confident that our results show a realistic picture of the occurrence of anoxia in both target species. These times of low oxygenation seem to occur commonly and appear to be part of the sponge functioning.

That sponges can have anoxia has been observed previously in a variety of species (Hoffmann et al. 2005a, b, Schläppy et al. 2007, Hoffmann 2008). However, our data shows that oxygenation is heterogeneous across the sponge, that oxygenation is most intense near an osculum, so that more remote areas are not as well oxygenated and must even rely on diffusion. Ventilation is the main oxygenation process and seems to be alternately active in different zones of the sponge. It is possible that the set of choanocyte chambers and canals

leading to an osculum function as an independent unit (as an autonomous module). Observations made in the field (Mendola unpublished data) and in the laboratory (Schläppy unpublished data) showed that one osculum can be totally inactive while the neighboring osculum has a high oscular flow rate. This also supports the idea of modular functioning of *D. avara*. Our data indicate that oxic and anoxic zones can be present at various locations across the sponges and that the change from aerobic to anaerobic and vice-versa is occurring abruptly and not gradually. This means that within the deeper layers in sponges a highly dynamic oxygen regime is present, to which the bacterial populations must be adapted in order to pertain.

5.2 Oxygenation and distance from target osculum

Oxygen profiles carried out away, midway and close to an osculum showed highly variable tissue oxygenation patterns in space and time (Fig. 7, 8). The expectation of oxygenation being a function of the distance to a target osculum was met in the field (Fig. 7) but less so in the laboratory (Fig. 8). Oxygenation patterns were not, as might have been expected, the most oxygen depleted away from the osculum (Fig. 8). If *D. avara* really has a 'modular' ventilation patterns, then it is possible that our measurements were made in different units and are so variable for this reason.

Oscular flow speed measured in the laboratory was sometimes related to how well the sponge was oxygenated, but not always. The presence of a lag time between ventilation and oxygenation is possible and would explain why ventilation and oxygenation data do not always match. In *Aplysina aerophoba*, the situation is very different and Hoffman et al. (2008) showed a clear relation between sponge tissue oxygenation and pumping activity. However, this species has a simple chimney-like architecture unlike *D. avara* which is more massive, often with many oscules, making it difficult to predict the architecture of the canal system. The tissue sampled with the electrode may have only been partially linked to the target osculum where the exhalent flow was measured.

5.3 Oxygenation and ambient flow

Another factor which influenced oxygenation patterns in sponges was the level of ambient flow and sponge ventilation behaviour. The larger specimens in this study showed the ability to modify their pumping behaviour according to the presence or absence of ambient flow (Fig. 9), and according to ambient flow speed (Fig. 10). This implies that the sponges were able to detect the presence or absence of ambient flow and modified their ventilating behavior

accordingly, although we have no direct evidence as to the method of detection. Furthermore, the sponges reacted rapidly (within minutes) to a change of ambient flow magnitude by changing their ventilation. When exposed to varying regimes of ambient flow, the oxygenation within the body of a *D. avara* specimen fluctuated little (approx. 180 – 200 µM), as long as the ambient flow was above 1 cm s^{-1} (Fig. 10). However, when ambient flow was stopped, the sponge maintained oxygen concentration above 100µM within its tissues and did not become anoxic, suggesting a compensatory mechanism through increased ventilation.

When a similar experiment was conducted with a small *D. avara* individual which lacked an osculum (and thus probably a functional aquiferous system), ambient flow had a much larger impact on the oxygen levels within the sponge. The cessation of ambient flow, in this case, resulted in an immediate decrease of oxygen within the sponge. Sponge cell respiration and probably the respiration of sponge-associated microbes at the location of measurement must have exceeded the supply of oxygen through diffusion, so residual oxygen within the sponge tissues was depleted within 39 minutes. Varying levels of ambient flow did not make a substantial change in the maximum level of oxygen content within the sponge tissue (Fig. 11), suggesting that, above a certain minimum ambient flow, the benefits of increased flow are not proportional. Our results support Vogel's findings (1975, 1977) that sponges can take advantage of ambient flow, which comes at a low cost to them. These results point to the importance of ambient flow to small sponges, for example explants (sponge pieces) often used for sponge aquaculture.

5.4 Consequences of sponge tissue anoxia

The consequences of temporal or spatial anoxic niches within the study species are several-fold. Firstly, it allows the presence of obligate anaerobic or facultative anaerobic micro-organisms in the sponge body. Such microbes and their processes have been found in several species of sponges such as *Rhopaloeides odorabile* (Webster et al. 2001, Hoffmann 2005b). Secondly, anoxic niches allow anaerobic microbes to become active. Whether anaerobic conditions last long enough for anaerobic microbial processes such as denitrification, anammox or sulfate reduction to occur remains to be investigated. Finally, the sponge-associated microbes must be able to tolerate and be active even under rapidly changing oxygen conditions.

By varying the internal oxygen condition within its body, a sponge may be able to maintain a diverse population of associated bacteria, which can potentially be used as a food source (bacterial farming) or as a means to reduce the prevalence of the sponge cell metabolic waste

products, such as ammonium. Alternatively, sponge-associated microbes may simply take advantage of an inherent behaviour - the periodic shutting down of the ventilating activity. In order to investigate this further, the presence or absence of key anaerobic microbial processes should be assessed in these two species of sponges and the mechanisms triggering ventilation understood. Only then could the interactions between the oxygenation of the sponge host and the metabolic activity of its associated microbes be elucidated.

6. Acknowledgments

This work was funded by the EU SPONGES project N^{o} 017800. Invaluable logistic assistance was kindly provided by Marta Ribes, CSIS Barcelona. We thank Silke Dahms for assistance in the field. MW acknowledges the support through a PhD scholarship by the Max-Planck-Society and the German Academic Exchange Service (DAAD).

7. References

Boury-Esnault N, (2002) Order Chondrosida Boury-Esnault and Lopès, 1985. Family Chondrillidae Gray, 1872. In Hooper JNA, van Soest RWM (eds) Systema Porifera: A Guide to the Classification of Sponges. Kluwer Academic/Plenum Publishers, New York

Canfield DE, Marais DJ, 1991. Aerobic sulfate reduction in microbial mats. Science 251:1471-1473

Fell P, (1998) Ecology and physiology of dormancy in sponges. Schweizerbart'sche Verlagsbuchhandlung, Stuttgart

Galera J, Turon X, Uriz M, Becerro M, (2000) Microstructure variation in sponges sharing growth Ffrm: The encrusting demosponges *Dysidea Avara* and *Crambe Crambe*. Acta Zool. (Stockholm), 81**:** 93-107

Gerrodette T, Flechsig AO (1979) Sediment-induced reduction in the pumping rate of the tropical sponge *Verongia Lacunosa*. Mar. Biol. 55**:** 103-110

Hoffmann F, Larsen O, Rapp HT, Osinga R (2005a) Oxygen dynamics in choanosomal sponge explants. Mar. Biol. Res. 1**:** 160-163

Hoffmann F, Larsen O, Thiel V, Rapp HT, Pape T, Michaelis W, Reitner J (2005b). An anaerobic world of sponges. Geomicrobiol. J. 22**:** 1-10

Hoffmann F, Røy H, Bayer K, Hentschel U, Pfannkuchen M, Brümmer F, de Beer D (2008) Oxygen dynamics and transport in the Mediterranean sponge *Aplysina Aerophoba*. Mar. Biol. 153**:** 1257-1264

Hoffmann F, Schläppy M-L (submitted) Sponges (Porifera) and Sponge Microbes. In Reitner J, Thiel V (eds) Encyclopedia of Geobiology. Springer Verlag, Heidelberg

LaBarbera M, Vogel S, (1976) An inexpensive thermistor flowmeter for aquatic biology. Limnol. Oceanogr. 21**:** 750-756

Pile AJ, Patterson MR, Savarese M, Chernykh VI, Fialkov VA (1997) Trophic effects of sponge feeding within Lake Baikal's littoral zone. 1. In Situ Pumping Rate. Limnol. Oceanogr. 42**:** 171-178

Reiswig HM (1971) In Situ Pumping Activities of Tropical Demospongiae. Mar. Biol. 9**:** 38-50

Revsbech NP (1989) An oxygen microelectrode with a guard cathode. Limnol. Oceanogr. 34**:** 474-478

Santavy DL, Willenz P, Colwell RR (1990) Phenotypic study of bacteria associated with the Caribbean Sclerosponge, *Ceratoporella Nicholsoni*. Appl. Environ. Microbiol. 56**:** 1750-1762

Schläppy M-L, Hoffmann F, Røy H, Wijffels RH, Mendola D, Sidri M, de Beer D (2007) Oxygen dynamics and flow patterns of *Dysidea Avara* (Porifera: Demospongiae). J. Mar. Biol. Ass. U. K. 87

Schumann-Kindel G, Bergbauer M, Manz W, Szewyk U, Reitner J (1997) Aerobic and anaerobic microorganisms in modern sponges: A possible relationship to fossilization-Processes. Facies 36**:** 268-272

Swatschek D, Schatton W, Müller WEG, Kreuter J (2002) Microparticles derived from marine sponge collagen (scmps): Preparation, characterization and suitability for dermal delivery of all-trans retinol. Europ. J. Pharm. Biopharm. 54**:** 125-133

Uriz MJ, Rosell D, Martin D (1992) The sponge population of the Cabrera Archipelago (Balearic Islands): Characteristics, distribution and abundance of the most representative species. P.S.Z.N.: Mar. Ecol. 113**:** 101-117

Vogel S (1974) Current-induced flow through the sponge, *Halichondria*. Biol. Bull. 147**:** 443-456

Vogel S (1977) Flows in organisms induced by movements of the external medium. In Padely TJ (ed) Scale effects of animal locomotion. Academic Press, New York pp 285-297

Weber M, Färber P, Meyer V, Lott C, Eickert G, Fabricius KE, de Beer D (2007) *In Situ* applications of a new diver-operated motorized microsensor profiler. ES&T 41**:** 6210 -6215

Webster NS, Wilson KJ, Blackall LL, Hill RT (2001) Phylogenetic diversity of bacteria associated with the marine sponge *Rhopaloeides Odorabile*. Appl. Environ. Microbiol. 67**:** 434-444

Chapter 8

The H_2S microsensor and the dissociation constant pK_1: problems and solutions

The H_2S microsensor and the dissociation constant pK_1: problems and solutions

Weber, M.[*1,2], Lichtschlag, A.[*1], Jansen, S.[3], de Beer, D.[1]

[1] Max Planck Institute for Marine Microbiology, Celsiusstrasse 1, 28359 Bremen, Germany

[2] HYDRA Institute for Marine Sciences, Elba Field Station, Via del Forno 80, 57034 Campo nell'Elba (LI), Italy

[3] Netherlands Organisation for Applied Scientific Research, Delft, Netherlands

Authors e-mail:
m.weber@hydra-institute.com
alichtsc@mpi-bremen.de
stefan.jansen@tno.nl
dbeer@mpi-bremen.de

[*] These authors contributed equally to this work.

This chapter will be submitted as a note to a peer-reviewed international journal.

1. Introduction

For the calculation of S_{tot} from hydrogen sulfide microsensor signals, the dissociation constant pK_1 is needed. Also for the calibration of the H_2S microsensor in a medium with a pH > 4 the pK_1 is necessary for H_2S concentration calculations. Hence its accuracy is important for a precise determination of S(II)-species. Here we describe and discuss the pK_1 problems and suggest a new calibration protocol.

Hydrogen sulfide is one component of the sulfide equilibrium system:

$$(1) \qquad \left[S_{tot}^{2-}\right] = \left[H_2S\right] + \left[HS^-\right] + \left[S^{2-}\right]$$

Presence and concentration of the S(II)-species depend on the dissociation constants K_1 $\left(H_2S \xleftrightarrow{H_2O} HS^- + H^+\right)$ and K_2 $\left(HS^- \xleftrightarrow{H_2O} S^{2-} + H^+\right)$. The equilibrium is influenced by pH, ionic strength and temperature of the medium (Kühl & Steuckart, 2000) (Fig. 1). The pK is the negative logarithm of this dissociation constant K.

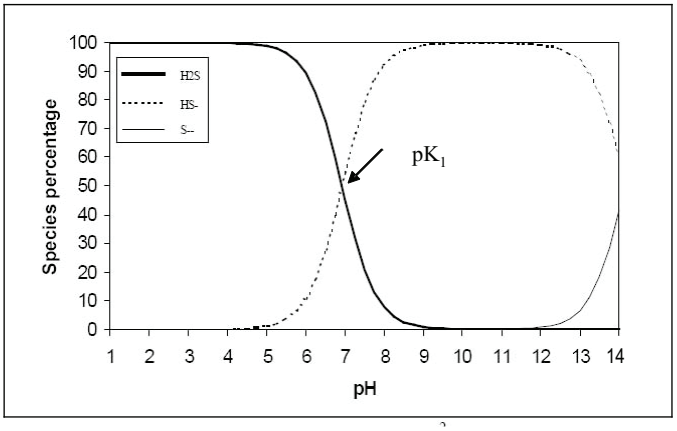

Figure. 1. S(II)-species percentage as a function of pH at given ionic strength and temperature with the negative logarithm (pK_1) of the dissociation constants K_1 $\left(HS^- \xleftrightarrow{H_2O} S^{2-} + H^+\right)$. (Kühl & Steuckart 2000).

The H_2S concentration at a given total S(II) concentration (S_{tot}^{2-}) can be calculated as

$$(2) \qquad \left[H_2S\right] = \left[S_{tot}^{2-}\right] \div \left(1 + \frac{K_1}{\left[H_3O^+\right]} + \frac{K_1K_2}{\left[H_3O^+\right]^2}\right)$$

For pH < 9, as is the case in most natural systems, the dissociation of HS^- to S^{2-} is negligible and the equation can be simplified to:

(3) $$\left[H_2S\right] = \left[S_{tot}^{2-}\right] \div \left(1 + \frac{K_1}{\left[H_3O^+\right]}\right); \qquad K_1 = 10^{-pK_1}$$

In solutions with pH < 4, also the dissociation of H_2S to HS^- is negligible and the equation can further be simplified to:

(4) $$\left[H_2S\right] = \left[S_{tot}^{2-}\right]$$

For the calculation of equation (3) the pK_1 and the pH (=-log $[H_3O^+]$) need to be known (Jeroschewski et al. 1996). The pH can be measured and the pK_1 can be calculated according to Millero et al. (1988) using the following equation:

(5) $$pK_1^* = -98.080 + 5765.4 \div T + 15.04555 \times \ln(T) + \left(-0.157 \times \left(S^{0.5}\right)\right) + \left(0.0135 \times S\right)$$

where T is the temperature in Kelvin (0 K = 273.15°C) and S is the salinity (Fig. 2). It is very important to note that this equation is only valid for seawater! For media with another ionic composition respectively ionic strength, refer to further literature and see part 3). Therein the problems of the correct pK_1-determination are elucidated and solutions are presented.

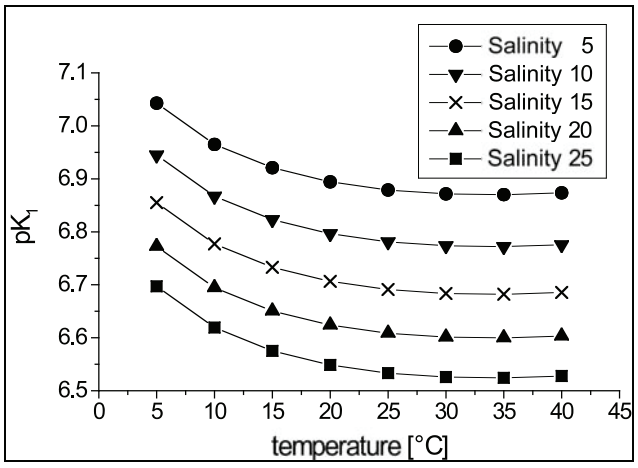

Figure 2. pK_1-values for H_2S concentrations at certain temperatures and salinity using the equation from Millero et al. (1988).

The hydrogen sulfide microsensor is an amperometric type miniaturised sensor (Jeroschewski et al. 1996, Kühl et al. 1998) measuring H_2S partial pressure: H_2S gas penetrates the silicon

membrane of the sensor tip and is converted to HS^--ions in an alkaline electrolyte. Ferricyanide oxidizes this HS^- to sulphur and ferrocyanide is formed. The ferrocyanide is reoxidized at the anode of the sensor tip. The resulting current corresponds to the H_2S concentration.

The electrolyte is photosensitive, mainly to UV and blue light (www.unisense.com). The detection limit of a new sensor is about 0.1 μM. The sensor signal is linear in a concentration range between 0-300 μM H_2S and becomes non-linear at concentrations > 300 μM. In the linear range a 2-3 point calibration of the microsensor is sufficient, whereas in the non-linear range a more precise calibration is recommended.

According to literature and the Unisense manual of July 2003 (the reader should know that the current Unisense manual is modified), it was suggested to calibrate the H_2S sensor in a 100-200 mM phosphate buffer (pH 7-7.5). Increments of a stock solution (100-500 mM S_{tot}) were added to a known volume of degassed buffer. Subsamples were taken and fixed in 2% ZnAc after each calibration step. S_{tot} was determined photometrically (Cline 1969, Budd & Bewick 1952) and H_2S concentration was calculated using equation (3). Usually the pK_1 = 7.05 was used as it was done by previous authors (Wieland & Kühl 2000, Kühl & Jørgensen 1992). Doing so, we discovered a discrepancy between S_{tot} concentrations measured with H_2S microsensors and S_{tot} concentration measured in the pore water with analytical methods.

As a consequence we decided to determine the precise pK_1 for the phosphate buffer we had used for the calibration of the microsensor using the 2-way-calibration-method" (§ 3). Then we compared results obtained using the defined pK_1 6.9 (see ** in Tab. 1 and § 3) with those of the previously used pK_1 = 7.05 (see * in Tab. 1) and revealed up to ± 30% deviance in the final H_2S concentration. A pK_1-offset of 0.05 leads to over- or underestimation of 8.9% ± 1.2 (SD) and an offset of 0.1 pK_1 units to 17% ± 1.7 (Tab. 1) of the measured H_2S concentration.

Table 1. The effect on the final H_2S concentration using over-/underestimated pK_1 values for the H_2S microsensor calibration (using a phosphate buffer, pH 7.5).

mean value			pK_1 deviance	0.05 unit		0.1 unit	
pK_1	H_2S [mM]	H_2S difference [%]	H_2S difference	[mM]	%	[mM]	%
7.10	0.52	140.5		0.04	7.69	0.08	15.38
7.05	**0.48**	**129.7***		0.04	8.33		
7.00	0.44	118.9		0.03	6.82	0.07	15.91
6.95	0.41	110.8		0.04	9.76		
6.90	**0.37**	**100.0****		0.03	8.11	0.06	16.22
6.85	0.34	91.9		0.03	8.82		
6.80	0.31	83.8		0.03	9.68	0.06	19.35
6.75	0.28	75.7		0.03	10.71		
6.70	0.25	67.6		0.02	8.00	0.04	16.00
6.65	0.23	62.2		0.02	8.70		
6.60	0.21	56.8		0.02	9.52	0.04	19.05
6.55	0.19	51.4		0.02	10.53		
6.50	0.17	45.9	**Mean value**		**8.89**		**16.99**
			Standard deviation		**1.18**		**1.74**

* pK_1 literature value for phosphate buffer calibration
** pK_1 determined "2-way-calibration-method"

In the following we describe:

2.1) The H_2S microsensor calibration protocol, which we suggest to use from now on.

2.2) Data showing the effect on H_2S microsensor sensitivity and/or measuring accuracy of: 2.2.1) degassing; 2.2.2) salinity/ionic strength; 2.2.3) temperature; 2.2.4) pH; 2.2.5) a) temperature and salinity on the pK_1 using formula (4) and b) pH on the H_2S concentration using equation (3).

2.3) The "2-way-calibration-method" for the pK_1-determination of any given solution.

2. Material, Methods & Results

2.1 Calibration protocol

We suggest performing the calibration of the H_2S microsensor in a subsample of the solution where measurements will be carried out (further referred to as calibration solution, e.g. seawater with salinity 36). If the calibration solution is acidified to pH < 4 no pK_1 is needed for the calibration.

1. Get a H_2S microsensor started (see also www.unisense.com).
2. The calibration should be performed under *in situ* conditions: in the calibration solution the same temperature and salinity (respectively ionic strength) should be maintained as will prevail during your measurements (see 2.2 and Fig.3).
3. The calibration solution is acidified with HCl to a pH < 4; as it is most probably not a buffered medium and you will add a base as stock solution (Na_2S) it is better to acidify to a pH < 2.
4. A defined volume (e.g. 100 ml) of the calibration solution is put on a stirrer (degassing is not needed (see 2.1 and Fig.3), the sensor inserted and the signal detected.
5. 2-4 times increments (e.g. 100 µl) of a 100-500 mM Na_2S stock solution are added, shortly and gently (!) stirred (no teflon stirrer) for mixing, and subsamples and sensor

readings are taken between each addition. Consider that at pH < 4 all S(II) in form of H_2S gas and can easily be flushed out by vigorous stirring! A subsample (e.g. 100 µl) of the calibration solution is fixed in 2% ZnAc (e.g. 5 ml) so that an end concentration of 20-50 µM is reached. Subsamples can be stored in the dark and cold (4°C) for several weeks.

6. The pH in the medium must be checked after the calibration. It maximally should be 3.9; this is important because only in this case $H_2S = S_{tot}$ (see formula (4)).
7. S_{tot} of the subsamples is measured photometrically (Cline, 1969; Budd and Bewick, 1952). Results correspond directly to the H_2S signal measured with the H_2S microsensor (see equation (4)).

2.2 Data on the H_2S sensor sensitivity and measurement accuracy

2.2.1 We tested if the calibration solution needs to be anoxic. For that a calibration according to the new calibration protocol (see § 2.1) with degassed (N_2-flushed) and air-saturated seawater (salinity 36, pH 2.5) was done.

Because the sensor signal remains constant during the calibration degassing of the calibration solution is not needed (Fig. 3). Half lifetime of H_2S depends on pH, temperature and ionic strength and is circa 24 h in air saturated seawater (salinity 36) (Millero et al. 1987).

2.2.2 We tested if the new H_2S microsensor calibration is salinity (respectively ionic strength) sensitive. For that a calibration was carried out in 100 ml (pH 2.5): a) deionised water (salinity 0), b) seawater (salinity 36), c) deionised water + 15 g NaCl (salt was added to simulate a hypersaline medium = salinity 150) and d) seawater + 15 g NaCl (salinity 186).

In our tests the microsensor signal in the calibration solutions with salinity 150 and 186 was strongly affected (Fig. 3). Further our data showed that the ionic strength difference from e.g. deionised water compared to e.g. phthalate buffer (phthalate buffer = 0.1 M potassium hydrogen phthalate solution adjusted to a pH 2.2 - 4 by HCl addition) is also reflected in the sensor signal (Fig. 4).

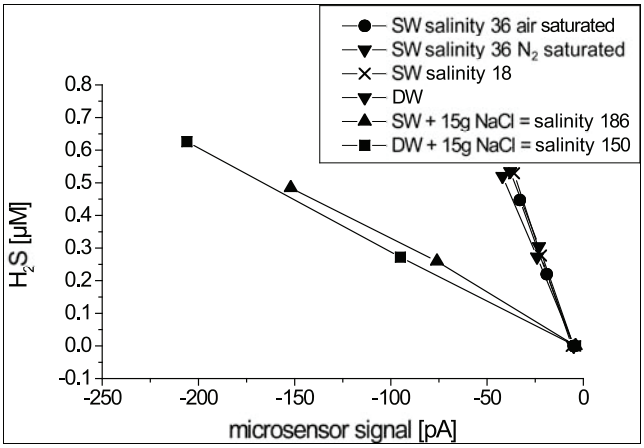

Figure. 3. H_2S microsensor calibrations at 21°C in seawater (SW) and deionised water (DW) with various salinities, air and N_2 flushed.

2.2.3 We tested if the new H_2S microsensor calibration is temperature sensitive. For that a calibration at two different temperatures (15 and 23°C) was carried out with: a) phosphate buffer (pH = 7.5), b) phthalate buffer (pH < 4) and c) 10 mM HCl.

As stated in the original reference (Jeroschewski et al. 1996), we confirmed that the H_2S microsensor is temperature sensitive. Thus it is important to perform the calibration at *in situ* temperature (Fig. 4).

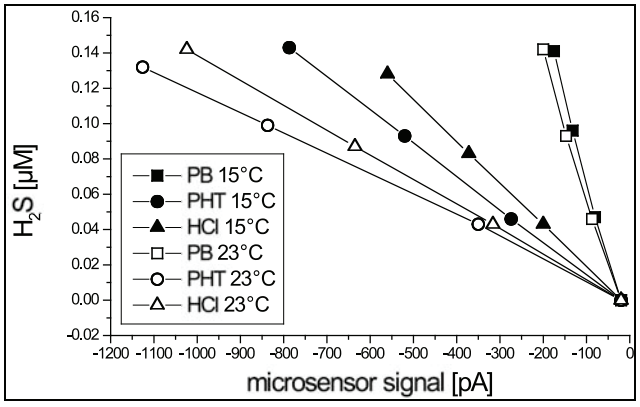

Figure 4. H_2S microsensor calibrations at two different temperatures (15 and 23°C) with a) 200 mM phosphate buffer pH = 7.5 (PB), b) phthalate buffer pH 3.8 (PHT) and c) 10 mM HCl as calibration solutions.

2.2.4. We tested if the new H_2S microsensor calibration is pH sensitive. For that a stepwise acidification of the calibration solution (here seawater salinity 36) from pH 3.9 to pH 1 was done.

The microsensor signal stayed constant; hence it is not influenced by the decreasing pH (data not shown).

2.2.5 We calculated a) the pK_1-deviance of imprecise temperature and salinity measurements when using equation (5) and b) the H_2S concentration deviance of imprecise pH measurements using equation (3).

a) Temperature offset ± 1°C affects the pK_1 in the first decimal. The effect of salinity is strongest at low salinity. An offset between salinity 5 and 18 changes the pK_1 in the first decimal, but at salinity values > 18 in the second and > 33 in the third decimal only (Tab. 2). Even though the effect is little, using formula (5) it should be aimed to measure temperature and salinity with an accuracy of ± 1 unit. As shown in the introduction and Tab. 1 a pK_1 deviance in the second decimal already can have a sever effect on the H_2S concentration.

b) A pH offset of ± 0.05 units at e.g. pH 7.5 leads to an over-/underestimation of 8.9-9.5% (see * in tab. 3) and an offset of ± 0.1 pH unit to 17.1-19.7% (see ** in tab. 3) deviance of the measured H_2S concentration. The deviance decreases with higher pH. However using equation (3) pH measurements should be aimed at best accuracy possible. Because of this we suggest to use the calibration protocol described above (see § 2.1).

Table 2. pK_1-deviance caused by imprecise temperature and salinity measurements using the equation (5) from Millero et al. (1988). Note that the equation is for seawater salinity 5 – 40 at 5 – 25°C only!

	Temp (°C)	Salinity	pK_1 (Millero et al., 1988)
brackish water	23	5	6.7265
brackish water	23	18	6.5870
brackish water	23	19	6.5822
brackish water	23	20	6.5779
seawater	23	33	6.5537
seawater	23	34	6.5536
seawater	23	35	6.5537
seawater	24	35	6.5389
seawater	23	35	6.5537
seawater	22	35	6.5688
seawater	16	35	6.6651
seawater	15	35	6.6822
seawater	14	35	6.6996
seawater	6	35	6.8499
seawater	5	35	6.8701

Table 3. H_2S concentration deviance caused by imprecise pH measurements using the equation (3) from Jeroschewski et al. (1996).

Calibration solution	pK_1	pH	H_2S [mM]	H_2S difference [mM]	%
Phosphate buffer 200 mM	6.9	7.00	0.48	0.26	120.5
	6.9	7.05	0.45	0.23	106.5
	6.9	7.10	0.42	0.20	92.7
	6.9	7.15	0.39	0.17	79.3
	6.9	7.20	0.36	0.14	66.3
	6.9	7.25	0.33	0.12	53.8
	6.9	7.30	0.31	0.09	41.8
	6.9	7.35	0.28	0.07	30.4
	6.9	7.40	0.26	0.04	**19.7****
	6.9	7.45	0.24	0.02	**9.5***
	6.9	**7.50**	**0.22**	**0.00**	**0.0**
	6.9	7.55	0.20	0.02	**8.9***
	6.9	7.60	0.18	0.04	**17.1****
	6.9	7.65	0.16	0.05	24.8
	6.9	7.70	0.15	0.07	31.9
	6.9	7.75	0.13	0.08	38.3
	6.9	7.80	0.12	0.10	44.3
	6.9	7.85	0.11	0.11	49.7
	6.9	7.90	0.10	0.12	54.7
	6.9	7.95	0.09	0.13	59.2
	6.9	8.00	0.08	0.14	63.3

* Resulting H_2S concentration deviance with an offset of 0.05 pH unit offset
** Resulting H_2S concentration deviance with an offset of 0.1 pH unit offset

2.3 Determination of pK_1 using the "2-way-calibration-method"

(e.g. 200 mM phosphate buffer pH 7.5, 23°C)

In case you used the phosphate buffer or another solution with pH >4 for the calibration of the H_2S sensor, and you are unsure about the correct pK_1, we suggest to determine the pK_1 afterwards using the following protocol.

Theory: Two calibrations in 2 different calibration solutions (here called: calibration solution I and II) are carried out with the same microsensor, and then the pK_1 is calculated. For this the calibration solution I must have the same properties (salinity/ionic strength, pH, temperature) as the solution you formerly calibrated in. In calibration solution I S(II) exists as $H_2S + HS^-$. Calibration solution II must be prepared as suggested in the new calibration protocol (salinity, ionic strength and temperature as in the solution you have measured in, acidified to pH < 4) all S(II) is in the form of H_2S (see Fig.1); by adding exactly the same concentration of stock solution in both calibration solutions, the sensor signal that is corresponding to the HS^- concentrations in solution I can be calculated. The sensor signal corresponding to the H_2S concentration is known from the calibration in solution II, because the S_{tot} corresponding to this sensor signal can be determined photometrically. The relation of the amount of H_2S/HS^- determines the pK_1 and can be calculated by combining the calibration I and II (see Tab. 4).

Practical application:

1. Get a fresh H_2S microsensor started (Unisense.com).
2. Take 100 ml of the formerly used calibration solution (here calibration solution I = 200 mM phosphate buffer, pH 7.5) and measure the pH as precise as possible (check the temperature settings and calibrate the pH probe).

3. Perform a 3-4 point calibration, fixate subsamples for later S_{tot} determination (see § 2.1) and check the pH again.
4. Take 100 ml of the calibration solution II with equal ionic strength as the medium you have measured in (here seawater salinity 36) and acidify it with HCl to pH < 2 (the pH has to be < 4 for the whole calibration procedure, thus to assure a pH < 4 also after the addition of the Na_2S stock a pH of < 2 is recommended).
5. Perform a 3-4 point calibration (with the same microsensor and at the same temperature!), take subsamples for later S_{tot} determination and check the pH again.
6. To make both calibrations comparable you now have to calculate how much S_{tot} would be present in the different calibration solutions if the sensor signals in both calibrations would be identical (Tab. 4). For this (i) calculate the regression of calibration solution I (here phosphate buffer) and then (ii) calculate the S_{tot} at the corresponding sensor signals from the calibration solution II.
7. Now you can use equation (3) with the pK_1 as the only unknown variable: The S_{tot} and pH are known, and the pK_1 needs to be fitted until the value for S_{tot} matches the value you measure in your calibration solution I.

Note: usually the pH cannot be measured more accurately than the first decimal (see § 2.2.4). Thus we suggest using a pK_1 value with the accuracy of one decimal only!

Table 4. The pK_1-determination of a given solution using the "2-way-calibration-method".

I	Calibration	y = -11,396x + 0,0331		
Calibration solution I		sensor signal	Stot = H_2S+HS^-	
Phosphatebuffer		0.00	0.0	
pH 7.5		-0.02	0.3	
23°C		-0.04	0.5	
II	Using	y = -11,396x + 0,0331		In calibration solution I
Calibration solution II		sensor signal	S_{tot} = H_2S	S_{tot} = H_2S would be
seawater salinity 36		0.00	0.0	*0.0*
pH < 4		-0.12	0.3	*1.4*
23°C		-0.24	0.5	*2.7*
III	Using formula (3):	$[H_2S] = [S^{2-}_{tot}] / \left(1 + \frac{K_1}{[H_3O^+]}\right)$		
			H_2S uM	In calibration solution I S_{tot} = H_2S would be
	pH	*7.50*	0.0	*0.0*
	Pk_1	*6.90*	0.7	*1.4*
			1.4	*2.7*

Further possibilities for pK_1 determination were suggested and used:

- Titration (de Beer & Lichtschlag)
- Calibration with phosphate buffers at different pH and the common intercept corresponds to the pK_1 (Jansen & Weber)

3. Conclusions & Recommendations

When doing your measurements/experiments always measure pH, temperature and ionic strength/salinity as precise as possible. Be aware of the potential over-/underestimation caused by imprecise temperature, salinity and/or pH measurements, when

a) determining the pK_1 with the equation (5) of Millero et al. (1988)
b) doing the H_2S calibration with a solution pH > 4 (not recommended by the authors!) using the equation (3) of Jeroschewski et al. (1996)
c) calculating S_{tot} concentration using the equation (3) of Jeroschewski et al. (1996).

Precise pH measurements can usually be done accurately to the first decimal. That is why pK_1-values should be used with one decimal only. After all we suggest avoiding calibration in solutions with pH > 4; then the pK_1 can be neglected for the calibration. Anyhow always consider to measure pK_1 directly, if you are unsure about the calculations and literature.

Also measuring salinity needs to be thought through carefully. The most accurate measurement method is conductivity. However when working with seawater salinities 5 – 40 we consider a refractometer, calibrated against normal seawater, as sufficient. Other solutions than seawater need further investigations and are not covered within this study.

Take care using H_2S microsensors under "abnormal" conditions like hypersaline, hyperbaric, or very high temperature and check the sensor for its sensitivity if uncertain. Researchers interested in measuring under high pressure should consult the literature of e.g. Carroll and Mather (1989). If you work with hypersaline media, check Gamsjäger & Schindler (1969), Wieland & Kühl (2000), and for high temperature check Barrett et al. (1988), Hershey et al. (1988), Millero (1986) and Millero & Hershey (1989). In order to determine the threshold at which salinity and/or ionic strength values affect the microsensor signal, further tests are needed. However we strongly recommend calibrating in the same solution/medium, as where the measurements will be done.

Further, all H_2S microsensor users should consider mentioning the potential percentage deviance of the H_2S concentration of their results. We suggest that this provides all of us with a better understanding on the difficulties of H_2S microsensor measurements, but also on the absolute and relative values of the published H_2S data.

4. Acknowledgements

We thank Frank Millero, Nils-Peter Revsbech, Michael Kühl, Andrea Wieland, Bo Barker Jørgensen, Marcel Kypers, Tim Ferdelman, Hans Røy, Frank Wenzhöfer, Henk Jonkers, Volker Brüchert, Christian Lott, and Peter Stief for valuable communication. We gratefully

acknowledge all technicians of the Microsensor Department for providing the microsensors. MW acknowledges the support through a PhD scholarship by the German Academic Exchange Service (DAAD) and the Max-Planck-Society.

5. References

www.unisense.com/Files/Filer/Manuals/Sulfide_manual_A5_www.pdf (accessed 23.02.2009)

Barrett, T.J., Anderson, G.M. and Lugowski, J. 1988. The solubility of hydrogen sulphide in 0.5 m NaCl solutions at 25-95°C and one atmosphere. Geochimica Et Cosmochimica Acta 52:807-811.

Budd, M.S. and Bewick, H.A. 1952. Photometric determination of hydrogen sulfide and reducible sulfur in alkalines. Analytical Chemistry 24: 1536-1540.

Carroll, J.J. and Mather, E. 1989. The solubility of hydrogen sulphide in water from 0 and 90 °C and pressures to 1 MPa. Geochimica Et Cosmochimica Acta 53:1163-1170.

Cline, J. 1969. Spectrophotometric determination of hydrogen sulfide in natural waters. Limnology and & Oceanography 14: 454-458.

Gamsjäger, H., and P. Schindler. 1969. Solubility and Activity Coefficients of H_2S in Electrolyte Mixtures. Helvetica Chimica Acta 52:1395-&.

Hershey, J. P., T. Plese, and F. J. Millero. 1988. The pK_1^* for the Dissociation of H_2S in Various Ionic Media. Geochimica Et Cosmochimica Acta 52:2047-2051.

Jeroschewski, P., C. Steuckart, and M. Kühl. 1996. An amperometric microsensor for the determination of H_2S in aquatic environments. Analytical Chemistry 68:4351-4357.

Kühl and Jørgensen, 1992. Microsensor Measurements of Sulfate Reduction and Sulfide Oxidation in Compact Microbial Communities of Aerobic Biofilms. Applied and Environmental Microbiology 58:1164-1174.

Kühl and Steukart, 2000. Sensors for in situ analysis of sulfide in aquatic systems. In: In situ monitoring of aquatic systems: chemical analysis and speciation. Eds: Buffle, J. and Horvai, G. pp 121-159.

Kühl, M., C. Steuckart, G. Eickert, and P. Jeroschewski. 1998. A H_2S microsensor for profiling biofilms and sediments: application in an acidic lake sediment. Aquatic Microbial Ecology 15(2): 201-209.

Millero, F. J. 1986. The thermodynamics and kinetics of the hydrogen sulfide system in natural waters. Marine Chemistry 18:121-147.

Millero, F. J., and J. P. Hershey. 1989. Thermodynamics and kinetics of hydrogen sulfide in natural waters. Acs Symposium Series 393:282-313.

Millero, F. J., T. Plese, and M. Fernandez. 1988. The dissociation of hydrogen sulfide in seawater. Limnology and Oceanography 33:269-274.

Millero, F., S. Hubinger, M. Fernandez, and S. Garnett. 1987. Oxidation of H_2S in seawater as a function of temperature, pH, and ionic strength. Environmental Science and Technology 21:439-443.

Truper, H. G., and H. G. Schlegel. 1964. Sulphur metabolism in Thiorhodaceae 1. Quantitative measurements on growing cells of *Chromatium okenii*. Antonie Van Leeuwenhoek Journal of Microbiology and Serology 30:225-&.

Wieland, A., and M. Kühl. 2000. Short-term temperature effects on oxygen and sulfide cycling in a hypersaline cyanobacterial mat (Solar Lake, Egypt). Marine Ecology-Progress Series 196:87-102.

Chapter 9

Conclusion and Outlook

Conclusion and Outlook

Based on the previous chapters of this thesis we conclude that bacteria are important for the harmful effects of sediment on reef-building warm-water coral colonies during sediment exposure. Our research demonstrated that the exposure to organic-rich fine sediment is particularly dangerous for coral reefs, and that the demise of sediment-covered corals is mediated by microbial activity.

We deduce that the broadest possible definition of sediment, "matter that settles to the bottom of a liquid", is essential when studying sedimentation stress on corals, and in an extended view, also when studying its effect on other organisms. It could be shown that certain sediment properties and their combined effects do play the major role in the damaging of corals. Fine sand did not harm the covered corals, and silt only had negative effects when it was organic-rich. As organic-rich sediments are also rich in microbes, it is to be expected that bacteria play an important role in the damaging of corals by sedimentation. We have proven that microbial activity causes damage on corals during sediment-coverage, and showed that the harmful effect of sediments increased with higher concentrations of organic matter in the sediment. Therefore, we conclude that a threshold of organic matter amount is needed in order to trigger the deadly microbial processes. It is obvious that the bioavailability of the organic matter determines how fast the microbial activity is triggered and how long it will endure. Based on our observations in the field and from experiments, we deduce that the amount of reactive organic matter, which is necessary to generate lethal conditions for the coral, is small. This is frequently observed during sedimentation events in areas affected by terrestrial runoff, but unlikely to occur during the sedimentation of resuspended organic-poor calcareous and coarse offshore sediments. Once initiated the deadly process is proceeding fast, within hours to 1-2 days, so that there is little chance for the affected coral to survive (Chapter 2-4).

The observations that led to the hypothesis that hydrogen sulfide from sulfate reduction could kill sediment-covered corals were misleading. While studying the 2-5 mm thin sediment layer on the coral, we encountered a complex system where interferences of biological (microbes and coral) and chemical processes occur. The increased activity of organic compound-degrading microorganisms that reduced pH and scavenged oxygen was enough to kill the corals. And the increase in hydrogen sulfide from decaying coral tissue accelerated the killing process substantially. Although this study showed that the killing of sediment-covered corals is microbially mediated, the exact initial killing process remains unknown. It is possible that fermentation end-products are more harmful under lower pH than at seawater pH. As the pH

is a very important parameter for cell functioning, subsequent physiological studies on corals could reveal why pH 7 under anoxic conditions was lethal and could set off this chain reaction. We further suggest that decreased pH at anoxic conditions could also have impacts on other organisms, such as calcareous algae, sponges, or microorganisms, and that the occurrence of this phenomenon in coral reefs is probably underestimated. For example locally increased particulate or dissolved organic carbon concentrations could increase microbial activity, decreasing oxygen and pH simultaneously. We would test this idea with similar experiments as described in this thesis, i.e. by a combination of viability tests, high-resolution methods for microenvironments, microbial rates, and microbial diversity studies. This hypothesis should be tested in tank experiments first, and then the occurrence in the reef should be evaluated. Whereas the exact mechanism leading to coral death is not entirely elucidated, the important message for coastal management is that microbial activities enhanced from the degradation of organic matter kill corals efficiently. Thus organic-rich silt is more dangerous than organic-poor sediments (Chapter 2-4).

We confirmed that the fresh coral mucus reduces sulfate reduction rates, and it was observed that the coral mucus alone was not enough to trigger lethal microbial activity on corals. This indicates that coral mucus has biocidal effects on microbial processes within the sediment layer. This possibly protects the corals against damage induced by microbes. However if concentrations of toxic metabolites from microbial processes increase substantially, or a quorum of pathogens has gathered, the coral mucus protection capacities will probably not withstand any longer (Chapter 4).

Our results showed that first the oxygen scavenging and pH decreasing microbial processes dominated, and then with some delay substantially concentrations of sulfide were generated. Sulfide release exceeded the measured sulfate reduction rates, thus the degradation of the organic sulfur compounds formed a significant additional sulfide source in very early diagenesis. This phenomenon may be of significance in the degradation of plankton blooms, coral mucus, and plant material or, as in our study, of sediment-buried sessile organisms (Chapter 4).

The existing calibration protocols of the hydrogen sulfide microsensor were critically assessed, and found to be in need of careful consideration. Suggestions for improvements lead to strong increase of accuracy. We think that the effect of extreme conditions such as high pressure or hypersalinity onto dissociation constants and microsensor functioning should be carefully investigated, as research on extreme environments becomes more and more important (Chapter 8).

The value of field measurements for complementing data obtained in mesocosms and laboratory experiments is obvious. Laboratory experiments may lead to artefacts, and thus wrong conclusions, but field experiments are difficult and costly. The observations made in the laboratory on the effects of sediment-coverage on corals and on the ventilation of sponges, were confirmed by direct measurements in the field. When animals are studied in their natural habitat they probably remain unstressed. Moreover, it is sometimes not possible to bring the samples to the laboratory, because they are too big (e.g. large corals), or others like corals with accumulated sediment cannot be sampled without destroying the thin sediment layer. Animals may behave differently in the laboratory, but also microbial processes need to be investigated under natural conditions as a comparison to lab-studies (Chapter 3, 4 and 7).

In order to link lab and field data it is preferable to use the same technique. We developed the diver-operated microsensor system DOMS, allowing similar microsensors measurements in the field as in the laboratory. We argue that with the extended techniques presented here, more insights can be gained on different organisms and their interactions in their natural habitat. Specific habitats, as e.g. small caves, rock pools, or fragile/sensible ecosystems like coral reefs or microbial mats, are now accessible to the study with microsensors. And because research on changing environmental conditions by sedimentation, eutrophication, temperature increase, or acidification become of greater public interest, results from manipulative microsensor experiments in the laboratory can be complemented by microsensor studies in the field. Despite the fact that in situ work is much more difficult, time-consuming, less precise, more difficult to interpret and more expensive than laboratory work, it is essential. We need to assess whether concepts found in the lab are relevant in the field, and the increasing technological possibilities need to be exploited optimally to achieve this goal (Chapter 5 and 6).

Acknowledgements

First of all I want to express sincere thanks to all who contributed to the outcome of this thesis. I would not be able to present it here without countless wonderful people and help I received!

More specific I would like to thank Prof. B.B. Jørgensen and Prof. K. Bischof for the evaluation of the thesis and for the support. I thank Dr. D. de Beer, Prof. W. Hagen, MSc LS K. Kohls and BSc S. Häusler for being the committee members of the thesis defence. Special thanks go to Katharina Fabricius and Dirk de Beer. Without your support and trust this joint project would not have started. I would like to let you know that you taught me many things I do not want to miss, that you inspired me, that you challenged me and that I spent a precious time. Thank you very much for your supervision. I would do it again! I cordially thank all co-workers of the seven chapters included in this thesis. It was a pleasure to work with you. I acknowledge the Max Planck Society and the German Academic Exchange Service for the support by PhD stipends.

I thank all colleagues for fruitful and inspiring discussions and times. At the Max Planck Institute for Marine Microbiology, I thank the microsensor department team 2004-2009, all TAs of the institute, especially of the microsensor group, the electronical and mechanical workshops, the IT department team, the library, the directors, and the entire administration for their continuous support. Special thanks go to Bo and Dirk for their valuable help with the "Last-minute-MTA". At the Australian Institute for Marine Science in Townsville, I thank the Water Quality team 2004 and 2005, the analytical technology team, the controlled environment aquaria team, the engineering facility team, marine operations team, the crews of the RV "Lady Basten" and "Cape Ferguson", the PC2 lab team, the tropical aquaculture facility team, the radiation lab team, the IT department team, the library, the director, and the entire administration for their assistance on the other side of this planet. I want to express my deepest thanks to Alison, Katharina, Glen, Tim, Craig, Anke, Sven, Michelle, Lindsay, Frank and all others for your support after the accident, which made me few mg lighter and 4 mm shorter. At the HYDRA Institute for Marine Sciences in Fetovaia, I thank the crews of 2004, 2006, 2007 and numerous visitors who assisted during fieldwork. Special thanks to Andrea, Boris, Silke, Stephan and Christian for your continuous support while "watching the grass grow" (quote from Katharina). At all three institutes, which agreed to contribute to this thesis, I felt welcome at any time. This was a great experience and I want to let all people working at these institutes know, that this is something special.

Last but not least, endless thanks to my husband, family and friends! Thanks for your continuous support and for believing in me. Live your dreams!

Erklärung

Gem. § 6(5) Nr.1-3 PromO

Ich erkläre, dass ich

1. die Arbeit ohne unerlaubte fremde Hilfe angefertigt habe,
2. keine anderen, als die von mir angegebenen Quellen und Hilfsmittel benutzt habe, und
3. die den benutzen Werken wörtlich und inhaltlich entnommenen Stellen als solche kenntlich gemacht habe.

(Datum, Ort) (Unterschrift)

Statement

Corr. § 6(5) Nr.1-3 PromO

I state that I

1. have finished this work without illegal help,
2. have used no other sources and aid, than stated, and
3. have cited any references.

(Date, Location) (Signature)